

Executive Summary

Safety is paramount to the wellbeing of the individual and is the focus for engineering innovation spanning various industries and sports. In football, helmets are typically constructed with a strong polycarbonate shell and an inner foam lining made from expanded polypropylene (EPP) or expanded polystyrene (EPS). Utilizing and studying the lightweight and energy absorption properties of an octet truss lattice structure, a superior padding can be created as an alternative to traditionally used EPS or EPP.

Ideally, the octet truss's unique lattice structure will decrease the strength of sudden impacts when compared to traditional foam paddings. Similarly, by focusing on improving safety for football players and preventing sport-related injuries, the research done in this project and similar projects forces the National Football League (NFL) to invest in and conduct their own helmet research (Williams).

One constraint of this project is the size of the models since the creation and simulation of a full-scale NFL helmet is out of the project's scope. Weight/Comfortability are also vital to this project as there should not be an excessive load on a football player's head. Cost is another constraint as if this project were to be done for-profit, hours would need to be billed and commercial licenses would need to be obtained for any software being used. Lastly, lack of accessibility to a lab and lab equipment due to the pandemic is limiting the research done in this project.

It was possible to complete the project by assuming that an Ansys simulation is comparable to physical tests done in a lab, properties remain constant through tests and that unit cells follow linear relationships when scaled to the full cell structure. Additionally, the evaluation of alternatives is based on the strength, durability, energy absorbing capabilities and environmental impacts of the unit cells.

This report presents completed SolidWorks models of unit cells varying in link radiiuses (0.5 mm, 1 mm and 1.5 mm) and lengths (9 mm, 10.80 mm, 13.50 mm and 18.0 mm), and completed unit cells assembled from previously mentioned unit cells (3x3x3, 4x4x4, 5x5x5, 6x6x6). Due to unexpected circumstances, the 4x4x4 R1.0 cell structure simulation was incomplete and is not included in this report. Compression tests were simulated on Ansys using a fine (1 mm) mesh and coarse (3 mm) mesh for all the unit cells and a coarse mesh for the cell structures. After the simulations, analyses for force versus displacement, energy versus displacement, specific energy absorption versus displacement and stress versus strain was conducted for the unit cells and cell structures. Additionally, a comparison between the unit cell's fine and coarse mesh was done. Also, an impact test was simulated to mimic the effect of a forearm hitting a 2x2 sheet made of the 3x3x3 R0.5 cell structure. Lastly, the optimal cell structure was determined using the specific energy absorption and theoretical densities, and rankings were created with the aid of a decision matrix.

Table of Contents

1.0	Introduction.....	1
1.1	Problem Statement	1
1.2	Objectives and Scope	1
1.3	Literature Review.....	2
1.3.1	Social Impacts	2
1.3.2	Health and Safety Impacts	3
1.3.3	Environmental Impacts	4
1.3.4	Economic Considerations	5
2.0	Background.....	5
2.1	Constraints.....	6
2.2	Assumptions	7
2.3	Criteria for Evaluation.....	8
3.0	Design Methodology.....	8
3.1	Design Parameters.....	9
3.2	Alternative Evaluation Procedures.....	9
3.3	Analysis Techniques	10
3.3.1	Aspect of the Unit Cells.....	10
3.3.2	Ansys Simulation	10
3.3.3	Theoretical Density and Mass Calculations.....	14
3.3.4	Unit Cell Results	14
3.3.5	Cell Structure Absorption Results	21
3.3.6	Impact Test.....	23
3.4	Design Evaluation	25
4.0	Project Management	28
4.1	Details of Design Plan.....	28
4.2	Plan of Attack.....	29
4.3	Division of Work.....	29
4.4	Project Status and Challenges	30
5.0	Conclusions and Recommendations	30
6.0	References.....	32
7.0	Appendices.....	34
7.1	Unit Cell Drawings.....	34

7.1.1	Unit Cells: Link Length of 9.0 mm.....	34
7.1.2	Unit Cells: Link Length of 10.80 mm.....	37
7.1.3	Unit Cells: Link Length of 13.50 mm.....	40
7.1.4	Unit Cells: Link Length of 18.00 mm.....	43
7.2	Cell Structure Drawings	46
7.2.1	3x3x3.....	46
7.2.2	4x4x4.....	49
7.2.3	5x5x5.....	52
7.2.4	6x6x6.....	55
7.3	PMMA Material Properties.....	58
7.4	Theoretical Densities and Mass.....	58
7.5	Additional Ansys Simulation Captures	60
7.5.1	Unit Cells	60
7.5.2	Cell Structures.....	109
7.6	Tabular Results for Simulations.....	131
7.6.1	Fine 1 mm Mesh Unit Cells	131
7.6.2	Coarse 3 mm Mesh Unit Cells.....	132
7.6.3	Coarse 3 mm Mesh Cell Structures	133
7.7	Ansys Detailed Forces and Energies.....	134
7.7.1	Unit Cell Fine Mesh (1 mm) Results	134
7.7.2	Unit Cell Coarse Mesh (3 mm) Results	140
7.7.3	Cell Structure Mesh (3 mm) Results.....	146
7.8	Force and Energy Absorption Graphs.....	152
7.8.1	Unit Cell Fine (1 mm) vs. Coarse (3 mm) Mesh Results Comparison	152
7.8.2	Cell Structure Mesh (3 mm) Results.....	156
7.9	Specific Energy Absorption (SEA) Graphs	163
7.9.1	SEA of Fine Mesh (1mm Mesh) Unit Cells.....	163
7.9.2	SEA of Coarse Mesh (3mm Mesh) Unit Cells.....	165
7.9.3	SEA of Cell Structures (3mm Mesh)	166
7.10	Stress Versus Strain Graphs	168
7.10.1	Unit Cells with Fine and Coarse Mesh vs. their accompanying Assembled Cell Structures	168
7.10.2	Varying Radiiuses with Constant Length	174
7.10.3	Varying Lengths with Constant Radiiuses.....	180

7.11	Impact Test on Single and Multiple 3x3x3 Cell Structures.....	184
7.11.1	Impact Test on Single 3x3x3 Cell Structure	184
7.11.2	Impact Test on 2x2 Sheet of Cell Structures	187
7.12	Decision Matrix Tools	189
7.12.1	Ranking Metrics.....	189
7.12.2	Ranking.....	192

1.0 Introduction

Additive manufacturing (AM) is a process which builds 3-Dimensional (3D) objects layer by layer. Complex geometries, such as octet-truss lattice structures, can be manufactured more easily using AM compared to traditional manufacturing methods due to the effectiveness of building layer by layer. Studies suggest that octet-truss lattice structures have lightweight and high energy absorption properties and often outperform foam cushioning such as expanded polystyrene (Hughes-Mussio, Kelly and Reeves). Given the octet truss lattice structure's energy absorption and lightweight properties, it is suitable as an alternative padding to EPS foam found in traditional football helmets. In the final phase of this project, the effects of displacement, forces applied, and energy absorption properties of twelve (12) unit cells and their lattice structures were compiled from simulations using finite element analysis (FEA) software. This data was analyzed to uncover the unit cell that fit the conditions of a possible foam substitute.

1.1 Problem Statement

Personal safety is paramount to the wellbeing of the individual and is a focal point for engineering innovation that spans many industries. Contact sports activities such as football put a lot of stress on a player's head and body. Sports activities were the third leading cause of traumatic brain injuries requiring hospital care in 2003-2004 (Gimbel and Hoshizaki). Sports leagues are significant investors into research and development of personal protective equipment (PPE), with one of the largest being the NFL. In 2019, the NFL reported they invested 16 million USD into the Engineering Roadmap, a campaign managed by Football Research Inc., to combat their record breaking 291 concussions reported in the 2017 season (Williams). They need the latest in material technology to keep their players protected and in their best state. Persistent impacts to the head of either low or high energies adversely affect the player's cognitive and neurological function (Gimbel and Hoshizaki). Common football helmets are constructed with a strong outer shell made of polycarbonate and an inner lining of foam such as expanded polypropylene (EPP) and expanded polystyrene (EPS), implemented to help dissipate and absorb impact energy. The octet truss structure, a lattice pattern consisting of repeating cells, is designed to absorb energy while being lightweight. The benefits of using this structure in place of the current foam found in football helmets can be uncovered by testing the structure's response to impacts and compression in football simulations.

1.2 Objectives and Scope

Group 9 aims to reach the following goals in the design of the octet truss foam liner:

- Create SolidWorks models of unit cells and assembled cell structures.
- Simulate compression and impact tests on unit cells and cell structures on the Ansys, a finite element analysis (FEA) software.
- Compile data from simulations and compare to current EPS/EPP foams.
- Draft partial mesh liners using the octet truss structure (and simulate tests on Ansys)

This report presents completed SolidWorks models of unit cells and cell lattices with various truss radii (0.5mm, 1.0mm, 1.5mm) and truss length (9.0mm, 10.8mm, 13.5mm, 18.0mm). Ansys compression tests are carried out on all 12 unit cells and 11 cell lattices. Compression data was collected from these simulations, which generated stress, strain, and force reaction values. Analysis was carried out on these values, with calculations on average stress and strain and specific energy absorption (SEA). Through this analysis the best parameters for the octet truss will be highlighted. This will help shed more light on the strengths of the octet truss shape and its extent of implementation. To simulate practical conditions, an impact test was executed with a cylinder representing an arm on a 2x2 sheet of a 3x3x3 cell structure. This experimental setup may be beneficial in the future to test the structure's capability in real world conditions.

In compliance with the lockdown restriction in Ontario, the location of the project, on-campus research facilities and resources are unavailable for use at the University of Guelph. Therefore, the scope of the project focuses on the application of known material properties of cured 3D printed parts based on prior research conducted by Royal City Engineers and literature review. A prototype of the models built in SolidWorks is out of the scope and consequentially in-person analysis such as 3D printing and curing will not be conducted. This project intends to build theoretical knowledge of the extent to which varying dimensions of the octet truss structure will have on the ability to absorb energy.

1.3 Literature Review

While the objectives are the primary focus, impacts of the design must also be considered. The primary goal of this project is to normalize a design that highlights the value of making contact sports as safe as possible while still being entertaining to watch. As well, research into an alternative foam liner is necessary as the production of EPP and EPS have considerable impact on the environment. By developing the octet truss model, it can be introduced as a framework for a foam liner that capitalizes on its inherent strength while using environmentally sustainable material.

1.3.1 Social Impacts

The NFL has been campaigning for a better understanding of sports injuries and how to protect their players. They have even begun investing into helmet research themselves, with their 16 million USD investment into the Engineering Roadmap (Williams). The NFL's stance on player protection will influence their fans to protect themselves as well. News about design development will help enforce their message about personal safety. For example, a new foam liner design helps bring focus to helmet technology, especially due to the rather consistent use of EPP and EPS foam as the football helmet design evolved. This in turn allows consumers to evaluate their safety while playing football and build a greater importance to wearing PPE.

Developing better helmets isn't the only path to protecting players. Heads up tackling is a safer method of tackling focused on leading with one's shoulder instead of their head. This method is based on self-preservation, where it is assumed the head protection is not completely

energy absorbing. During the late 70s and early 80s, players did lead with their shoulder, similar to rugby tackling (Staples). However, great development in head protection allowed players to act more with their head to capitalize on raw tackling power. This caused more head trauma cases as players believed helmets were now impervious to surface impact. Medical data collected in the late 2000s showed a greater amount of head injury cases due to this shift in playstyle (Staples). Research projects such as this strive to find a technology that can eliminate this problem, but there is still a lot of work to do; current football technology cannot eliminate the possibility of concussive impacts, only decrease it. With the help of newly trained coaches such as former Seattle Seahawks coach Rocky Seto, more football teams are returning to old rugby style tackles (Staples). Seto believes that this is the correct way to play, with sturdy shoulders to achieve leverage (Staples).

With advancing head armor technology, there runs a risk of players favoring their head in tackles, which leads to more head injuries. This octet truss research is meant to build on head protection, but football players are encouraged to take the extra step and favour their shoulders and the rest of their body instead of their head during tackling. Better tackling education and helmet development with octet truss technology work together to decrease the long-term impacts of head injuries and concussions on the football field.

1.3.2 Health and Safety Impacts

This novel foam substitute has great impact on health and safety through the design. It is aimed towards decreasing the strength of impacts during football. Professional football games include a lot of tough contact between players, and a huge risk during play is getting a hit to the head. Concussions are just another part of the game, but health officials in the league are pushing to reduce this statistic. While designing for the most professional in the industry, this octet truss model can also be translated into commercial purposes, making it available to the people who love to play football and other contact sports.

EPS foam is very versatile and one of its applications is house insulation. To protect the house from fires, this insulation would be treated with hexabromocyclododecane (HBCD). This is an additive used to help polystyrene particles achieve flame retardant properties. Other end products that contain HBCD are treated furniture and upholstery in vehicles and draperies (Canada). When EPS is recycled, HBCD particles can be transferred into secondary products of EPS foam, which may then be used in football helmets. Continued production of EPS poses a risk to consumers as HBCD has been found to cause harmful effects to humans when found in the body, as shown in Figure 1. HBCD can disrupt liver and thyroid hormone secretion, disrupt fertility and cause cancer when ingested (Huang, Shah and Hu). This accumulation in the body may also come from inhalation, which is possible for football players as the helmet surrounds the head. Alternatives must be found to decrease the production cycle of polystyrene and EPS as it has great impact on the health of players and the population.

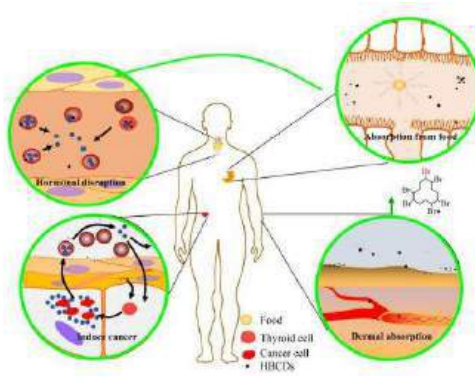


Figure 1: Health effects of HBCD found in EPS foams when entering human body (Huang, Shah and Hu).

1.3.3 Environmental Impacts

Both EPP and EPS are petroleum-based products (Madehow). Fossil fuels have considerable harmful effects on the environment, including pollution and ozone layer thinning. While most plastics are based on fossil fuels, bioplastics are gaining more ground. These bioplastics, such as polylactic acid, have similar properties to polypropylene and polystyrene, while being sourced from fermented starch from plants (Rogers). Ethically sourced plastics are suitable alternatives for helmet foam liners as they bear much less of an environmental impact than petroleum-based plastics.

HBCD is a synthetic material, and since it is physically added into the foam, there is a potential for HBCD to leak from the material and disperse into the environment. EPS waste that is not disposed properly will also deposit the HBCD into the environment. When EPS is dumped into water sources, the HBCD can then be discovered in the water and along the sediment. It has extremely slow biodegradation in water and soil, with half-lives ranging from 182 days to 5 years (Canada). The extended presence of HBCD allows marine life to ingest it from the sediment bed, resulting in its increased accumulation in the environment.

HBCD has been found to be bioaccumulative, posing a risk to the aquatic life in the area (Canada). HBCD particles can be transferred through the aquatic food chain resulting in larger fish harboring the largest concentration of the pollutant. The fish are then caught and sold in markets as seafood. Thus, HBCD can ultimately end up in humans, resulting in adverse effects on public health. While recycling of EPS is most desired, plastic waste will inevitably be disposed of as garbage and leech into the environment. As stated before, alternatives of conventional plastic needs to be used to lessen the adverse environmental impacts.

In comparison PMMA products are not classified as hazardous waste (Cefic). Thus, there does not exist any leaching chemical that could be toxic to the environment. There is a possibility of PMMA not being correctly recycled, which may lead to dumping of PMMA in environmental sites. In this worst case scenario, PMMA will not leach any chemicals into the environment (Cefic). As well, there are no corrosive gases emitted when acrylic is burned

(Cefic). Both EPS and PMMA are plastics, but PMMA has virtually no chemical or toxic effect when littered, making it a desirable material for this project.

1.3.4 Economic Considerations

The design is modeled on SolidWorks and is ready to be realized on 3D printers. However, the COVID-19 pandemic prevents us from using printing facilities, so the tests are simulated on Ansys instead. Under the assumption of using 3D printing, this prototype is expected to be developed on PMMA resin.

PMMA is a polymer, which can be broken down in a simple industrial process called depolymerization. The components of singular MMA that arise from this have very high levels of purity, allowing the polymer to be easily recyclable at the end of product life (PMMA). This cuts down on material use, as helmet liners that are damaged can be recreated with the same material due to the malleability of MMA and PMMA. As well, a sulphuric acid component used in this recycling process can be used for other end products, such as soil fertilizer (PMMA). Thus, the value of PMMA extends to creating other products when used PMMA is safely disposed and recycled (PMMA). Due to the nature of compression tests and impact tests, full recycling of PMMA helps with recuperating costs and lessens environmental impact, as virtually none of the PMMA goes to waste.

2.0 Background

To truly understand the use of lattice structures in current helmet designs, it is important to understand how history has allowed this design to be necessary in the first place. Although the NFL is a relatively newer league, football has been played all the way back to the 19th century. Football helmets themselves were not documented until the end of the 19th century, early 20th century. At that point, the gear only consisted of a leather headwear, not providing the support that would prevent serious injuries or death in any way. As the production of metals and plastics increased over the 20th century, helmet manufacturers started to integrate these into their designs. In the late 60's when football-related injuries started sharply increasing, safety standards had to be put in place, thus the founding of the National Operating Committee on Standards for Athletic Equipment (NOCSAE) triggered research efforts and brought awareness to head injuries and had protections implemented (Levy, Ozgur and Berry).

Now before the use of lattice structures in helmets, there was a huge proponent for foam structures to be used. To this point, it is the most effective piece of material to line the inner shell of a football helmet with. Specifically, the Expanded Polypropylene (EPP) and Expanded Polystyrene (EPS) Foams. EPP foam is unique in that it has “crushing or cell wall bending during compression, causing a plateau region in the stress-strain curve, this allows for a comparatively low increase in stress over a large strain interval, which in turn translates to good energy absorption, along with relatively low stresses” (Morton, Reyes and Clausen). EPS foam has features which closely resemble the EPP foam, including elastic deflection of cell walls, air compression and buckling of cell walls, which helps in energy absorption by the foam. The foam

can be used with different densities, each with their own benefits. The high-density EPS foam will absorb a larger amount of energy than low density ones, but at the cost of greater accelerations and forces being localized at the impact point. Low density foams are beneficial on the side of cost, size, and aerodynamics. The solution lies in the ability to increase the thickness of low-density EPS foams to achieve similar levels as the high-density ones. But with every option there is always a give and take (Landro, Sala and Olivieri).

Research and development into foam cushioning technology has given more focus on alternative foam types. Recent foams that are of interest to investors are vinyl nitrile (VN) foams, as it has distinct material properties compared to current EPP foam. A recent study in 2020 by Bailly et al. characterizes three vinyl nitrile samples with different densities of 97.5, 125, and 183 kg/m³ at different strain rates. It was found that VN foams achieved the same amount of energy absorbed compared to EPP foams while remaining denser and more efficient. This leads to reduced stress for same impact energy applied to EPP foams (Bailly, Petit and Desrosier). For instance, a VN foam of density 125kg/m³ transmitted a stress of 1.05 MPa while EPP foam of density 94.6 kg/m³ transmitted a stress of 1.57 MPa when at their most efficient during compression (Bailly, Petit and Desrosier). However, a downside to implementing VN is the heavier weight for the same energy, which can cause balance and comfort issues for athletes.

2.1 Constraints

Size

The scope of this project does not include replicating a full-scale NFL helmet. In terms of size constraints, the dimensions of the unit cells are calculated to fit within a 76.3674 mm (~3 inch) volume cube. By varying the lengths and radiiuses of the unit cell, cell structures of 6x6x6, 5x5x5, 4x4x4, 3x3x3 are achieved. The scope of this project is to understand which one of these structures will handle the vertical compression test and other variables to the greatest extent.

Weight/ Comfortability

The inner composition of a helmet should not be an extra load on the player's head, that is why it is important to limit the lattice structures to a minimum weight. This ties in with the fact that a heavier helmet, due in part to a denser material composition, will impede the athlete's play on the field. Therefore, comfortability will be a constraint in this design, influenced again by how heavy the lattice octet truss structure will be. Ease of play and comfortability with a helmet should not come in the way of improving safety standards, the two should be allowed to coexist, as the evolution of the football helmet has shown (Levy, Ozgur and Berry).

Cost

The greatest constraint in any project is the capital cost. At this iteration of the lattice structure design, the octet truss is not meant to be fully implemented into a full-scale football model. Since there will be no 3-D printing and use of machinery to test this model, the cost is

relatively low. The man hours working on this model will be in SolidWorks and Ansys. These are very expensive software to obtain for home use, but the remote access through the University of Guelph has driven down the cost of this project significantly.

Hypothetically, if remote access were not available for this project, the various programs that are used would have to be included in the budget. This includes:

- SolidWorks – \$110.00 CAD
- Ansys – Free Student Version
- Microsoft Office - \$169.00 CAD
- Microsoft teams – Free Software

The largest cost would come from labour or man hours spent on this interim report so far. Using the Fee Guideline for Professional Engineering Services from the Ontario Society of Professional Engineers, there is a breakdown on hourly rates for each responsibility level. In the case of this project, this group can be assigned responsibility level C, with an hourly rate of \$175 CAD. The reason for this can be summarized in the wording of how much supervision is needed for engineers at this level: “Work is not generally supervised in detail and amount of supervision varies depending upon the assignment. Usually, technical guidance is available to review work programs and advise on unusual features of assignment (Fee Guideline for Professional Engineering Services).” This perfectly encapsulates how dependent this group is on supervision from an advisor, most of the work is handled within the team, but technical guidance from an advisor is available, which is what the weekly advisory meetings are used for. Albeit, this guidance is for certified professional Engineers, this fee serves as an outline on what a ‘real-world’ compensation would look like. The time spent on this project is indicated from the Guelph course weighting breakdown, where it is stated that a course of [1.0] credits, requires 20-24 hours of study per week, taking off the 2 hours of lecture time per week, the hourly rate of \$175 CAD can be charged to approximately 18-22 hours spent on this project per week, per person.

Accessibility

In a normal year, this group would be able to use resources provided by the University to create a physical model, through 3-D printing. But since the pandemic has rendered that impossible, this group will need to adjust to online simulations to create a ‘life-like’ virtual model that will in the time being represent a working prototype. Since this iteration of the octet lattice structure is likely not the last, further tests can be performed using the results and observations found in this report in subsequent semesters, where access to University labs is possible.

2.2 Assumptions

1. In place of performing actual compression tests using University equipment, the model will be simulated using Ansys. The data collected from here, is assumed to be

comparable to actual compression tests to measure energy absorbing and strength properties of the octet truss structure.

2. In lieu of using 3-D printing to create a working prototype for the lattice structure, the model will be created on SolidWorks as planned but will not be printed. This version is assumed to reflect an actual working model and will be tested on Ansys.
3. Assume constant properties: Poisson's ratio of 0.35, thermodynamic equilibrium, constant volume, constant temperature, steady state, solid material, continuous, and homogenous structure (Askeland, Fulay and Wright).

2.3 Criteria for Evaluation

1. **Strength:** Using data from Ansys, find the maximum amount of stress that the lattice structure can take to test strength of material.
2. **Durability:** Other criteria measured by Ansys data is how much elastic/plastic deformation is present in the results, the greater the deformation before failure, the more durable the material is.
3. **Effectiveness of Absorbing Energy:** How the energy from the compression tests dissipated through the material. Ansys can show where the most stress/strain is being concentrated through contours on the model.
4. **Environmental consideration:** Compare the emissions of producing EPS/EPP Foams compared to producing PMMA for 3-D printing. One way is understanding where the materials come from for each material, and how much energy is consumed in preparing it for use in helmets.

3.0 Design Methodology

The purpose of the following evaluation is to determine the optimal composition of the octet truss lattice structure for the application of replacing EPS/EPP foam in existing American football helmets. SolidWorks was used to construct 3D models of the design and Ansys was used for simulations of displacement. The final report presents the accumulation of progress in the analysis of unit cells and fully constructed octet truss lattice structures. Simulations of the unit cells were conducted using the finest mesh possible corresponding to the size of the unit cell while maintaining the maximum number of elements allocated with the student version of Ansys. Similar analyses were conducted on the same unit cells with a coarse mesh to determine the accuracy of mesh sizing's. Details of each unit cell can be seen in the engineering drawings located in Appendix 7.1. Furthermore, the cell structures were assembled using each unit cell and the simulations were conducted by Dr. Bardelcik due to the limitation of Ansys and computing power. However, increased simulation times for the 4x4x4 R1.0 yielded no results. Details of each cell structure can be seen in the engineering drawings located in Appendix 7.2. Graphs regarding the simulations of the unit cell and the cell structure are organized with a reference parameter in the appendix, where either the radius or the length is constant to help the visual interpretation of the resulting data. Discussion and simulations of impacts tests were also conducted to simulate real world conditions in which the structures would be applied.

3.1 Design Parameters

The design of the octet truss lattice structure modified three parameters: the radius of a link, the length of the link, and the cell structure. All parameters were sized to fit a cubic shape cell structure measuring 76.3674 mm (~3 inches) along all edges. Both the length of the link and cell structure were designed to fit within the cubic shape. Changing the link radius will increase or decrease the relative density of the model, thereby, changing how the structure will react under displacement and loading conditions applied in the simulation. Table 1 illustrates the relation of each parameter to one another. The cells in the table correspond to parameters that intersect with each heading. For example, cell “I” corresponds to a link length of 18.0 mm and a link radius of 0.5 mm, where both parameters are used to construct a 3x3x3 cell structure.

Table 1: Correlation of Parameters

		Link Length (mm)			
		18.0	13.5	10.8	9.0
Link Radius (mm)	0.5	I	II	III	IV
	1.0	V	VI	VII	VIII
	1.5	IX	X	XI	XII
		3x3x3	4x4x4	5x5x5	6x6x6
Cell Structure					

3.2 Alternative Evaluation Procedures

The ultimate objective of the design is to investigate the behaviour of twelve (12) cell structures with their associated unit cells, specified in Section 3.1 Design Parameters, under displacement conditions to extract data for further analysis. Evaluation of cell structures and unit cells will be based on the energy vs. displacement curve derived from the integral of the force vs. displacement curve as well as the theoretical densities and masses of the unit cells calculated using Equation 1 and Equation 2 (Bardelcik, Yang and Ahmadpour). Ultimately, the specific energy absorption (SEA) calculations conducted using Equation 3 will help visualize and compare each cell structure and unit cell against one another (Ling, Cernicchi and Gilchrist). The cell structure and unit cell that exhibits high energy absorption and relatively low theoretical density will be the most desired design solution.

Equation 1: Theoretical Density

$$\bar{\rho}_{theoretical} = 6\sqrt{2}\pi \left(\frac{D}{2L}\right)^2$$

Equation 2: Theoretical Mass

$$m_{theoretical} = \rho_{material} \times V \times \rho_{theoretical}$$

Equation 3: Specific Energy Absorption

$$(SEA) = \frac{\text{Energy Absorbed}}{\text{Structural Weight}}$$

3.3 Analysis Techniques

The following section summarizes theoretical calculations and Ansys simulation results of the cell structures and unit cells being assessed. Dimensions of each unit cell are described in detail. Furthermore, results of the Ansys simulations for fine and coarse mesh are discussed in the context of the unit cells and cell structures.

3.3.1 Aspect of the Unit Cells

As mentioned in section 3.1 Design Parameters each combination of unit cells was created using SolidWorks and will be imported into Ansys for analysis. The initial link length was determined by the group before us, Royal City Engineers (Hughes-Mussio, Kelly and Reeves), at 9 mm using a SolidWorks file given by Dr. Bardelcik. A cubic cell structure (6x6x6) was constructed using the initial 9 mm length link in a unit cell, resulting 76.3674 mm (~3 inches) along all edges. This measurement would then be used to assemble the remaining unit cells. The group determined the height of a single unit cell by the resulting length by the number of faces (i.e., 6, 5, 4, 3) in the cell structure. A right-angle relation between the height of the unit cell and the length of two links along the hypotenuse was then calculated using the geometric relations. The single link length was determined by splitting the two-hypotenuse links. A summary of the calculations can be found in Table 1.

3.3.2 Ansys Simulation

For the analysis, the group simulated the unit cells with radiiuses of 0.5 mm, 1.0 mm and 1.5 mm and lengths of 9.0 mm, 10.8 mm, 13.5 mm, and 18.0 mm. The material properties and stress strain curve data (Figure 51), provided by Dr. Bardelcik, were imported into Ansys to mimic a unit cell 3D printed with Polymethyl methacrylate (PMMA). Then, meshes with a fine 1

mm element size (Figure 2) and coarse 3 mm element size (Figure 3) were applied to the unit cells for the simulation. Lastly, to simulate a compression test the bottom surface of the unit cell was treated as a fixed support (blue) and the top of the cell was assigned 50% displacement (yellow) relative to each unit cell's height as seen in Figure 4.

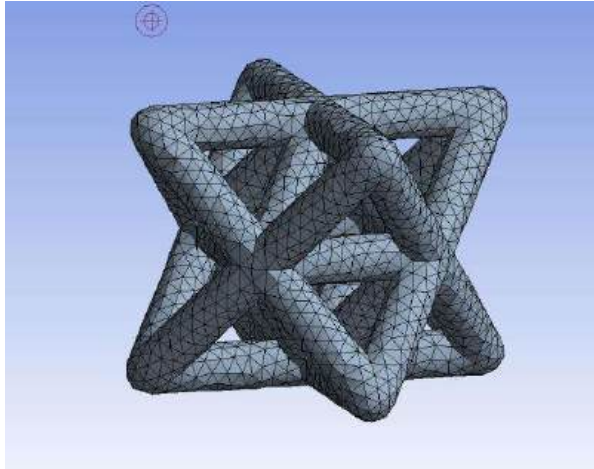


Figure 2: 1mm mesh for Ansys simulation (R1.5 L10.8)

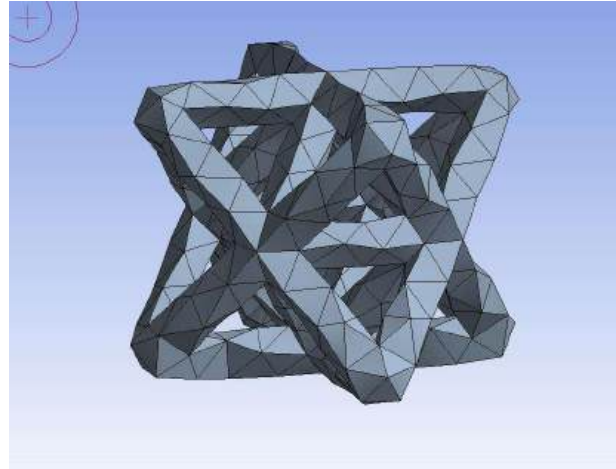


Figure 3: 3mm mesh for Ansys simulation (R1.5 L10.8)

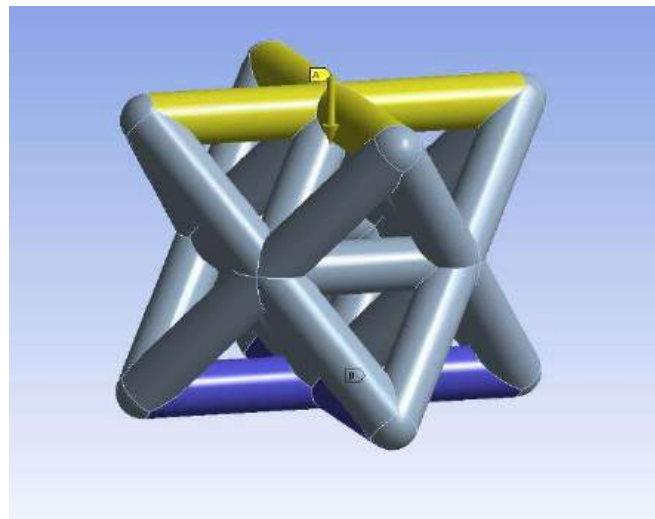


Figure 4: Fixed support (purple) and displacement (yellow) in Ansys (R1.5 L10.8)

During the analysis, the group examined the stress, elastic strain, total deformation and the force at the fixed support for both the 1 mm and 3 mm meshes, in which the tabular results can be seen in Appendix 7.6. The simulation of the stress, deformation, strain and force analysis for the unit cell with R1.5 mm L13.50 mm and a 1 mm mesh can be seen below in Figure 5, Figure

6, Figure 7 and Figure 8 respectively. Additionally, the simulations conducted on the remaining unit cells can be seen in Appendix 7.5.

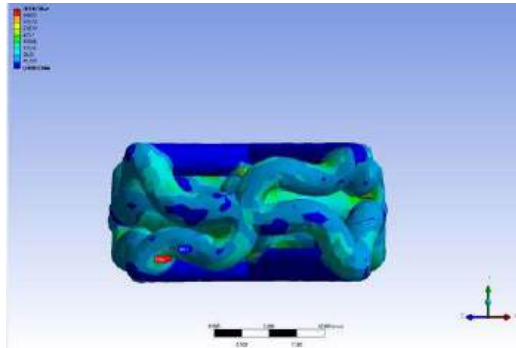


Figure 5: Stress for R1.5 mm L13.50 mm (1 mm mesh)

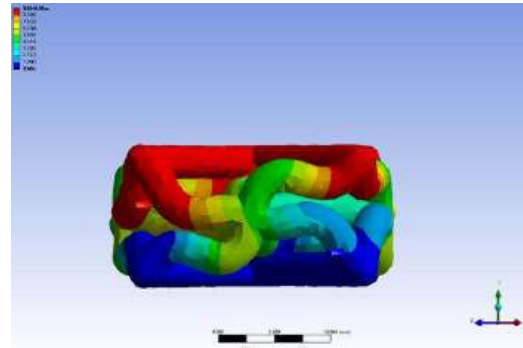


Figure 6: Deformation for R1.5 mm L13.50 mm (1 mm mesh)

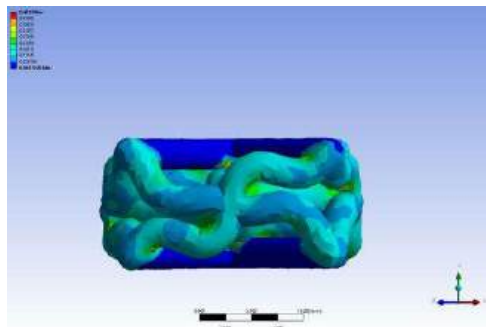


Figure 7: Elastic strain for R1.5 mm L13.50 mm (1 mm mesh)

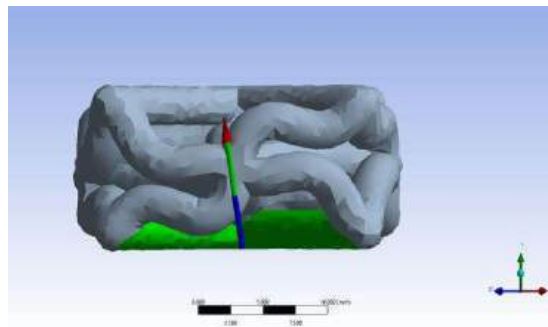


Figure 8: Force reaction for R1.5 mm L13.50 mm (1 mm mesh)

Similarly, the group constructed cell structures using the unit cells with radiiuses of 0.5 mm, 1.0 mm and 1.5 mm and lengths of 9.0 mm (6x6x6), 10.8 mm (5x5x5), 13.5 mm (4x4x4), and 18.0 mm (3x3x3). Please note that the 4x4x4 R1.0 cell structure simulation was incomplete due to unforeseen circumstances and so, is not included in this report. The same PMMA material properties and stress strain data used for the unit cells were used for the cell structures. Then, a mesh with a coarse 3 mm element size (Figure 9) was applied to the cell structures for the simulation. Lastly, to simulate a compression test the bottom surface of the unit cell was treated as a fixed support (blue) and the top of the cell was assigned 50% displacement (yellow) relative to each unit cell's height as seen in Figure 10.



Figure 9: 3mm mesh for Ansys simulation (3x3x3 R1.5)

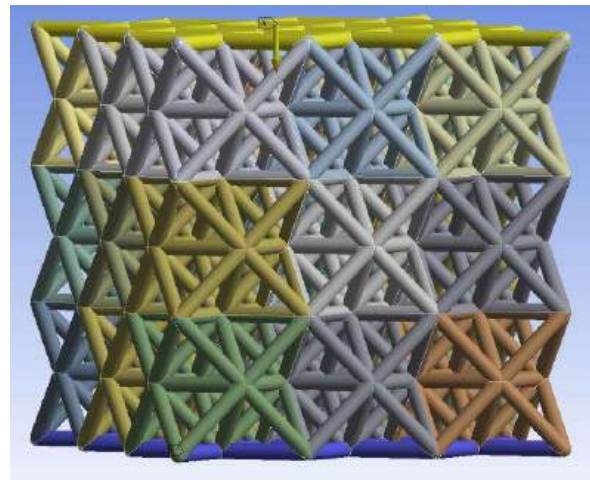


Figure 10: Fixed support (purple) and displacement (yellow) in Ansys (3x3x3 R1.5)

During the analysis, the group examined the stress, elastic strain, total deformation and the force at the fixed support for the 3 mm mesh, in which the tabular results can be seen in Appendix 7.6. The simulation of the stress, deformation, strain and force analysis for the 3x3x3 with R1.5 mm and a 3 mm mesh can be seen below in Figure 11, Figure 12, Figure 13, and Figure 14 respectively. Additionally, the simulations conducted on the remaining cell structures can be seen in Section 7.4.

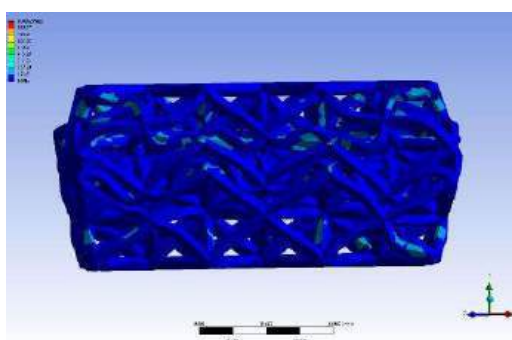


Figure 11: Stress for 3x3x3 R1.5 mm (3 mm mesh)

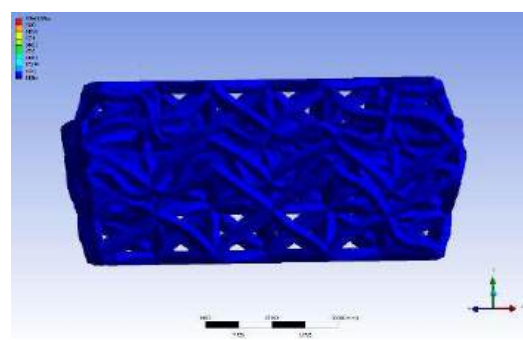


Figure 12: Deformation for 3x3x3 R1.5 mm (3 mm mesh)

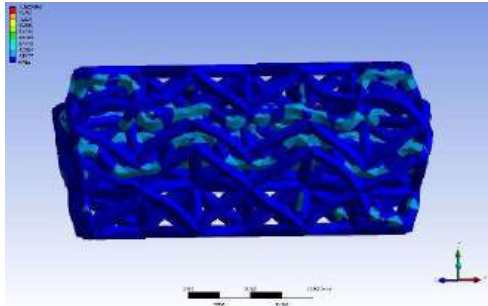


Figure 13: Elastic strain for 3x3x3 R1.5 mm (3 mm mesh)

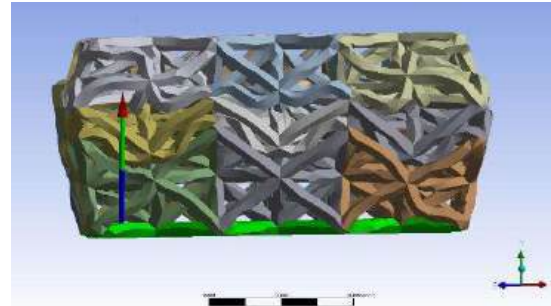


Figure 14: Force reaction for 3x3x3 R1.5 mm (3 mm mesh)

3.3.3 Theoretical Density and Mass Calculations

Using Equation 1, the theoretical densities of each cell structure and unit cell was calculated. Table 8 in Appendix 7.4 summarizes the theoretical densities each unit cell by percentage. The theoretical densities increase as the length of the link decreases. This inverse relation is due to the final formation of each associated cell structure. Furthermore, using Equation 3, the theoretical masses of each cell structure and unit cells was calculated. Table 9 in Appendix 7.4 summarizes the theoretical mass for each cell structure and unit cell. Material densities used in the calculation are referenced from Bardelcik et al. A cell structure of 6x6x6 will have more unit cells in contrast to a cell structure of 3x3x3, resulting in a significant higher density. Higher density unit cells have exhibited higher strength in simulations due to more distribution of energy along every ligament.

3.3.4 Unit Cell Results

The following section summarizes the resulting simulations of the fine mesh of 1 mm and the coarse mesh of 3 mm for all twelve (12) unit cells. Complete tabulated data for the fine mesh results can be seen in Appendix 7.7.1 and the coarse mesh results can be found in the subsequent section, Appendix 7.7.2. Furthermore, force and energy absorption graphs for the fine mesh and coarse mesh data can be found in Appendix 7.8.1. A comparison of the fine mesh and coarse mesh are discussed in detail to emphasize the quality of data in relation to the mesh sizing. Specific energy absorption (SEA) was calculated using Equation 3, where the mass of each unit cell and cell structure was determined through Ansys software. The SEA values as well as the mass values of each unit cell and structure are compiled in Appendix 7.7 and graphed in Appendix 7.9. Lastly, the stress versus strain graphs can be found in Appendix 7.10.

3.3.4.1 Comparison of the Fine Mesh and Coarse Mesh

Simulated displacements in Ansys yielded force applied to the unit cells. Detailed tables of the Ansys simulation can be found in Appendix 7.6. In Figure 15, the fine and coarse meshes for L9.0 mm were compared for all radii. In this force vs. displacement chart, it can be seen that that the greater the radius, the larger the force needed to be applied to displace the unit cell by 50% of its total height. Which is consistent with the fact that, a thicker radius would require more force to move it. The force applied (y-axis) moves in a “roller-coaster” like fashion, in that the force applied has multiple peaks and valleys when plotted. The initial drop in each curve (ex. after 3 mm for L9 1 mm Mesh R1.5) is caused by the lower ligaments of the unit cell completely collapsing in on itself, as the top face of the unit cell displaces downwards onto them. These lower ligaments start to distort, requiring less force to displace downwards. The force then starts to swing upwards again (ex. after 5.5 mm for L9 1 mm Mesh R1.5) because the ligaments have made it to the bottom of the unit cell. So, now the force increases to reach the 50% displacement, because it now must push on the lower face, which also happens to be the fixed support This can be clearly seen in Figure 8.

The mesh size indicates how accurate the results are. The smaller the mesh, means the more elements on the unit cell (as seen in Figure 2 & Figure 3). The more elements allow the cell to be accurately analyzed to understand what kind of stress, force and other variables are acting on it. In Figure 4, the greater the mesh size, the higher the force required to displace the unit cell. The coarser mesh (3 mm) will take longer to observe a dip in force applied than the finer mesh (1 mm), this could be due to the finer mesh being able to catch more intricate force applications sooner and longer. This is a possible reason of why there is more variation, or swings in the 1 mm mesh, because it is catching more precise force applications, that the coarser mesh misses. Overall, as the link lengths increase, it requires less and less force to displace the unit cell to 50% of its height. All force vs. displacement simulation graphs can be found in Appendix 7.8.1.1.1.

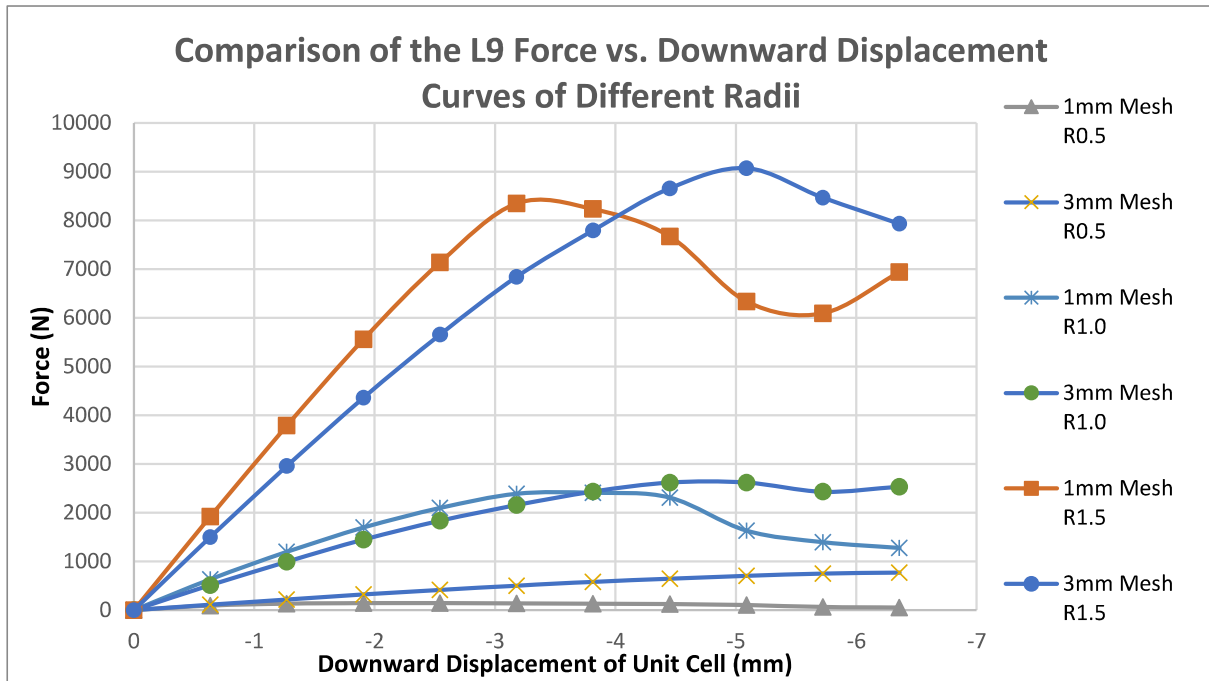


Figure 15: Comparison of Fine vs. Coarse Mesh Results using Force vs. Displacement data of Different Radii for Link length 9 mm Unit Cell.

Calculating the energy vs. displacement involved taking the integral of the force vs. displacement curve. To take the integral, the area under the curve was assessed using numerical integration in the form of the trapezoid rule using Microsoft Excel. As expected, the larger the radius, the more energy absorbed by the unit cell, because the thicker ligaments have more volume to absorb the energy. Increasing the link length will decrease the energy absorbed.

Figure 16 shows the comparison of fine mesh vs. coarse mesh energy calculated vs. displacement curve for a link length of 9.0 mm. The finer mesh sizing shows less energy absorbing numbers than the coarser mesh sizing, albeit the R1.5 mm unit cells have greater energy absorbing values for finer mesh. The consistent pattern shows the fine mesh has greater accuracy as it has lower energy absorbing values. This could be due to the process time being longer, so the number of elements analyzed should show that the energy absorbing values are not as great as coarse mesh lays them out to be.

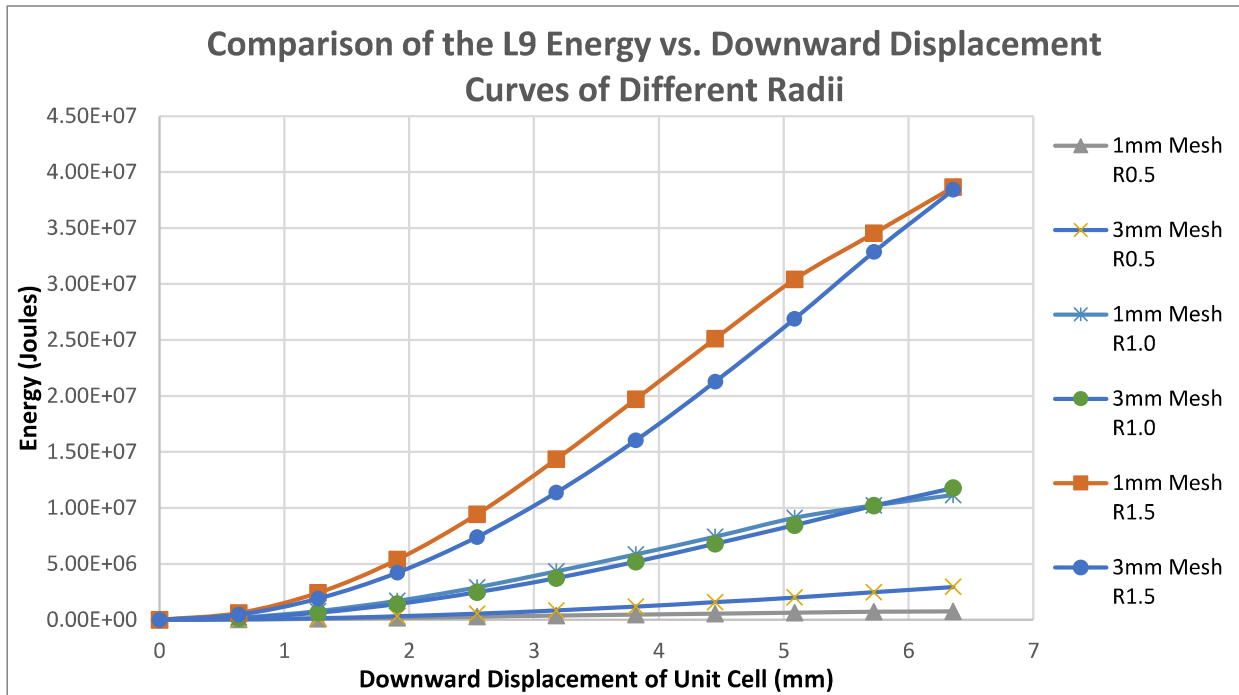


Figure 16: Comparison of Fine vs. Coarse Mesh Results using Energy vs. Displacement data of Different Radii for Link length 9 mm Unit Cell.

Similar to the force vs. displacement, the energy vs. displacement plot demonstrates that the short links of 9.00 mm absorbs more energy when compared to the other link lengths (Appendix 7.8.1.1.2) over a 50% displacement of the total height of each unit cell.

Therefore, for both force vs. displacement and energy vs. displacement plots, comparing the fine and coarse mesh values, there is a trend that appears. With finer mesh results, the program should be analyzing more elements, taking longer to process, producing more accurate results. In force vs. displacement, the finer mesh has more swings over its run time, because the program found more variations over the unit cell in its force detection. It can also be seen that both plots (Figure 15 & Figure 16) have smaller values for its y-axis for finer meshes, meaning the coarser mesh is giving inflated values, and that the actual results are not as high. Further evidence to this can be seen in how inconsistent the results are for all coarse mesh simulations, where a definitive trend cannot be placed. Overall, future simulations should be run with a finer mesh size to provide the most accurate results.

3.3.4.2 SEA Graphs and Discussion

SEA calculations are used for analysis of materials and structure tests. These were used to help with visualizing the energy absorption capacities of each unit cell and cell structure. The energy-displacement of each model was divided by the model's calculated mass in Ansys 2021 R1, which factors in the PMMA material density of 1.18g/cm^3 . The SEA values of the fine mesh unit cells, coarse mesh unit cells, and coarse mesh cell structures were compiled in Appendix 7.7, and graphed in Figure 17, Figure 18, and Figure 23, respectively.

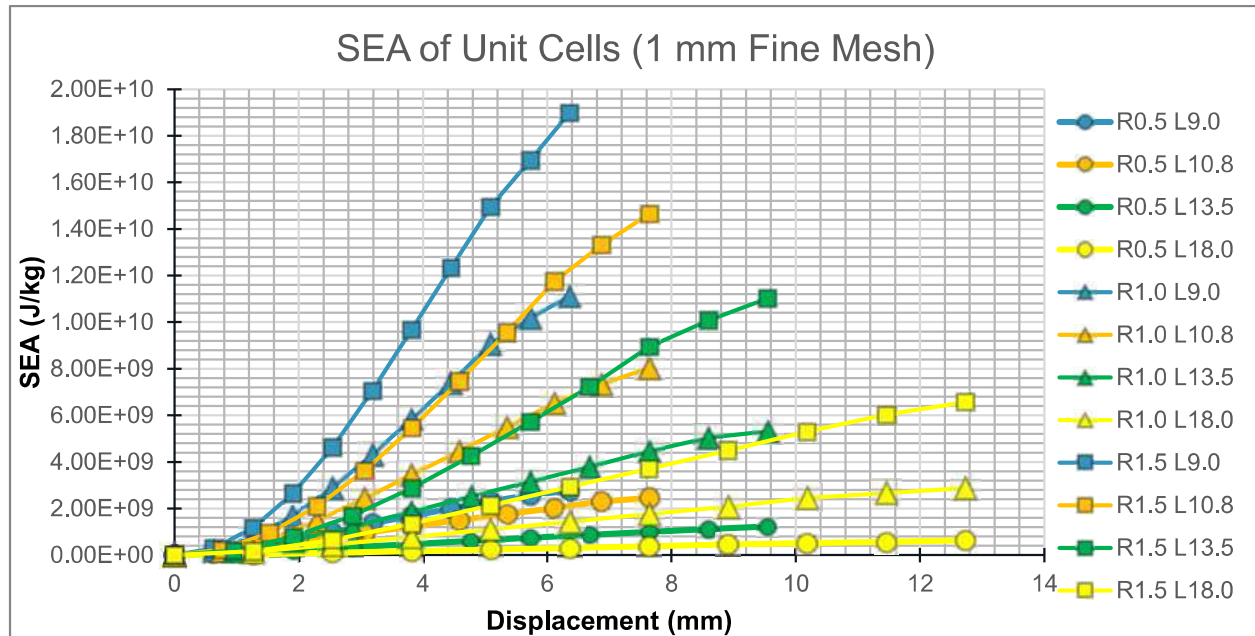


Figure 17: Specific Energy Absorption of Unit Cells with 1 mm Fine Mesh vs. Displacement data for Different Radii and Link lengths.

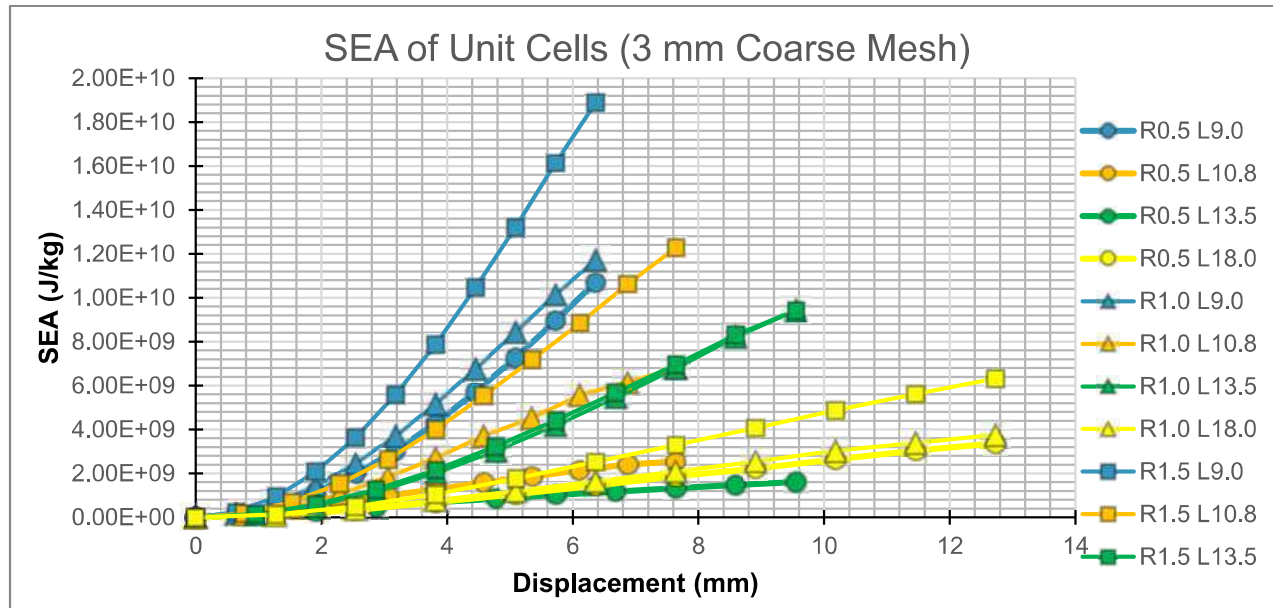


Figure 18: Specific Energy Absorption of Unit Cells with 3 mm Coarse Mesh vs. Displacement data for Different Radii and Link lengths.

Varied radii with constant truss length can be visually signified by how close the colored data are with the same color. These color groups are signified blue for $L=9\text{mm}$, orange for $L = 10.8\text{mm}$, green for $L=13.5\text{mm}$ and yellow for $L=18\text{mm}$, while the shapes of circle, triangle, and square represent $R=0.5\text{mm}$, $R=1.0\text{mm}$, and $R=1.5\text{mm}$, respectfully. Between the fine mesh and coarse mesh unit cells, the trends are generally the same since they each use the same models but

are meshed differently. However, fine mesh color groups overlap with each other, while the coarse mesh color groups are more separated especially between the L=9 and L=18 color groups. This shows that the truss length is less defined during meshing as the mesh elements become larger. This shows that a mesh of 3 mm is acceptable for superficial trends, but a finer mesh of 1 mm should be utilized for greater accuracy of energy absorption data from FEA simulation. Limitations in computer power and software licenses prevented the group from completing fine mesh of cell structures and is a recommendation for future research of octet truss technology.

In both mesh sizes, the structure parameters that achieve great energy absorption relative to displacement were R = 1.5mm and L = 9.0 mm. Thus, a larger truss radius and a shorter truss length leads to a design with large energy absorption specific relative to compression displacement.

3.3.4.3 Stress Strain Analysis

To further expand on the analysis of the results, a stress versus strain comparison was done for the unit cells and all the graphs can be found in Appendix 7.10: Stress Versus Strain Graphs. To begin the evaluation, the surface area for each cell was extracted from SolidWorks to begin the evaluation, the surface area for each unit cell was extracted from SolidWorks and calculated for the surface where displacement was applied (represented by the yellow ligaments in Figure 10). Next, the vertical force reactions from the Ansys simulations were used to calculate the stress (Equation 4: Formula for stress). Lastly, the strain was calculated using the displacement and total height of each cell (Equation 5: Formula for strain).

Equation 4: Formula for stress

$$\sigma = \frac{F}{A}$$

Equation 5: Formula for strain

$$\epsilon = \frac{\Delta L}{L}$$

Once the stress and strain calculations were completed for all the unit cells, the results were compared to each other. For the unit cells, the group studied the effects of varying ligament diameter with a constant link length for both a coarse and fine mesh (Appendix 7.10.2). The comparison between the three L9.0mm unit cells with a fine mesh can be seen in Figure 19.

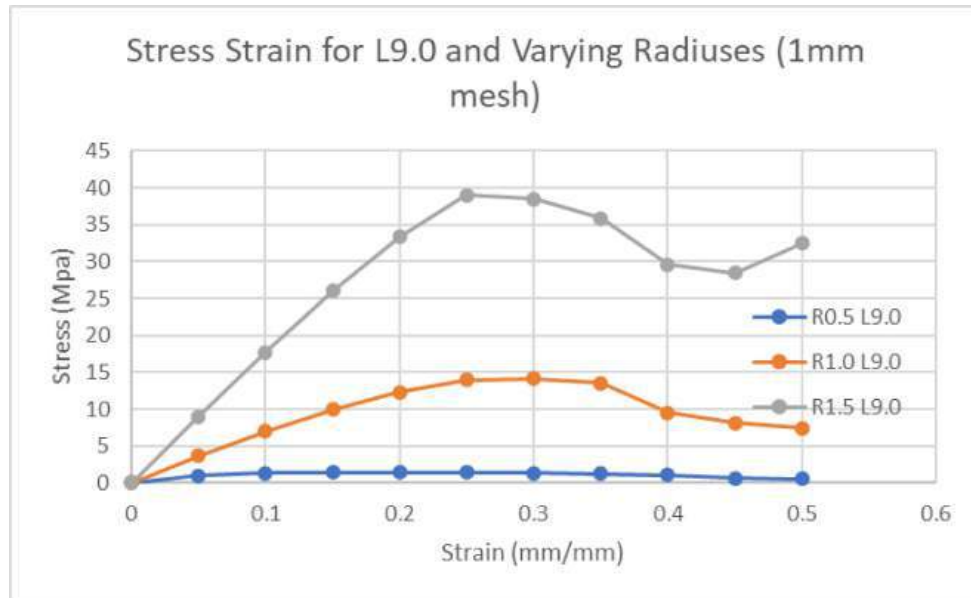


Figure 19: Stress Strain Curves of L9.0 mm Unit Cell with 1 mm Fine Mesh vs. Displacement data for Different Radii.

The group also considered the effects of varying ligament lengths with a constant link diameter for both the fine and coarse mesh (Appendix 7.10.3). The comparison between the four types of unit cells with a 1mm mesh can be seen below in Figure 20.

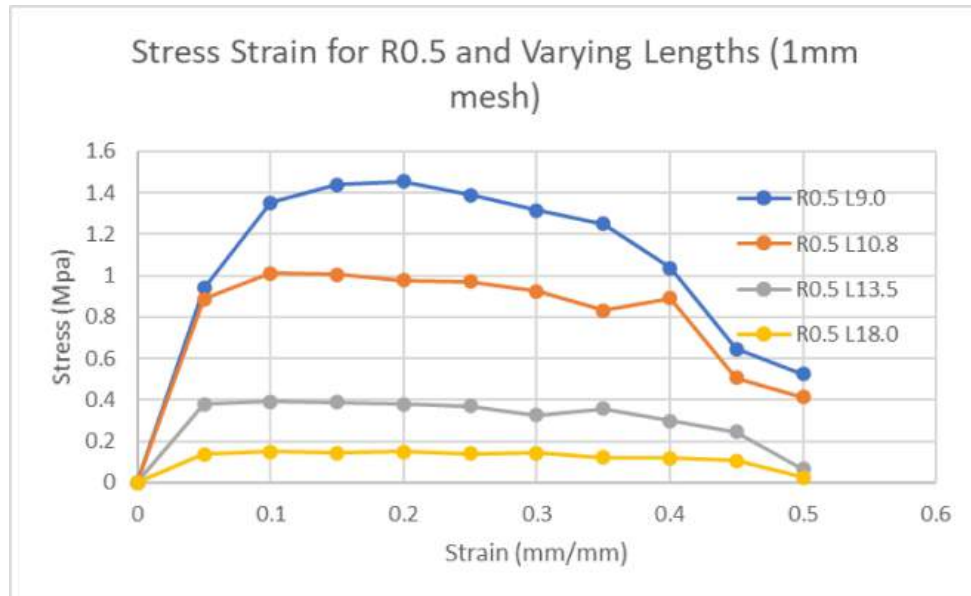


Figure 20: Stress Strain Curves of R0.5 mm Unit Cells with 1 mm Fine Mesh vs. Displacement data for Different Link Lengths.

3.3.5 Cell Structure Absorption Results

The following section summarizes the resulting simulations of the cell structures conducted by Dr. Bardelcik. However, the 4x4x4 R1.0 data is not included as simulation time for the structure was unforeseeably longer than expected. Complete tabulated data for a mesh size of 3 mm is shown in Appendix 7.7.3. All force, energy, and specific energy absorption graphs can be found in Appendix 7.8.2 and Appendix 7.9. The stress strain data and graphs can be found in Appendix 7.10.

3.3.5.1 Force and Energy vs. Displacement

Simulated displacements in Ansys yielded force applied to the cell structure. Detailed table of the Ansys simulation can be found in Appendix 7.7.3. Figure 21 depicts the 3x3x3 cell structure data extracted from the detailed table to create a force vs. displacement curve. The curve demonstrates that larger link radius will result in higher reaction forces. In contrast, the smaller link radius will produce lower reaction forces. The relationship between the radius and reaction forces are consistent in the simulation results for all cell structures considered. Appendix 7.8.2.1.1 shows each structure organized by constant cell structure whereas Appendix 7.8.2.2.1 shows each cell structure organized by radius.

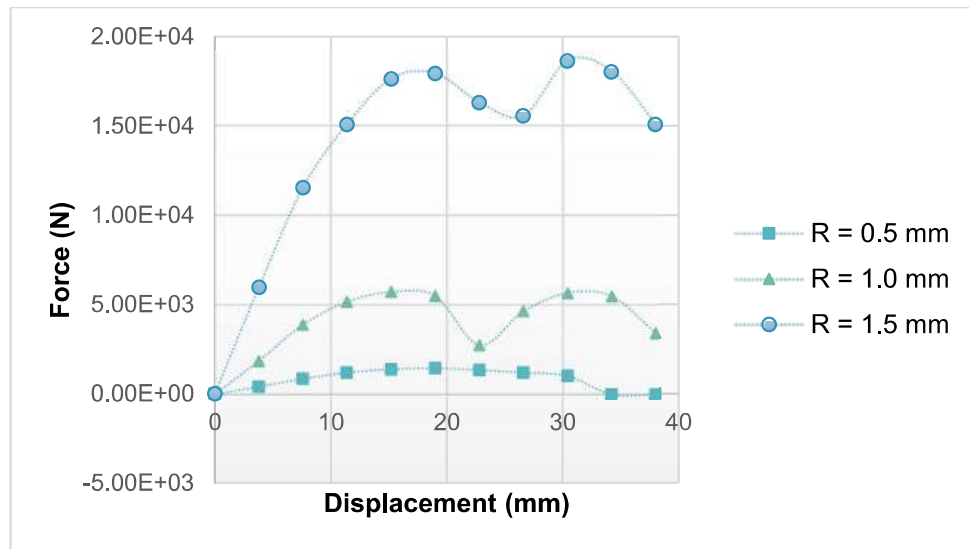


Figure 21: 3x3x3 Force vs. Displacement Curve

The corresponding energy graph is shown in Figure 22, where the same observation regarding link radius can be made. Appendix 7.8.2.1.2 shows each structure organized by constant cell structure whereas Appendix 7.8.2.2.2 shows each cell structure organized by radius.

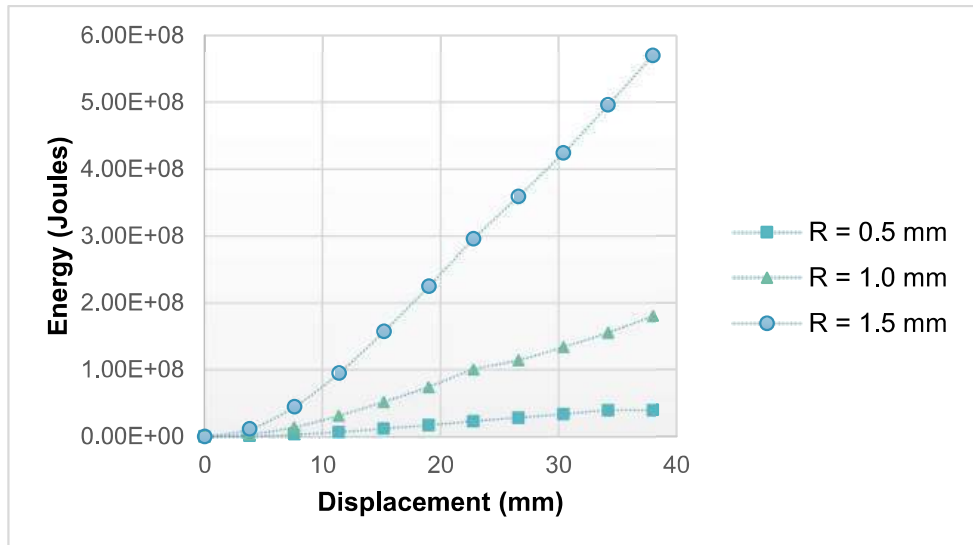


Figure 22: 3x3x3 Energy vs. Displacement Curve

3.3.5.2 SEA Graphs and discussion

The SEA values between each cell structure are graphed below in Figure 23. These structures use a coarse mesh of 3 mm as stated previously.

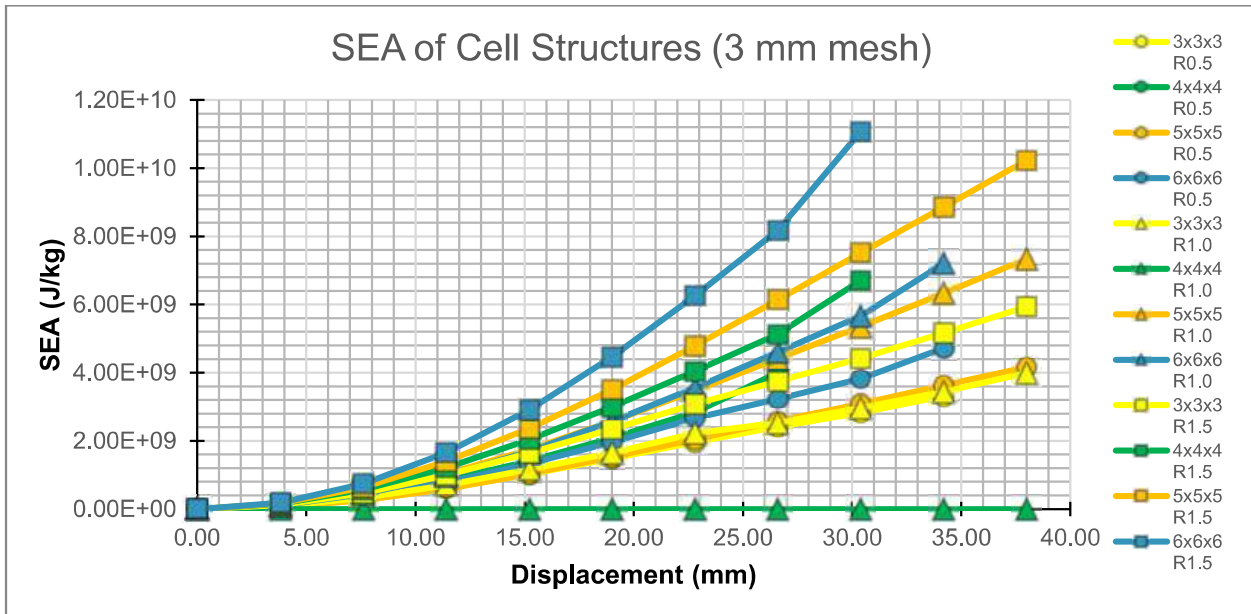


Figure 23: Specific Energy Absorption of Cell Structures with 3 mm Coarse Mesh vs. Displacement data for Different Radii and Link lengths.

This graph follows the same color grouping in the SEA graphs in section for unit cells. Detailed energy and SEA values are found in Appendix 7.7.3. Please note that there is no data for 4x4x4 R1.0 due to unforeseen circumstances. The energy absorption of the structure reaches up to 1.1×10^{10} J/kg, which is achieved at the largest truss radius and shortest truss length, R=1.5

and L=9.0. This coincides with findings on the unit cell SEA values. One thing to note is that the unit cell equivalent of these parameters has a larger SEA value of 1.9e10 J/kg. Unit cells are very durable and strong by themselves, and still retain much of their energy absorption capabilities when grouped in a lattice structure.

3.3.5.3 Stress Strain Comparison

In addition to the stress strain comparison done for the unit cells in Section 3.3.4.3, the same analysis was done for all the cell structures, minus the 4x4x4 R1.0 mm structure (Appendix 7.10: Stress Versus Strain Graphs). The surface area was again extracted from SolidWorks for the various cell structures and then computed for where the displacement was applied (represented by the yellow ligaments in Figure 10). Next, the vertical force reactions were used to calculate the stress (Equation 4) and the strain was calculated using the displacement and total height of each cell structure (Equation 5: Formula for strain).

Similarly, the group then analyzed the effects of varying ligament diameter with a constant link length (Appendix 7.10.2) and varying ligament length with a constant link diameter (Appendix 7.10.3). And the group evaluated the stress strain comparison between the unit cells and their fully assembled cell structures (Appendix 7.10.1). Figure 24 shows the plotted stress versus strain for the R0.5 L9.0-unit cell—with a coarse and fine mesh—and its assembled 6x6x6 cell structure.

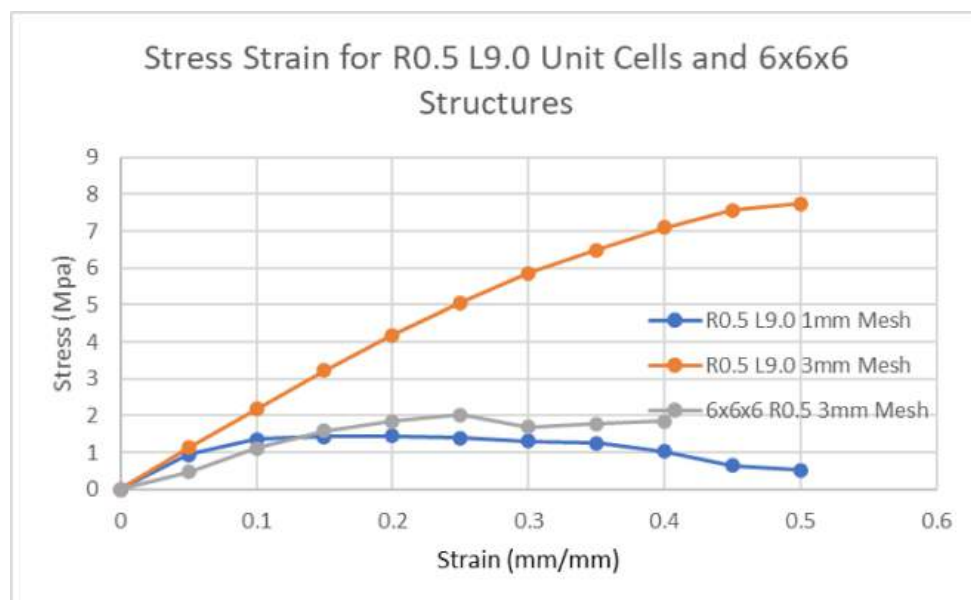


Figure 24: Stress Strain Curves of L9.0 mm R0.5 mm Unit Cells and its 6x6x6 Cell Structure vs. Displacement data for Fine and Coarse Mesh.

3.3.6 Impact Test

The obvious next steps in this design would be looking at how this octet truss structure can be applied to an impact simulation. Since the scope of this experiment did not specify a working prototype for the end of this iteration of the project, this group can still get very close

with a simulation done through Ansys. This group chose to simulate an arm (cylinder) hitting one of these cell structures to represent a hit made in football, but there should be a disclaimer added that this is a very early draft on what a “real” impact simulation will look like, and accurate data cannot be pulled from this test.

Firstly, it was decided the best cell structure model to use for this impact test was the 3x3x3 model, since its energy absorbing capabilities were the best of all the four different cell structure models, as seen in Appendix 7.8.2.1.2. Even though the R1.5 mm had the best energy absorbing values, the R0.5 mm was used in this case due to issues at the time of trying to simulate a 3 mm coarse mesh on the R1.5 mm. Another disclaimer should be added that the 4x4x4 cell structure models were not able to simulate in time for this report, so any data referring to those models was considered null. Now that the adequate cell structure is chosen, the next action is to create a 2x2 “sheet” of this cell structure, to let the arm have a large enough surface area to impact and provide accurate results. This sheet of cell structures will represent the inner lining of the helmet. A real-world helmet would have to fit multiple sheets of this cell structure, and do it in a curvilinear shape, but this method would go outside of the scope of this project, so a flat sheet would suffice. This sheet was made using the assembly portion of SolidWorks software, to mate 4 of these cell structures together.

Next, the arm, which has dimensions of 10 cm in diameter and 30 cm in length (or the average forearm size), was added a velocity on Ansys that would impact vertically in the Y-direction to the top of the 2x2 cell structure sheet. The velocity applied to the cylinder (arm) was that of an average NFL Safety, which on average, is the fastest position among all defensive players. The speed was taken from the famous 40-yard (~36m) dash of the 2019 NFL draft combine, where the average Safety ran 40-yards in 4.4 seconds (White), so, with some simple mathematical calculation, the speed applied to the cylinder was around 8312 mm/s.

The results of the simulation can be found in Appendix 7.11.2, showcasing the cylinder (arm) having a very observable impact on the cell structures. Not only does the energy of the hit go almost all the way to the bottom of the structure, showing the ability of it to transfer the energy of the impact into lower levels of the structure (Figure 25). But the actual simulation shows that when the cell structures are compressed to the maximum this cylinder will go, the “arm” appears to bounce back. Therefore, the cell structure in this test shows some elasticity properties, showing that it is very much capable of absorbing the energy of a hit from another player, and then deflect some of it back to assume the original shape of the structure. The numbers pulled from this simulation can only be analyzed by comparing it to the other cell structures that were made. Unfortunately, this was not possible due to time constraints and computing power. This simulation alone, due to the number of elements almost at the maximum allowable for the Ansys student version, took almost 12 hours to simulate.

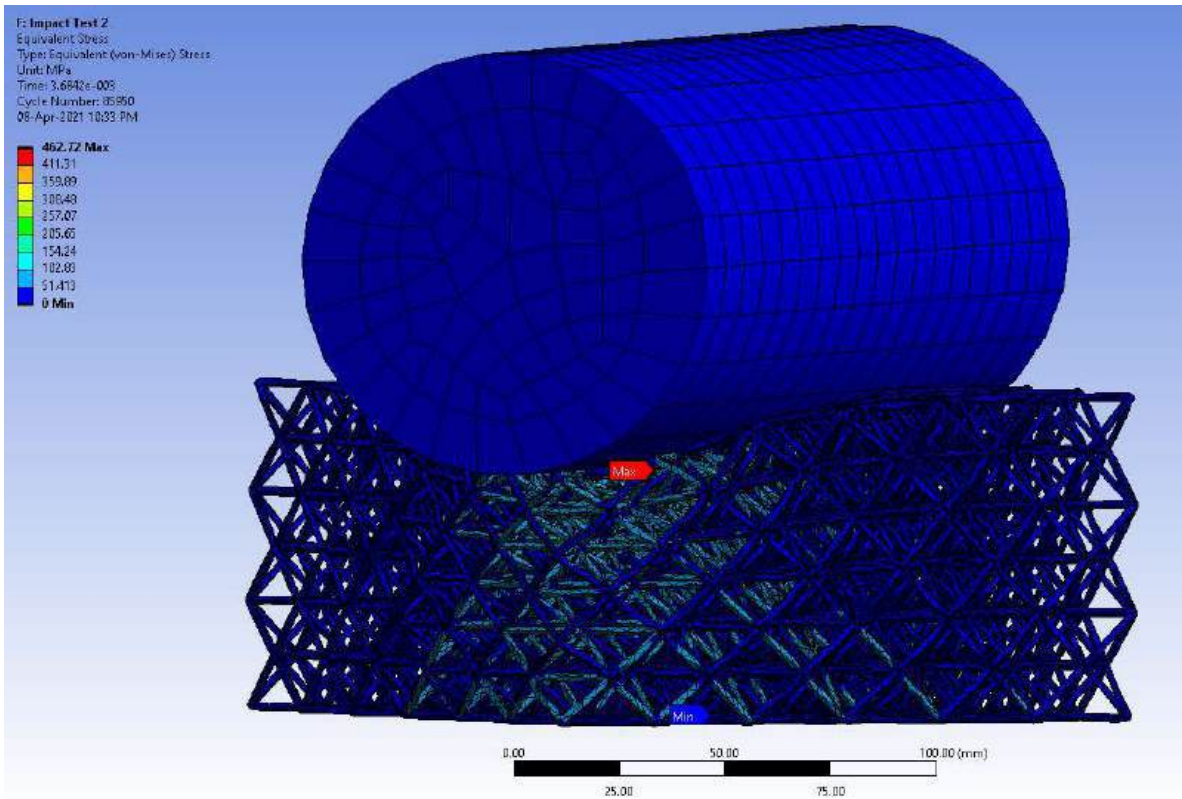


Figure 25: Equivalent Stress of Impact Test on Cylinder (arm) on multiple 3x3x3 Cell Structures (2x2 Sheet) with 3mm Mesh. Mesh Size varies on Cylinder.

3.4 Design Evaluation

Evaluation of the most optimal cell structure, not including the 4x4x4 R1.0 cell structure, and unit cell was determined using the SEA for fine mesh (1 mm) unit cells, coarse mesh (3 mm) unit cells, and cell structures simulated with a 3 mm mesh. Theoretical densities of the structures were also used as a factor in determination. To consider costs of implementation and material, volumetric analysis of each structure was conducted and considered as a factor towards optimal structure determination. Additionally, the ease of implementation was also deemed as an important factor for the ideal structure. Ease of implementation refers to the simplicity of application where applying each unit cell would result in an inherent difficulty, where the smaller the dimensions of the structure would result in easier implementation.

The maximum and minimum SEA values of each structure was used as a standard of ranking. The upper and lower ranges were determined by equally dividing the maximum and minimum SEA values in 10. Table 2 summarizes the ranking metrics developed for the fine mesh unit cell analysis. The ranking metrics was used to create a ranking of each SEA value seen in Table 3. A similar approach was used to develop the ranking for theoretical densities summarized in Table 4. Volumetric analyses of the unit cell and cell structure as well as simplicity of application ranking metrics can be found in Appendix 7.12.

Table 2: Fine Mesh Ranking Metrics

Rank	Lower Range	Upper Range
10	1.72E+10	1.90E+10
9	1.53E+10	1.72E+10
8	1.35E+10	1.53E+10
7	1.17E+10	1.35E+10
6	9.82E+09	1.17E+10
5	7.98E+09	9.82E+09
4	6.14E+09	7.98E+09
3	4.31E+09	6.14E+09
2	2.47E+09	4.31E+09
1	6.39E+08	2.47E+09

Table 3: Fine Mesh SEA Ranking

ID	SEA	Ranking
R0.5 L9	2.75E+09	2
R0.5 L10.80	2.46E+09	1
R0.5 L13.50	1.23E+09	1
R0.5 L18.00	6.39E+08	1
R1.0 L9	1.11E+10	6
R1.0 L10.80	8.04E+09	5
R1.0 L13.50	5.32E+09	3
R1.0 L18.00	2.88E+09	2
R1.5 L9	1.90E+10	10
R1.5 L10.80	1.46E+10	8
R1.5 L13.50	1.10E+10	6
R1.5 L18.00	6.57E+09	4

Table 4: Theoretical Densities Ranking

ID	Theoretical Densities	Ranking
R0.5 L9	0.08228	10
R0.5 L10.8	0.05714	10
R0.5 L13.5	0.03657	10
R0.5 L18	0.02057	10
R1 L9	0.32910	6
R1 L10.8	0.22854	8
R1 L13.5	0.14627	9
R1 L18	0.08228	10
R1.5 L9	0.74048	1
R1.5 L10.8	0.51422	4
R1.5 L13.5	0.32910	6
R1.5 L18	0.18512	8

A 4-factor weighted decision matrix was used to determine the optimal structure based on desired weighting of the SEA, theoretical densities, volume considerations, and simplicity of application. The total for each structure is calculated by performing a summation of weight factors multiplied by each ranking. A decision matrix can provide unbiased solutions using numerical values. Table 5, Table 6, and Table 7 summarizes a decision matrix for a fine mesh unit cell, a coarse mesh unit cell, and a cell structure, respectively.

The fine mesh decision matrix shown in Table 5 was developed to complement the SEA. Higher energy absorption will correspond with a high density and high 3D printed volume. Theoretical density, volume, and simplicity sum to the remaining weight factors. Therefore, a weighting of 50%, 20%, 20%, and 10% for the SEA, theoretical density, volume, and simplicity, respectively, would best suit the desired system. A highlight cell indicates the most optimal structure based on the weighting factor. Table 5 shows the optimal unit cell would be corresponding to a radius of 1.5 mm and a link length of 9 mm.

Table 5: Fine Mesh Decision Matrices

Fine Mesh Decision Matrix													
Factors	Weight (%)	ID											
		R0.5 L9	R0.5 L10.80	R0.5 L13.50	R0.5 L18.00	R1.0 L9	R1.0 L10.80	R1.0 L13.50	R1.0 L18.00	R1.5 L9	R1.5 L10.80	R1.5 L13.50	R1.5 L18.00
Total SEA	50	2	1	1	1	6	5	3	2	10	8	6	4
Theoretical Density	20	10	10	10	10	6	8	9	10	1	4	6	8
Volume	20	10	10	10	10	9	8	8	6	7	5	4	1
Simplicity	10	10	10	9	8	8	6	4	6	5	3	1	
Totals	100.00%	6	5.5	5.4	5.3	6.8	6.5	5.5	4.6	7.2	6.3	5.3	3.9

The coarse mesh decision matrix shown in Table 6 was developed for equally weighting of every parameter. Therefore, a weighting of 25%, 25%, 25%, and 25% for the SEA, theoretical density, volume, and simplicity, respectively, was assigned. The highlighted cell in Table 6 indicates that the unit cell with a radius of 0.5 mm and a link length of 9 mm is the most optimal choice based on the weighting assigned.

Table 6: Coarse Mesh Decision Matrix

		Coarse Mesh Decision Matrix											
Factors	Weight (%)	ID											
		R0.5 L9	R0.5 L10.80	R0.5 L13.50	R0.5 L18.00	R1.019	R1.0 L10.80	R1.0 L13.50	R1.0 L18.00	R1.5 L19	R1.5 L10.80	R1.5 L13.50	R1.5 L18.00
Total SEA	25	6	1	1	2	6	4	5	2	10	7	5	3
Theoretical Density	25	10	10	10	10	6	8	9	10	1	4	6	8
Volume	25	10	10	10	10	9	8	8	6	7	5	4	1
Simplicity	25	10	10	9	8	8	8	6	4	6	5	3	1
Totals	100.00%	9	7.75	7.5	7.25	7	7	5.5	6	5.25	4.5	3.25	

The cell structure decision matrix shown in Table 7 was developed to ensure simplicity of application was emphasized. Therefore, a weighting of 20%, 15%, 15%, and 50% for the SEA, theoretical density, volume, and simplicity, respectively, was given to each of the factors. The highlighted cell in Table 7 shows that the 5x5x5 with a radius of 1.5 mm and the 5x5x5 1.0 mm cell structure would be the most optimal for ease of implementation. Since both structures would result in the optimal cell structure, a manual decision can be made to select the final cell structure to be used.

Table 7: Cell Structure Decision Matrix

		Cell Structure Decision Matrix											
Factors	Weight (%)	ID											
		R0.5 6x6x6	R0.5 5x5x5	R0.5 4x4x4	R0.5 3x3x3	R1.0 6x6x6	R1.0 5x5x5	R1.0 4x4x4	R1.0 3x3x3	R1.5 6x6x6	R1.5 5x5x5	R1.5 4x4x4	R1.5 3x3x3
Total SEA	20	2	2	1	1	6	6	INVALID DATA	1	10	9	5	4
Theoretical Density	15	10	10	10	10	6	8	9	10	1	4	6	8
Volume	15	9	10	10	10	6	7	8	9	1	3	5	7
Simplicity	50	10	10	9	8	8	8	6	4	6	5	3	1
Totals	100.00%	1.9	1.9	1.7	1.7	2.1	2.4	#VALUE!	1.7	2.15	2.4	1.9	2

4.0 Project Management

In this section, the specific goals/details of the design plan are thoroughly discussed and explained. The project was divided into various stages with sufficient time assigned for each task to ensure that the group stayed on track to successfully complete this project. Additionally, group's successes and failures are expanded upon.

4.1 Details of Design Plan

After the interim report, the group simulated the remaining unit cells with a fine 1mm mesh and a coarse 3 mm mesh and assembled them into 76.3674 mm (~3 inch) cubes. The goal was to apply a vertical compression force to the cube and evaluate how changing the unit relative densities—by varying a link's length and thickness—impacted the material properties and energy absorption. Initially, 3D printing the various structures and performing live compression tests were within the scope but, due to the COVID-19 pandemic all the work was done virtually.

The group also worked with Dr. Bardelcik to obtain the simulation data and analyze the results due to the volume of simulations and lack of the group's processing power. Next, an impact test was done on Ansys to simulate real world interactions with the mesh as a lining material in protective equipment. Finally, while the results were being compiled and a conclusion was being made, the group began working on the poster, final report, and final memo.

4.2 Plan of Attack



Figure 26: Gantt chart displaying the steps taken to reach the final stages of the project.

Figure 26 shows the entire timeline of the project, depicting the steps the group took to successfully complete this project. Additionally, the above Gantt chart is an updated and completed version of the one provided in the Interim report to show newly added tasks. Lastly, with the provincial stay-at-home orders and the global pandemic, the project was expected to be completed entirely online so, the group is limited to using virtual resources—SolidWorks, Ansys, Microsoft Teams, etc.

4.3 Division of Work

The group aimed to divide work equally and effectively so, as the project progressed the division of labor remained fluid. While everyone was actively involved with discussions and the general direction of the project, each group member had their individual roles to fill. Initially, Elvin's main role was to create SolidWorks models for each unit cell and build cell structures while Benjamin and Arshpreet worked on Ansys simulations and Laith worked on

research/background. Overtime, Laith became an aid to both the SolidWorks modelling and Ansys simulations as the workload increased. Elvin moved onto completing calculations and graphing for the comparison of the simulations once all the SolidWorks models were completed. Arshpreet focused on the completion of the impact test and Benjamin helped the other group members where necessary. Lastly, the entire group contributed to the analysis and compilation of data along with the completion of the course deliverables.

4.4 Project Status and Challenges

Regarding project status, the group successfully completed the project on time and to the advisor's standards. However, throughout the project there were many challenges that had to be overcome to eventually lead to the group's success. The largest issues stemmed from the Ansys simulations and solving these issues consumed most of the group's time. Additionally, using the free, student version of Ansys limited the group to the number of elements that could be meshed which caused further challenges when meshing models. Solving these Ansys issues involved coordinating internally to reiterate the SolidWorks designs to create error free simulations. But, due to the limited processing power that the group had access to, Dr. Bardelcik needed to run the Ansys simulations for the large, cell structures.

To remain on schedule throughout the semester, additional manpower was required in various components of the project so, the group member's time was split between many tasks. Reshuffling and reprioritizing time allowed the group to complete tasks and meet deadlines. Additionally, the guidance from Dr. Bardelcik helped clear doubts and questions, which further contributed to the successful completion of the project.

5.0 Conclusions and Recommendations

The final stages of the design were successfully completed. Deadlines established in Section 4.0 were accomplished on time. The scope of the final design changed from the interim phase to include analyses of a fine mesh (1 mm) and a coarse mesh (3 mm), stress-strain data, specific energy absorption and impact tests. However, data for the 4x4x4 R1.0 cell structure was not included in the analysis due to an unforeseen increase in simulation time. In the conclusion of the project, a decision matrix was developed to numerically evaluate each structure based upon a user defined weighting of the SEA, theoretical density, volume, and simplicity of application.

To further analyze the results of the project, a stress strain comparison was done for the unit cells and cell structures (Appendix 7.10). The evaluation began with calculating the surface area for links exposed to displacement and extracting necessary properties from SolidWorks and Ansys. Then stress and strain were calculated, graphed, and examined. The group studied factors such as the differences between unit cells and assembled cell structures, varying ligament radius with a constant length and varying ligament length with a constant radius (Appendix 7.10.1, 7.10.2 and 7.10.3, respectively).

The energy calculations were employed in finding the SEA values of each unit cell and cell structure. Graphed SEA data of the octet truss structure shows that its energy absorption increases steadily as the structure is compressed (Appendix 7.9). Comparisons in each structure is made more apparent through the SEA graphs, which aid in finding the suitable dimensions for the octet truss model. Across the unit cell and cell structure SEA graphs, a wide truss radius and short truss length shows the greatest amount of absorption compared to compression displacement. SEA calculations remain an important tool for analyzing this structure's capabilities in this project and future research.

The impact test produced some very desirable results, starting with the fact that the impact of the cylinder allows the cell structure to absorb the energy and dissipate it to the lower ligaments of the structure (Appendix 7.11.2), in order to avoid further impact to the head of the individual below. The cell structure seems to have an elasticity aspect to it as well, demonstrating that it is very much capable of absorbing the energy of a hit from another player, and then deflecting some of it back to assume the original shape of the cell structure. Although there is not much comparison that can be done with the other cell structures created or to current technology, due to a constraint of time and computing power. The next group to take on this topic should test it against the other cell structures produced by this group and eventually to EPP and EPS foams that are already in use. They should also look at changing the different parameters of this simulation as well, for instance changing the arm's size and velocity, increasing the number of cell structures used at once, and many other parameters that this group was unable to achieve due to constraints on time and scope.

Ranking metrics were developed using the maximum and minimum values of each parameter analyzed to establish a comparison of which each structure can be evaluated. Together, the SEA, theoretical density, volume, and simplicity of application formed a 4-factor decision matrix. The weighting component can be adjusted to suit the values of the user. If theoretical densities are valued higher, then the weighting will have to be adjusted accordingly (i.e., 80). Decision matrices were developed for the fine mesh (1 mm) unit cell, the coarse mesh (3 mm) unit cell, and the cell structures simulated with a 3 mm mesh.

Continuation of the project was discussed with Dr. Bardelcik for a master's project. Recommendations for further simulations and implementation would include evaluation of different material properties and a convergence study of optimal mesh sizes. Additionally, real-world testing for the compression and impact tests would provide more concrete and consistent results when compared to the Ansys simulations done for this project. This comparison would validate both the models used throughout the project and the results compiled from Ansys.

6.0 References

- Askeland, Donald R, Pradeep P Fulay and Wendelin J Wright. *The Science and Engineering of Materials*. Stamford: Cengage Learning, 2010. Textbook.
- Bailly, Nicolas, et al. "Strain Rate Dependent Behavior of Vinyl Nitrile Helmet Foam in Compression and Combined Compression and Shear." *Applied sciences* (2020): 8286. Journal.
- Bardelcik, Alexander, et al. "The Effect of Wash Treatment on the Mechanical Properties and Energy Absorption Potential of a 3D Printed Polymethyl Methacrylate (PMMA)." (2020). Full Length Article.
- Canada, Environment. "Federal Environmental Quality Guidelines - Hexabromocyclododecane (HBCD)." May 2016. Website. 11 February 2021.
- Cefic. *Poly Methyl Methacrylate (PMMA)*. January 2015. <https://www.petrochemistry.eu/wp-content/uploads/2018/01/PMMA-Eco-profile-EPD-1-15-1.pdf>.
- Fee Guideline for Professional Engineering Services*. Guideline. Toronto: Ontario Society of Professional Engineers, 2012.
- Gimbel, Genille M. and Thomas B. Hoshizaki. "Compressive properties of helmet materials subjected to dynamic." *European Journal of Sport Science* 8.6 (2008): 341-389.
- Huang, Ling, et al. "Pollution and biodegradation of hexabromocyclododecanes: A review." *Frontiers of Environmental Science & Engineering* (2019): 11. Article.
- Hughes-Mussio, Mykael, et al. *CURAX*. 41x Report. Guelph, 2020.
- Landro, Luca D, Giuseppe Sala and Daniela Olivieri. "Deformation mechanisms and energy absorption of polystyrene foams for protective helmets." *Polymer Testing* (2002): 217-228.
- Levy, Michael L, et al. "Birth and Evolution of the Football Helmet." *Neurosurgery* (2004): 656-662.
- Ling, Chen, et al. "Mechanical behaviour of additively-manufactured polymeric octet-truss lattice structures under quasi-static and dynamic compressive loading." *Materials and Design* (2018): 1 - 13. Document.
- Madehow. *How Products are Made - Expanded Polystyrene Foam (EPF)*. n.d. Web site. 10 February 2021.

Morton, Daniel T, et al. "Mechanical response of low density expanded polypropylene foams in compression and tension at different loading rates and temperatures." *Materials Today Communications* (2020).

PMMA. *Sustainability*. 18 February 2019. <https://www.pmma-online.eu/sustainability/>.

Rogers, Tony. *Everything You Need To Know About Polylactic Acid*. 7 October 2015. Website. 10 February 2021.

Staples, Andy. "With Rugby and Robots, College Football's Top Teams Are Battling for the Perfect Tackle." 15 August 2017. *Sports Illustrated*. Article. <https://www.si.com/college/2017/08/15/college-football-tackling-methods-robots-targeting-rule>.

White, R.J. *2019 NFL combine: Top 40-yard dash times at each position as unheralded safety posts fastest run at Indy*. 04 March 2019. Article. April 2021.

Williams, Chase. *NFL investing \$60 million in safety innovation technology*. 24 October 2019. 10 February 2021. <<https://globalsportmatters.com/science/2019/10/24/nfl-investing-60-million-in-safety-innovation-technology/>>.

7.0 Appendices

7.1 Unit Cell Drawings

7.1.1 Unit Cells: Link Length of 9.0 mm

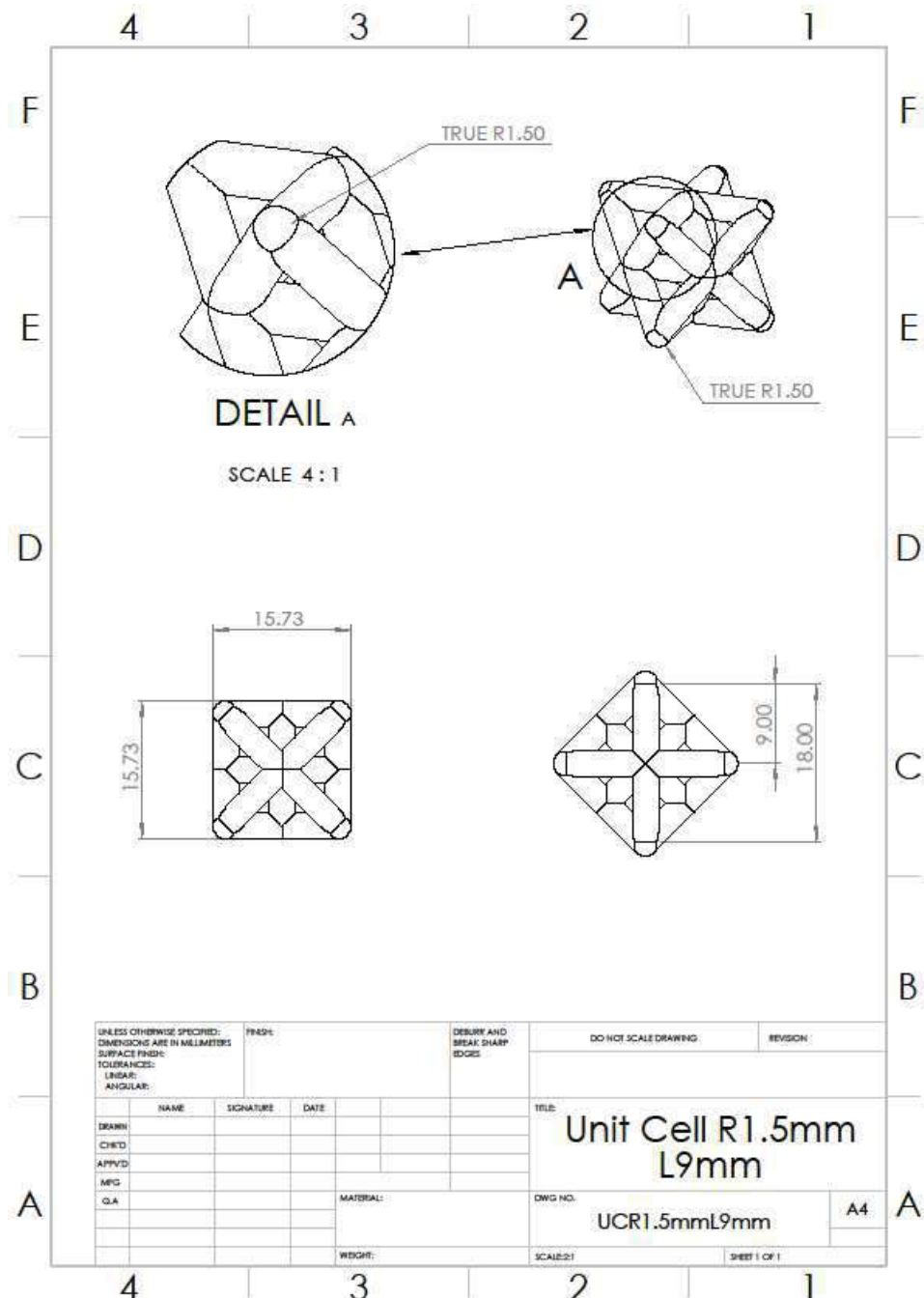


Figure 27: Radius 1.5 mm Length 9 mm Unit Cell SolidWorks Drawing

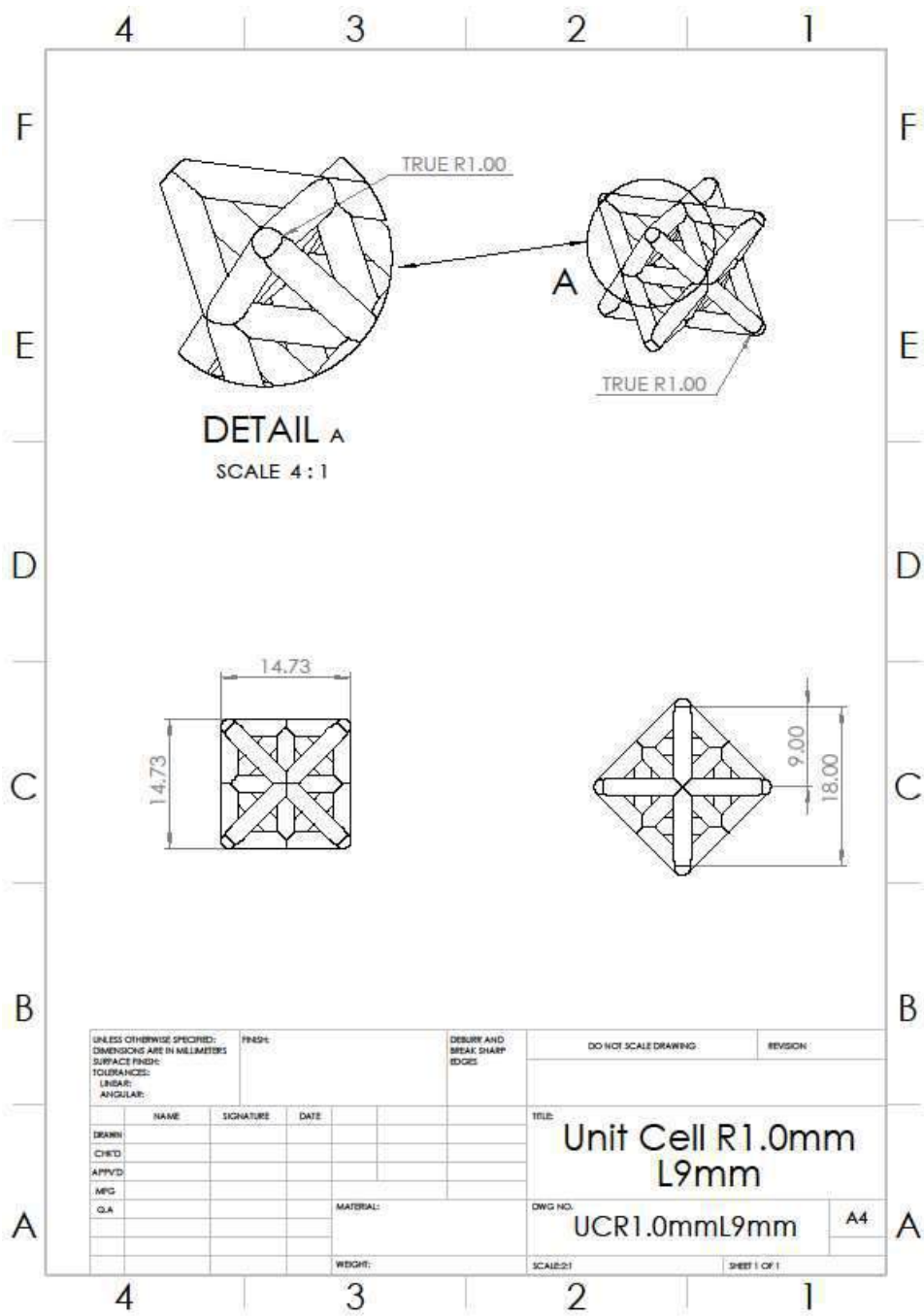


Figure 28: Radius 1.0 mm Length 9 mm Unit Cell SolidWorks Drawing

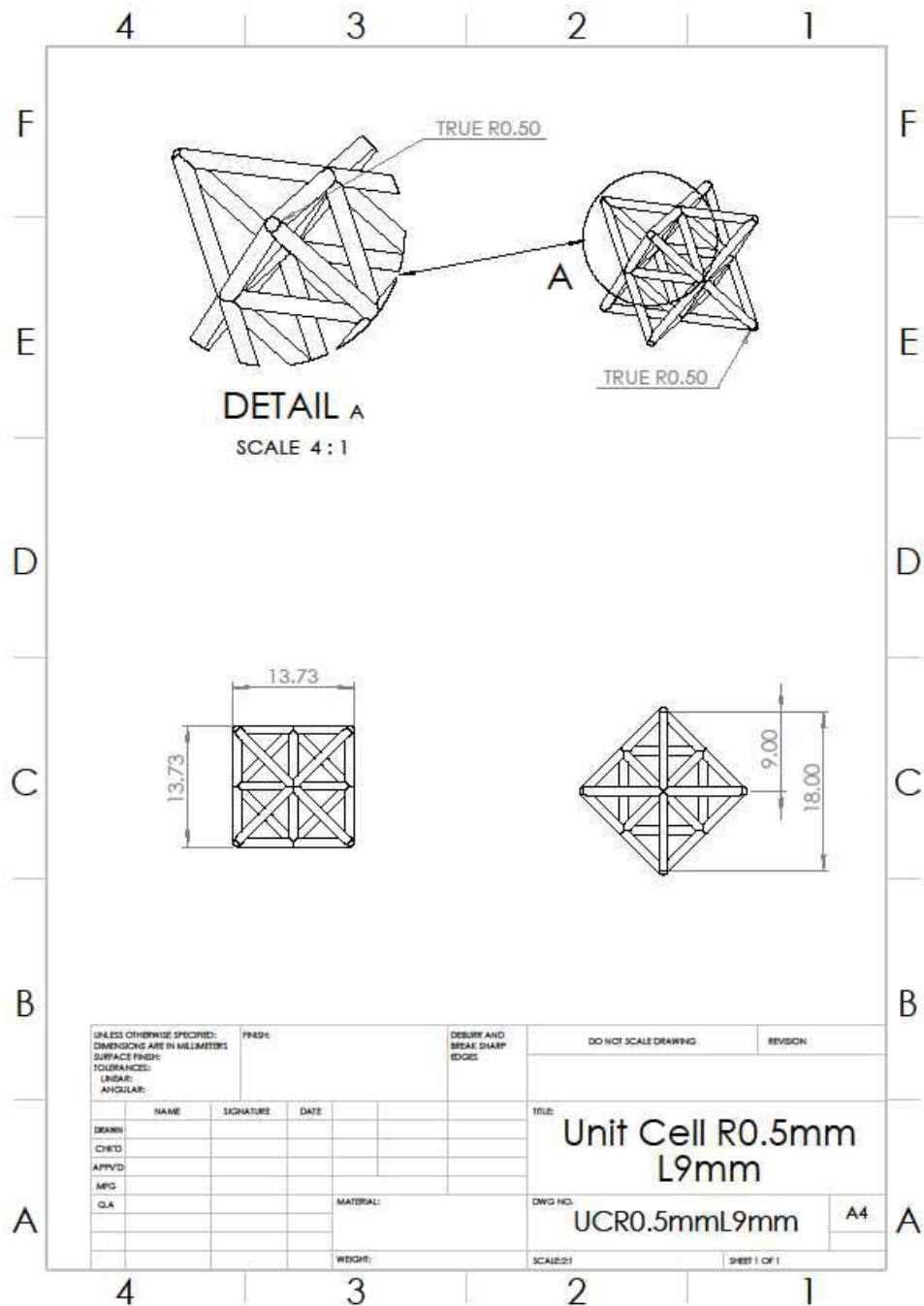


Figure 29: Radius 0.5 mm Length 9 mm Unit Cell SolidWorks Drawing

7.1.2 Unit Cells: Link Length of 10.80 mm

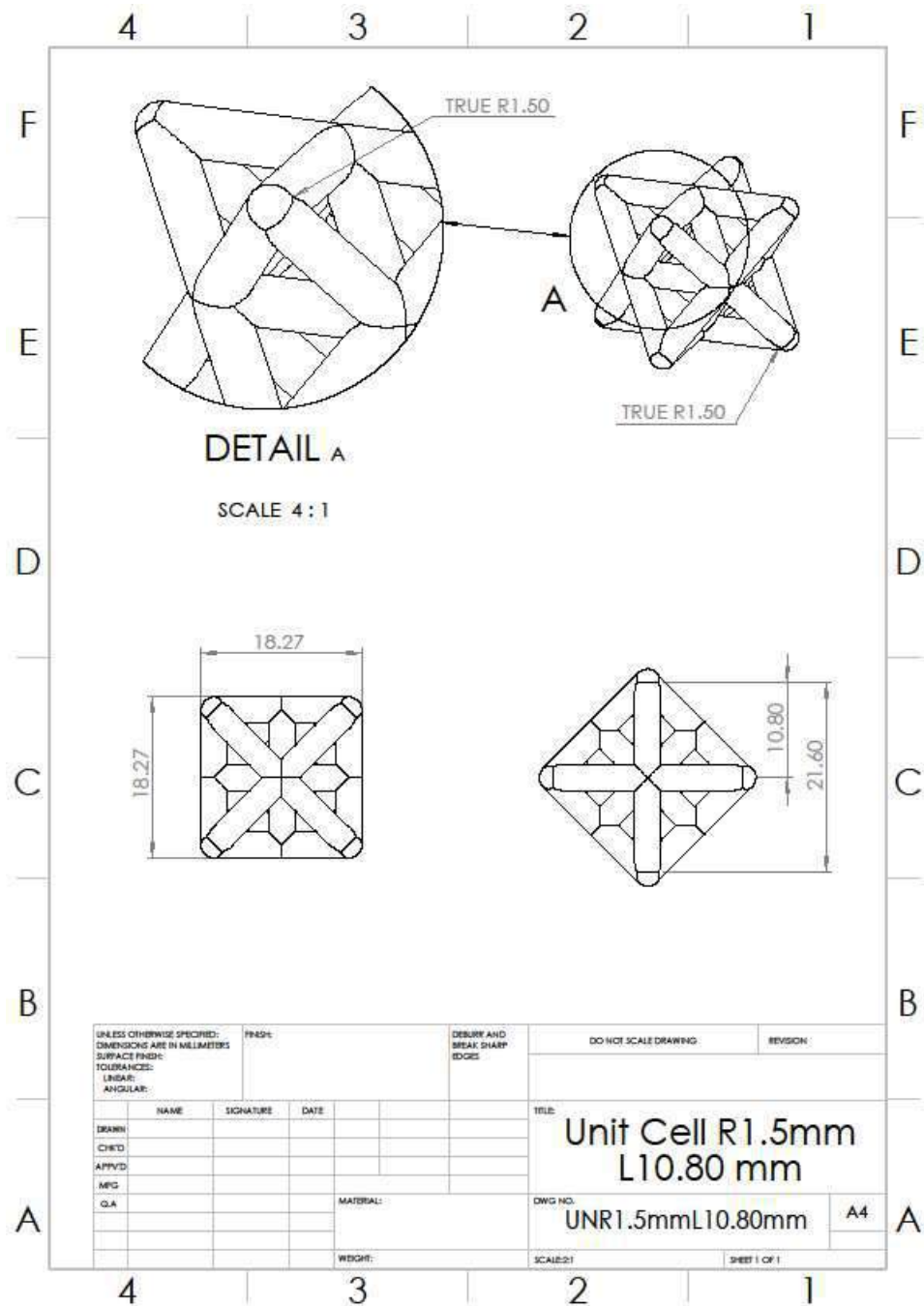


Figure 30: Radius 1.5 mm Length 10.80 mm Unit Cell SolidWorks Drawing

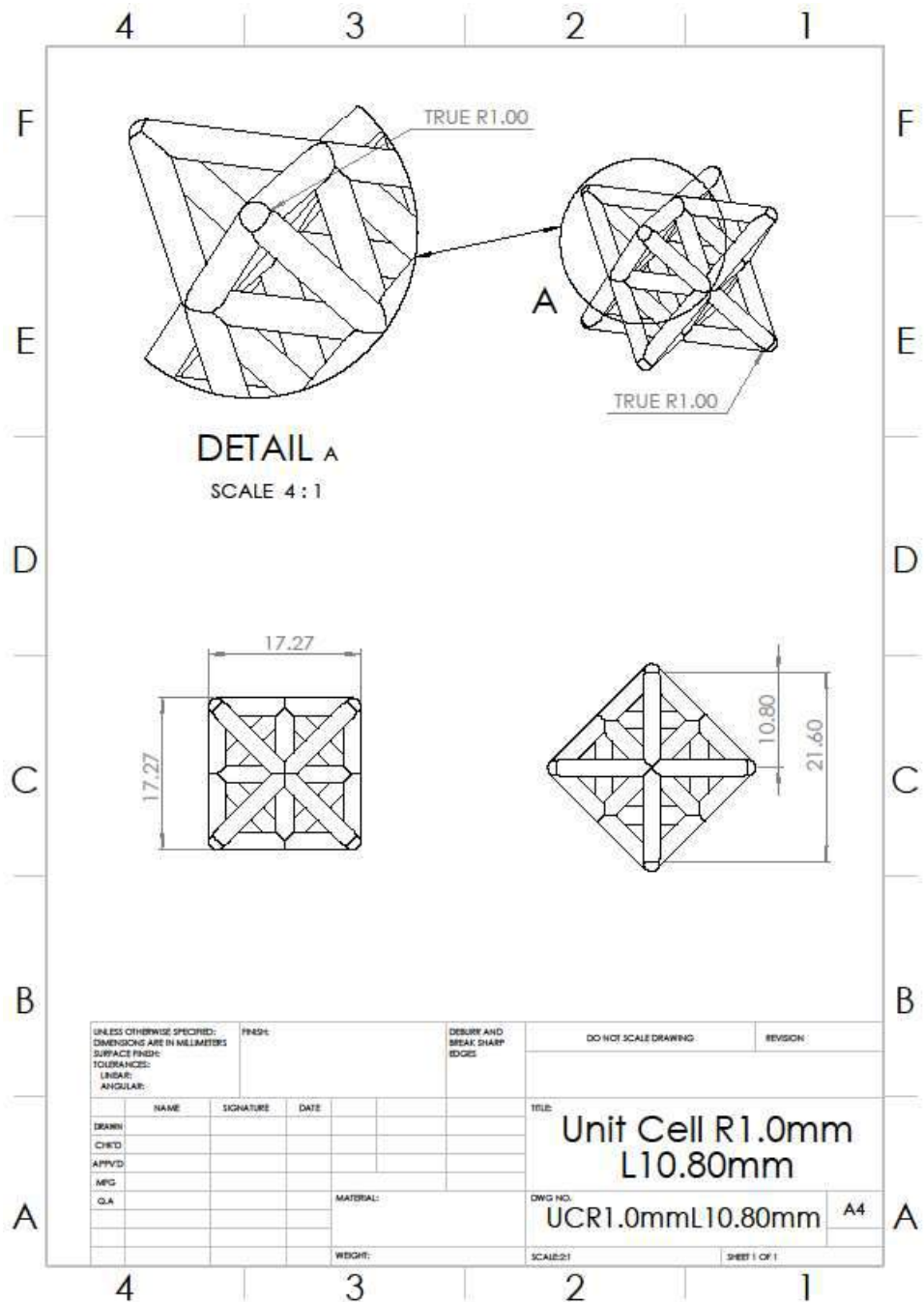


Figure 31: Radius 1.0 mm Length 10.80 mm Unit Cell SolidWorks Drawing

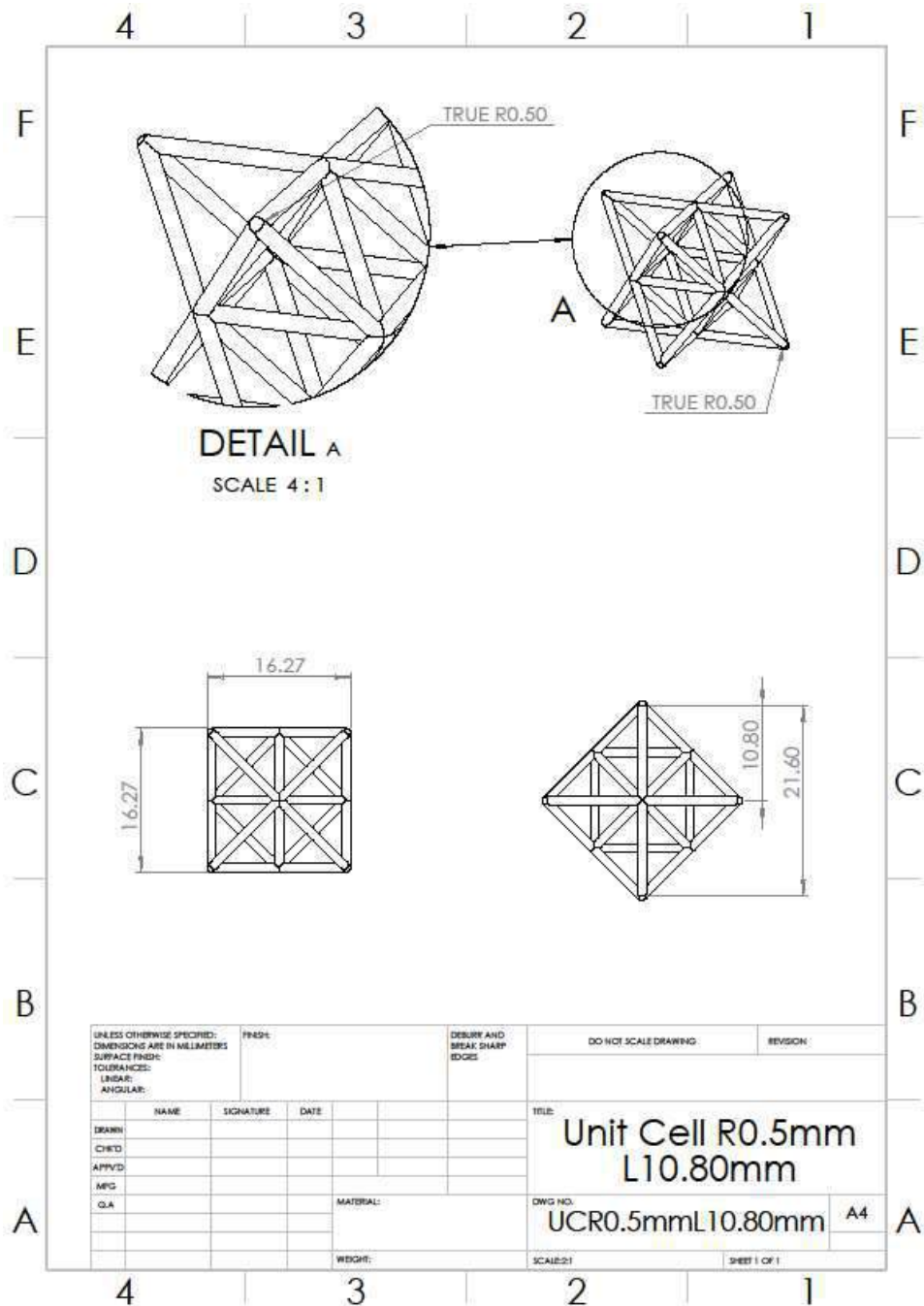


Figure 32: Radius 0.5 mm Length 10.80 mm Unit Cell SolidWorks Drawing

7.1.3 Unit Cells: Link Length of 13.50 mm

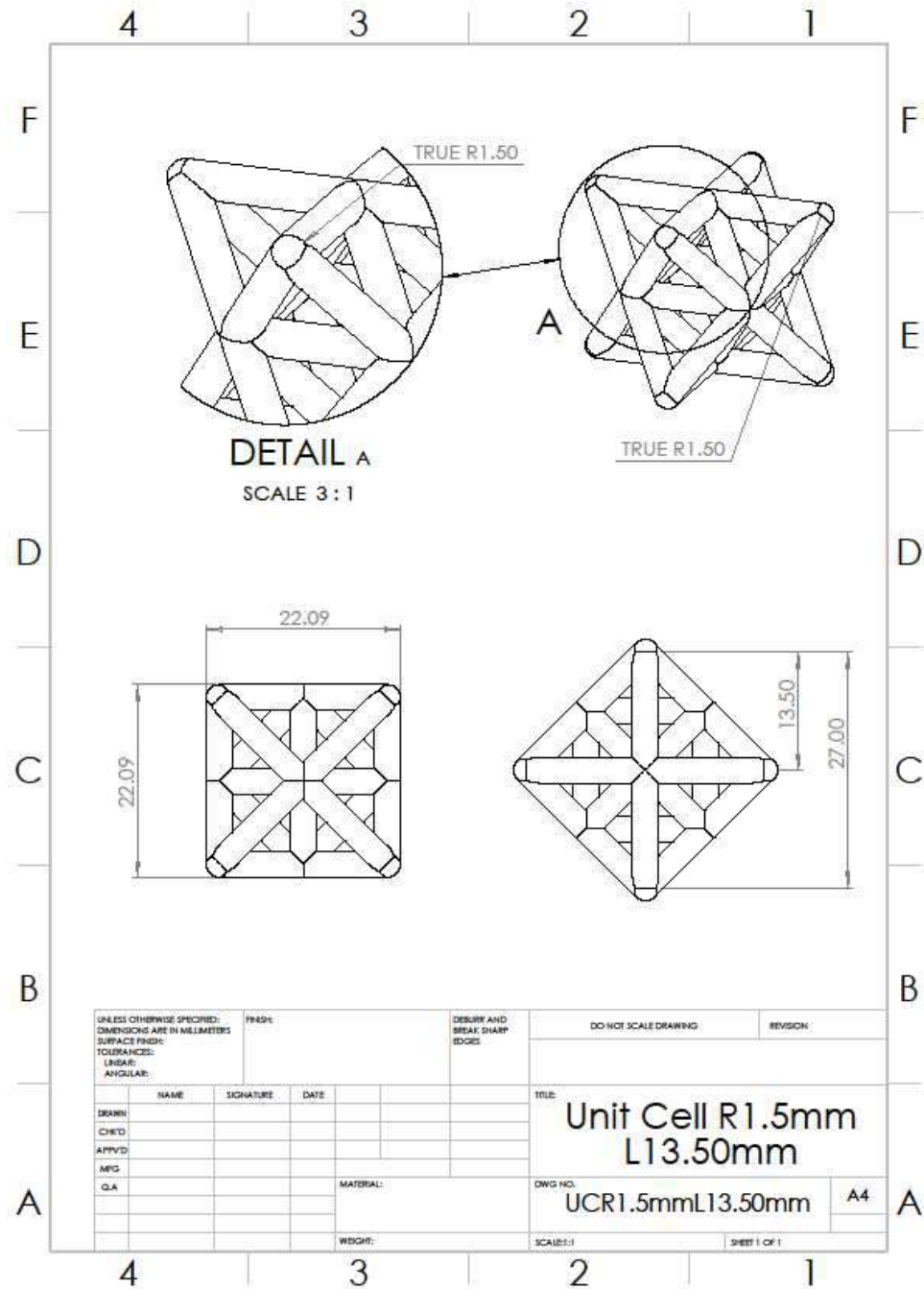


Figure 33: Radius 1.5 mm Length 13.50 mm Unit Cell SolidWorks Drawing

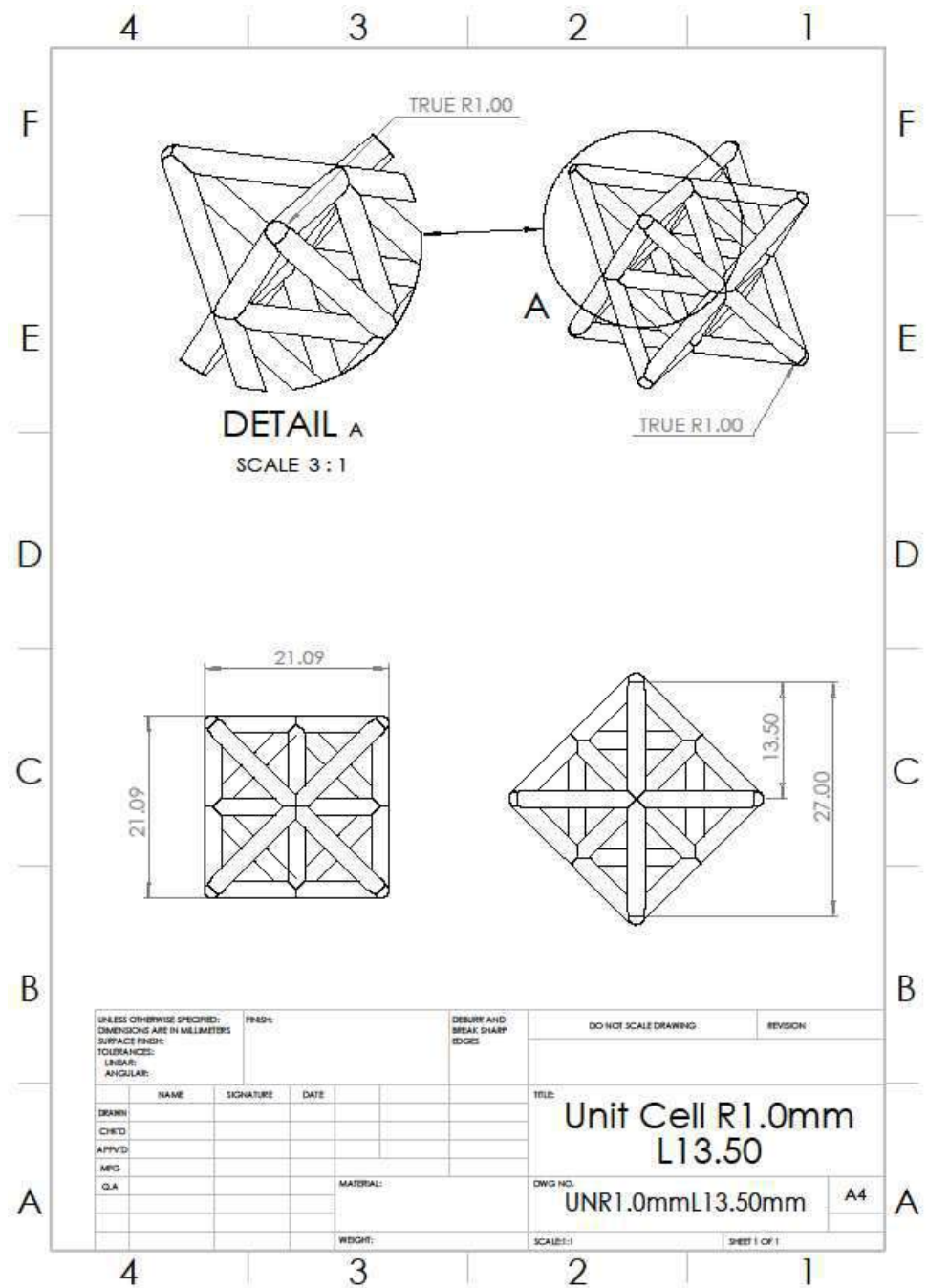


Figure 34: Radius 1.0 mm Length 13.50 mm Unit Cell SolidWorks Drawing

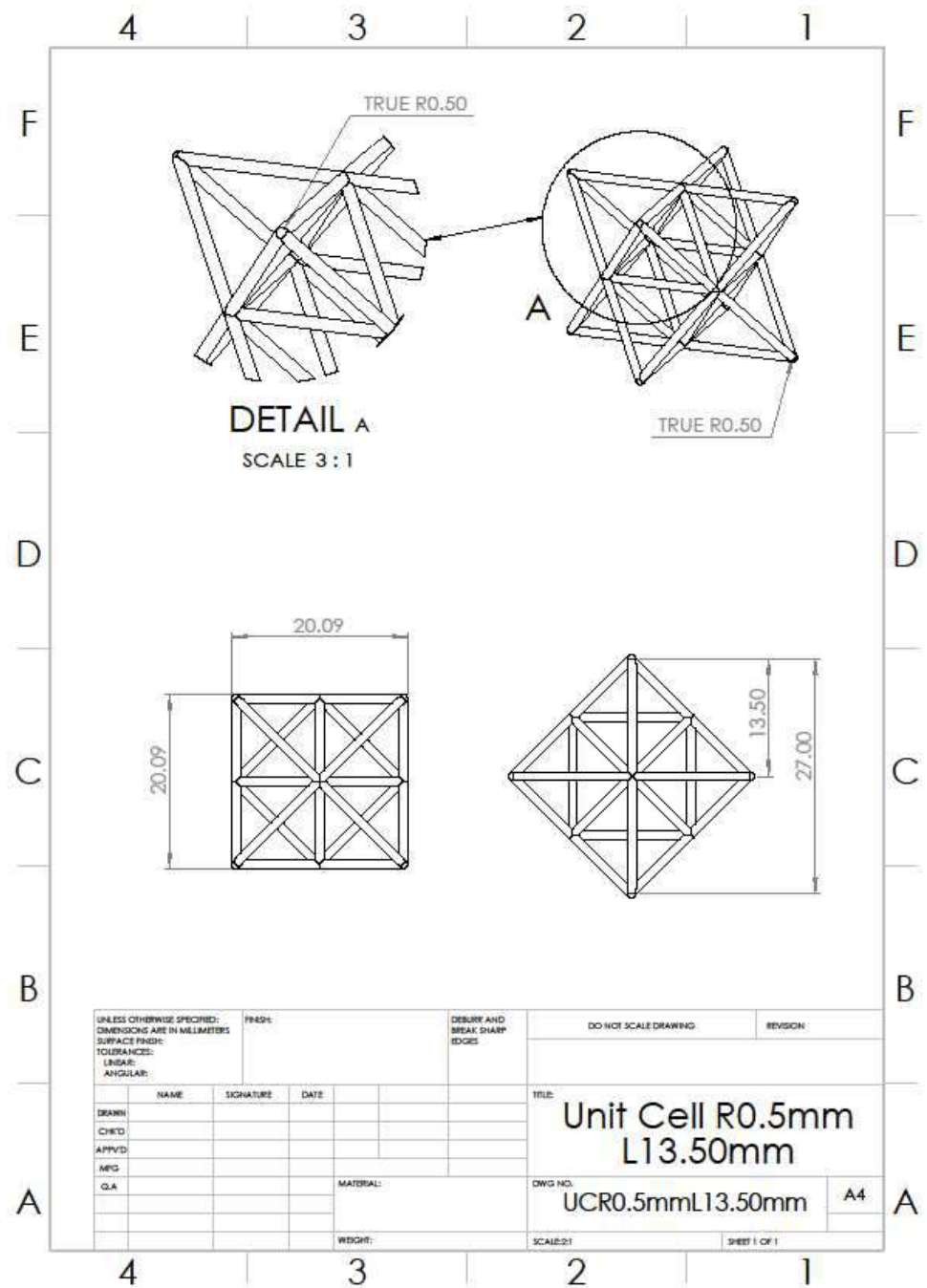


Figure 35: Radius 0.5 mm Length 13.50 mm Unit Cell SolidWorks Drawing

7.1.4 Unit Cells: Link Length of 18.00 mm

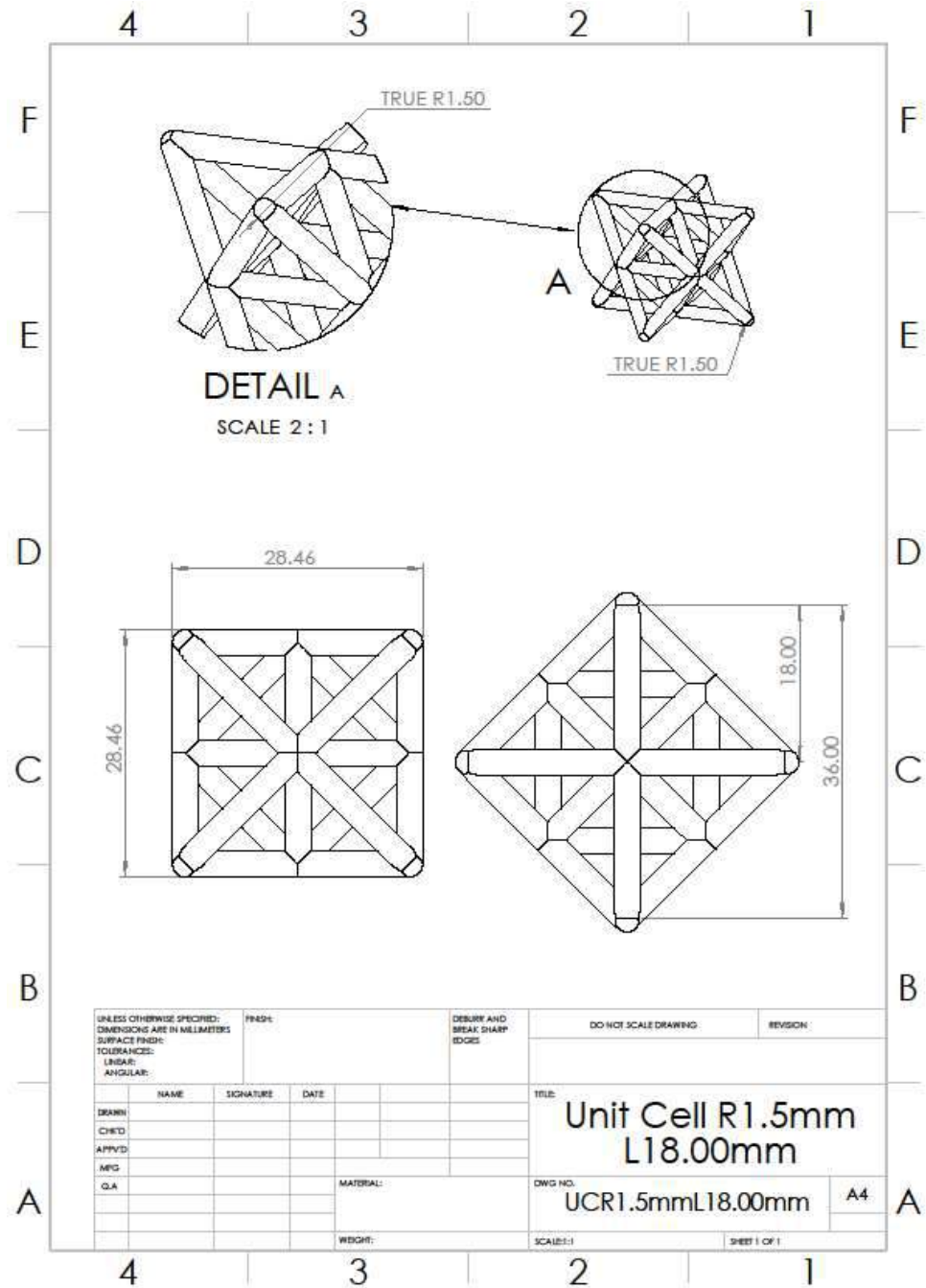


Figure 36: Radius 1.5 mm Length 18.00 mm Unit Cell SolidWorks Drawing

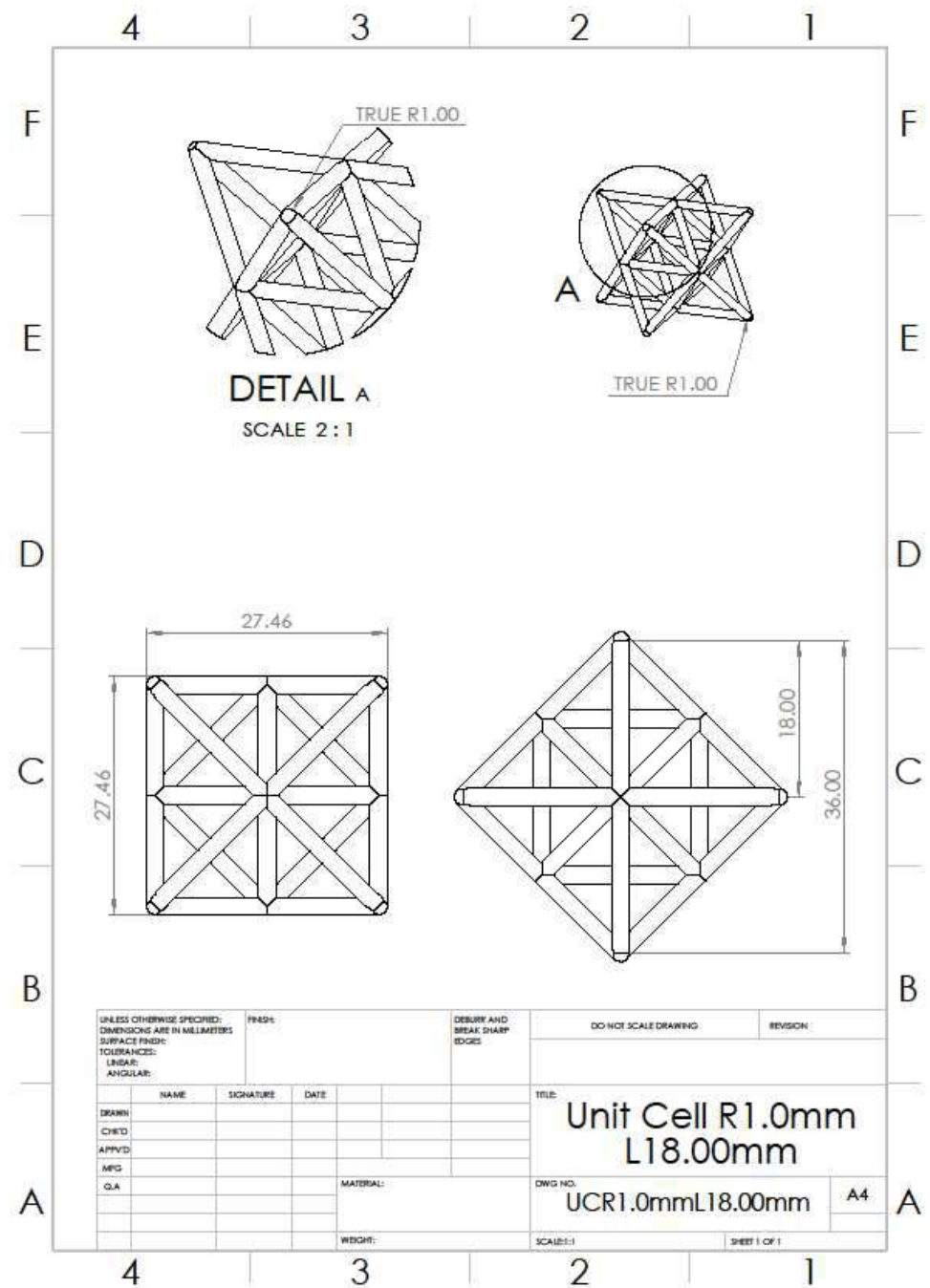


Figure 37: Radius 1.0 mm Length 18.00 mm Unit Cell SolidWorks Drawing

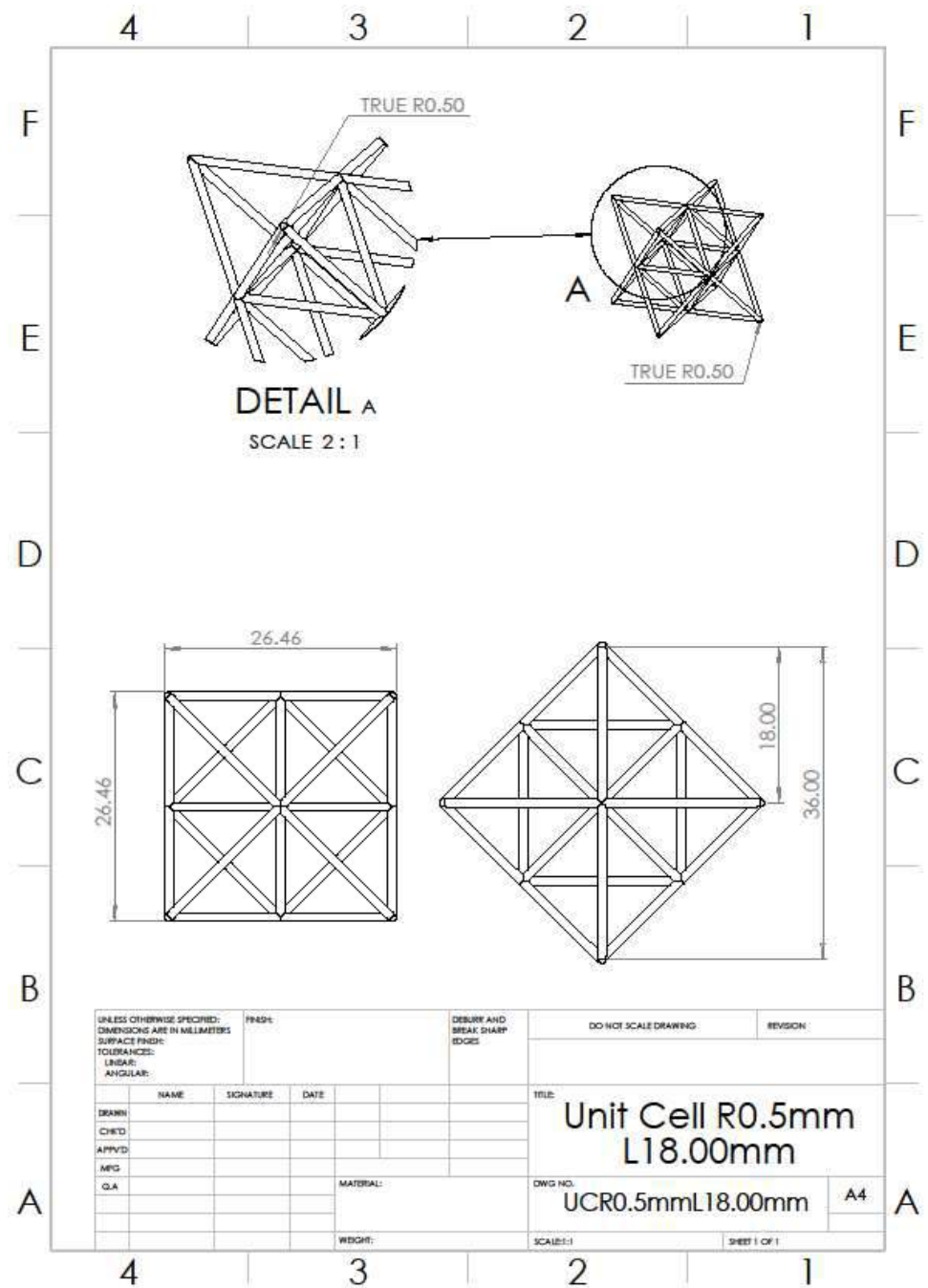


Figure 38: Radius 0.5 mm Length 18.00 mm Unit Cell SolidWorks Drawing

7.2 Cell Structure Drawings

7.2.1 3x3x3

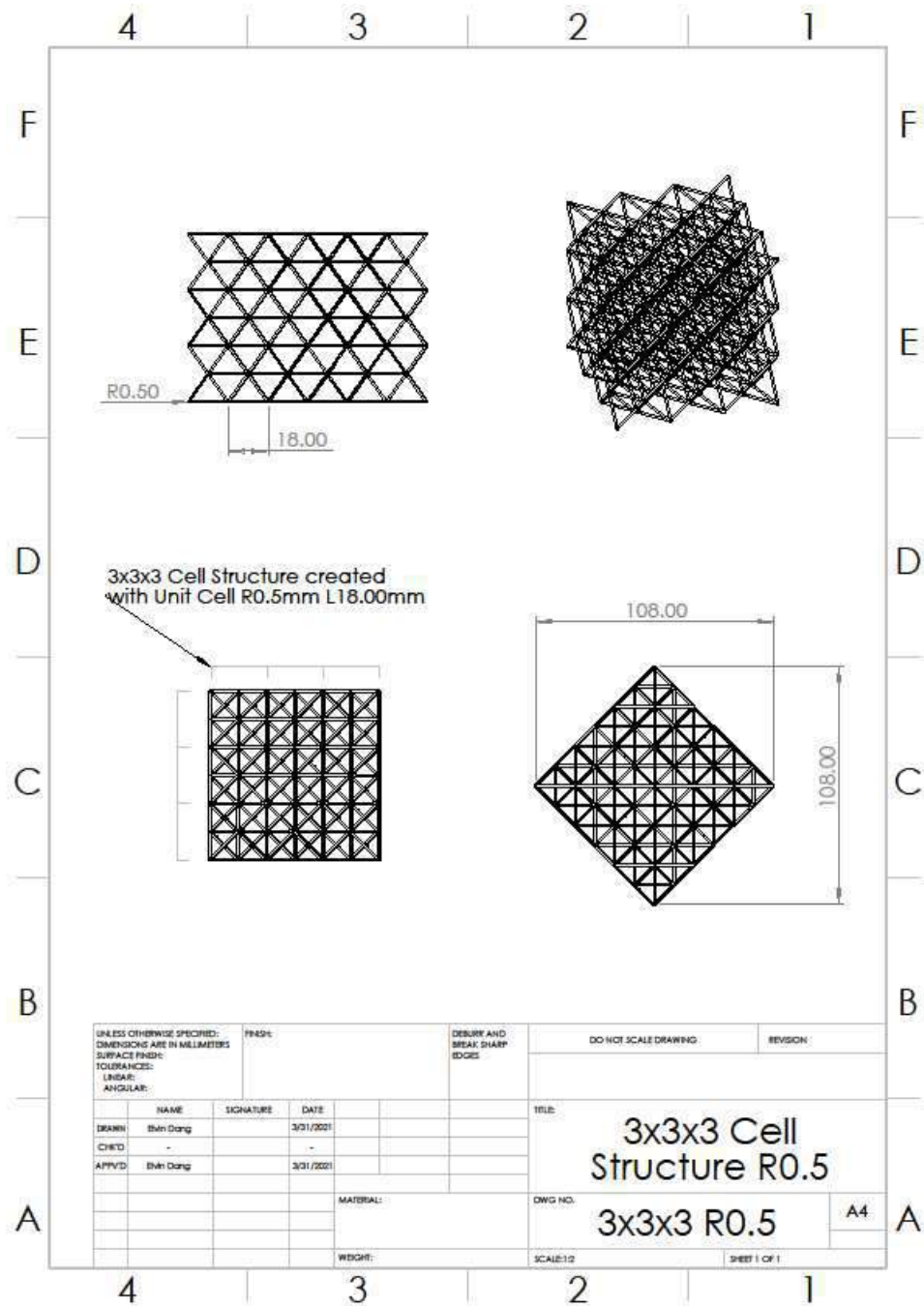


Figure 39: Radius 0.5 mm 3x3x3 Cell Structure SolidWorks Drawing

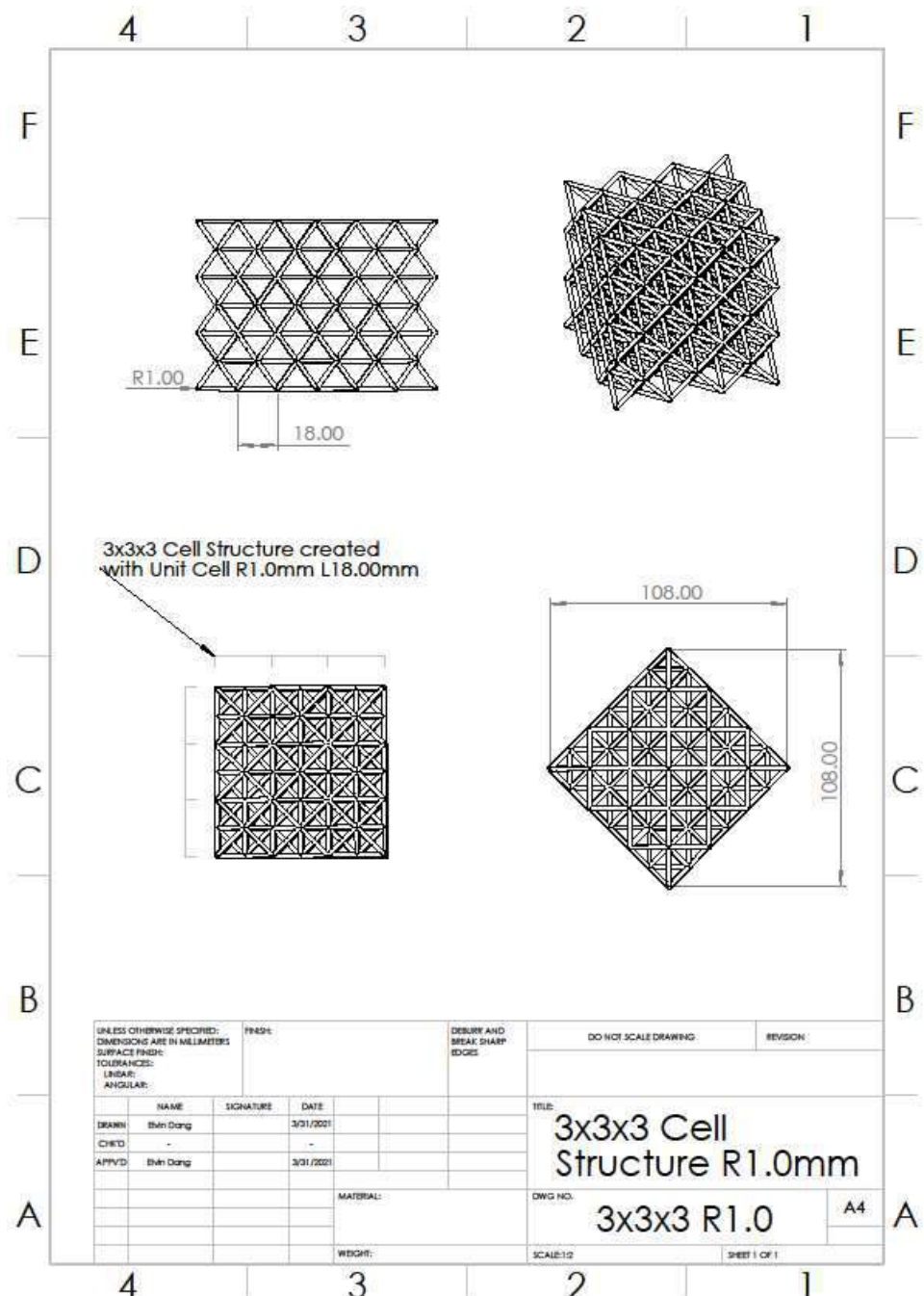


Figure 40: Radius 1.0 mm 3x3x3 Cell Structure SolidWorks Drawing

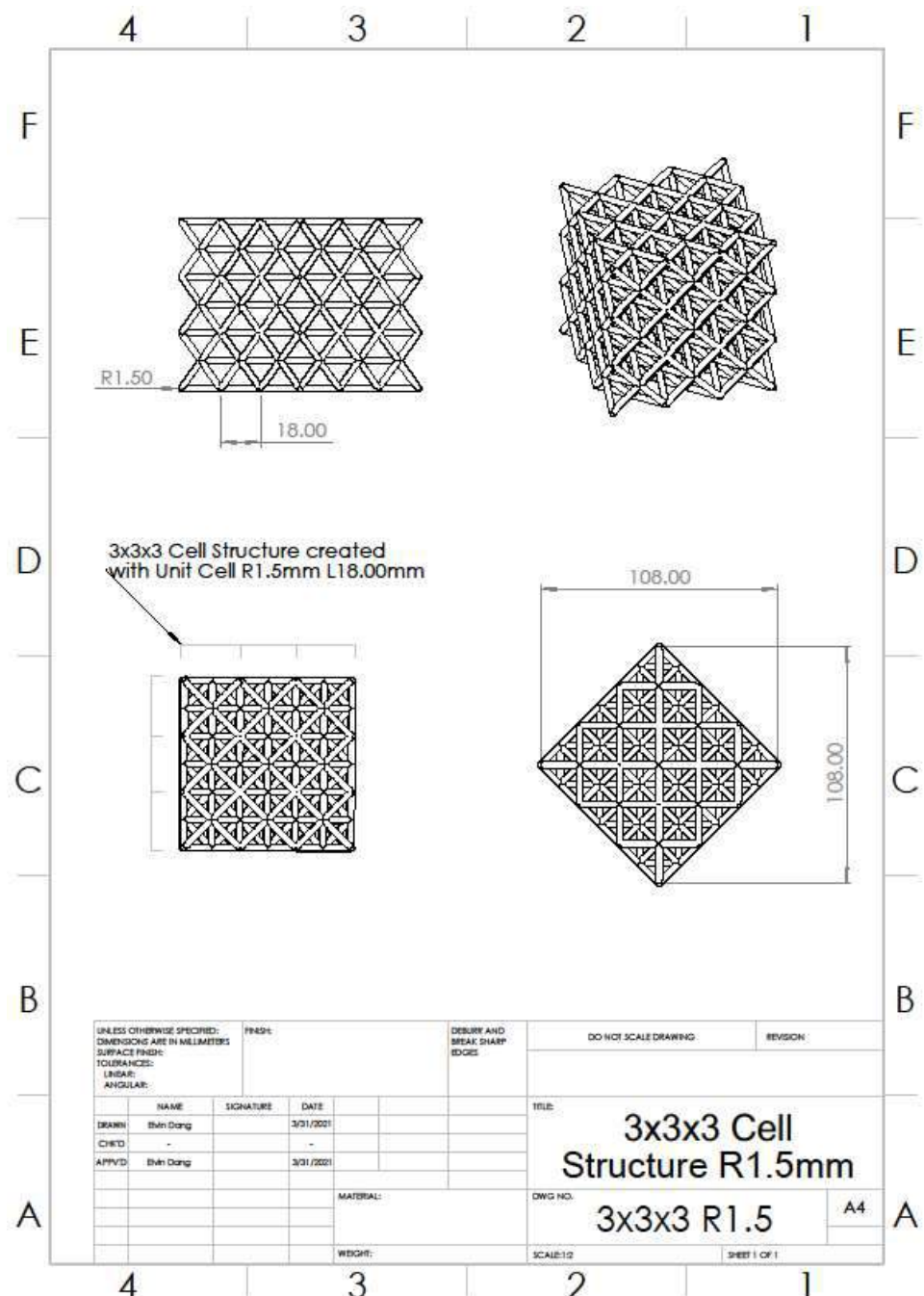


Figure 41: Radius 1.5 mm 3x3x3 Cell Structure SolidWorks Drawing

7.2.2 4x4x4

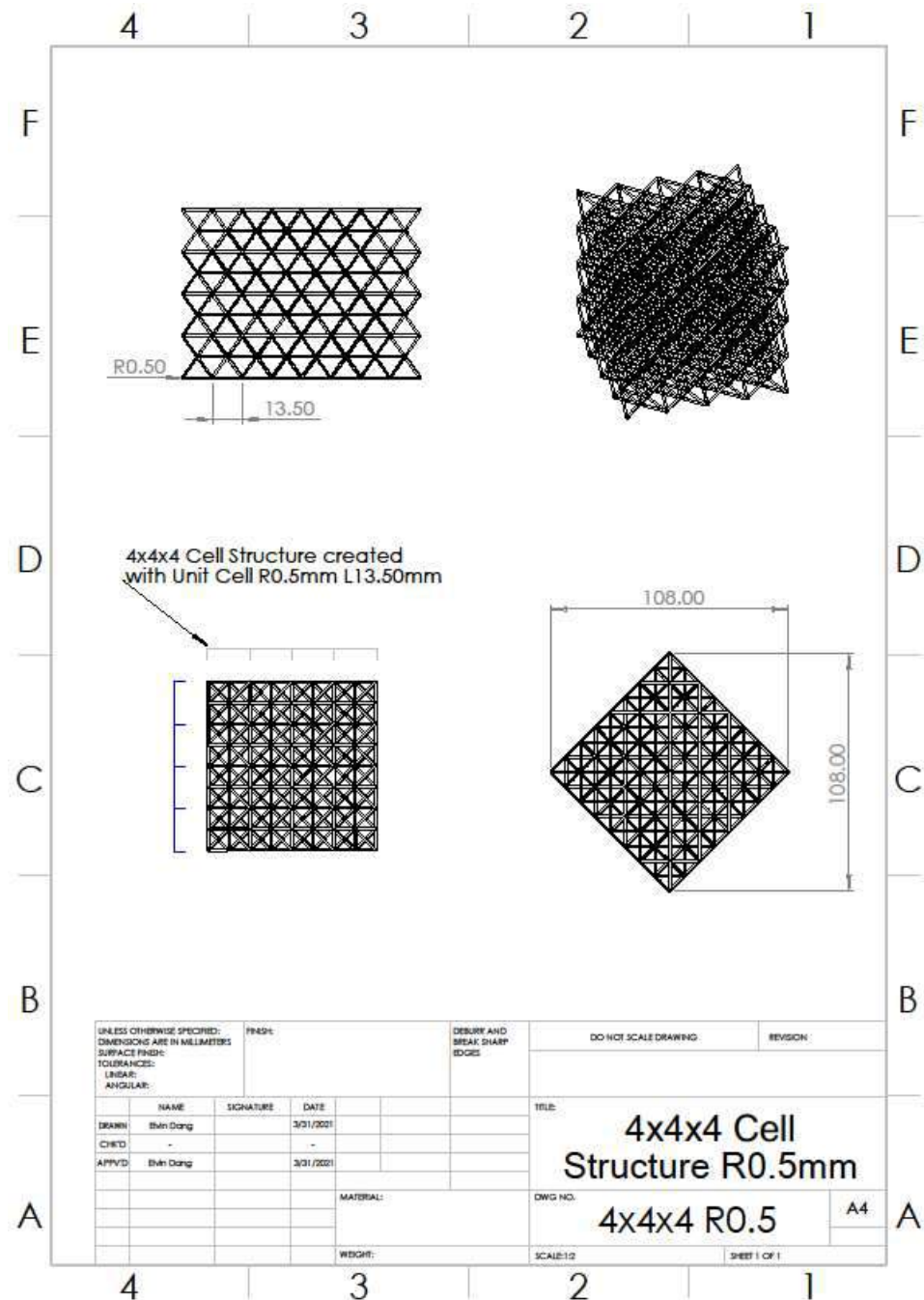


Figure 42: Radius 0.5 mm 4x4x4 Cell Structure SolidWorks Drawing

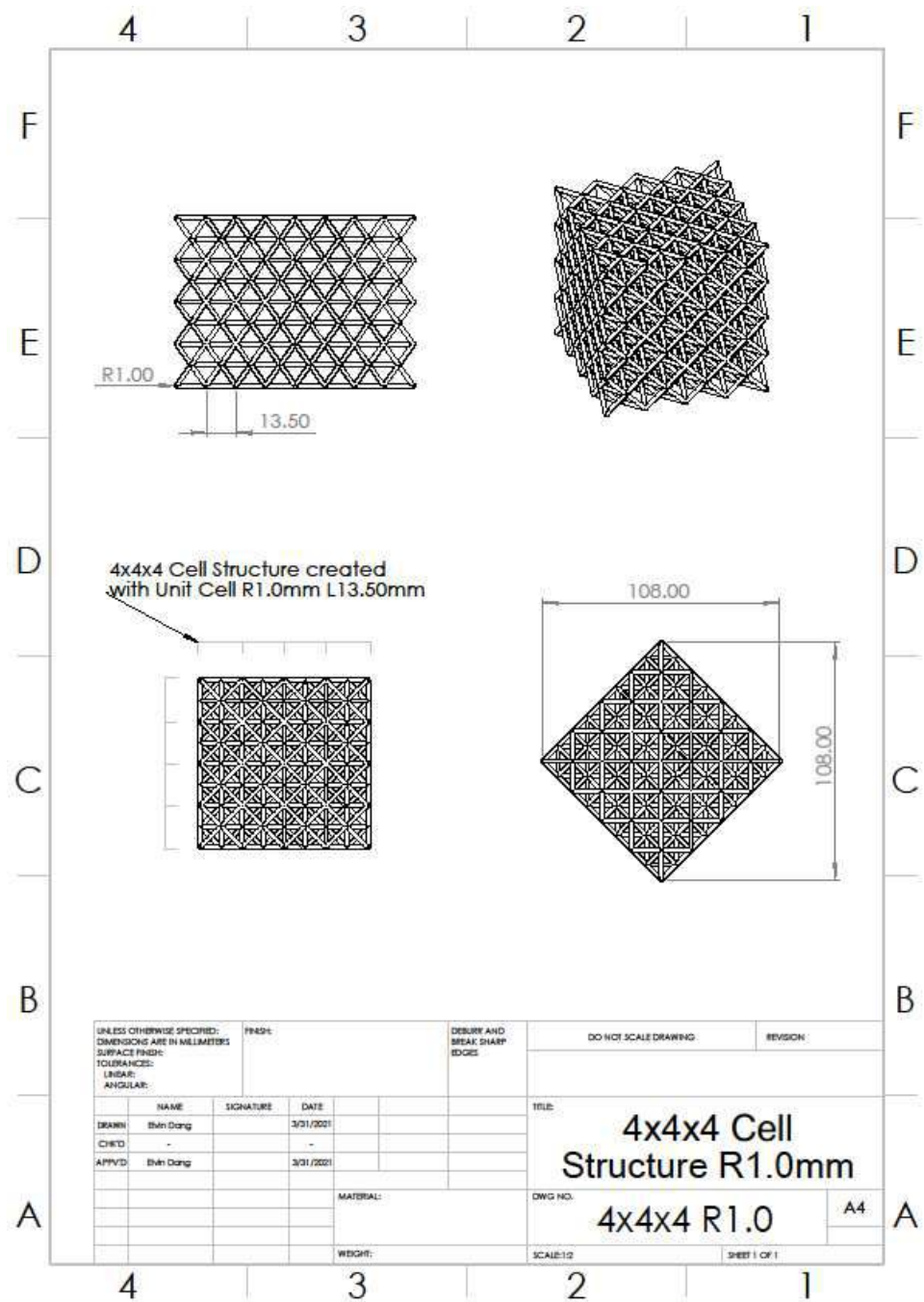


Figure 43: Radius 1.0 mm 4x4x4 Cell Structure SolidWorks Drawing

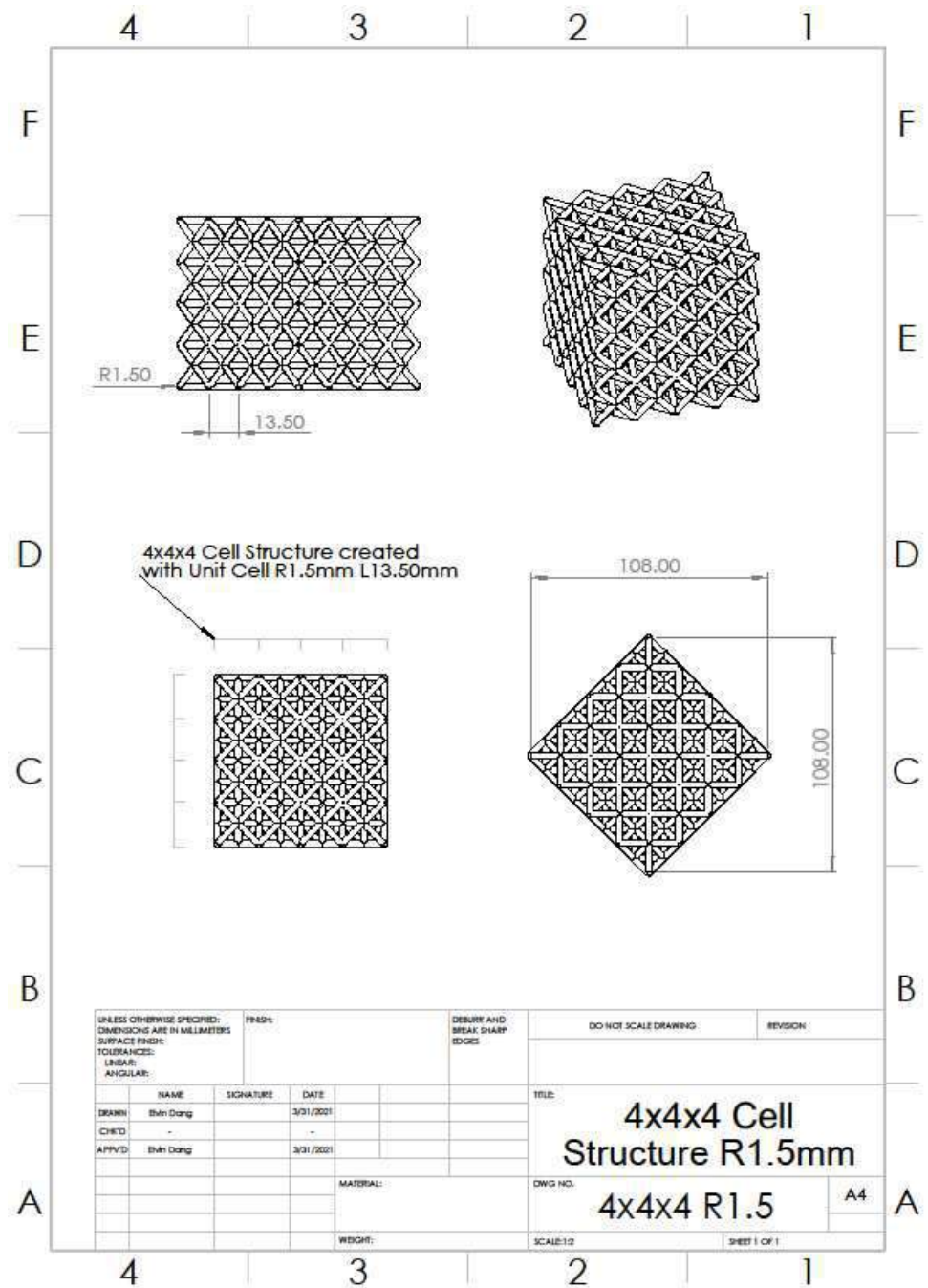


Figure 44: Radius 1.5 mm 4x4x4 Cell Structure SolidWorks Drawing

7.2.3 5x5x5

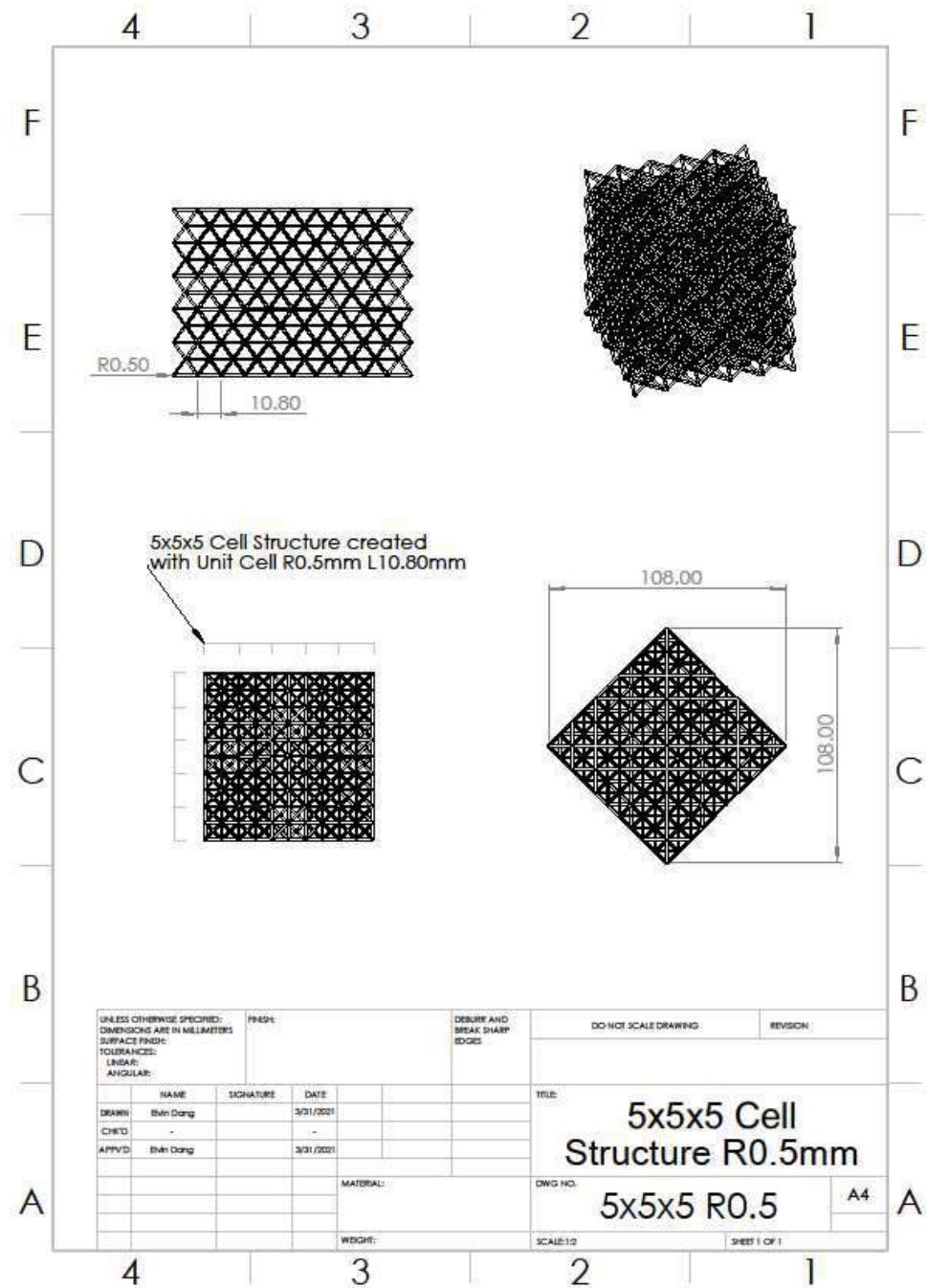


Figure 45: Radius 0.5 mm 5x5x5 Cell Structure SolidWorks Drawing

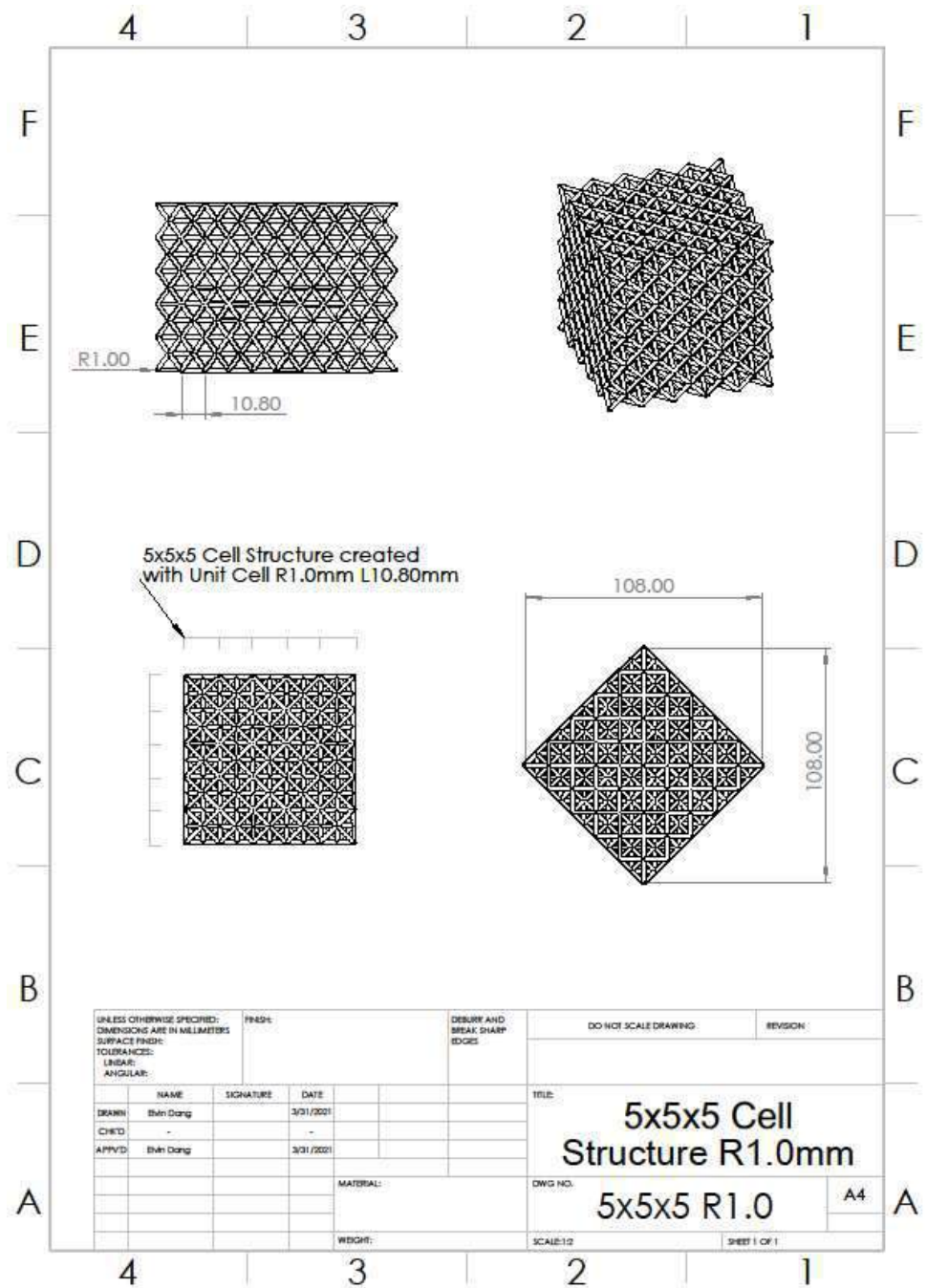


Figure 46: Radius 1.0 mm 5x5x5 Cell Structure SolidWorks Drawing

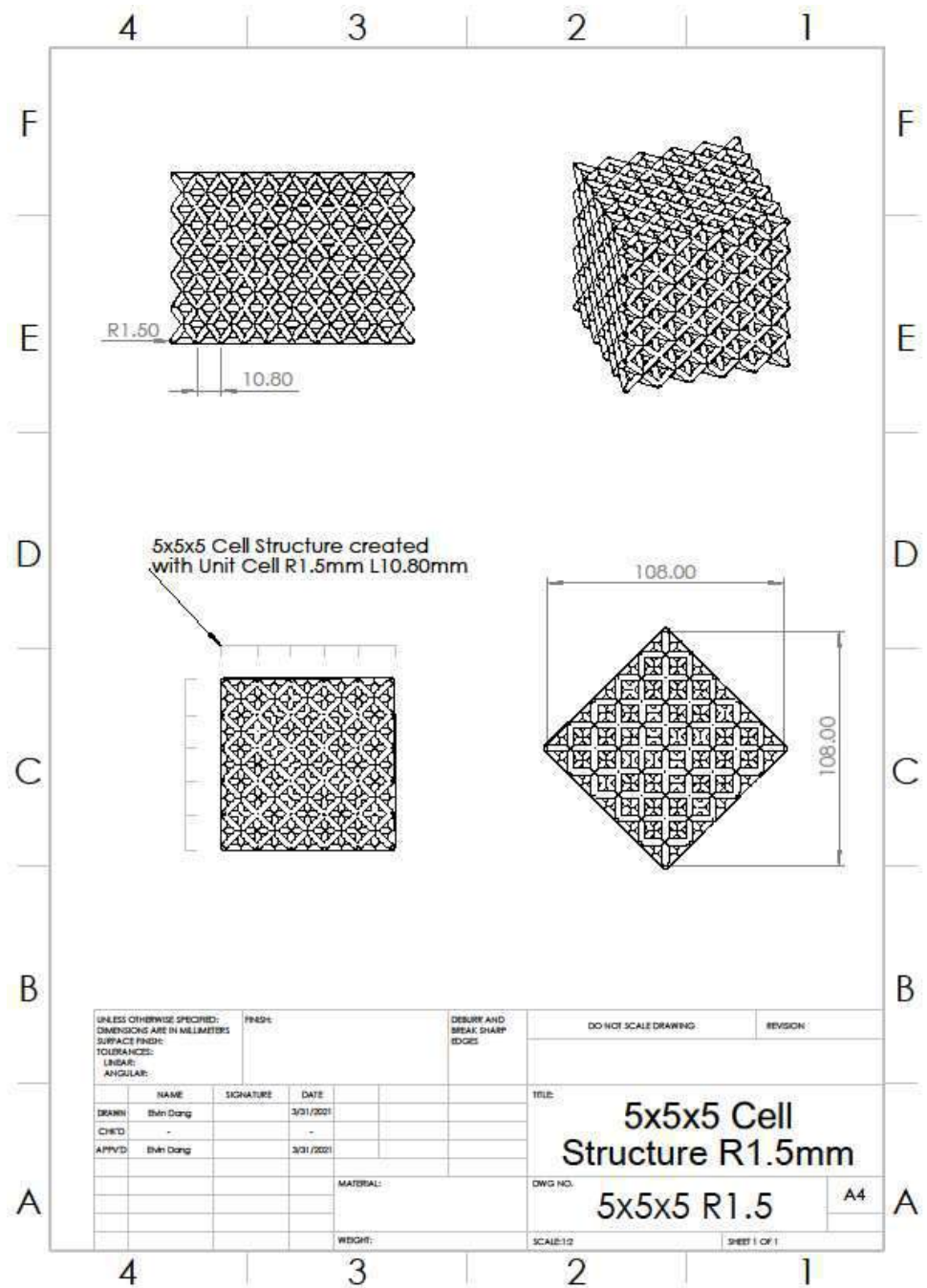


Figure 47: Radius 1.5 mm 5x5x5 Cell Structure SolidWorks Drawing

7.2.4 6x6x6

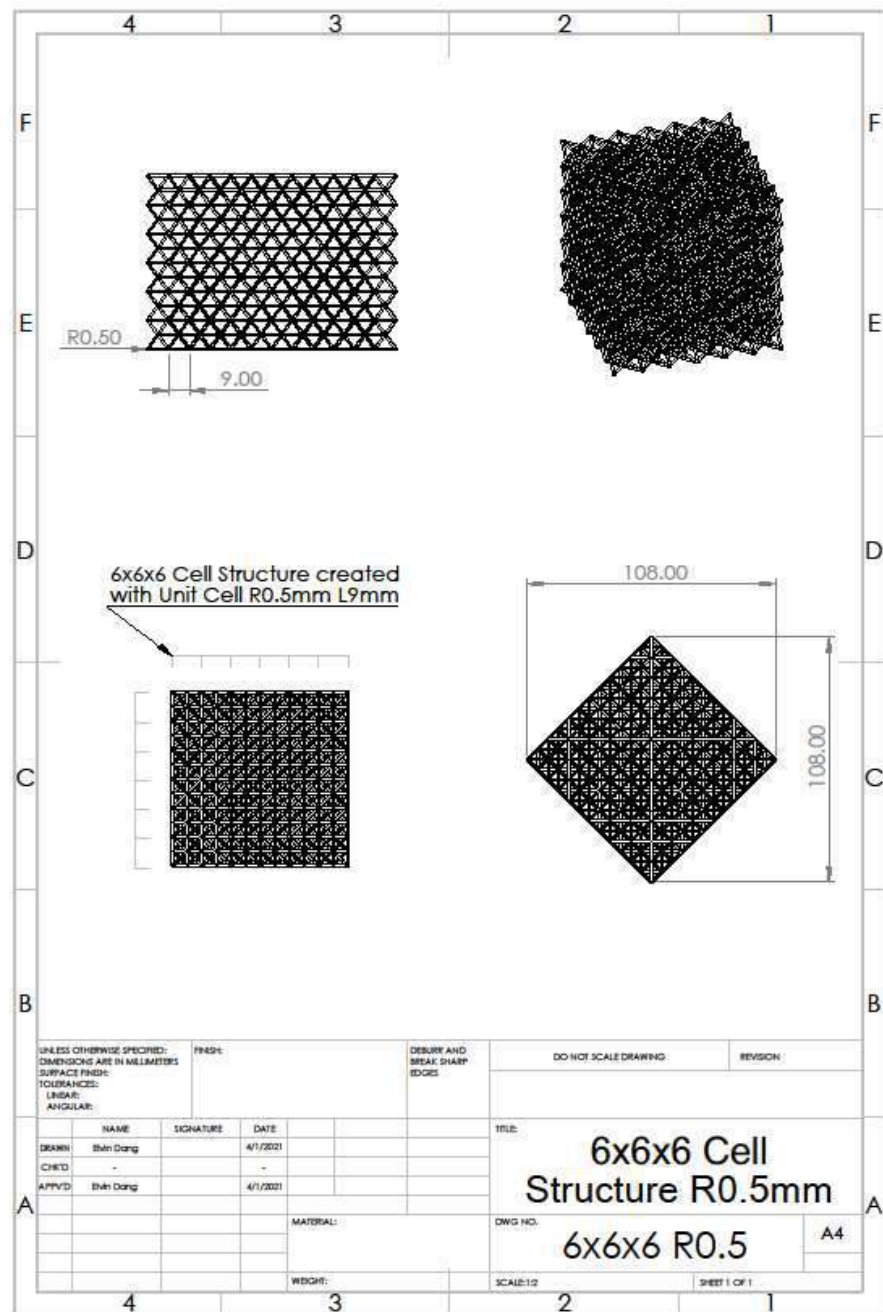


Figure 48: Radius 0.5 mm 6x6x6 Cell Structure SolidWorks Drawing

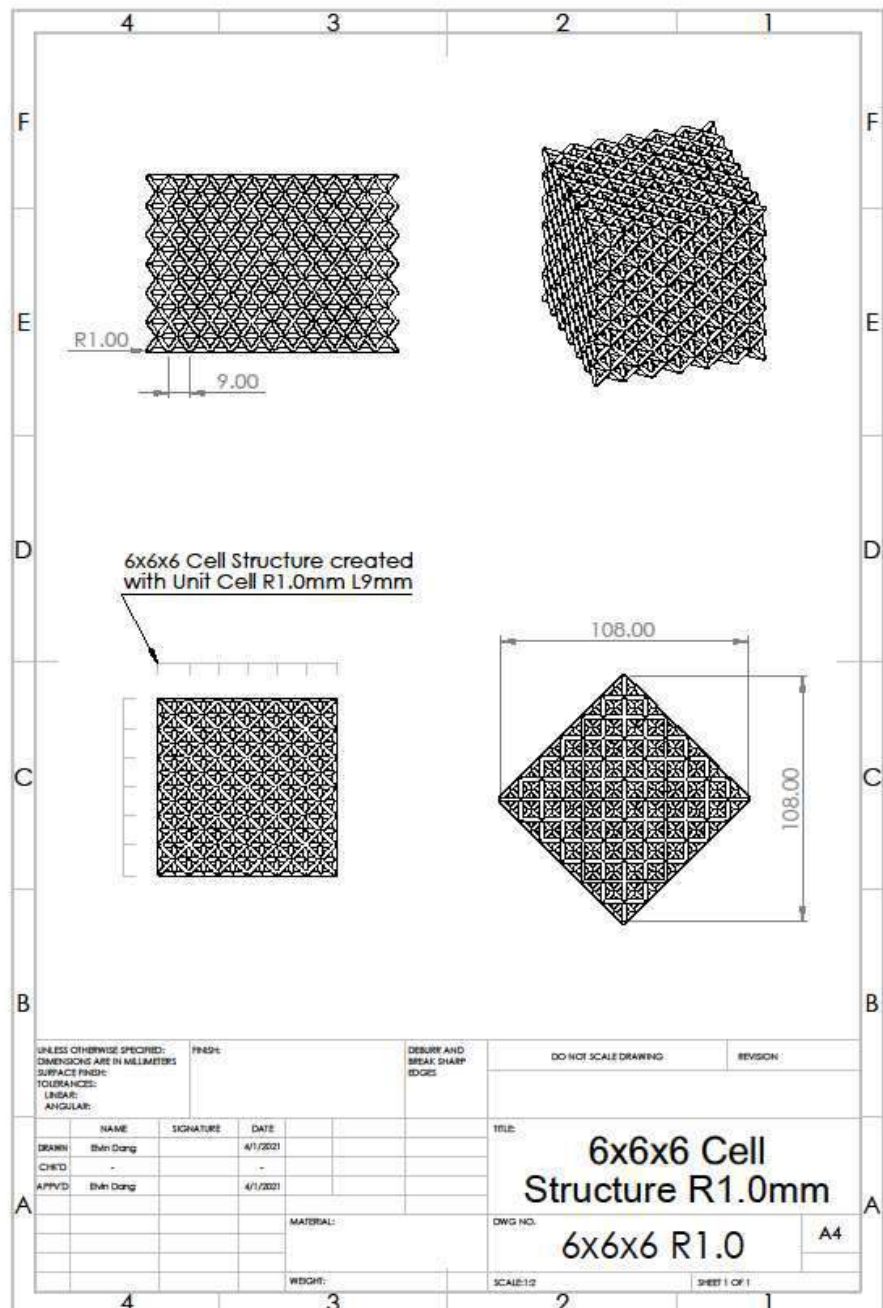


Figure 49: Radius 1.0 mm 6x6x6 Cell Structure SolidWorks Drawing

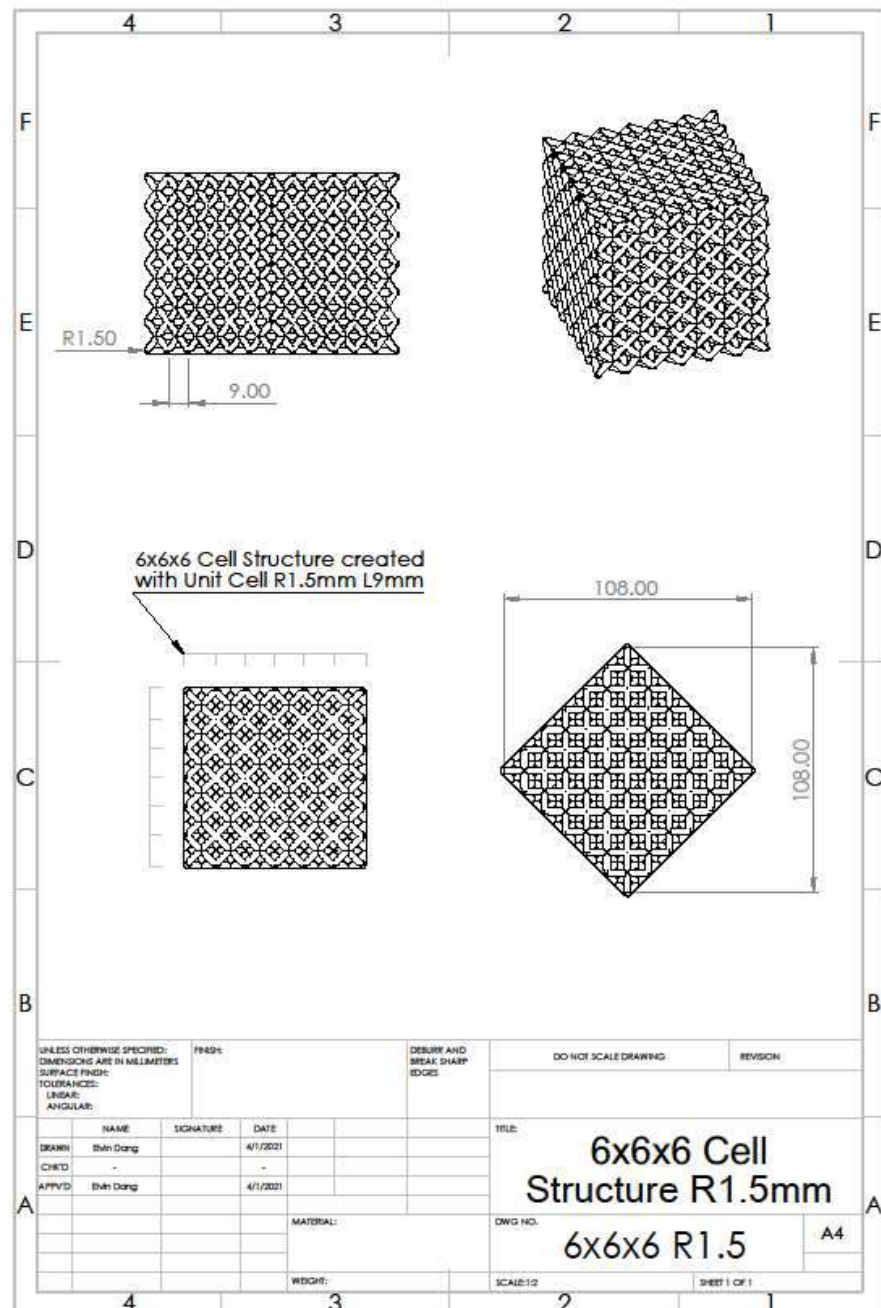


Figure 50: Radius 1.5 mm 6x6x6 Cell Structure SolidWorks Drawing

7.3 PMMA Material Properties

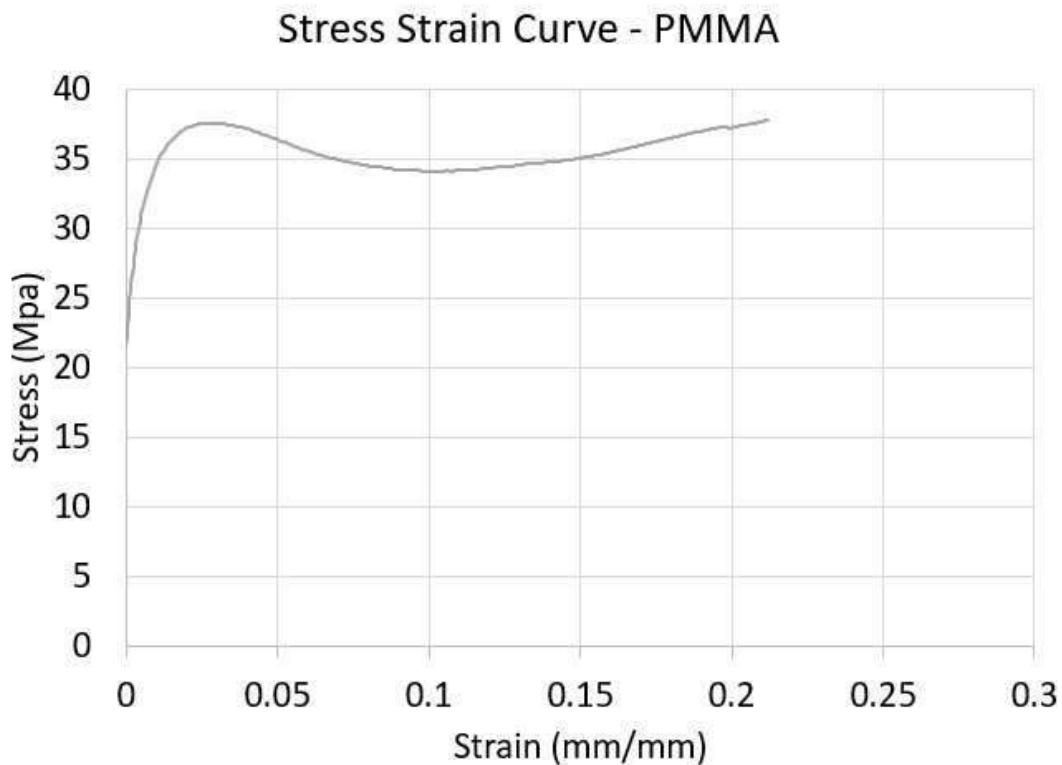


Figure 51: Stress Strain curve for primary material Unit Cells and Cell Structures - PMMA

7.4 Theoretical Densities and Mass

Table 8: Theoretical Density in Relation with Other Parameters

Link Radius (mm)	Link Length (mm)	Theoretical Density (%)	Associated Cell Structure
0.5	18.00	0.0206	3x3x3
1.0	18.00	0.0823	
1.5	18.00	0.1851	
0.5	13.50	0.0366	4x4x4
1.0	13.50	0.1463	
1.5	13.50	0.3291	
0.5	10.80	0.0571	5x5x5
1.0	10.80	0.2285	
1.5	10.80	0.5142	
0.5	9.00	0.0823	

1.0	9.00	0.3291	6x6x6
1.5	9.00	0.7405	

Table 9: Theoretical Mass Summary

Material Density (g/cm ³)	Volume of Solid Cube (cm ³)	Theoretical Density (%)	Theoretical Mass (g)	Associated Cell Structure
1.18	442.451	0.0206	10.74	3x3x3
1.18	442.451	0.0823	42.96	
1.18	442.451	0.1851	96.65	
1.18	442.451	0.0366	19.09	4x4x4
1.18	442.451	0.1463	76.37	
1.18	442.451	0.3291	171.82	
1.18	442.451	0.0571	29.83	
1.18	442.451	0.2285	119.32	5x5x5
1.18	442.451	0.5142	268.47	
1.18	442.451	0.0823	42.96	
1.18	442.451	0.3291	171.82	6x6x6
1.18	442.451	0.7405	386.60	

7.5 Additional Ansys Simulation Captures

7.5.1 Unit Cells

7.5.1.1 Radii of 0.5 mm

7.5.1.1.1 Unit Cell R 0.5 mm L 9.0 mm

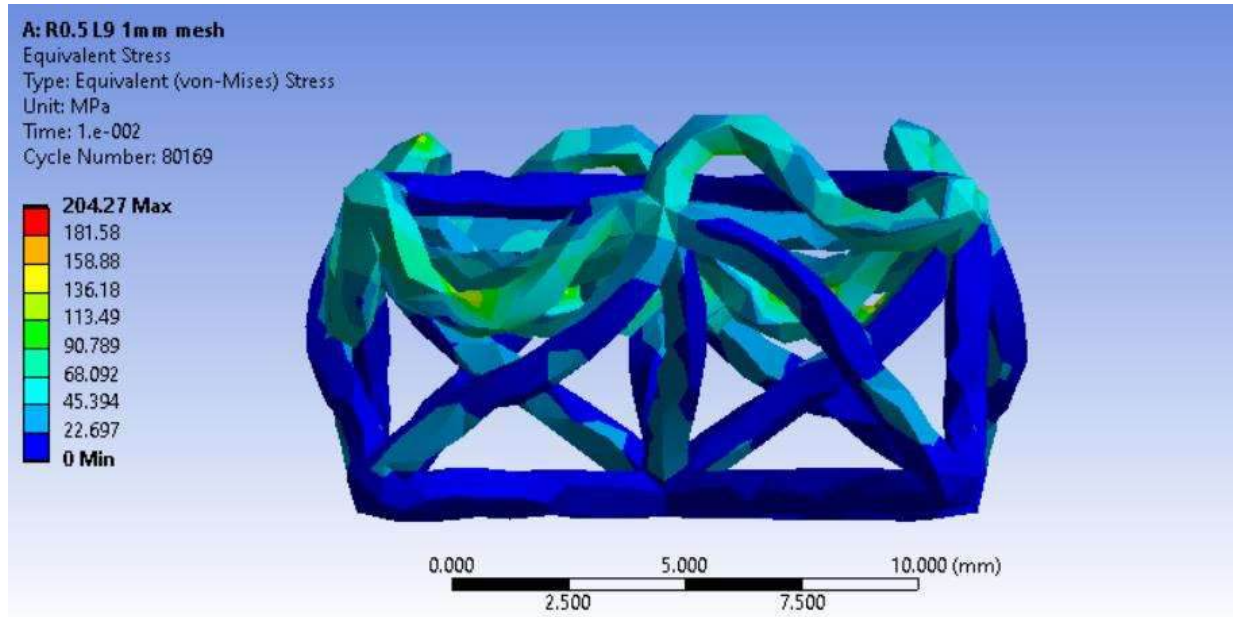


Figure 52: Equivalent Stress for R0.5 mm L9.0 mm with a 1 mm mesh.

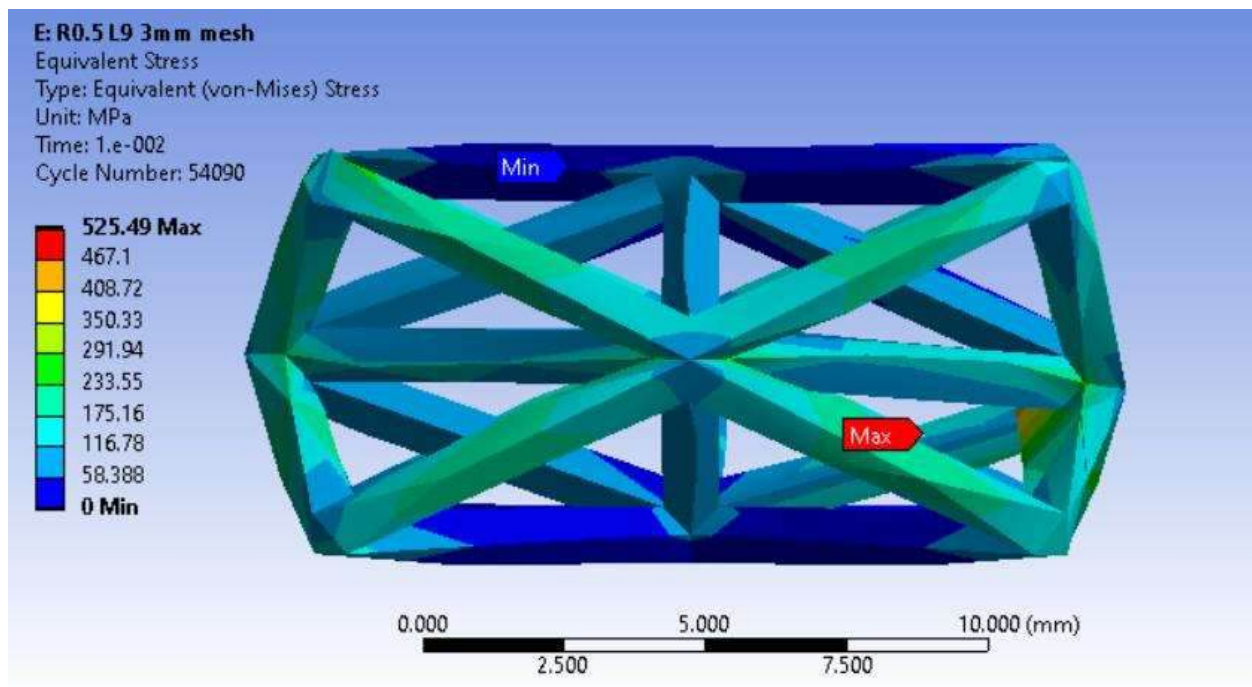


Figure 53: Equivalent Stress for R0.5 mm L9.0 mm with a 3 mm mesh.

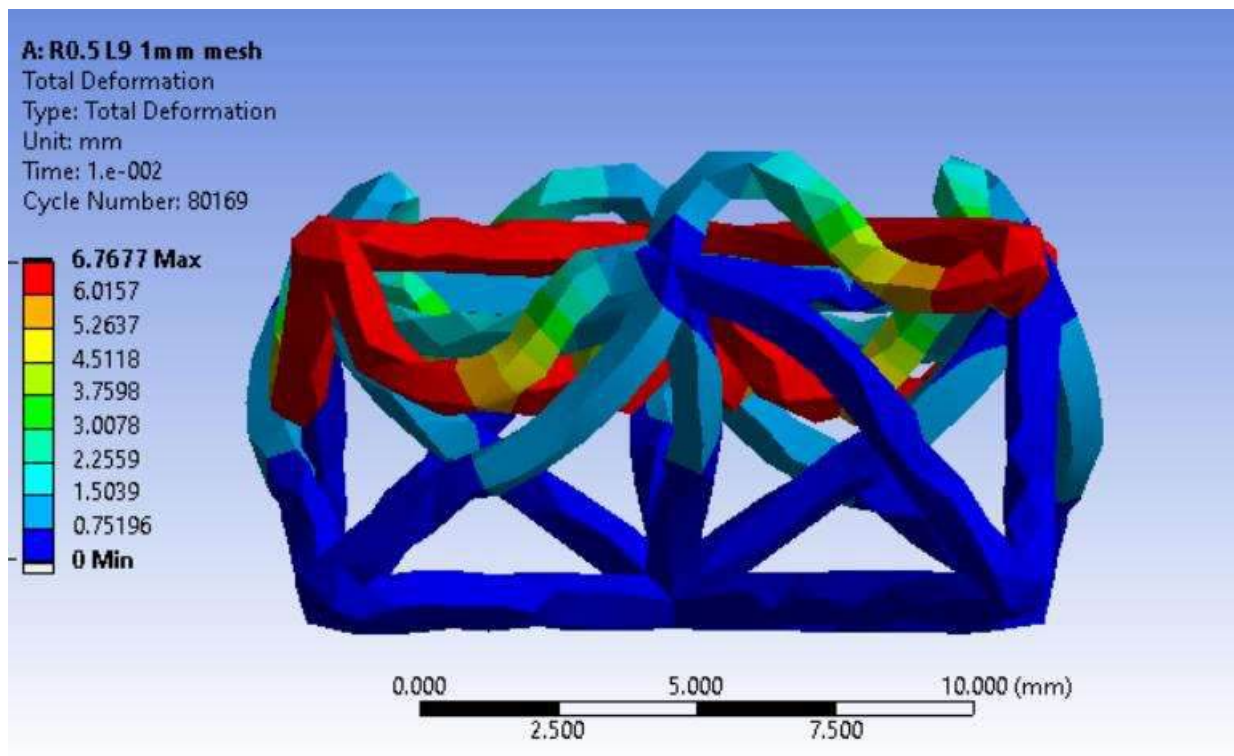


Figure 54: Total Deformation for R0.5 mm L9.0 mm with a 1 mm mesh.

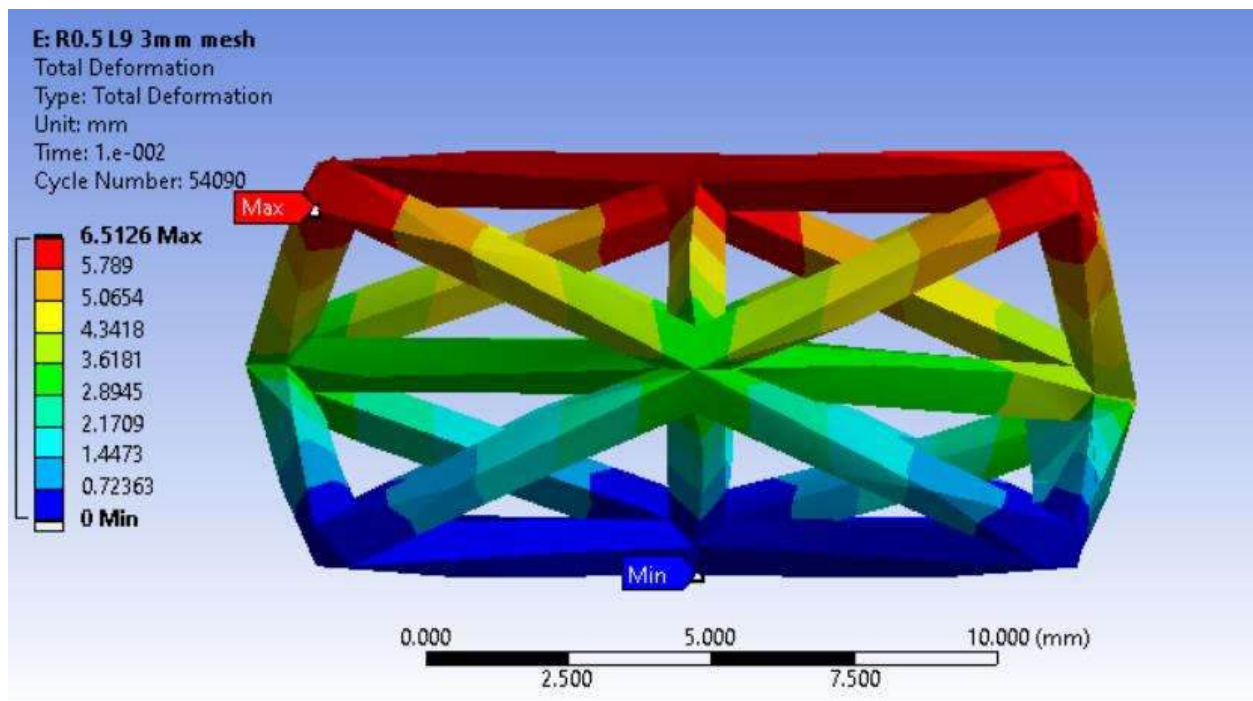


Figure 55: Total Deformation for R0.5 mm L9.0 mm with a 3 mm mesh.

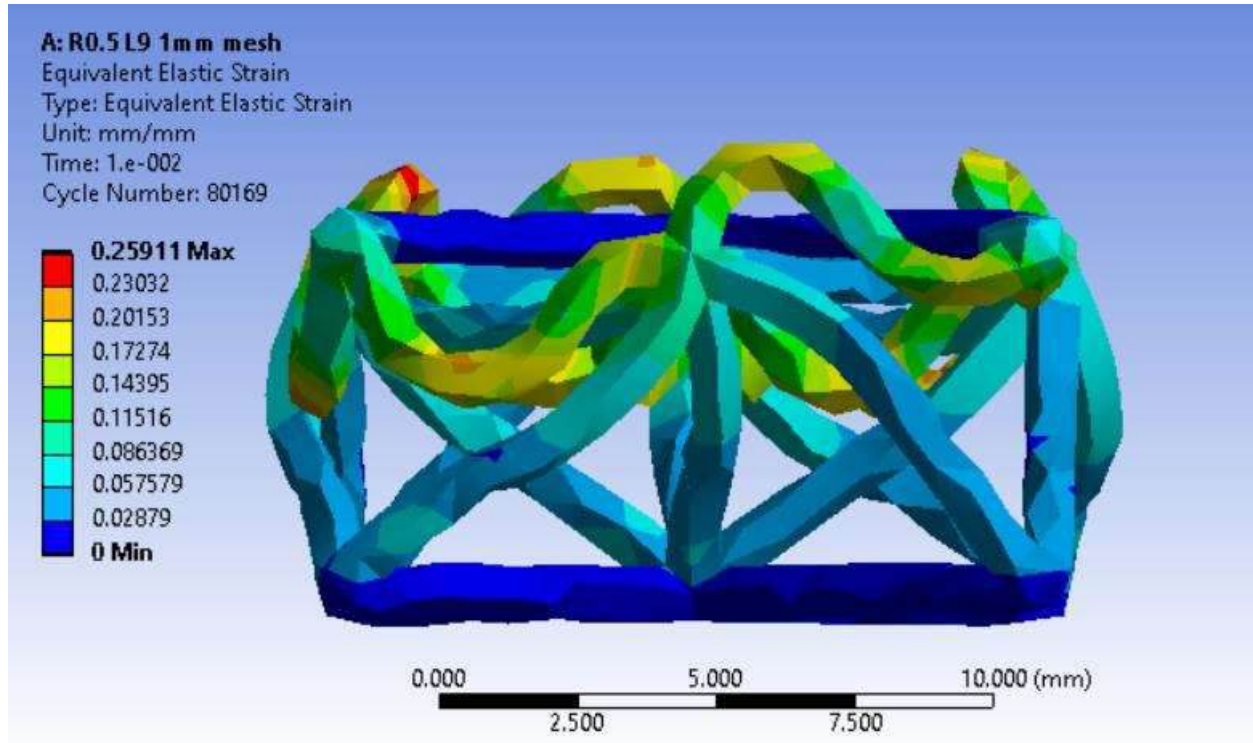


Figure 56: Elastic Strain for R0.5 mm L9.0 mm with a 1 mm mesh.

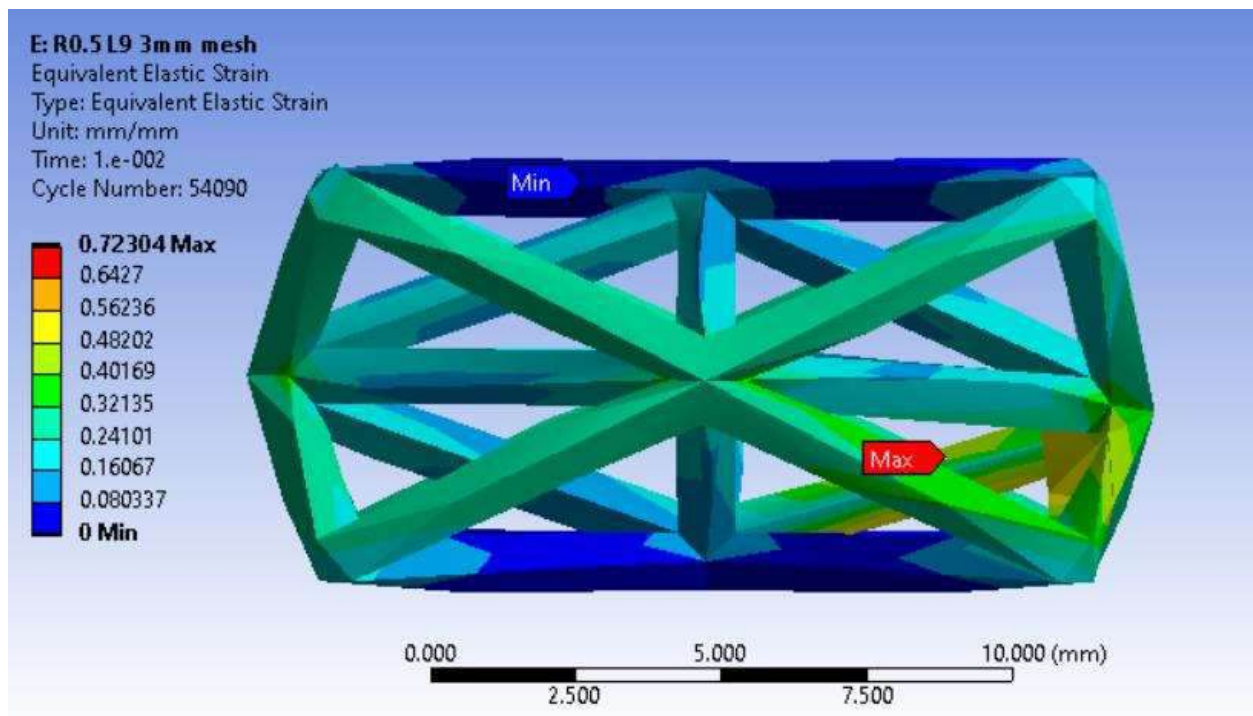


Figure 57: Elastic Strain for R0.5 mm L9.0 mm with a 3 mm mesh.

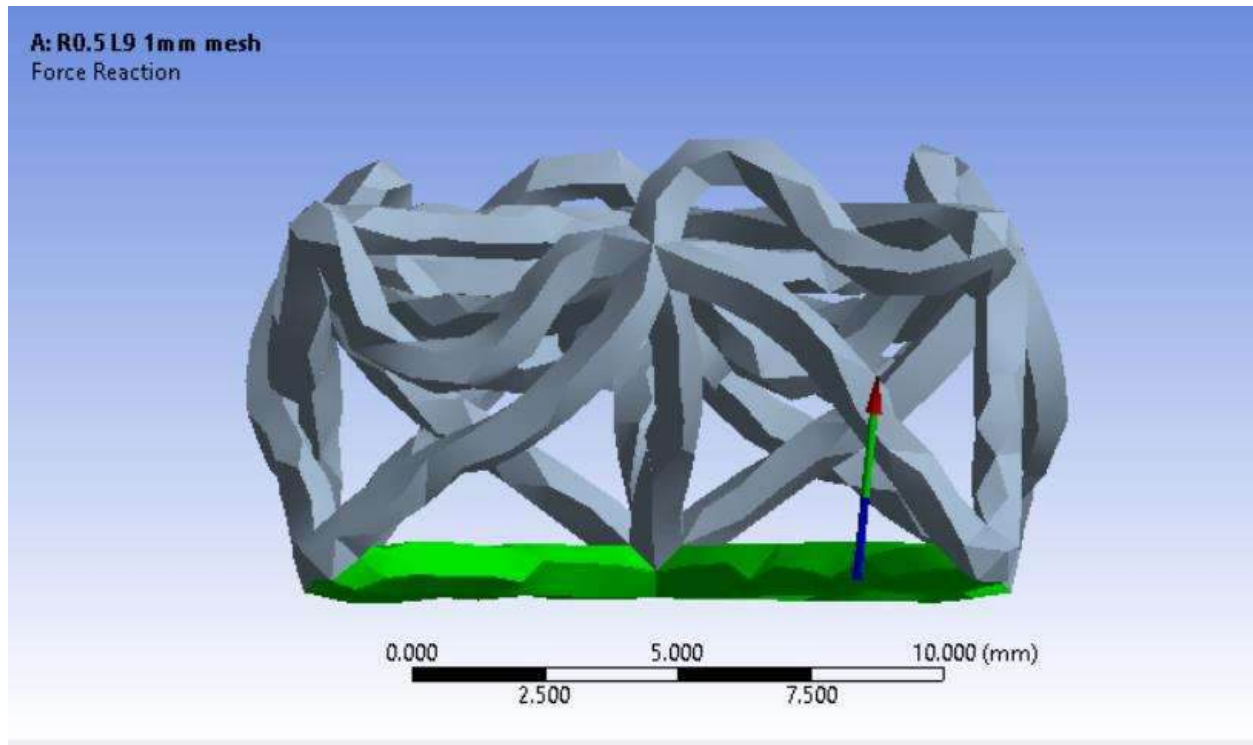


Figure 58: Force Reaction for R0.5 mm L9.0 mm with a 1 mm mesh.

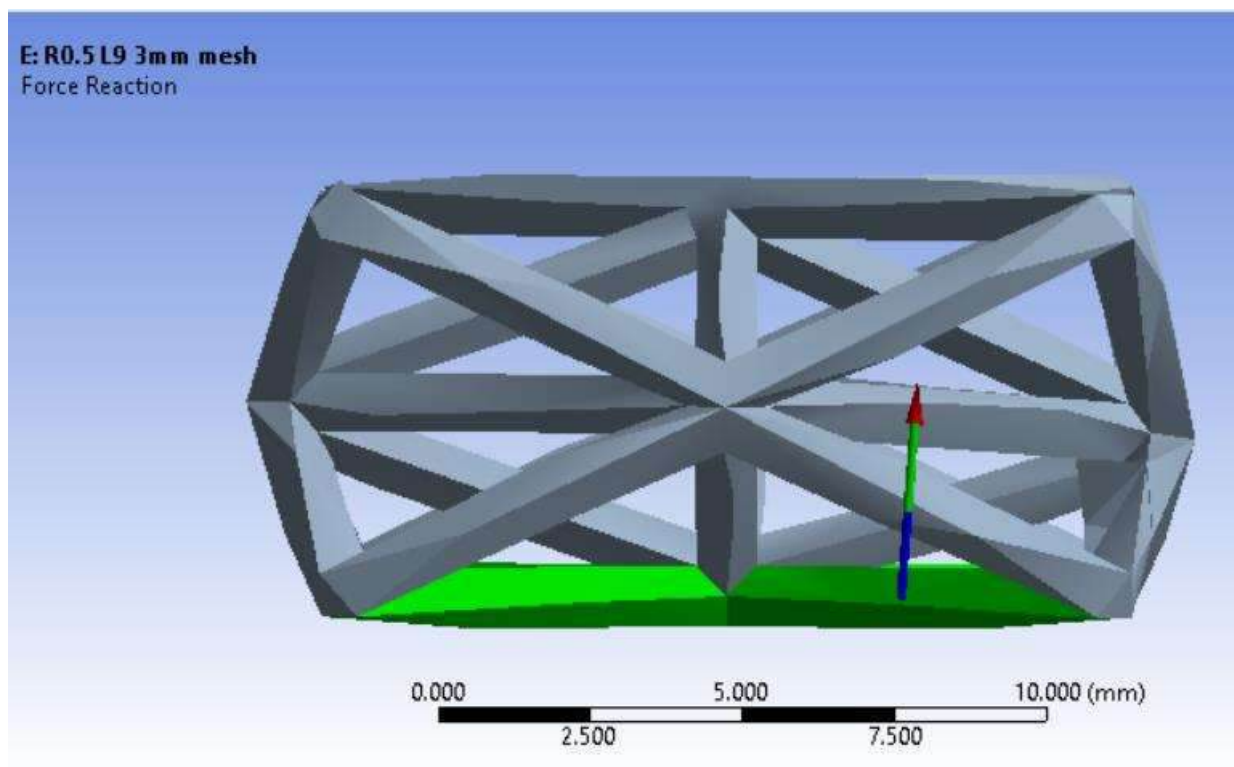


Figure 59: Force Reaction for R0.5 mm L9.0 mm with a 3 mm mesh.

7.5.1.1.2 Unit Cell R 0.5 mm L 10.80 mm

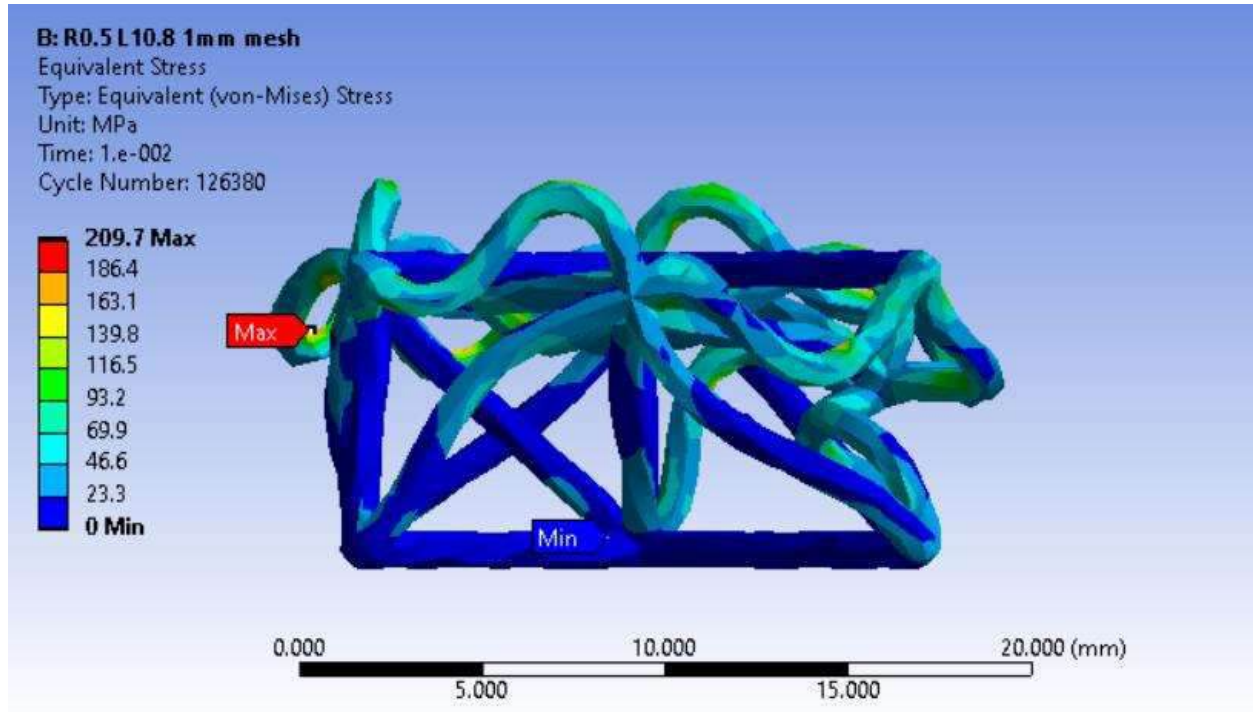


Figure 60: Equivalent Stress for R0.5 mm L10.80 mm with a 1 mm mesh.

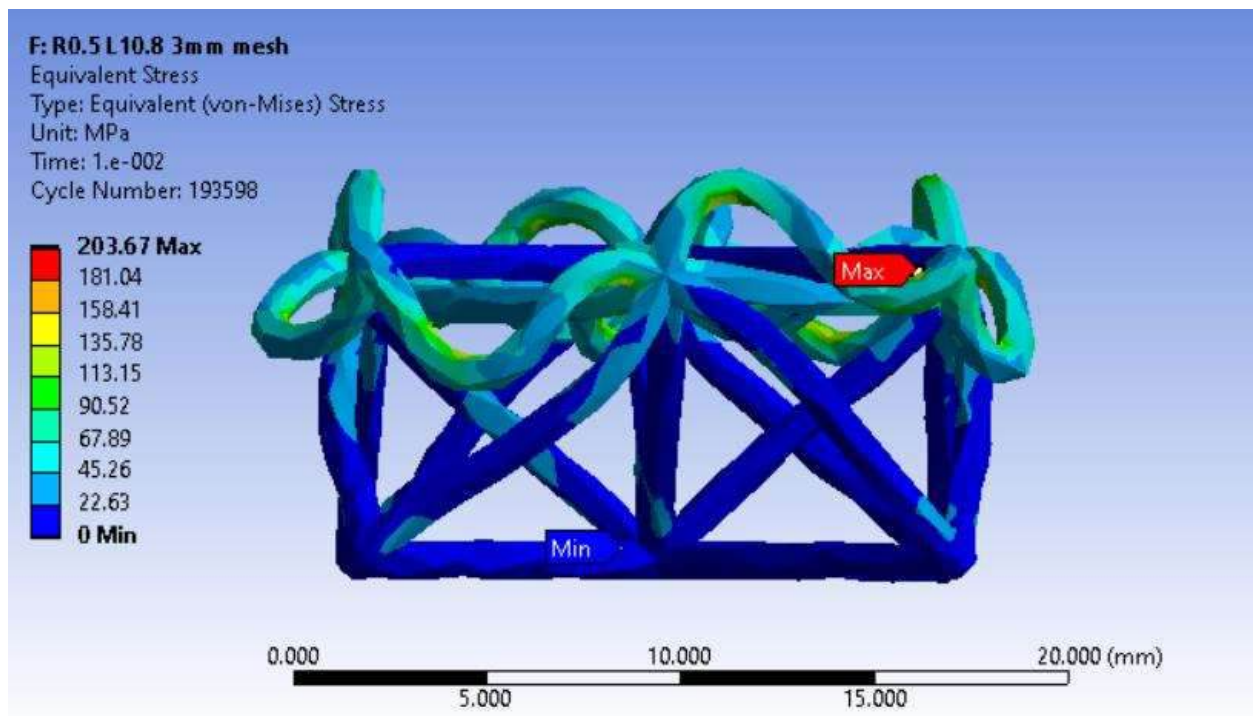


Figure 61: Equivalent Stress for R0.5 mm L10.80 mm with a 3 mm mesh.

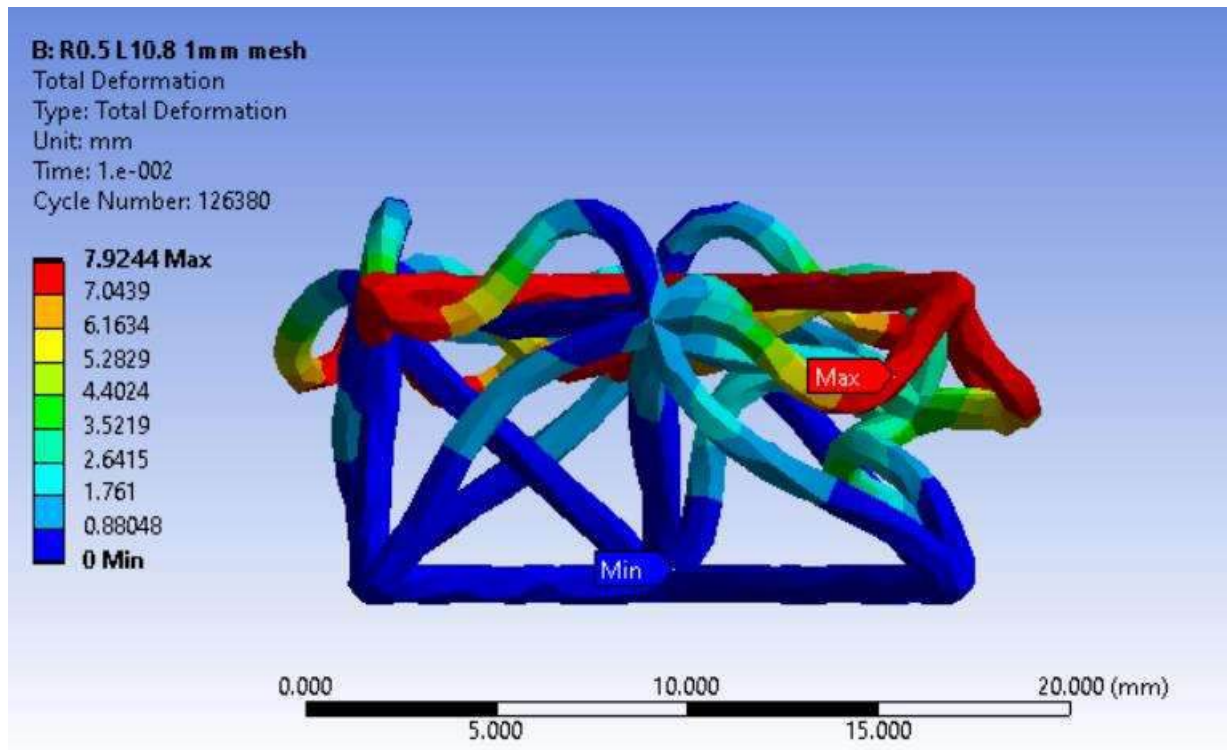


Figure 62: Total Deformation for R0.5 mm L10.80 mm with a 1 mm mesh.

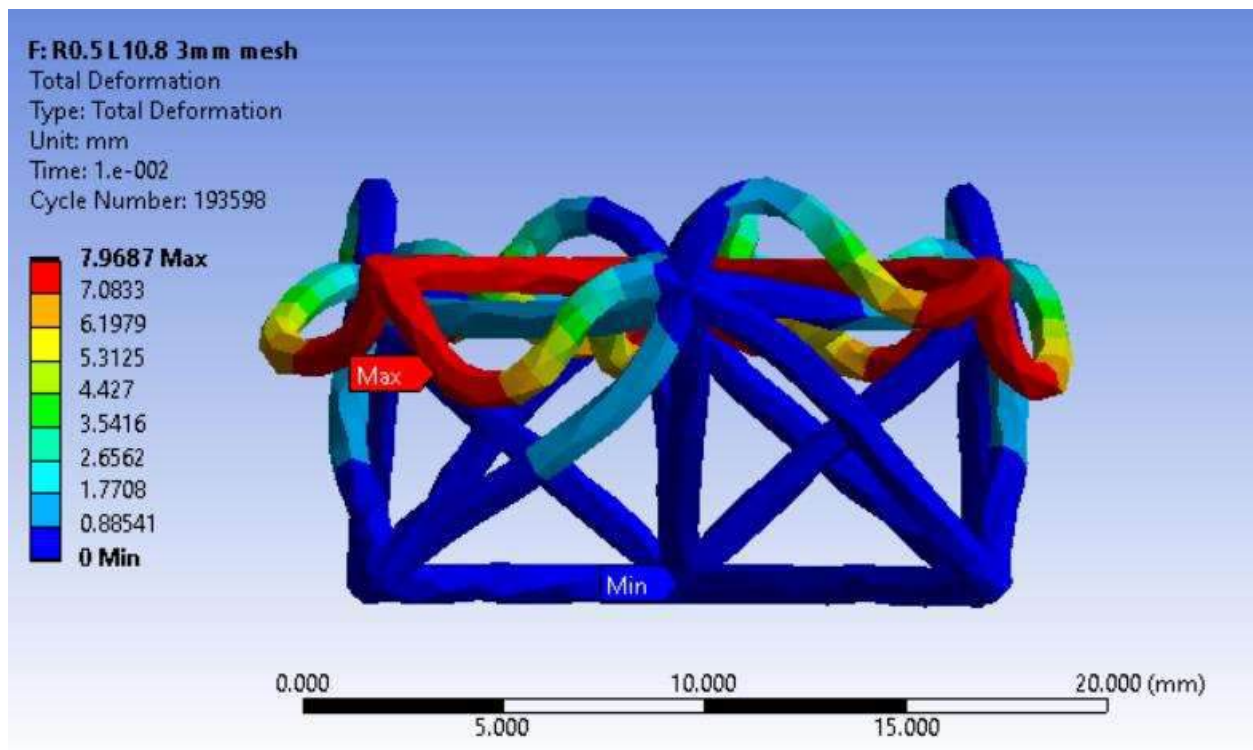


Figure 63: Total Deformation for R0.5 mm L10.80 mm with a 3 mm mesh.

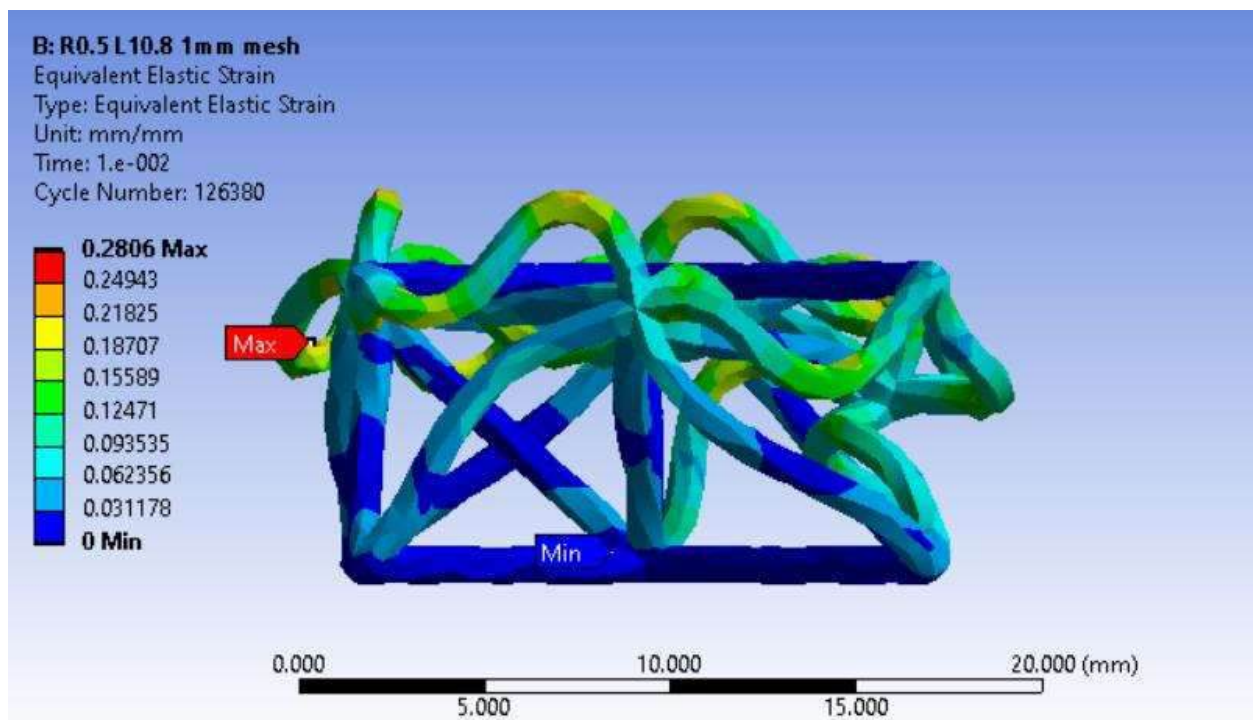


Figure 64: Elastic Strain for R0.5 mm L10.80 mm with a 1 mm mesh.

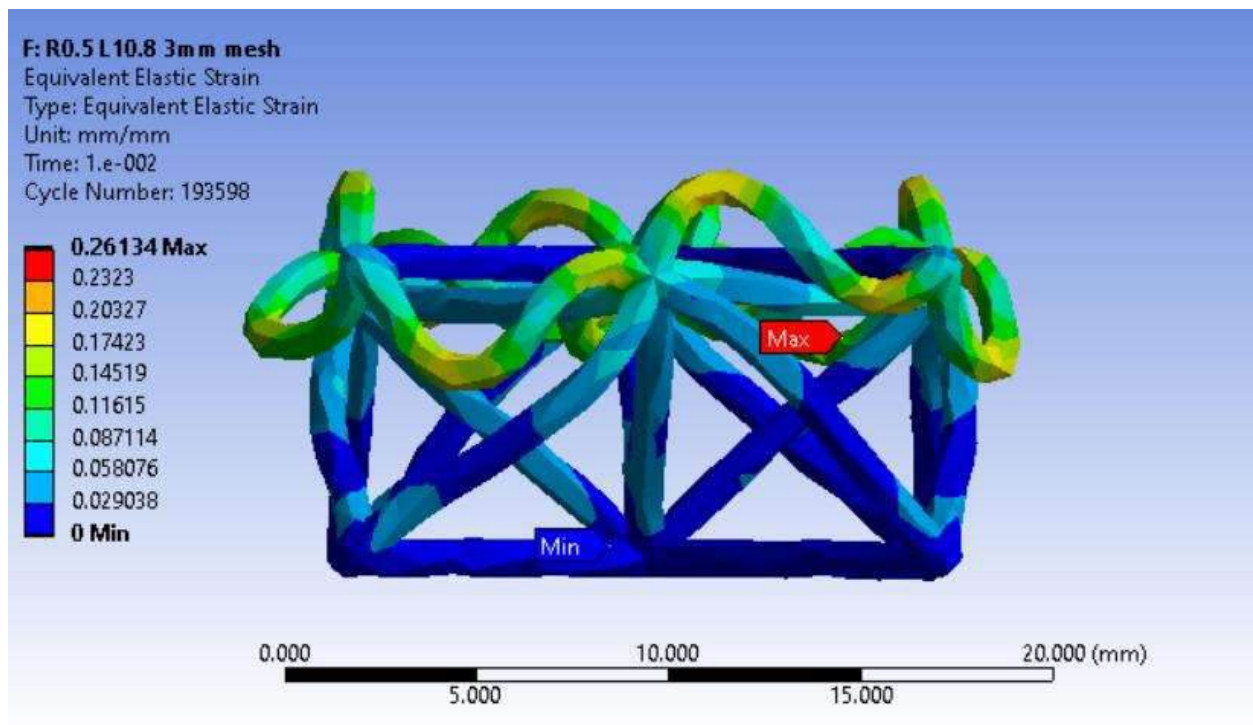


Figure 65: Elastic Strain for R0.5 mm L10.80 mm with a 3 mm mesh.

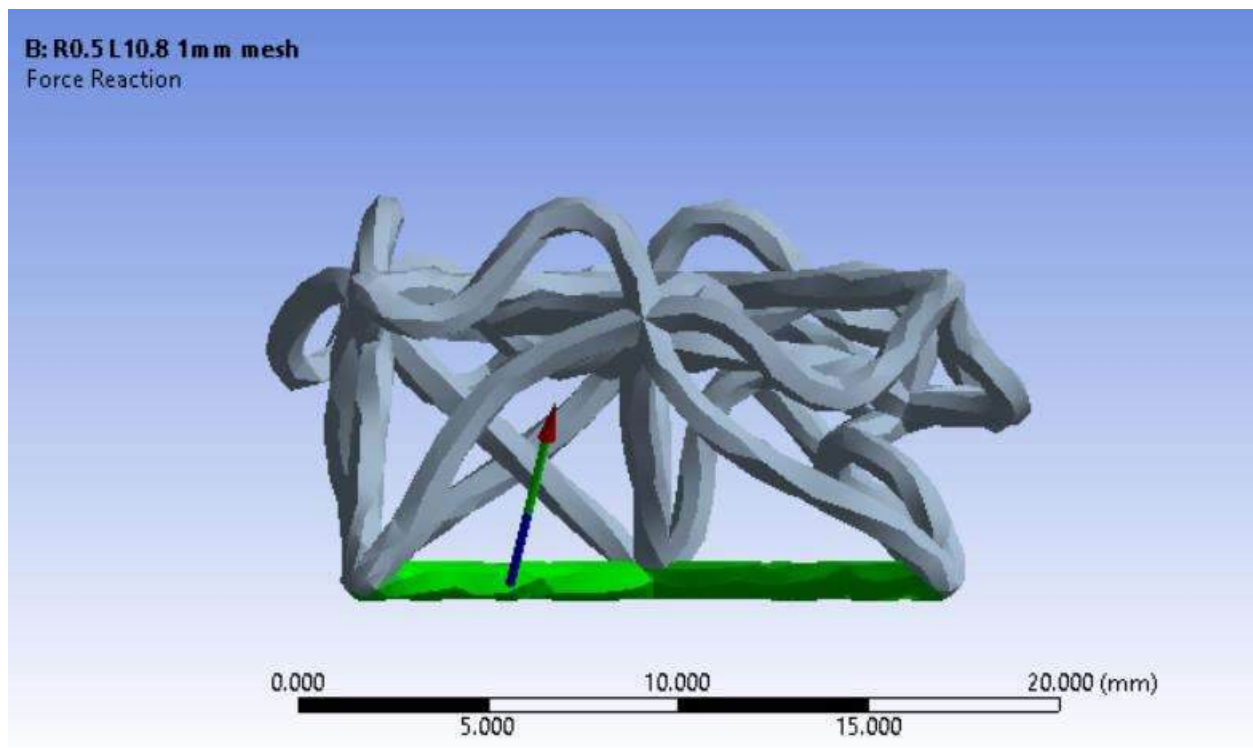


Figure 66: Force Reaction for R0.5 mm L10.80 mm with a 1 mm mesh.

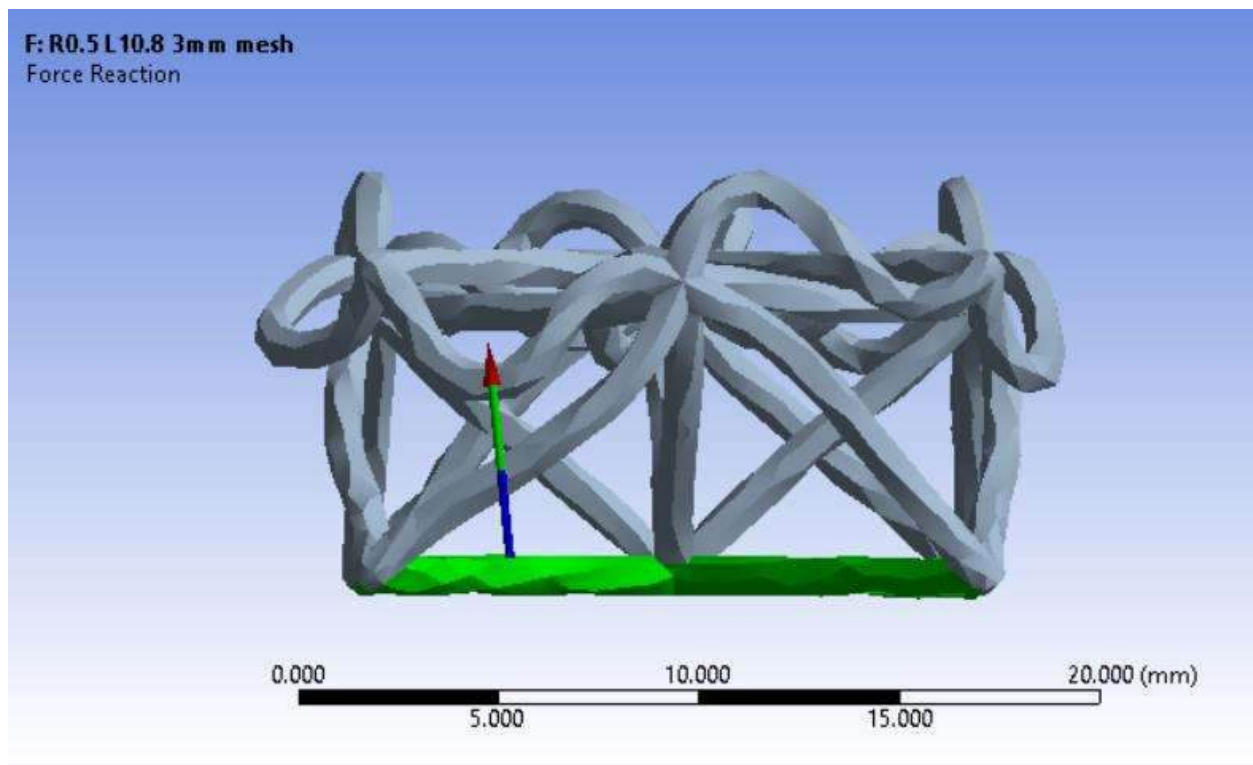


Figure 67: Force Reaction for R0.5 mm L10.80 mm with a 3 mm mesh.

7.5.1.1.3 Unit Cell R 0.5 mm L 13.50 mm

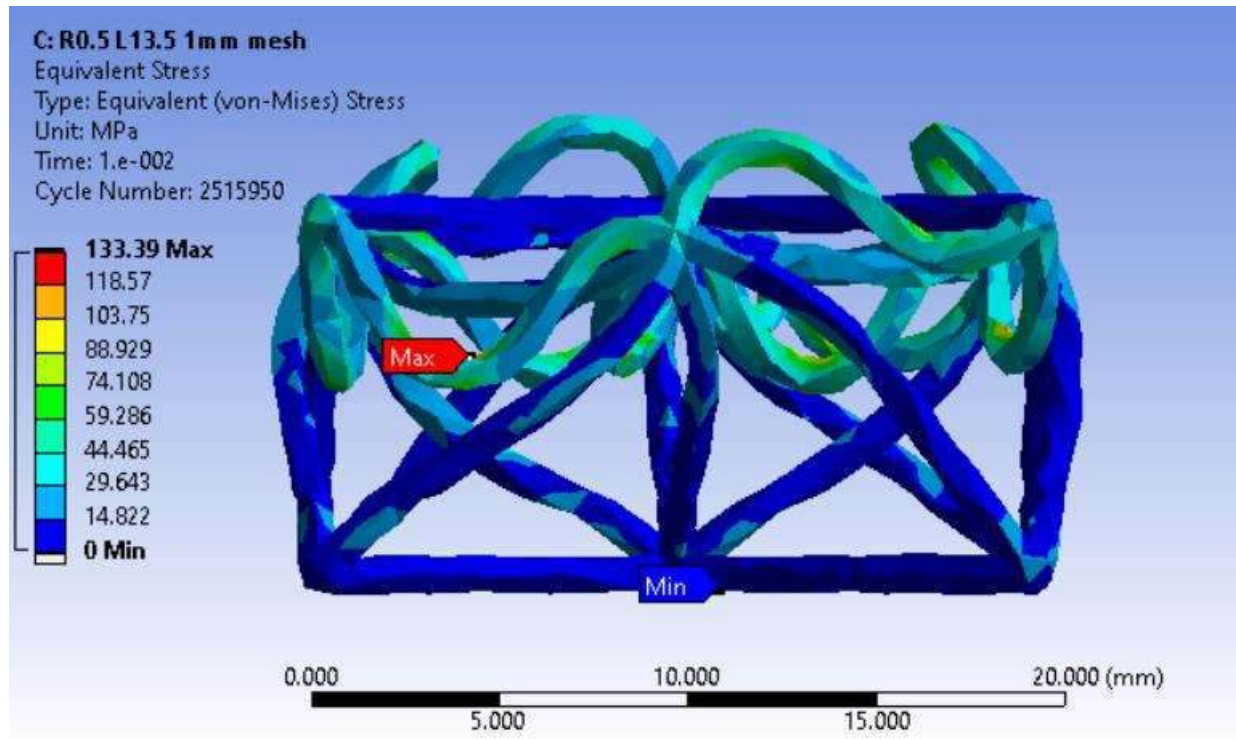


Figure 68: Equivalent Stress for R0.5 mm L13.50 mm with a 1 mm mesh.

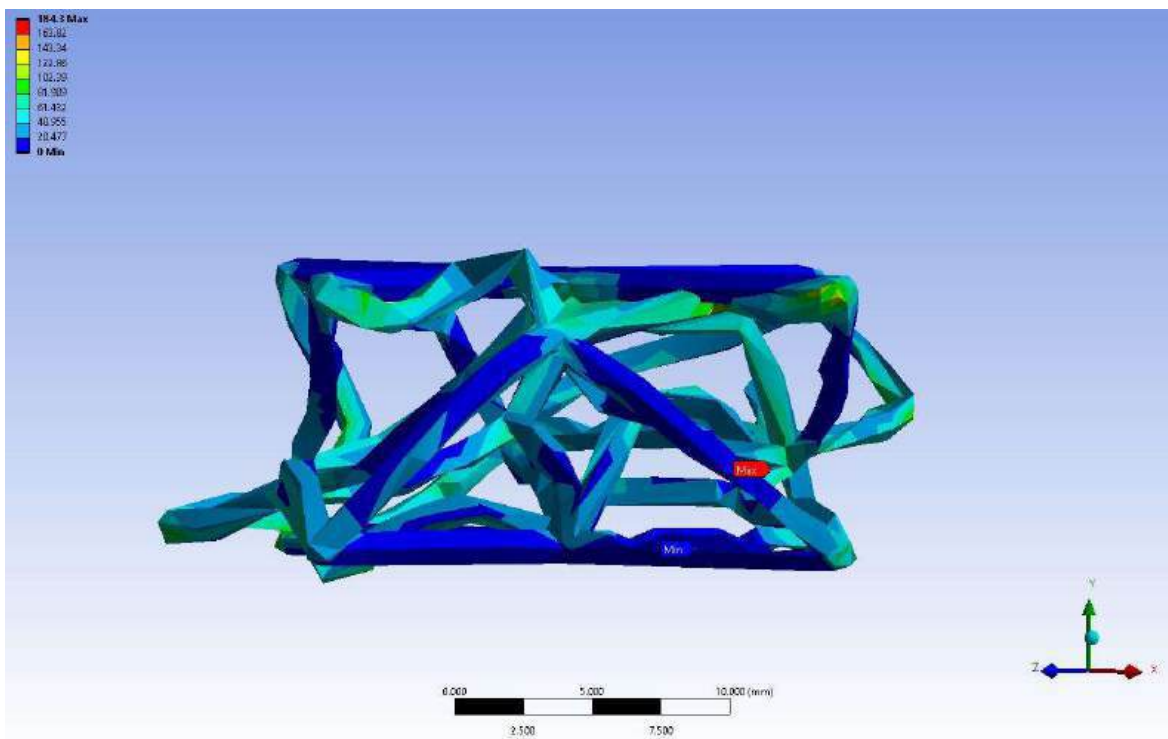


Figure 69: Equivalent Stress for R0.5 mm L13.50 mm with a 3 mm mesh.

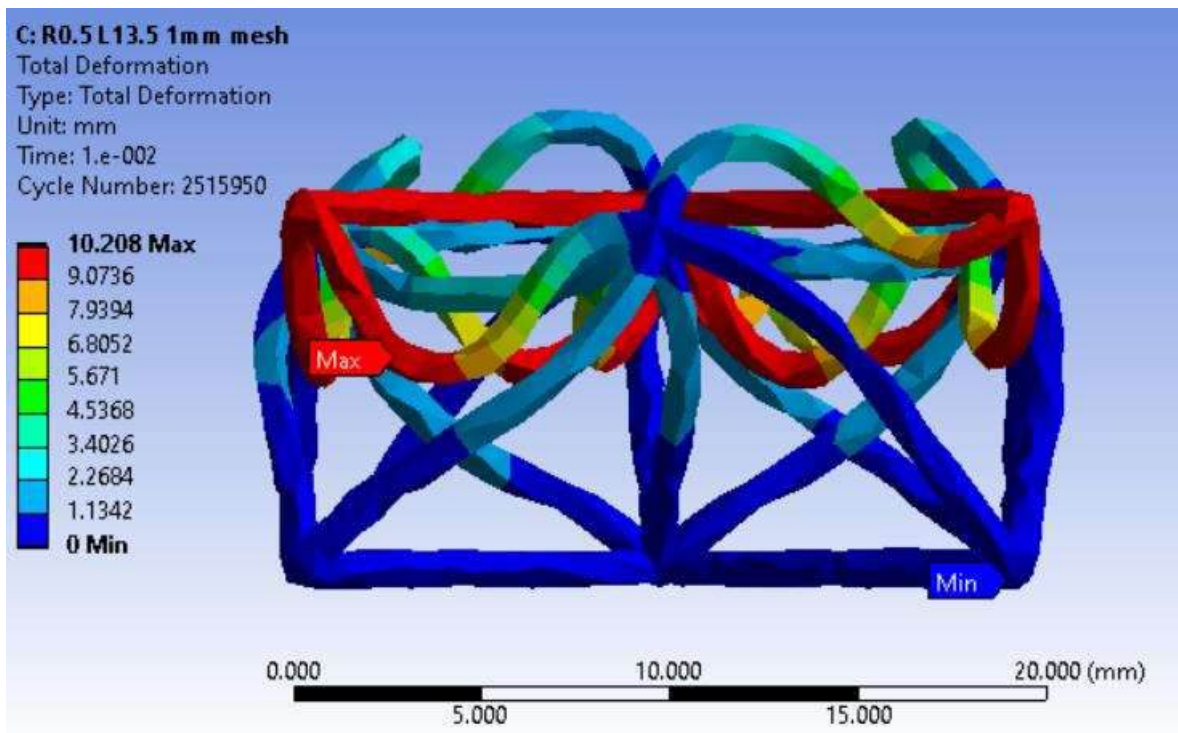


Figure 70: Total Deformation for R0.5 mm L13.50 mm with a 1 mm mesh.

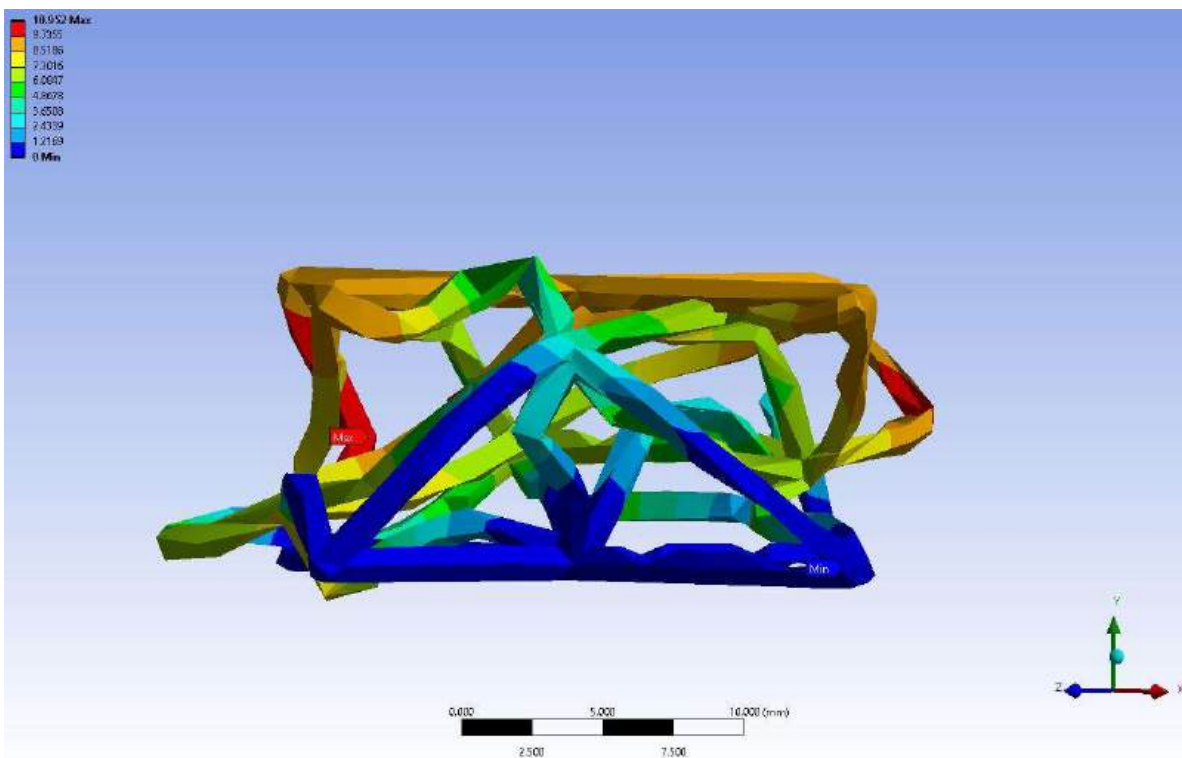


Figure 71: Total Deformation for R0.5 mm L13.50 mm with a 3 mm mesh.

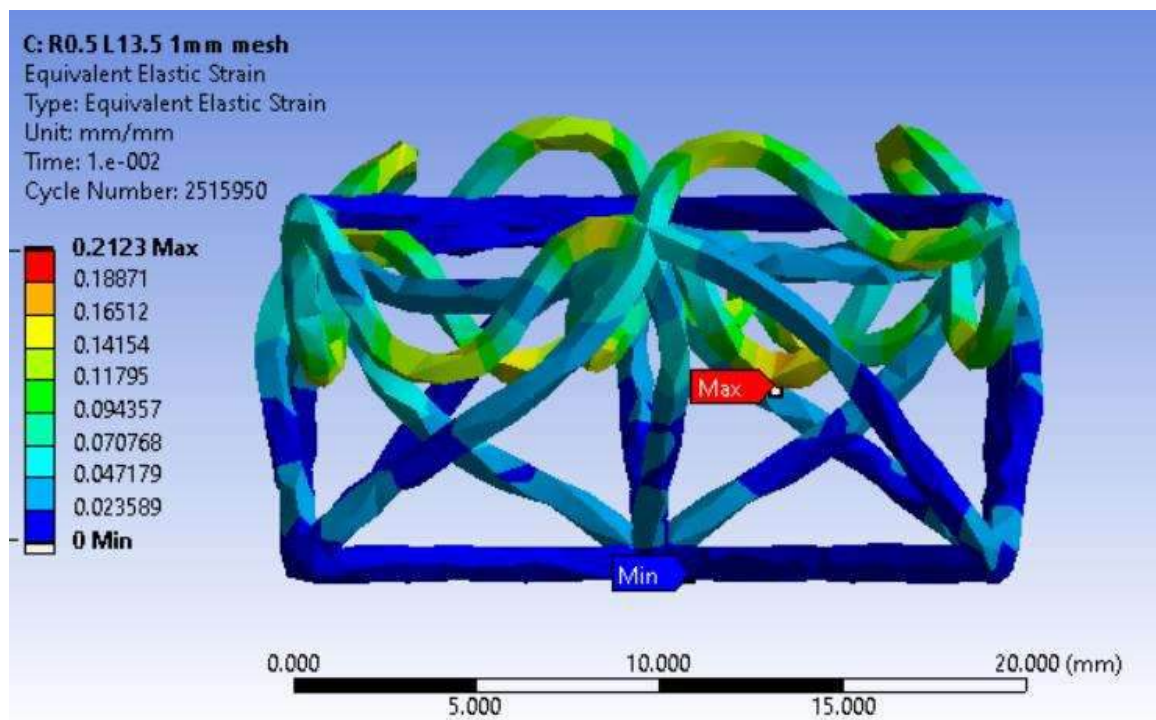


Figure 72: Elastic Strain for R0.5 mm L13.50 mm with a 1 mm mesh.

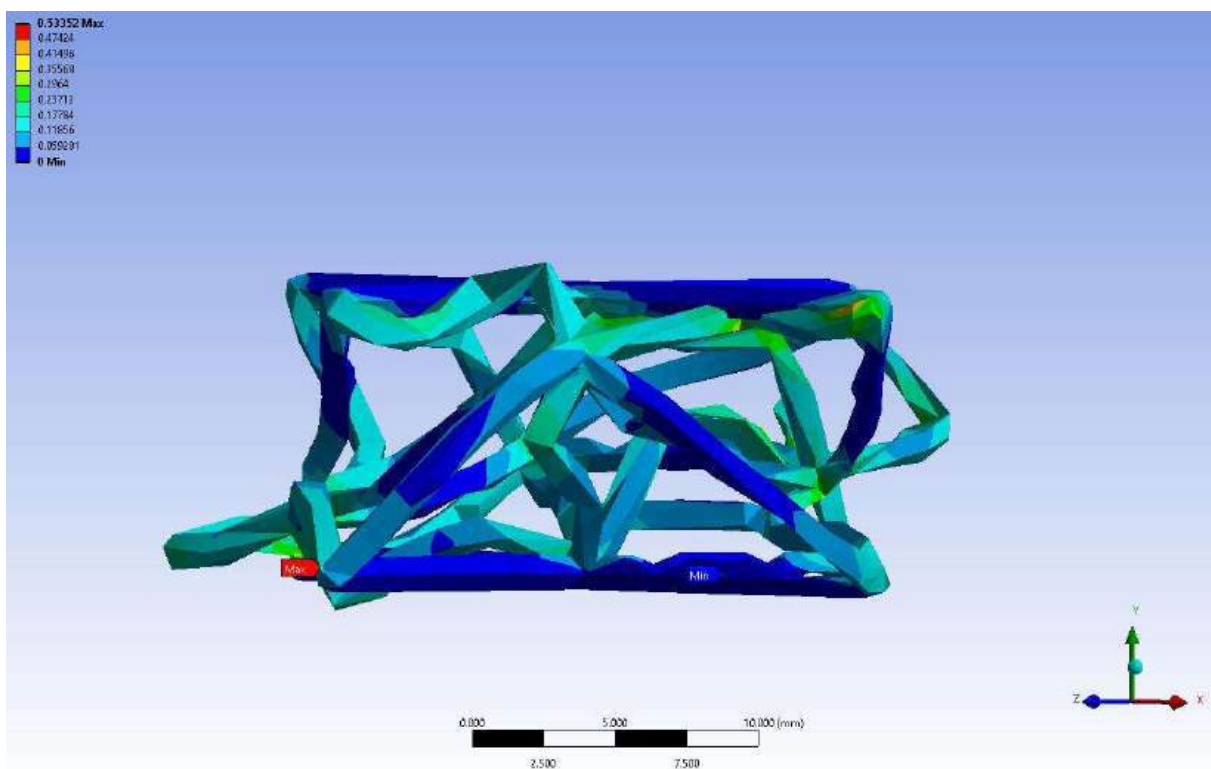


Figure 73: Elastic strain for R0.5 mm L13.50 mm with a 3 mm mesh.

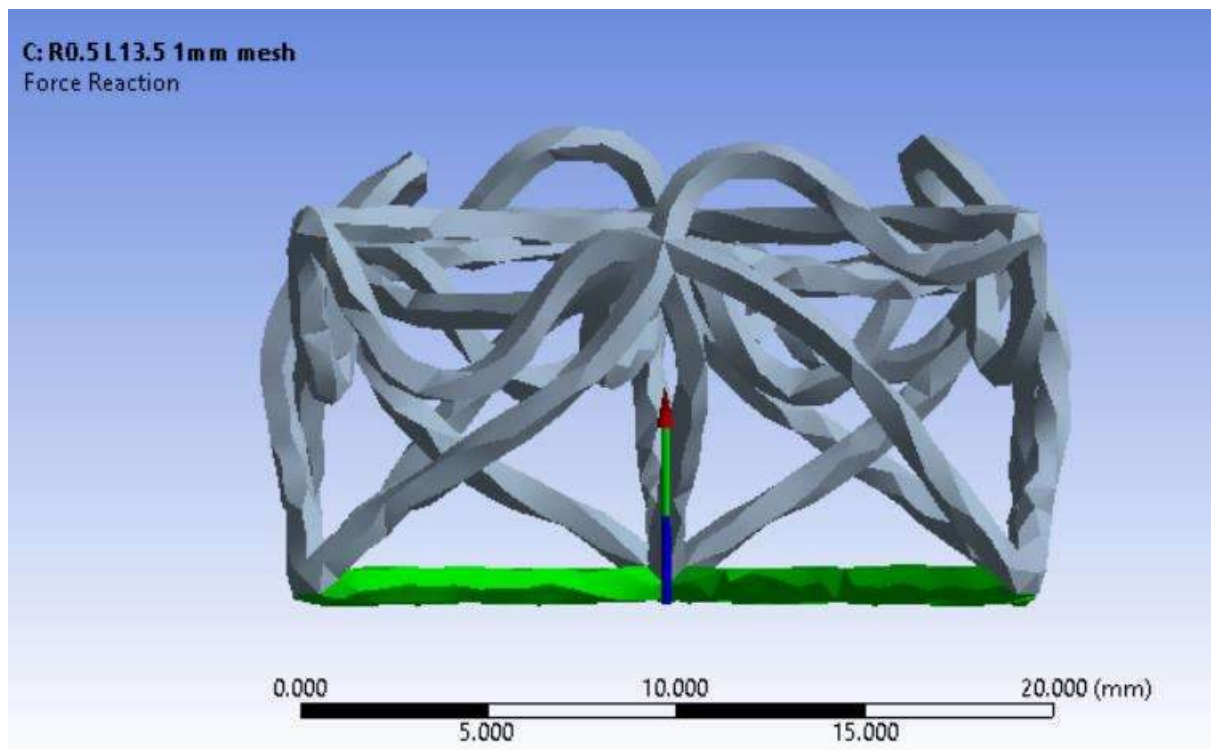


Figure 74: Force Reaction for R0.5 mm L13.50 mm with a 1 mm mesh

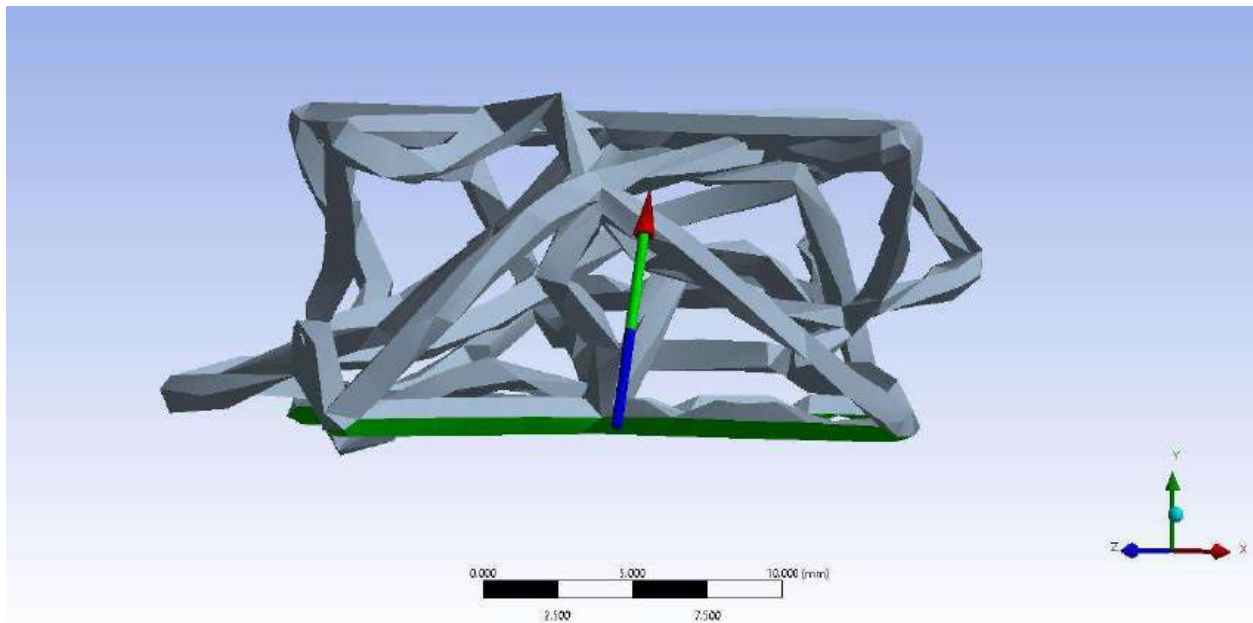


Figure 75: Force reaction for R0.5 mm L13.50 mm with a 3 mm mesh.

7.5.1.1.4 Unit Cell R 0.5 mm L 18.0 mm

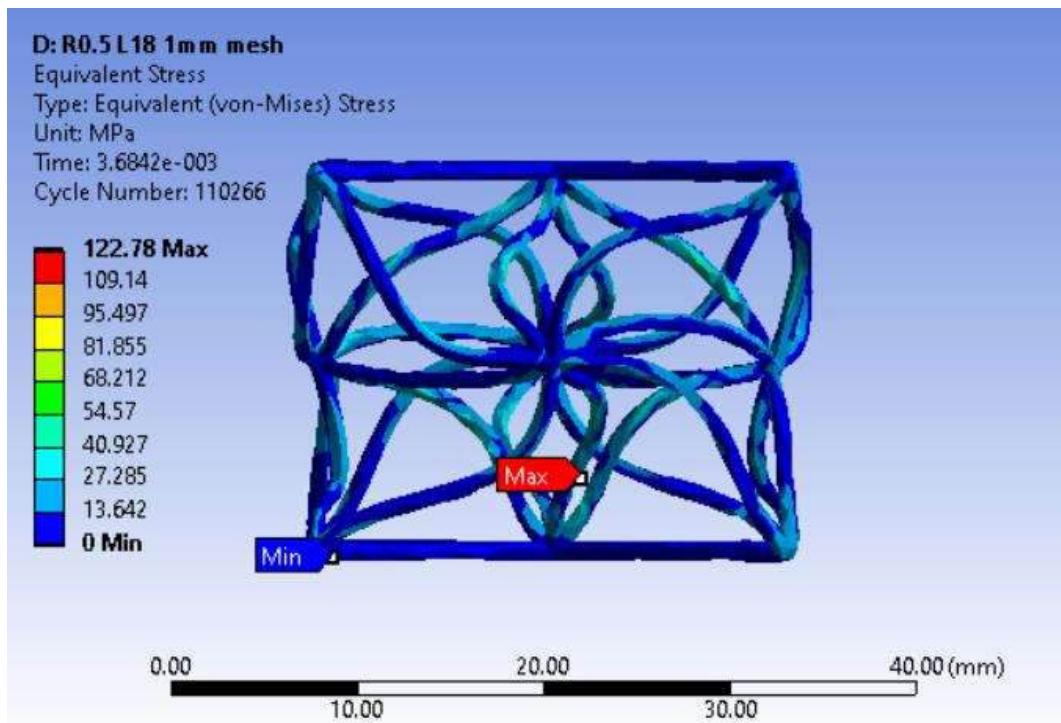


Figure 76: Equivalent Stress for R0.5 mm L18.0 mm with a 1 mm mesh.

7.5.1.2 Radii of 1.0 mm

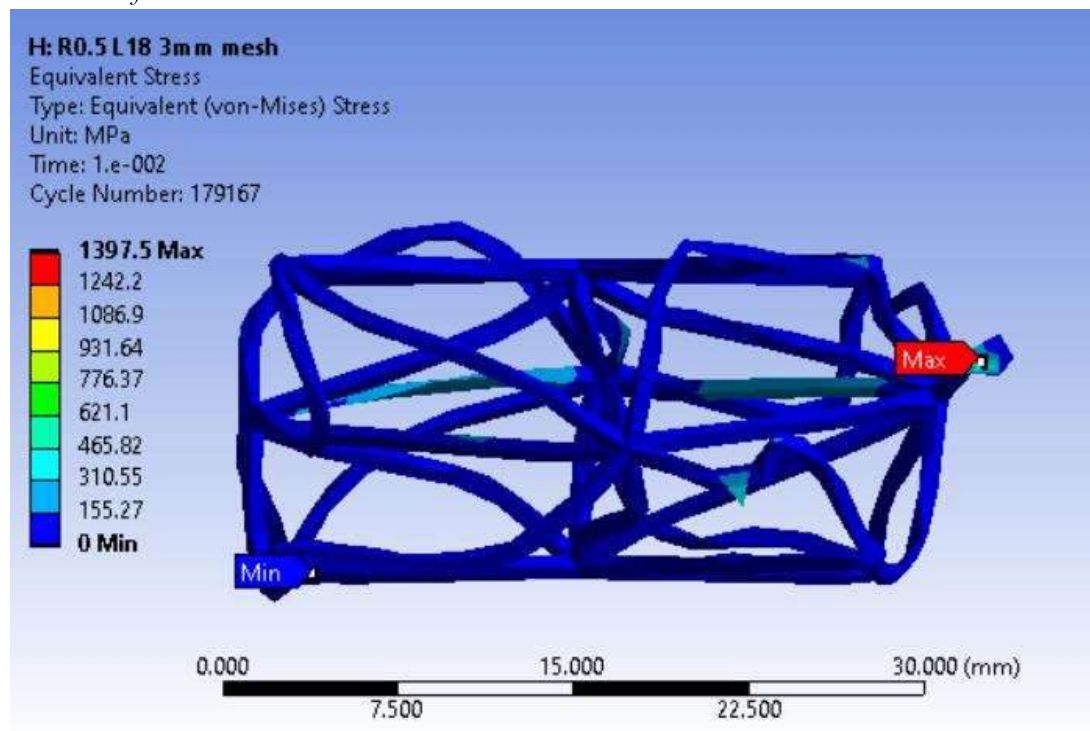


Figure 77: Equivalent Stress for R0.5 mm L18.0 mm with a 3 mm mesh.

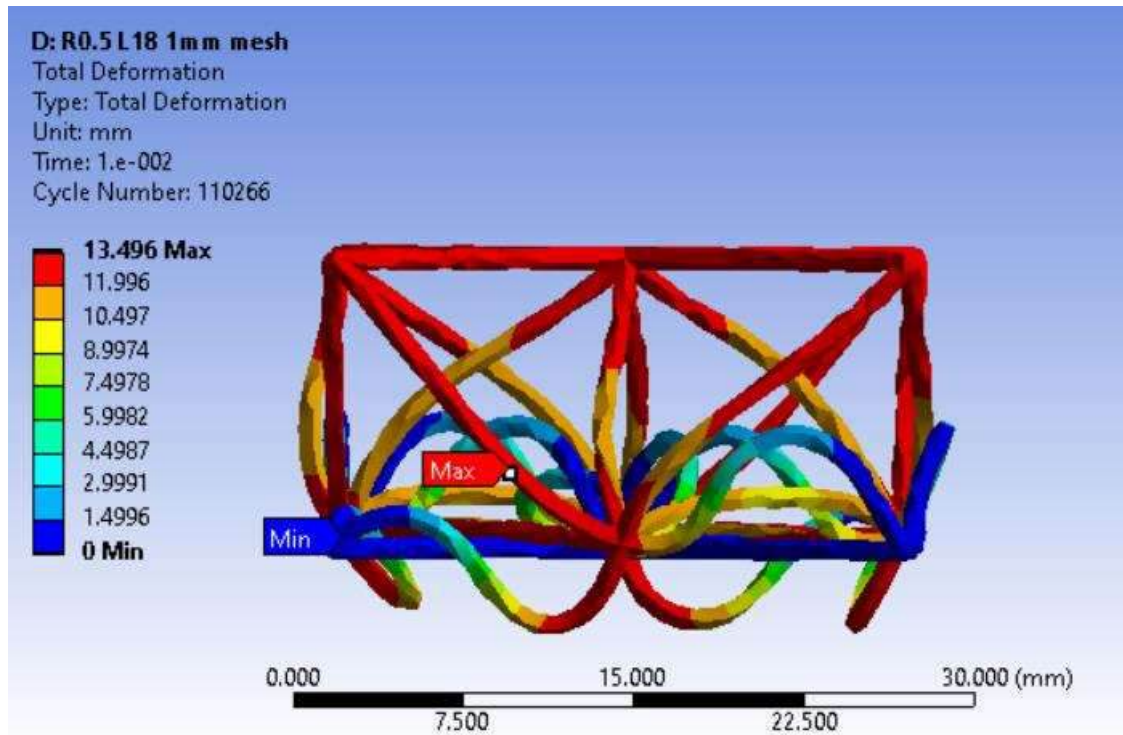


Figure 78: Total Deformation for R0.5 mm L18.0 mm with a 1 mm mesh.

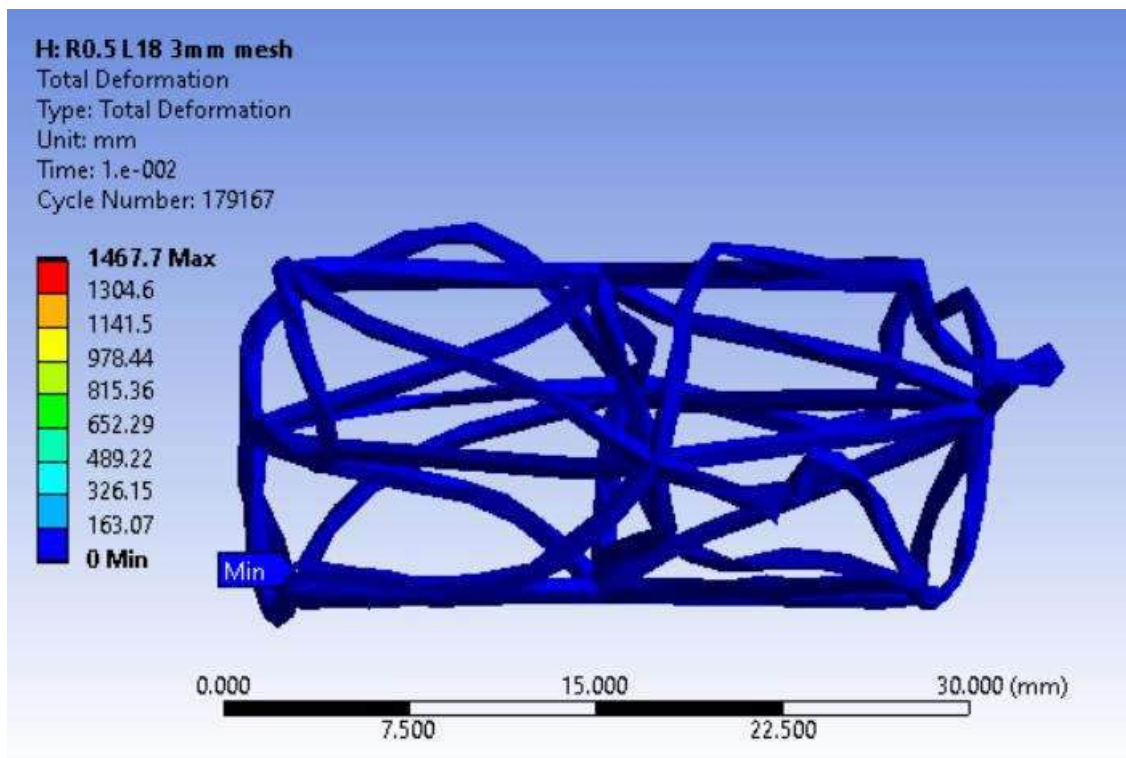


Figure 79: Total Deformation for R0.5 mm L18.0 mm with a 3 mm mesh.

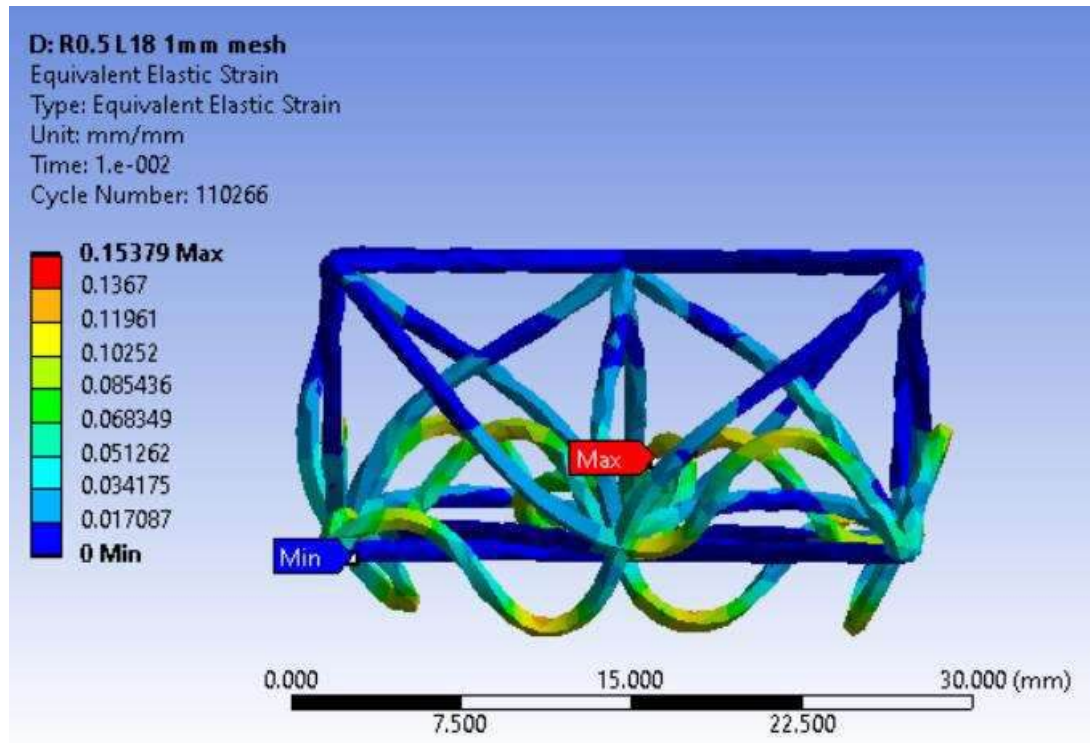


Figure 80: Elastic Strain for R0.5 mm L18.0 mm with a 1 mm mesh.

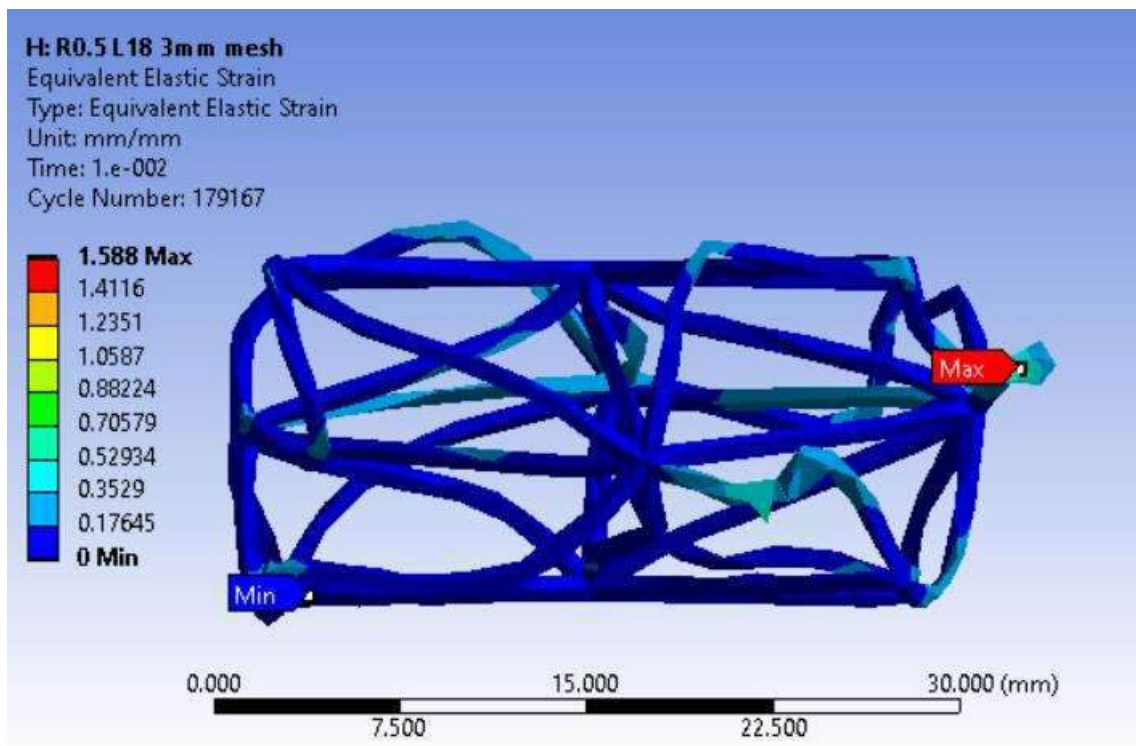


Figure 81: Elastic Strain for R0.5 mm L18.0 mm with a 3 mm mesh.

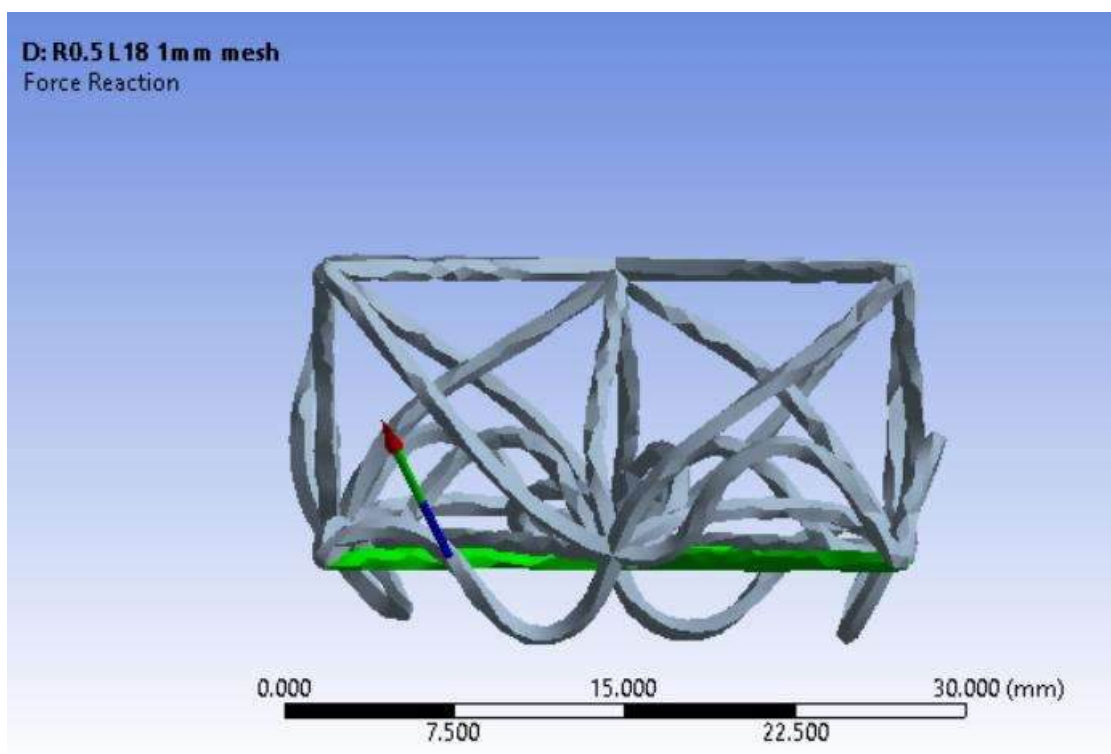


Figure 82: Force Reaction for R0.5 mm L18.0 mm with a 1 mm mesh.

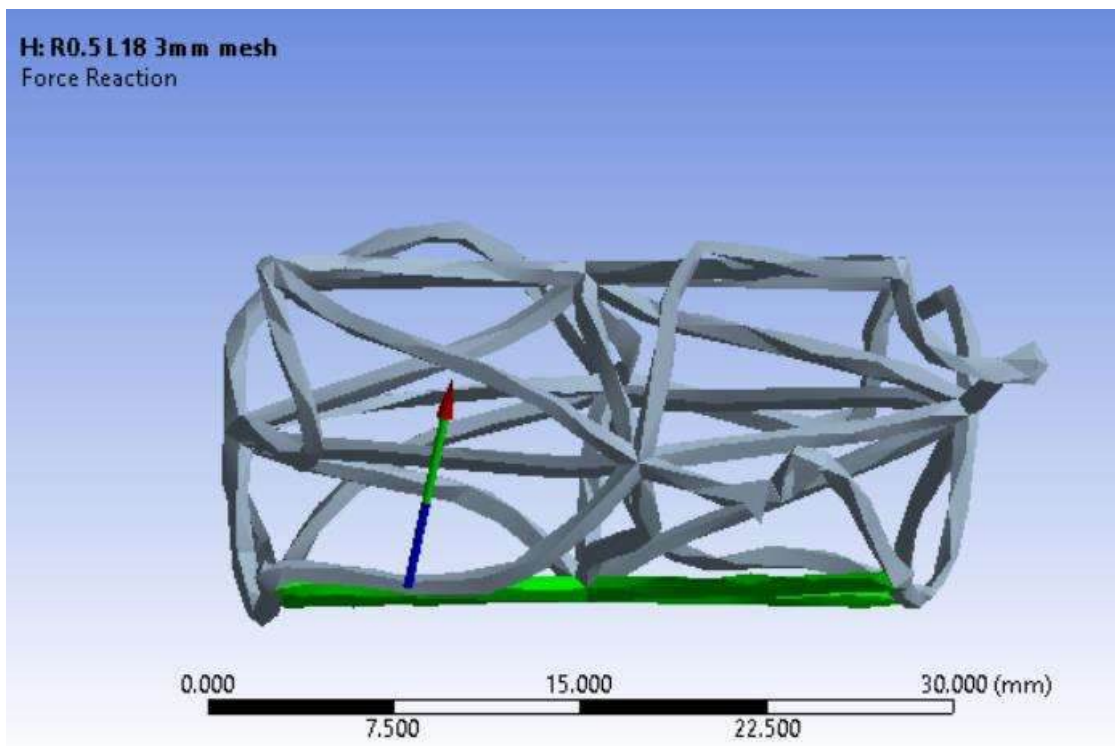


Figure 83: Force Reaction for R0.5 mm L18.0 mm with a 3 mm mesh.

7.5.1.2.1 Unit Cell R 1.0 mm L 9.0 mm

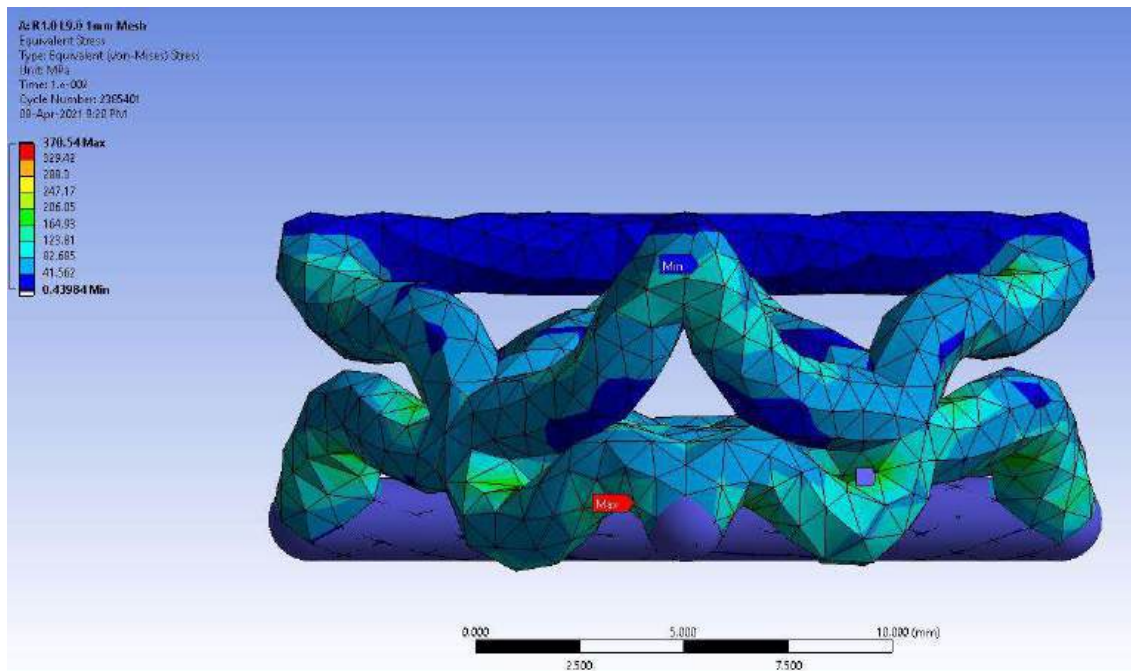


Figure 84: Equivalent Stress for R1.0 mm L9.0 mm with a 1 mm mesh (Purple region is the fixed support).

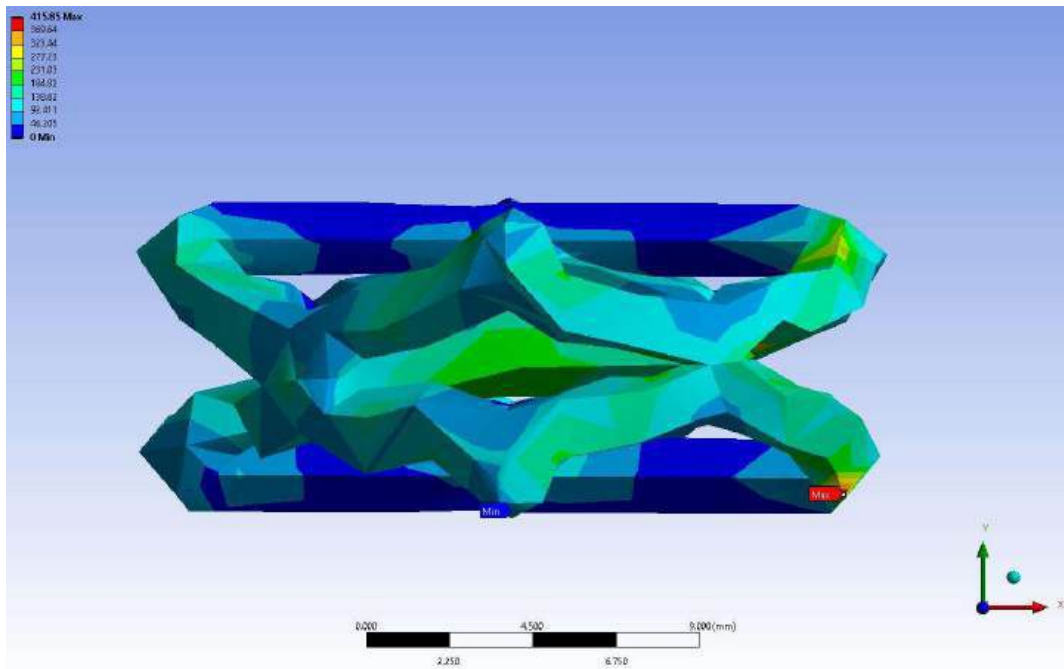


Figure 85: Equivalent Stress for R1.0 mm L9.0 mm with a 3 mm mesh.

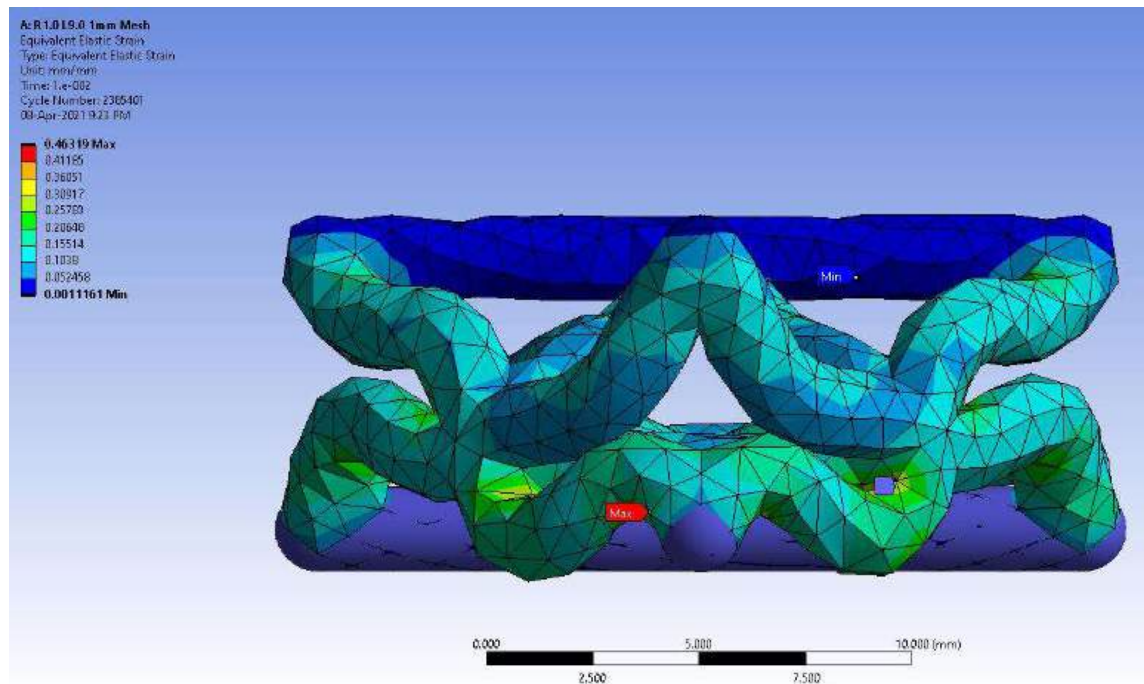


Figure 86: Elastic Strain for R1.0 mm L9.0mm with a 1 mm mesh.

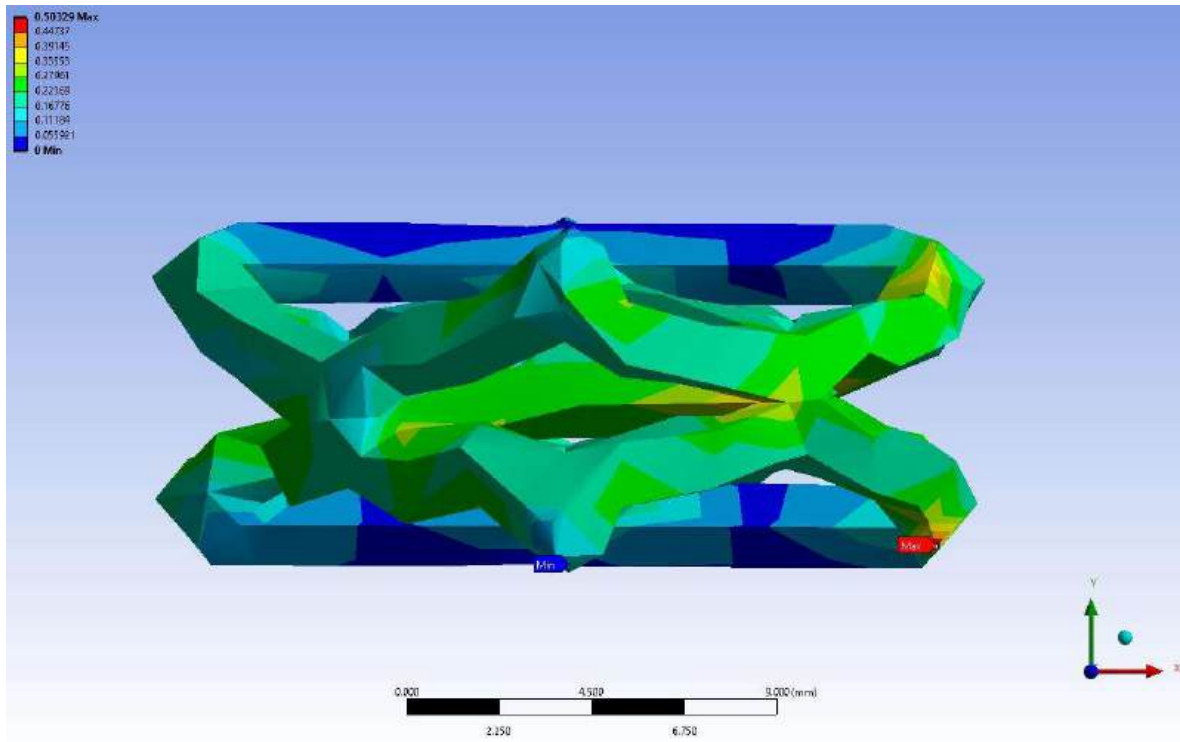


Figure 87: Elastic Strain for R1.0 mm L9.0mm with a 3 mm mesh.

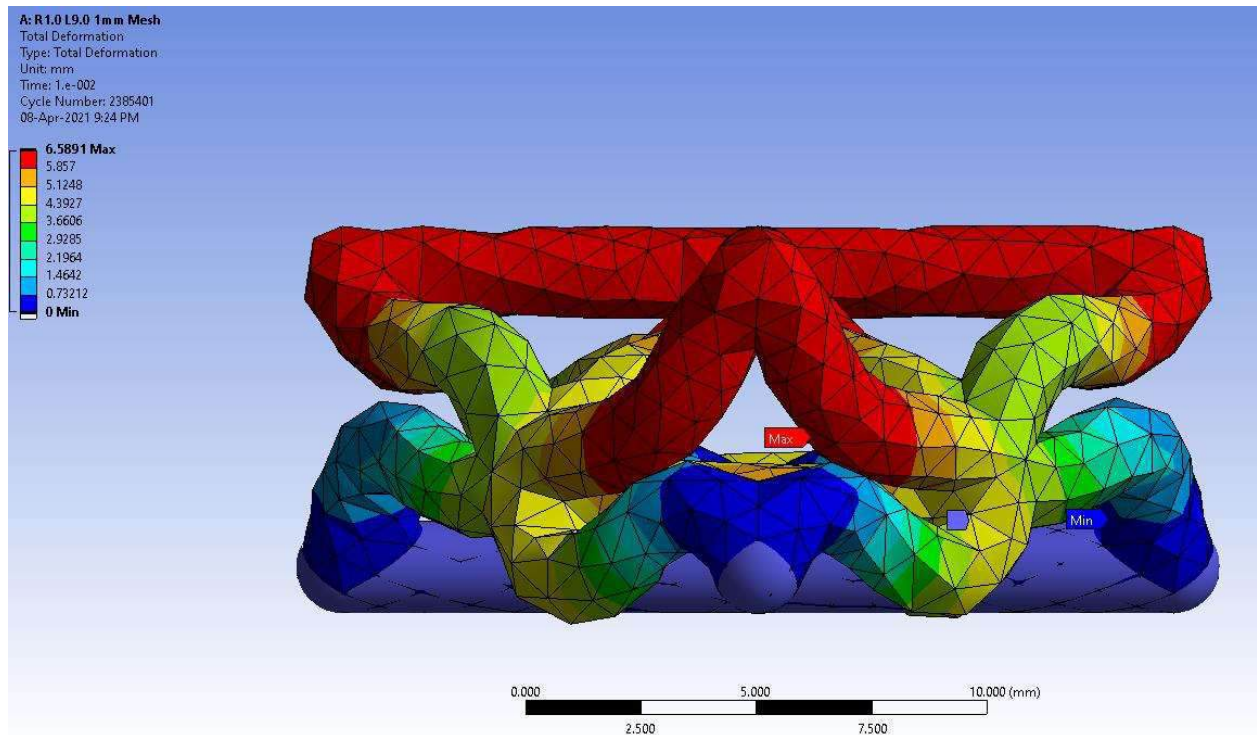


Figure 88: Total Deformation for R1.0 mm L9.0 mm with a 1 mm mesh.

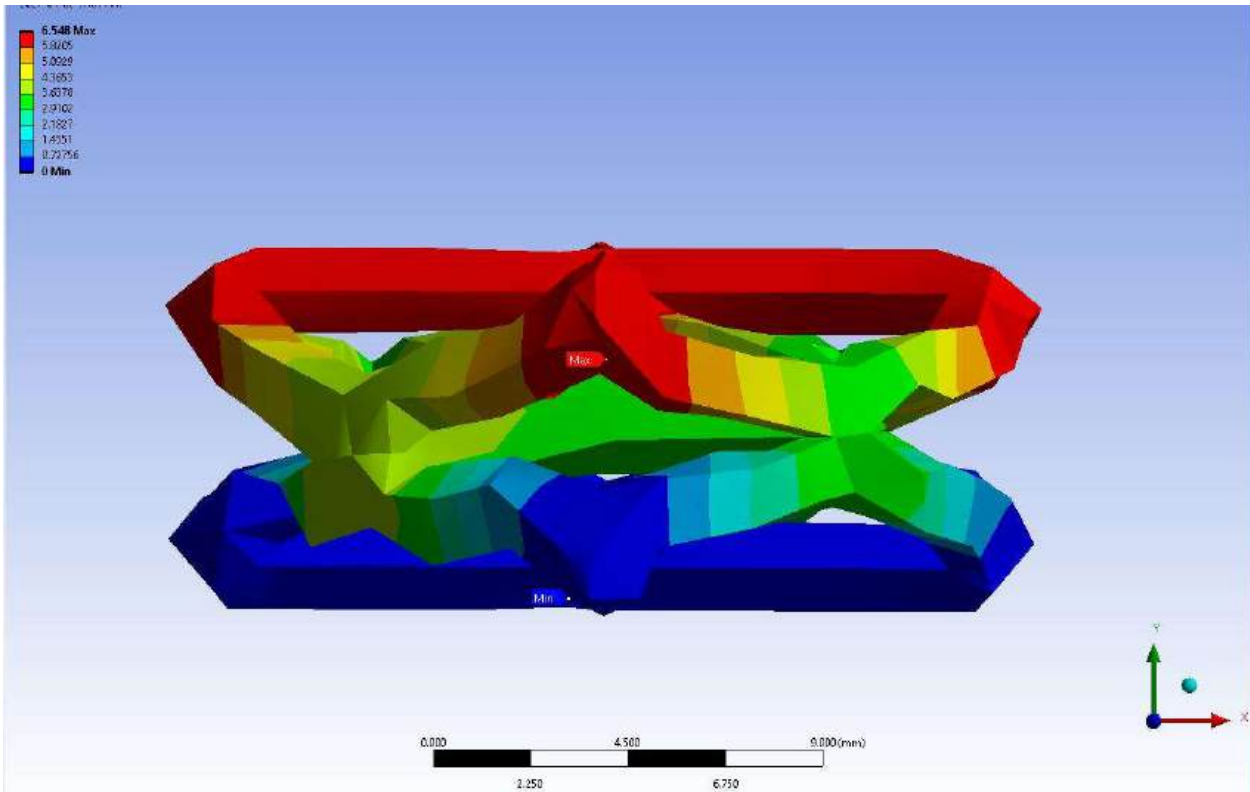


Figure 89: Total Deformation for R1.0 mm L9.0 mm with a 3 mm mesh.

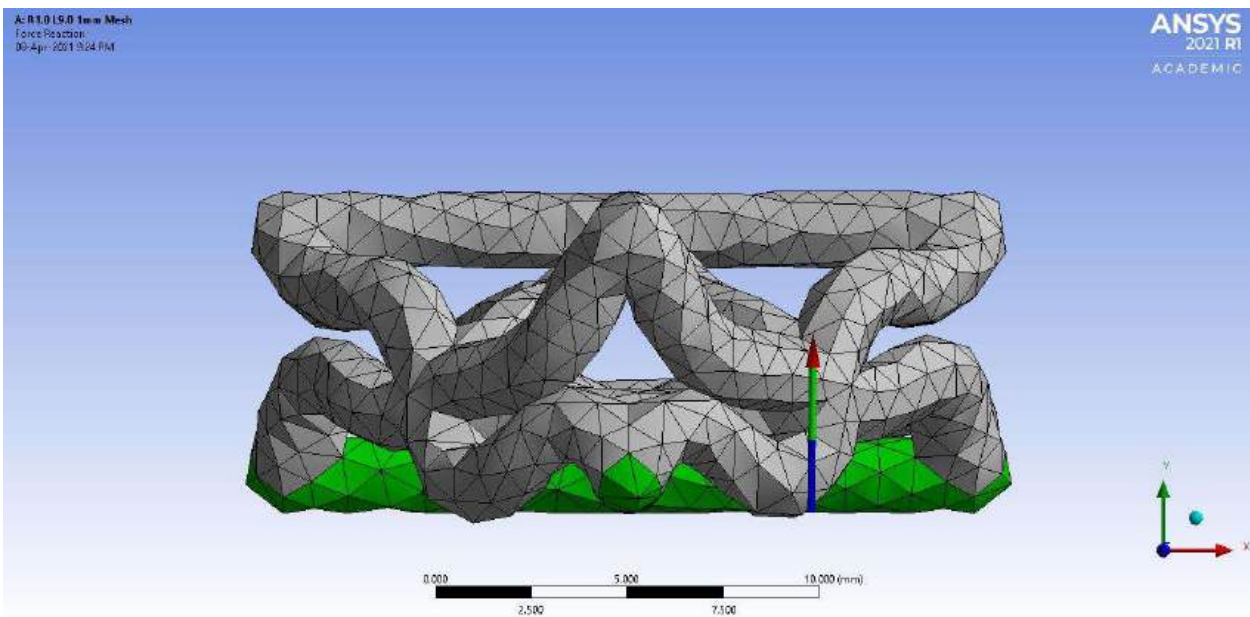


Figure 90: Force Reaction for R1.0 mm L9.0 mm with a 1 mm mesh.

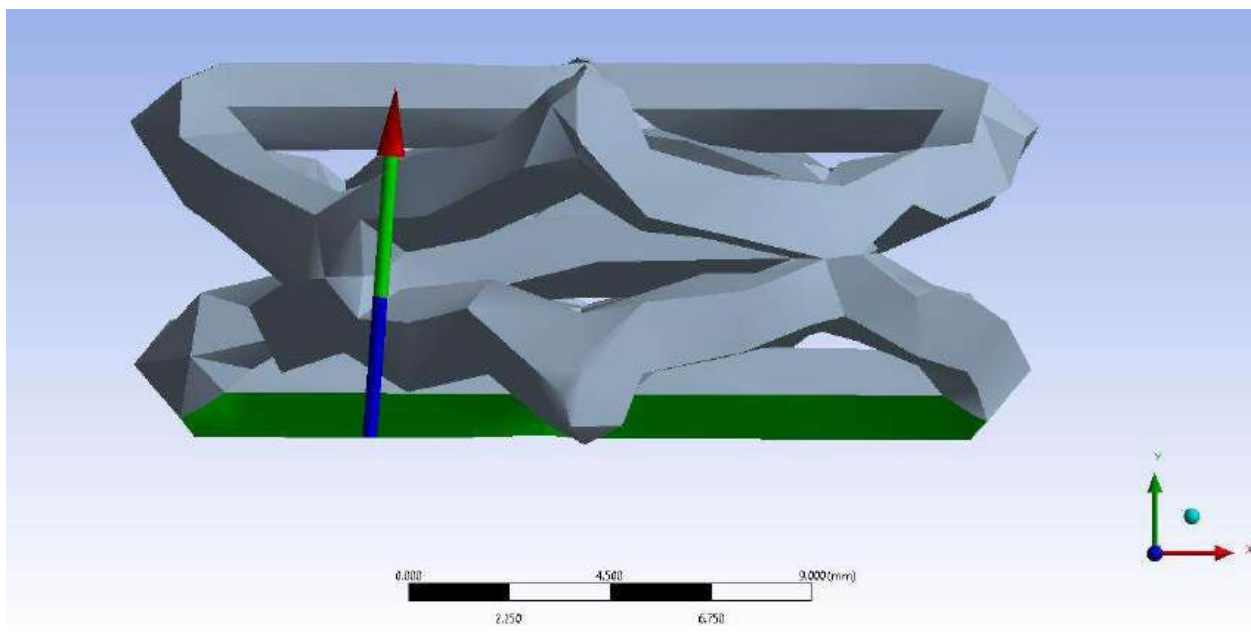


Figure 91: Force Reaction for R1.0 mm L9.0 mm with a 3 mm mesh.

7.5.1.2.2 Unit Cell R 1.0 mm L 10.80 mm

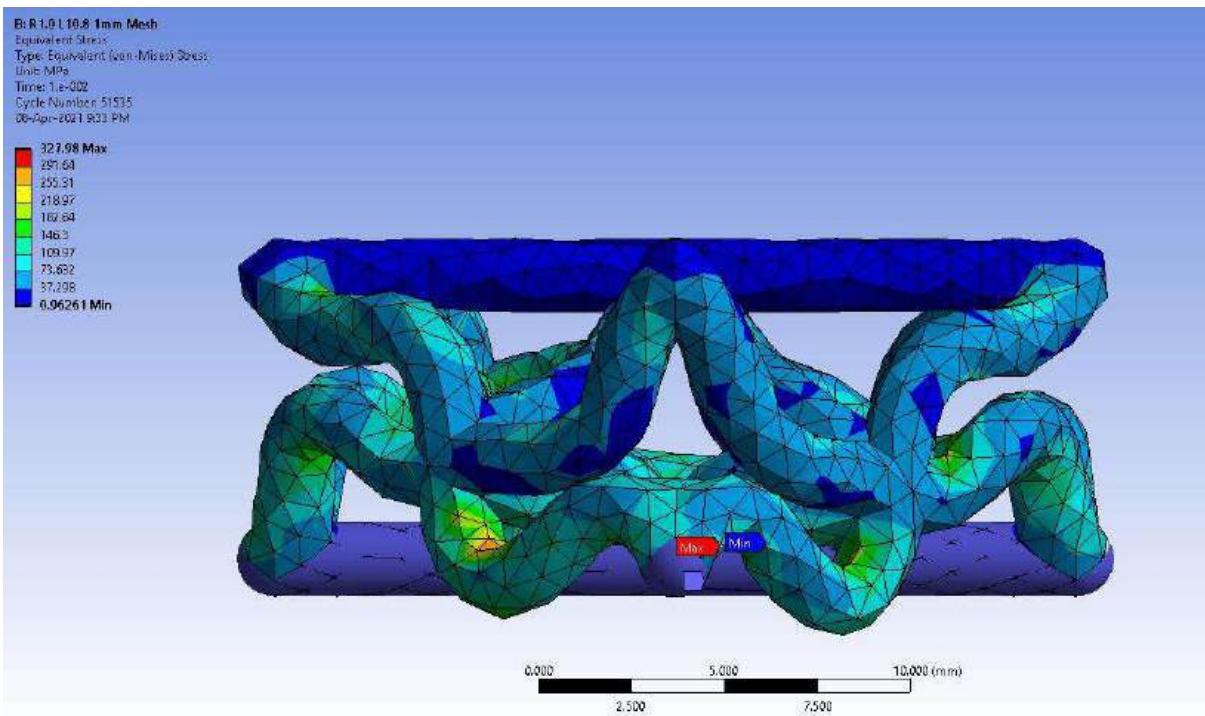


Figure 92: Equivalent Stress for R1.0 mm L10.80 mm with a 1 mm mesh (purple region is the fixed support).

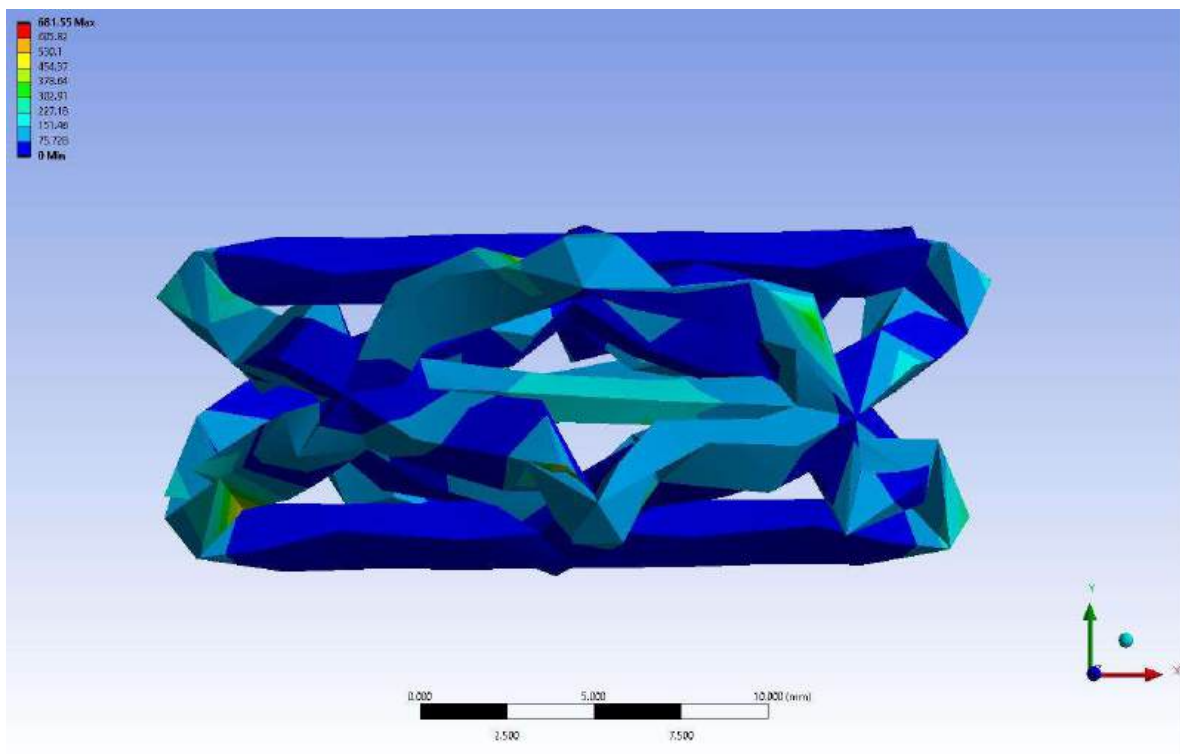


Figure 93: Equivalent Stress for R1.0 mm L10.80 mm with a 3 mm mesh.

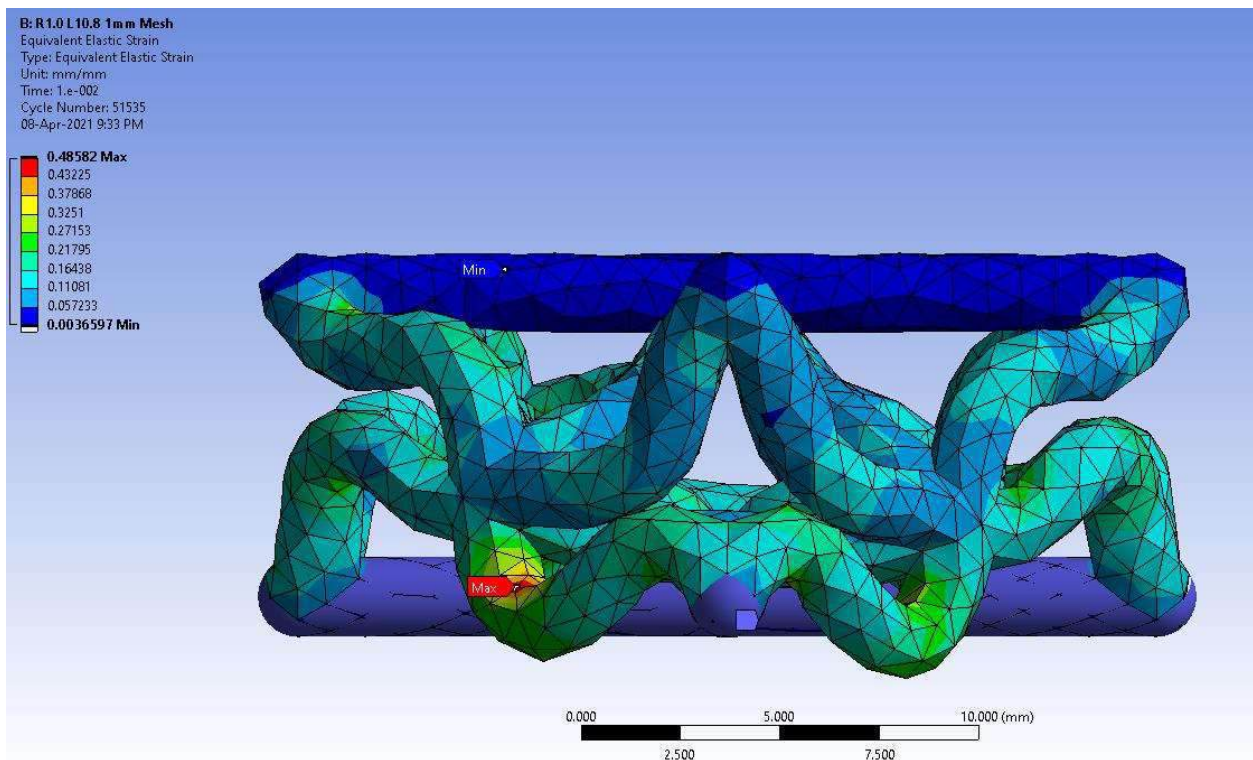


Figure 94: Elastic Strain for R1.0 mm L10.80 mm with a 1 mm mesh.

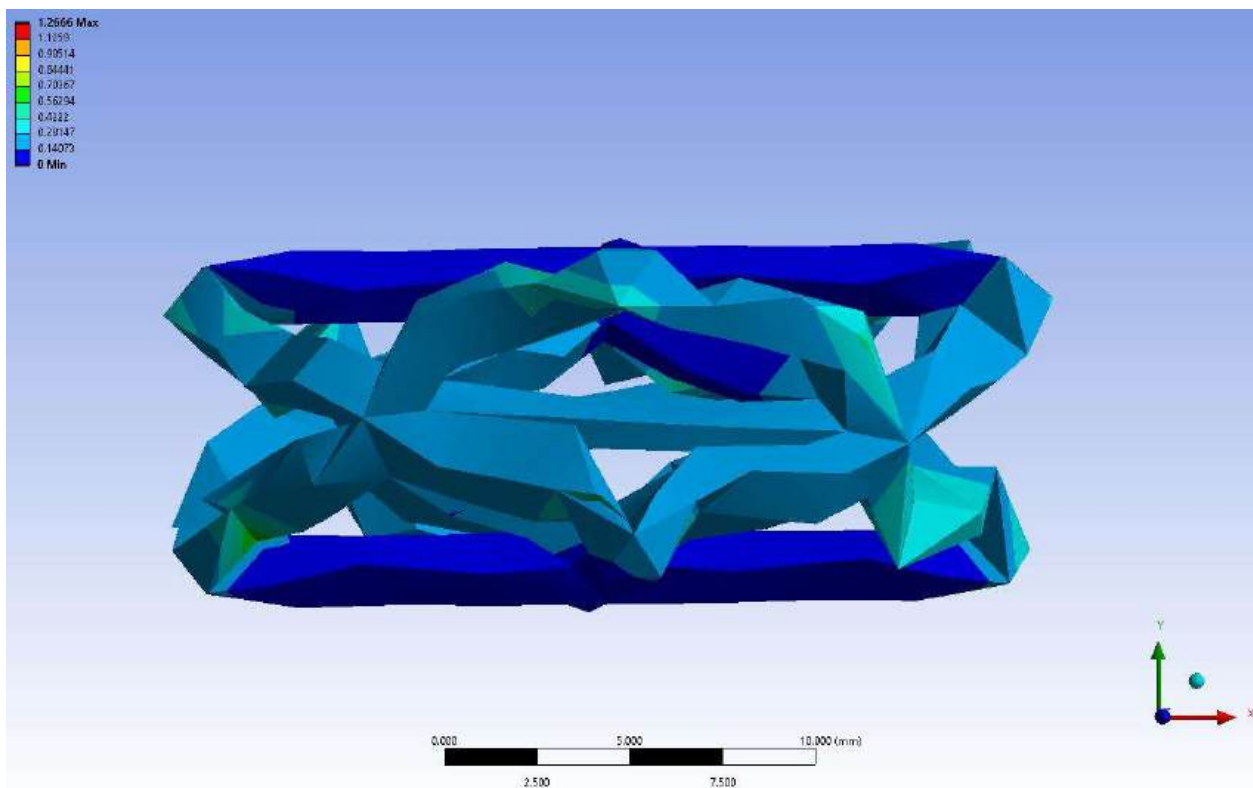


Figure 95: Elastic Strain for R1.0 mm L10.80 mm with a 3 mm mesh.

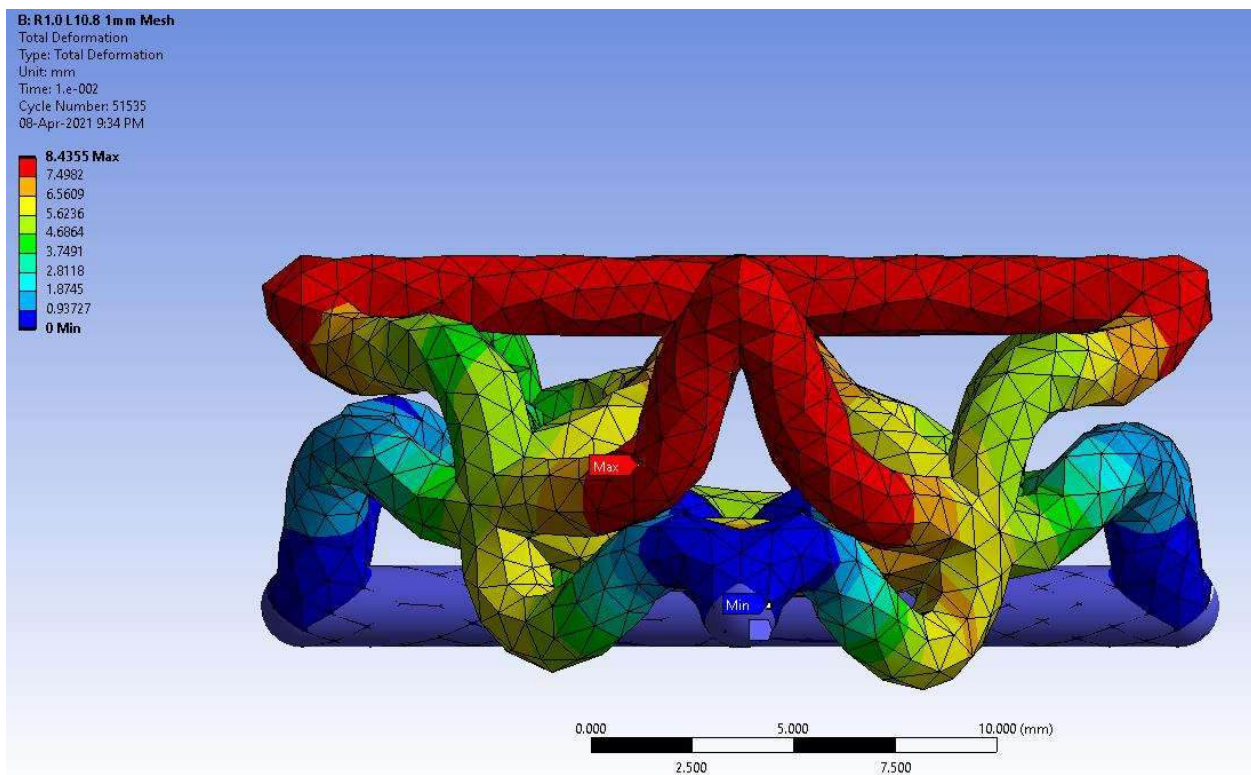


Figure 96: Total Deformation for R1.0 mm L10.80 mm with a 1 mm mesh.

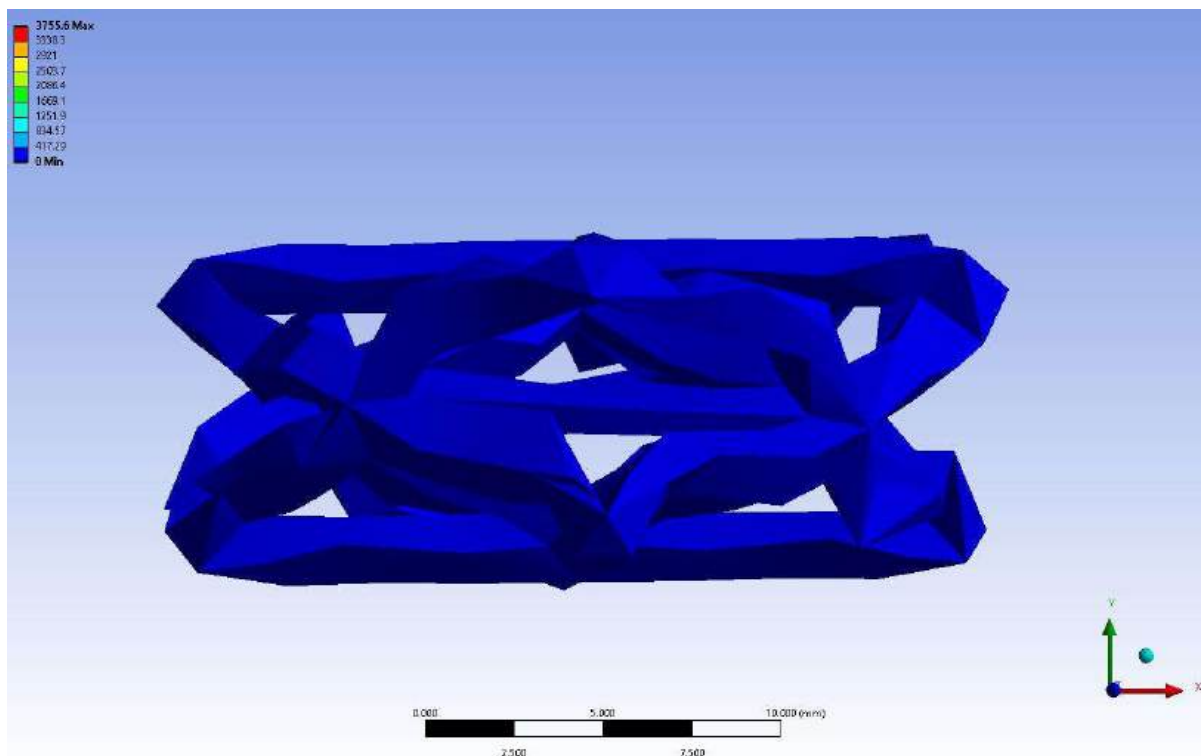


Figure 97: Total Deformation for R1.0 mm L10.80 mm with a 3 mm mesh.

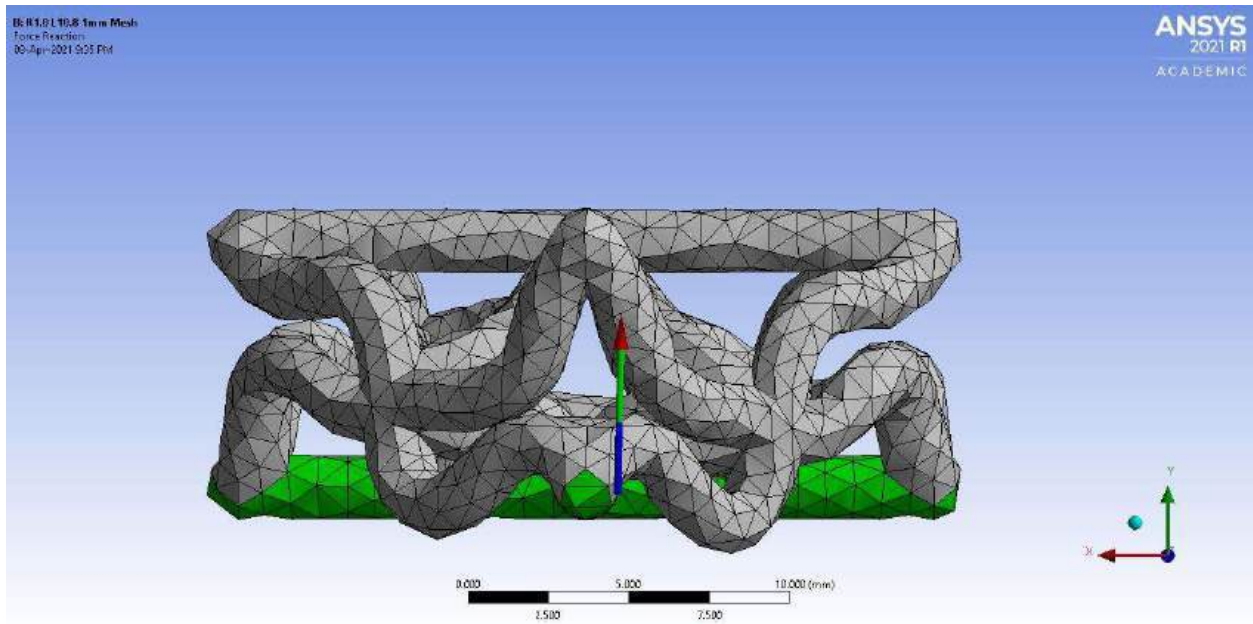


Figure 98: Force reaction for R1.0 mm L10.80 mm with a 1 mm mesh.

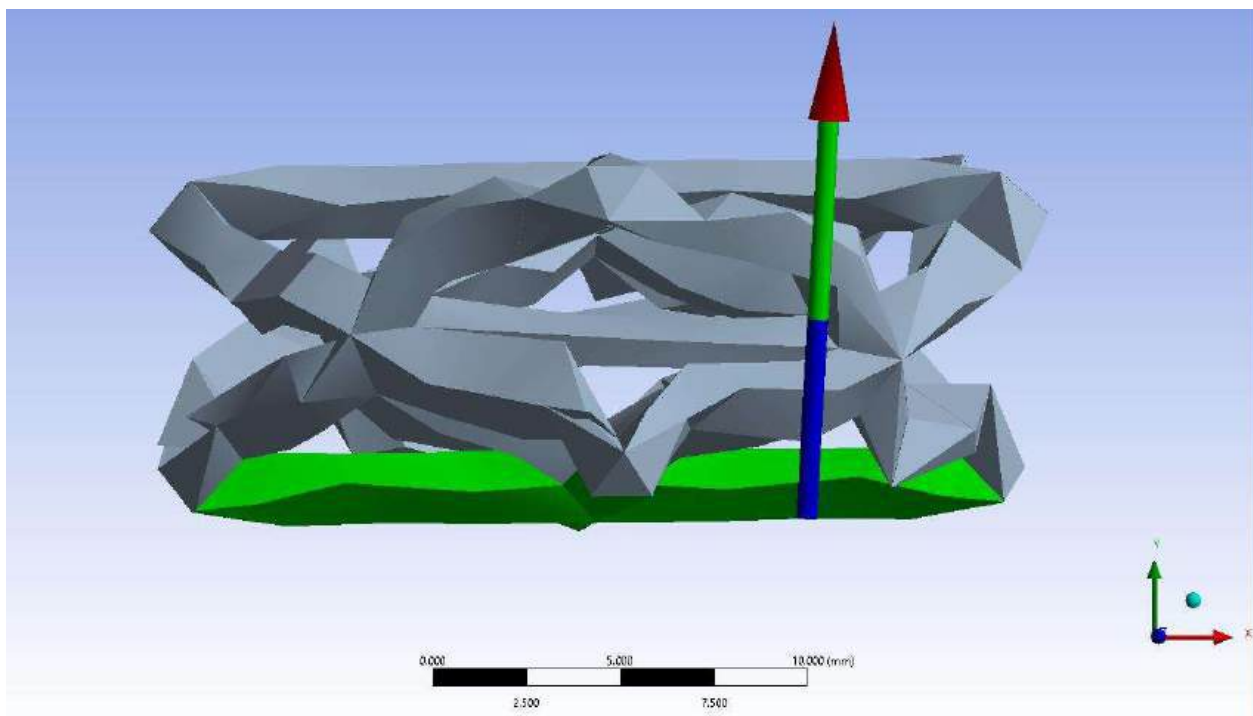


Figure 99: Force reaction for R1.0 mm L10.80 mm with a 3 mm mesh.

7.5.1.2.3 Unit Cell R 1.0 mm L 13.50 mm

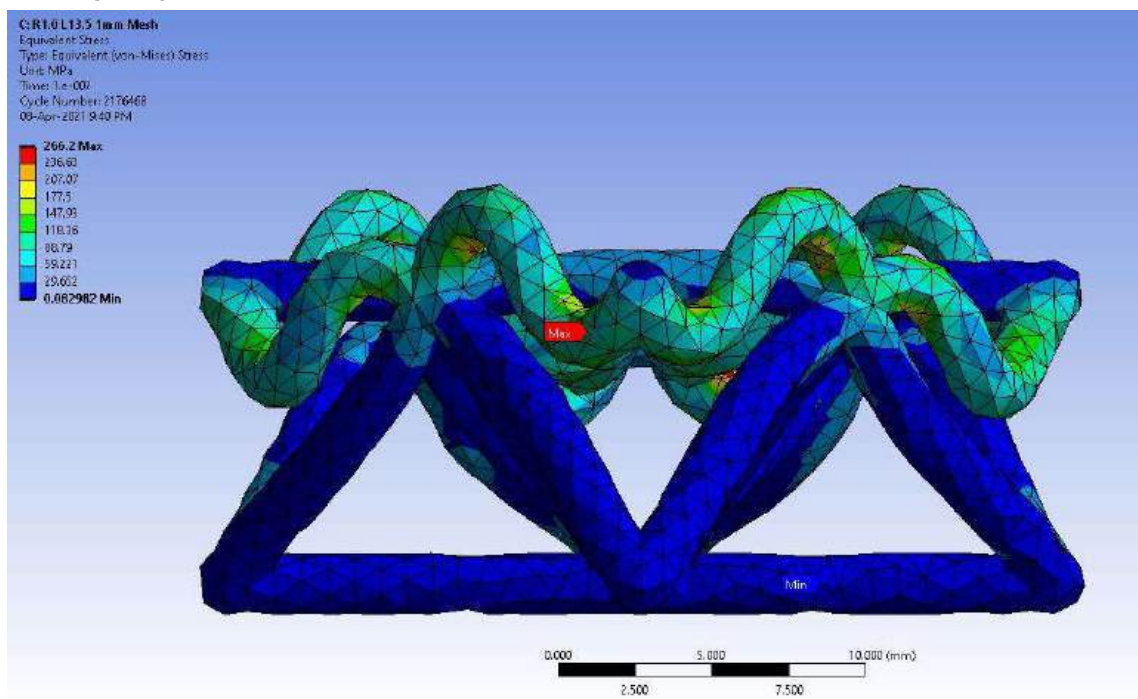


Figure 100: Equivalent Stress for R1.0 mm L13.50 mm with a 1 mm mesh.

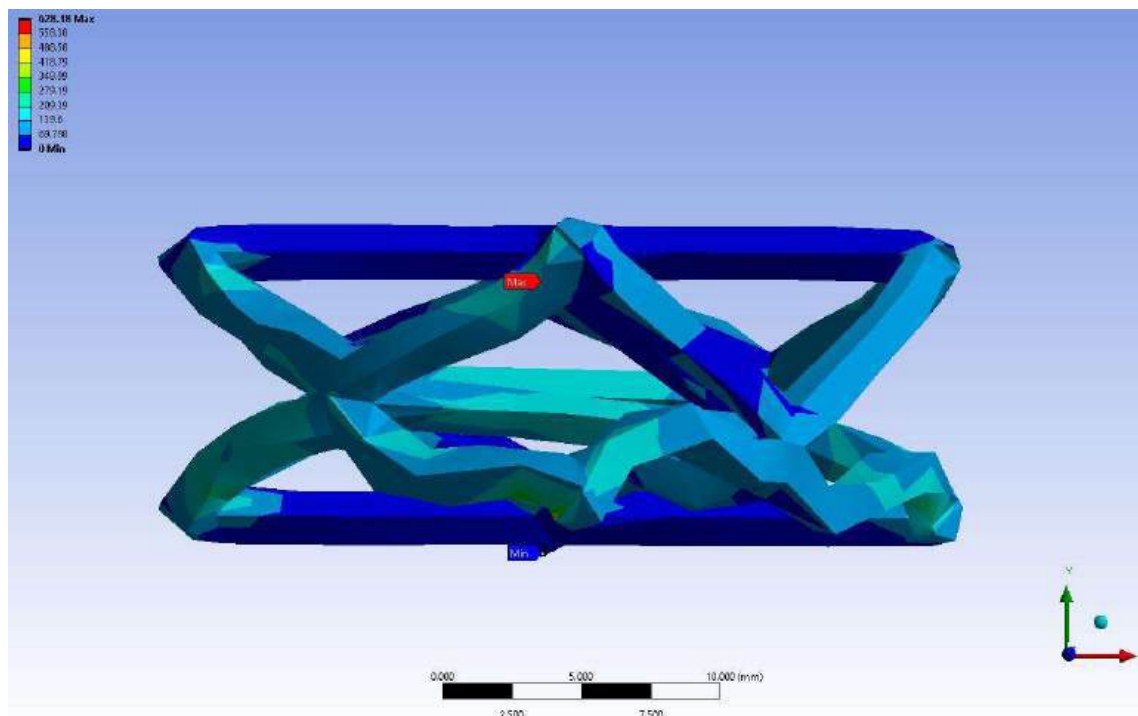


Figure 101: Equivalent Stress for R1.0 mm L13.50 mm with a 3 mm mesh.

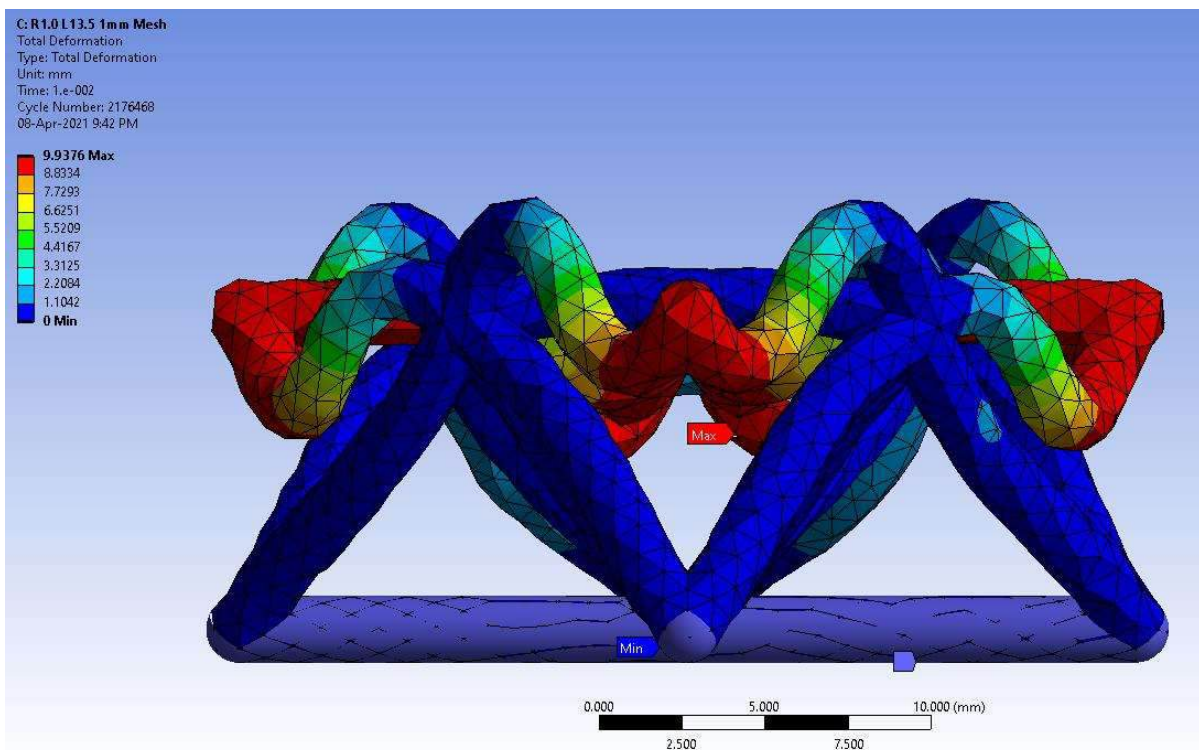


Figure 102: Total Deformation for R1.0 mm L13.50 mm with a 1 mm mesh.

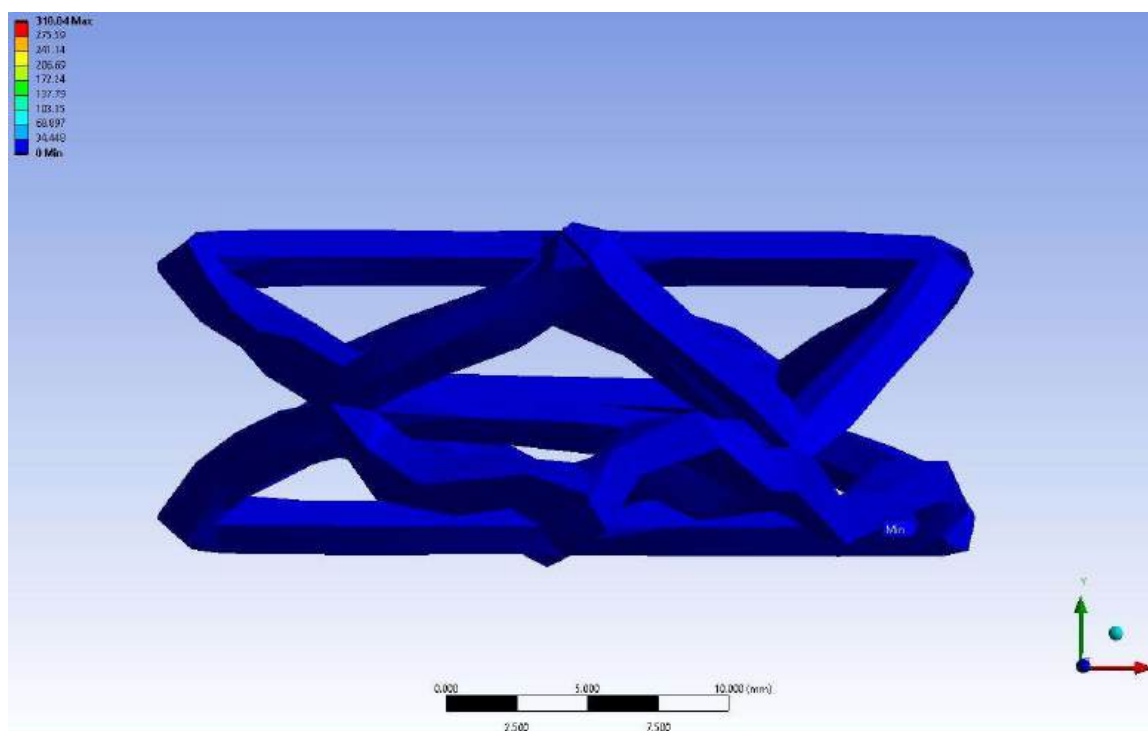


Figure 103: Total Deformation for R1.0 mm L13.50 mm with a 3 mm mesh.

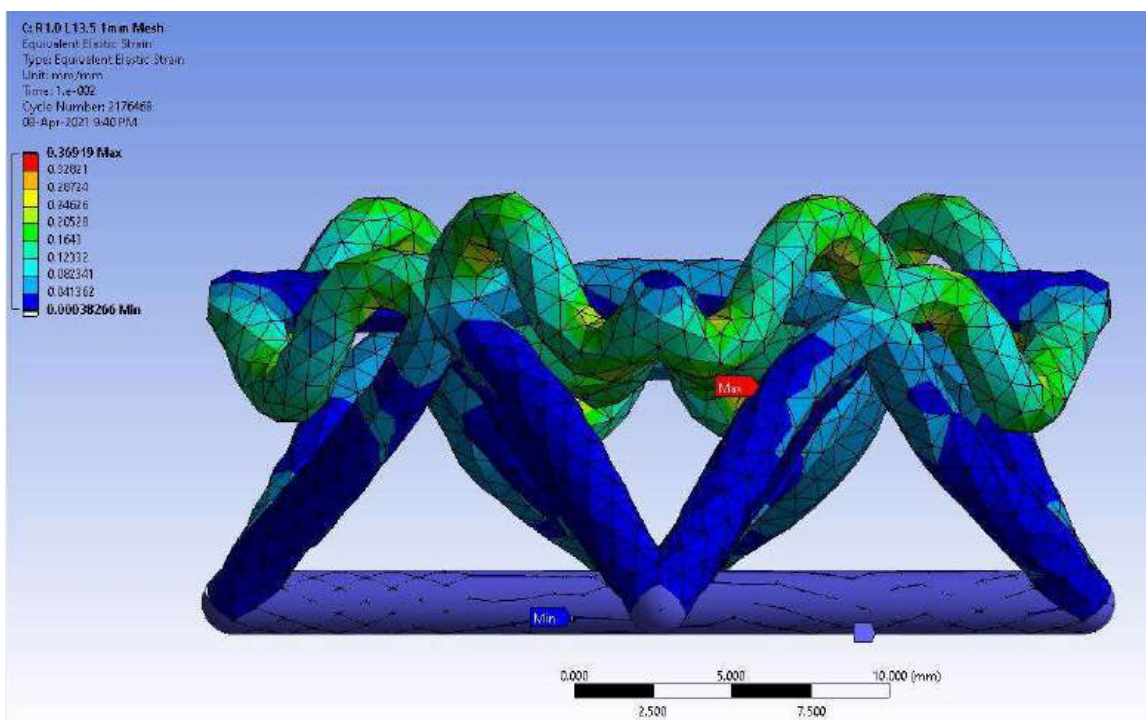


Figure 104: Elastic strain for R1.0 mm L13.50 mm with a 1 mm mesh.

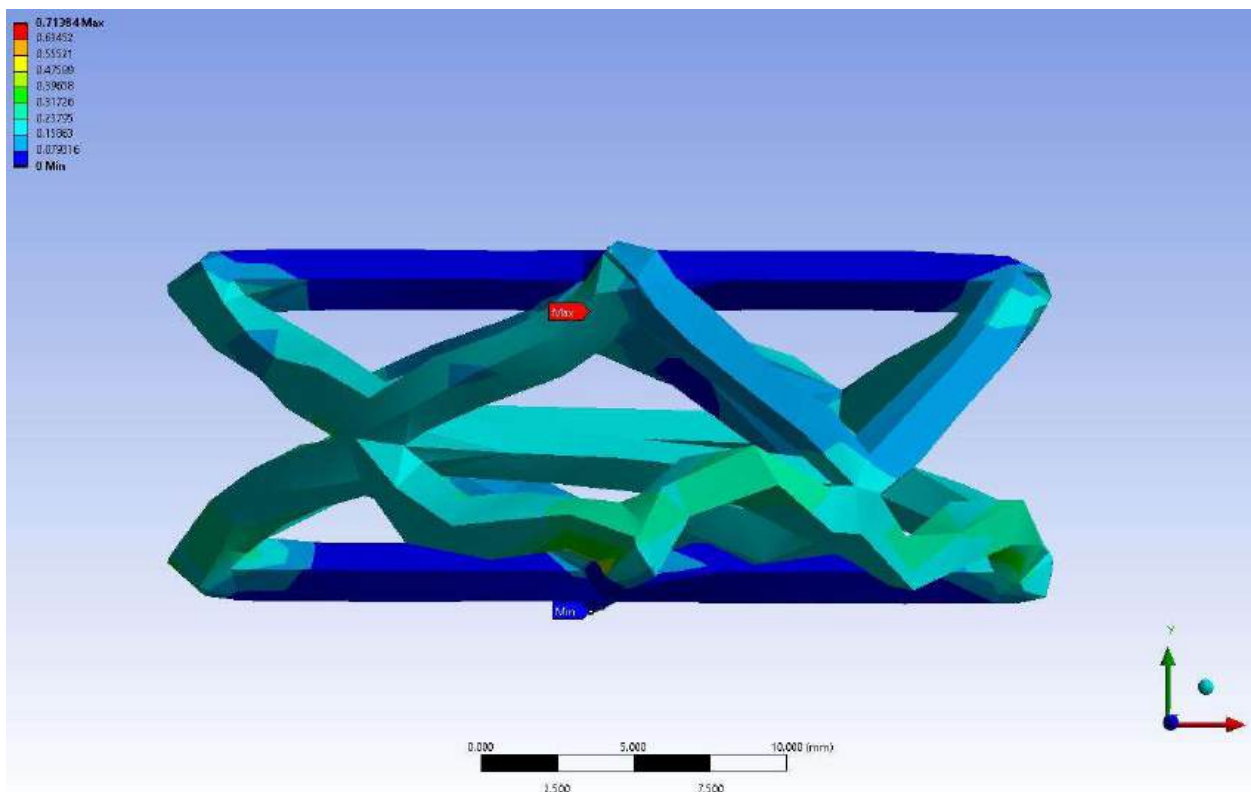


Figure 105: Elastic strain for R1.0 mm L13.50 mm with a 3 mm mesh.

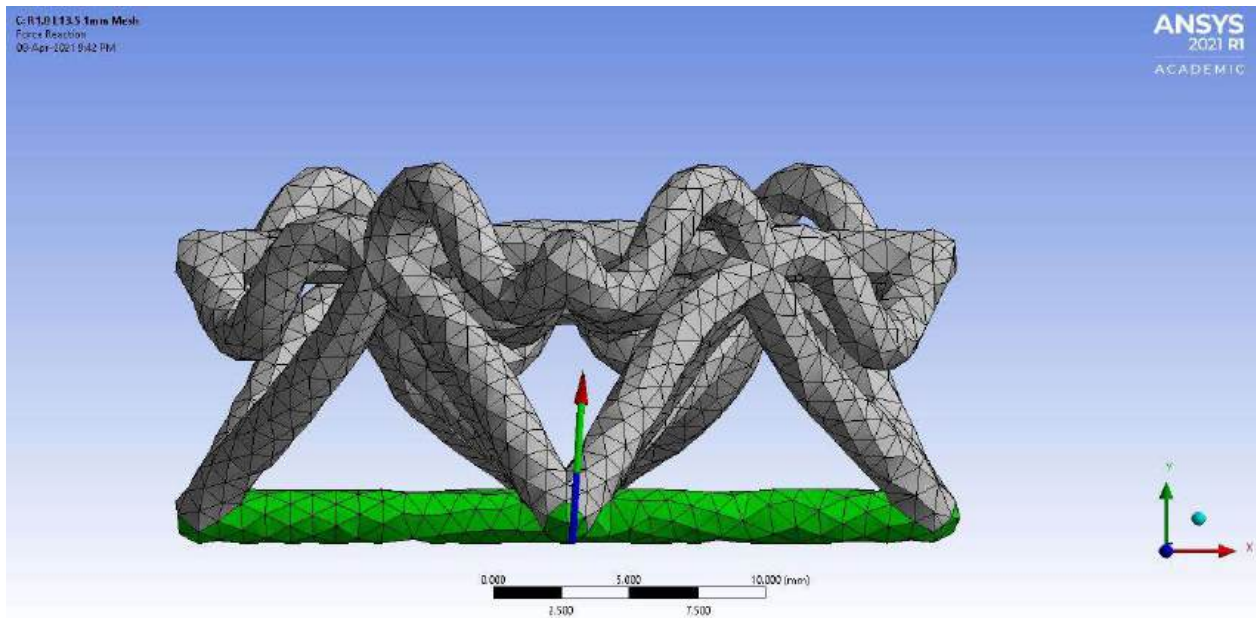


Figure 106: Force Reaction for R1.0 mm L13.50 mm with a 1 mm mesh.

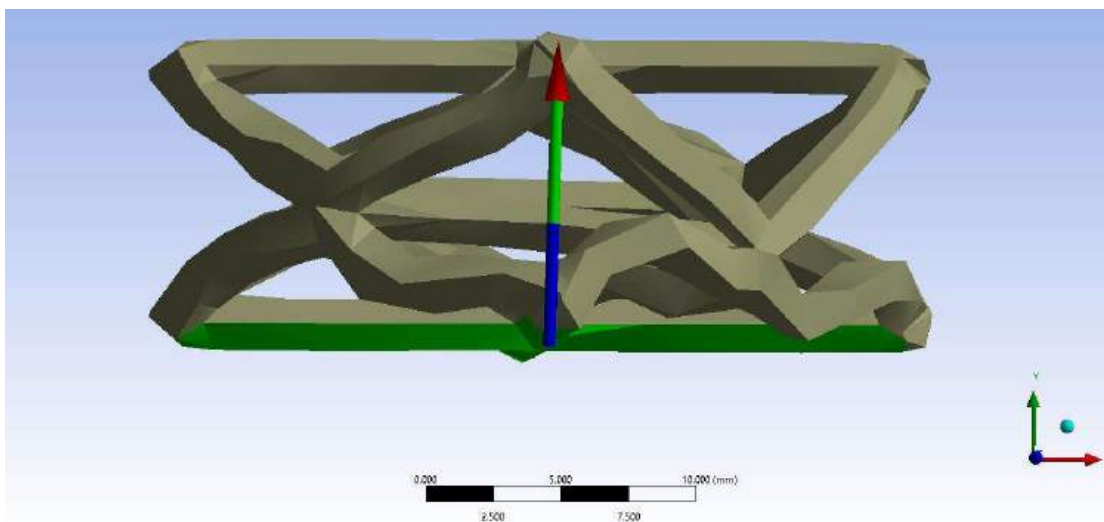


Figure 107: Force reaction for R1.0 mm L13.50 mm with a 3 mm mesh.

7.5.1.2.4 Unit Cell R 1.0 mm L 18.0 mm

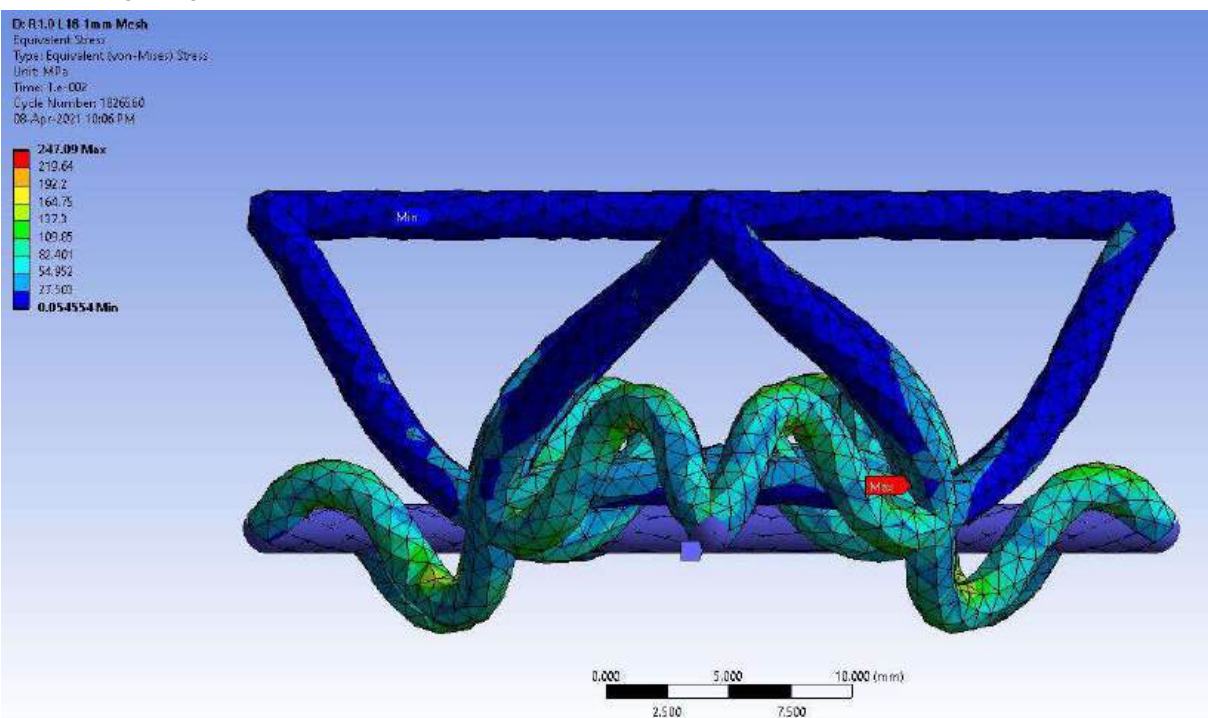


Figure 108: Equivalent Stress for R1.0 mm L18.0 mm with a 1 mm mesh (Purple Region is Fixed Support).

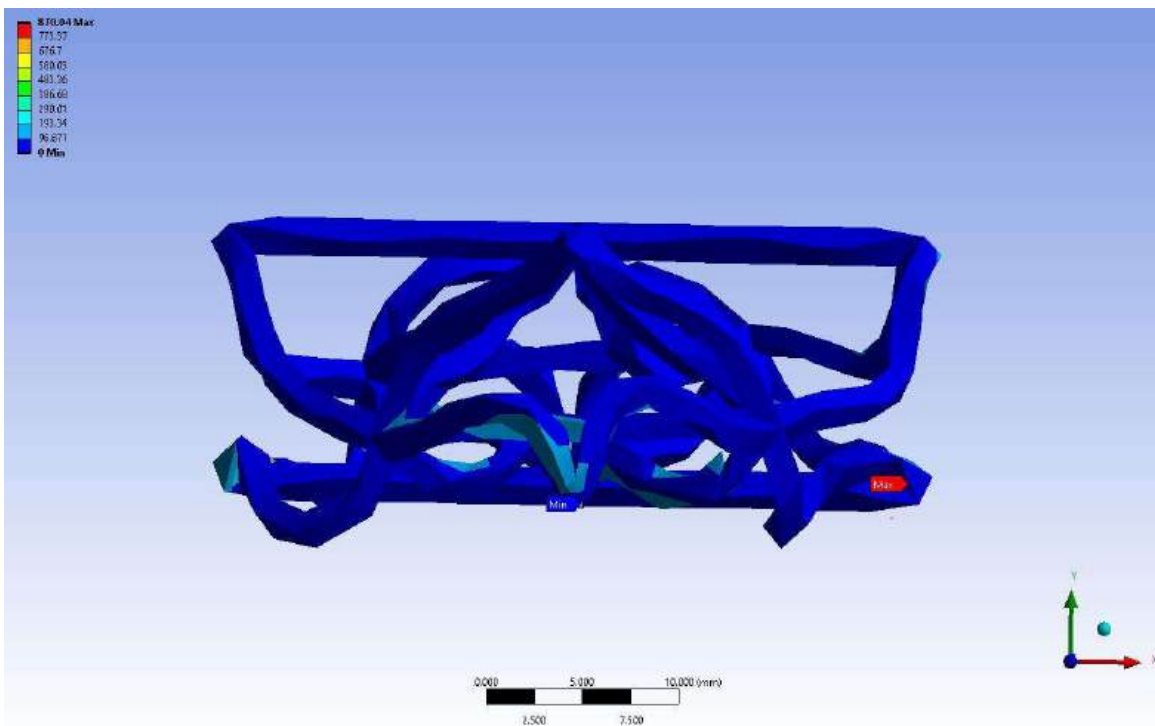


Figure 109: Equivalent Stress for R1.0 mm L18.0 mm with a 3 mm mesh.

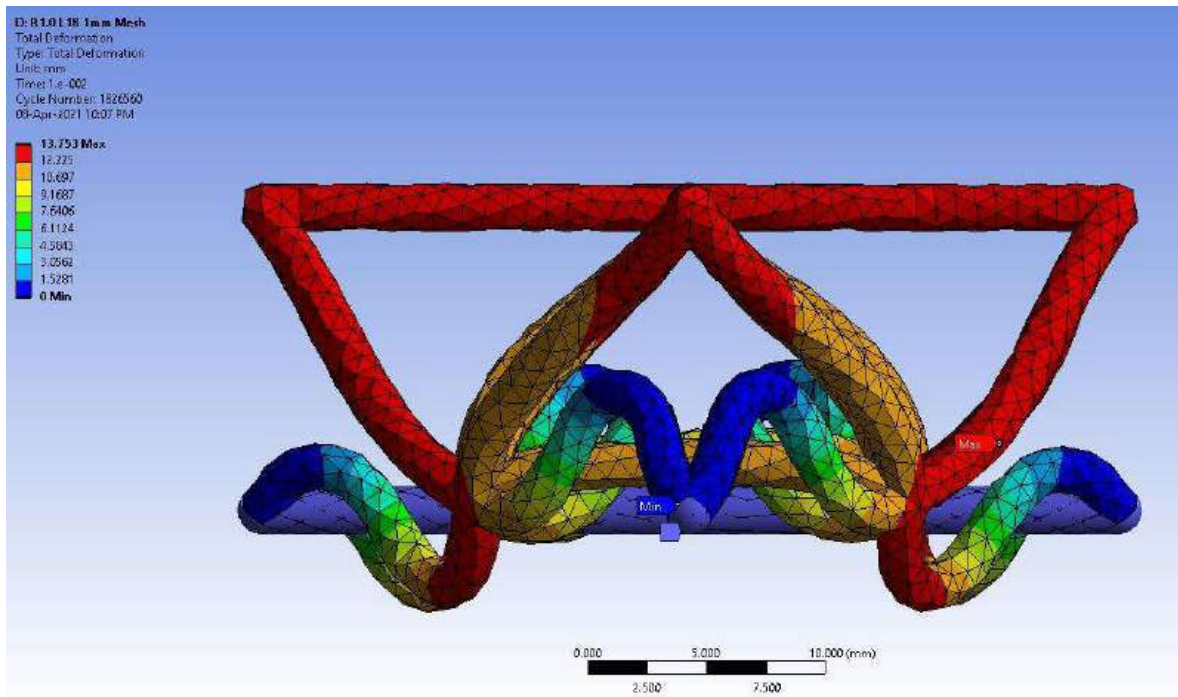


Figure 110: Total Deformation for R1.0 mm L18.0 mm with a 1 mm mesh.

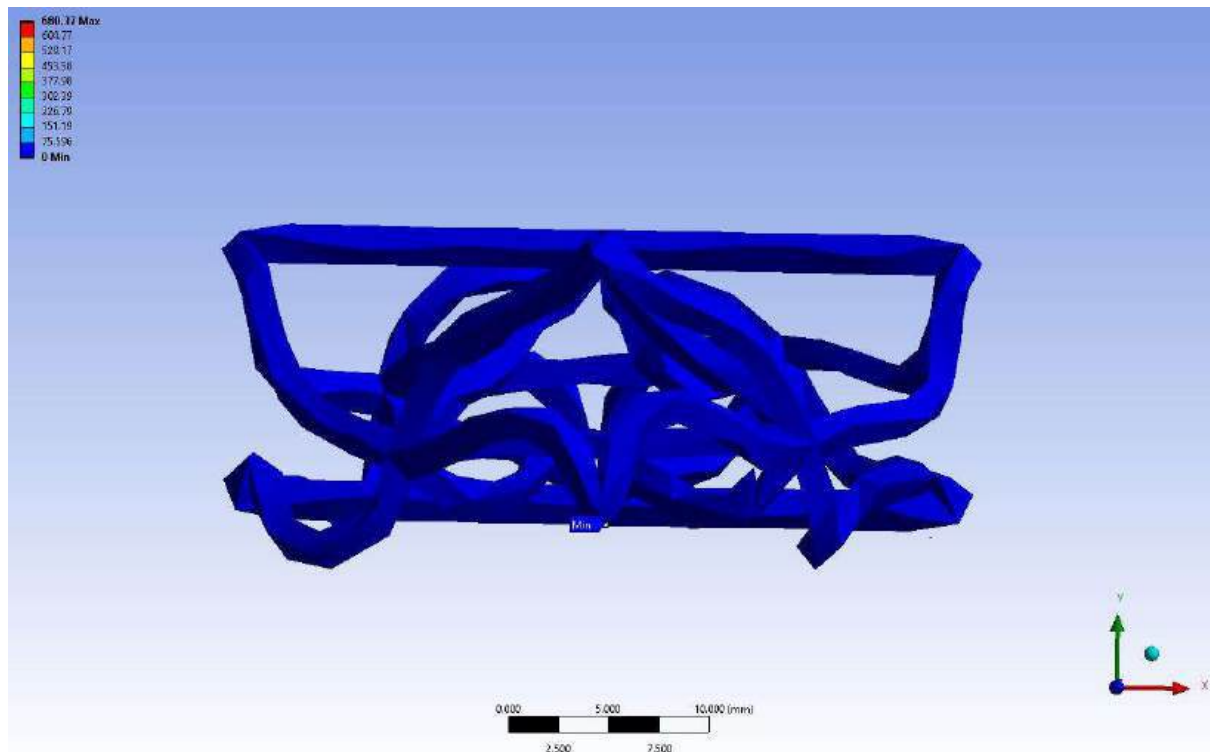


Figure 111: Total Deformation for R1.0 mm L18.0 mm with a 3 mm mesh.

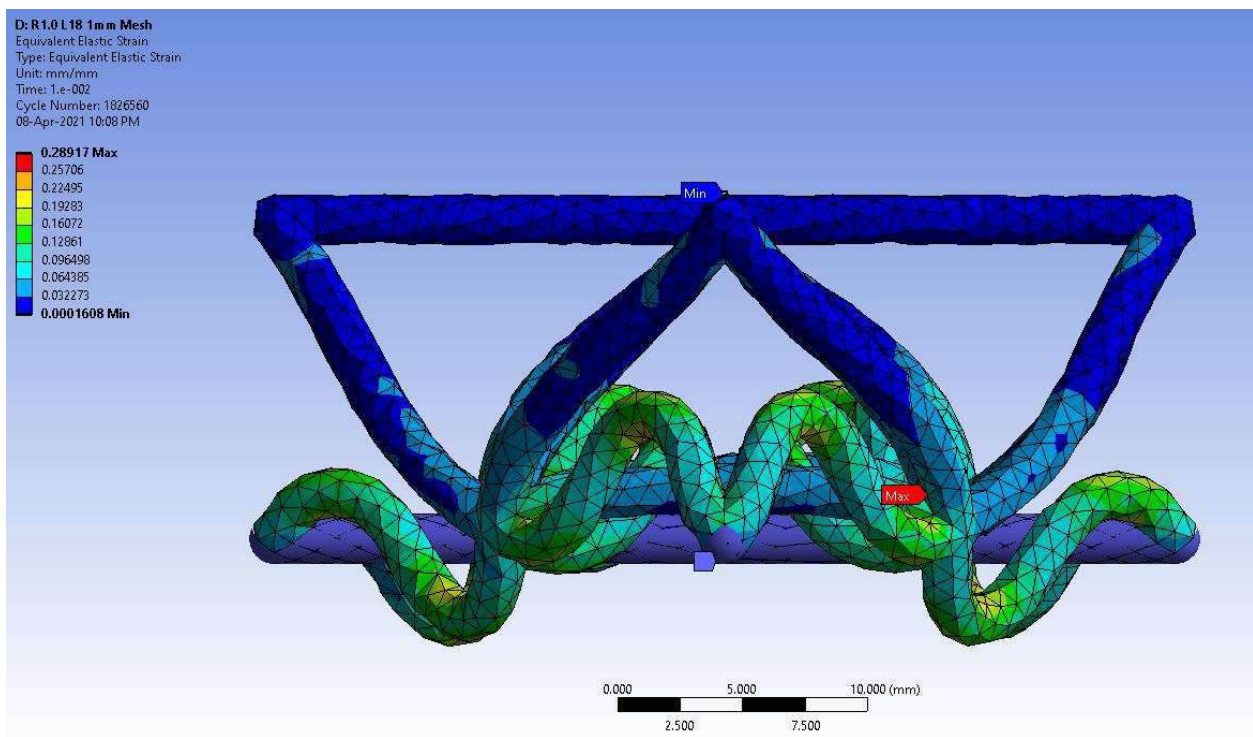


Figure 112: Elastic Strain for R1.0 mm L18.0 mm with a 1 mm mesh.

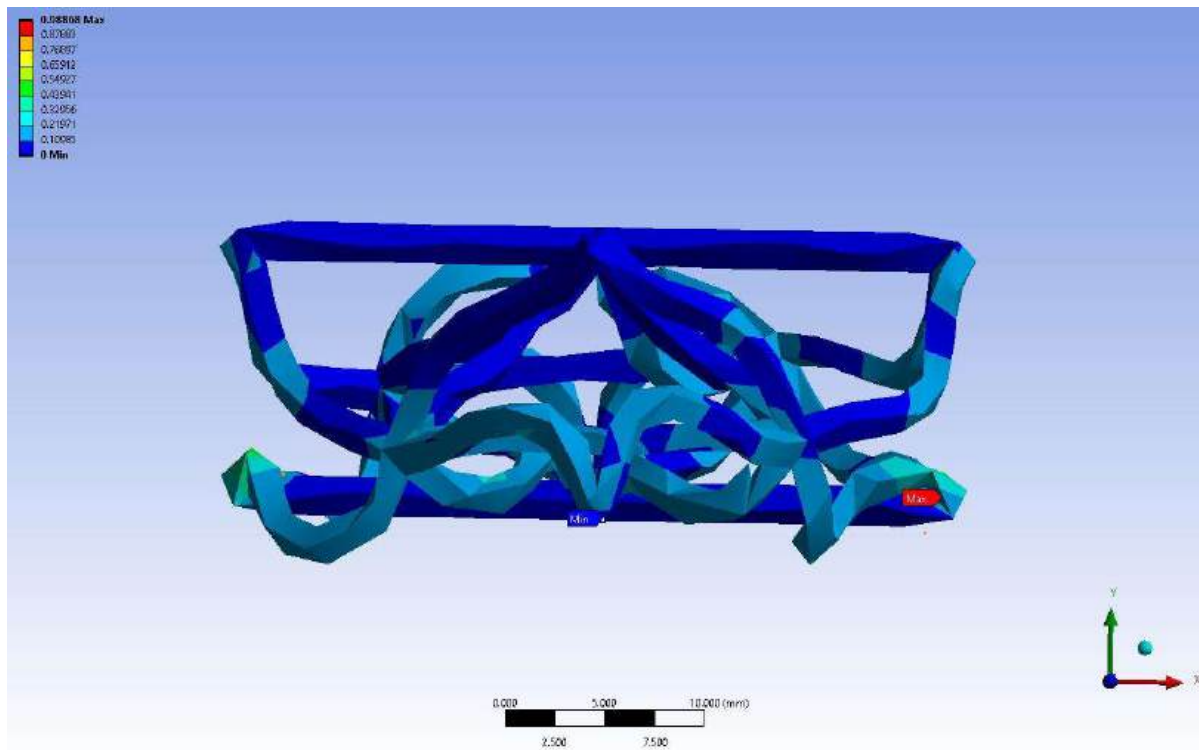


Figure 113: Elastic Strain for R1.0 mm L18.0 mm with a 3 mm mesh.

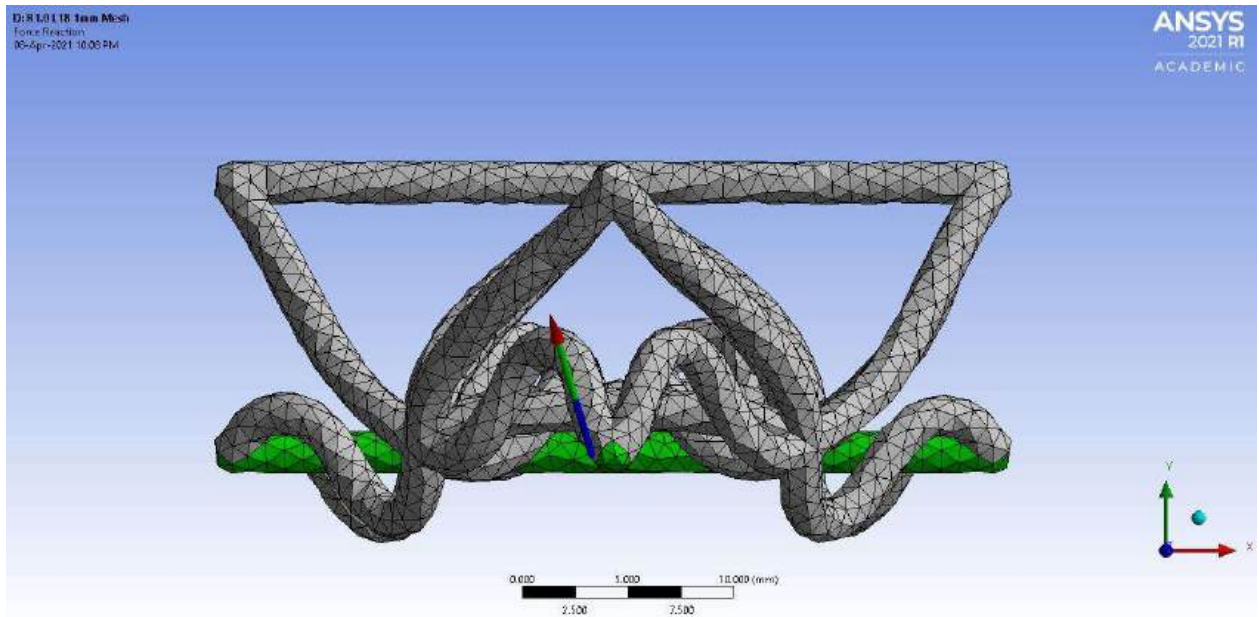


Figure 114: Force reaction for R1.0 mm L18.0 mm with a 1 mm mesh.

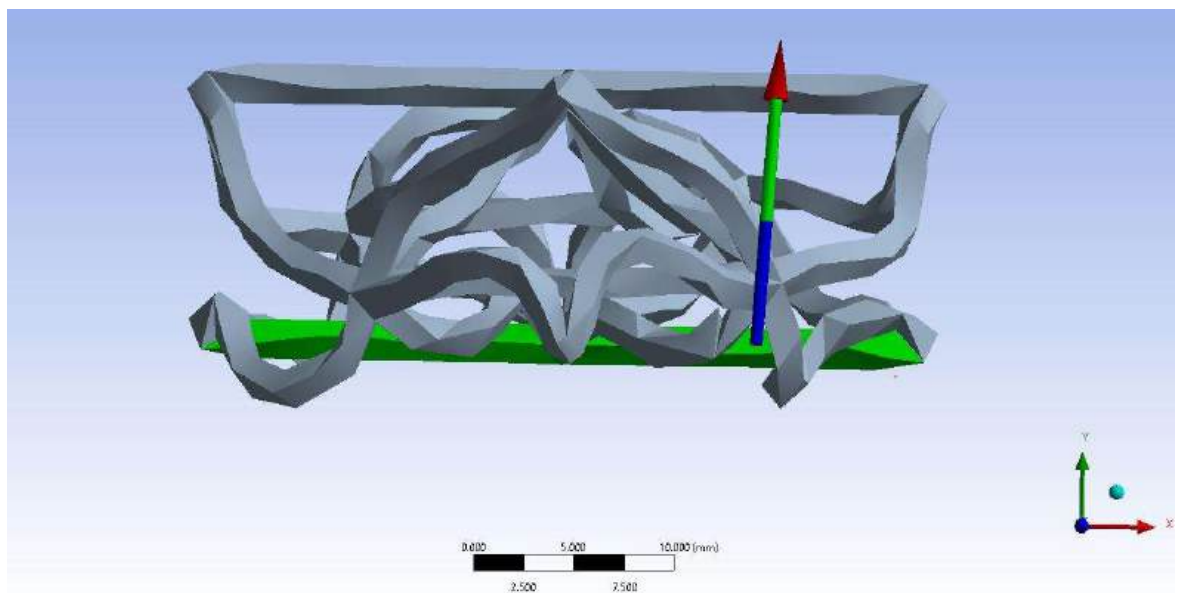


Figure 115: Force reaction for R1.0 mm L18.0 mm with a 3 mm mesh.

7.5.1.3 Radii of 1.5 mm

7.5.1.3.1 Unit Cell R 1.5 mm L 9.0 mm

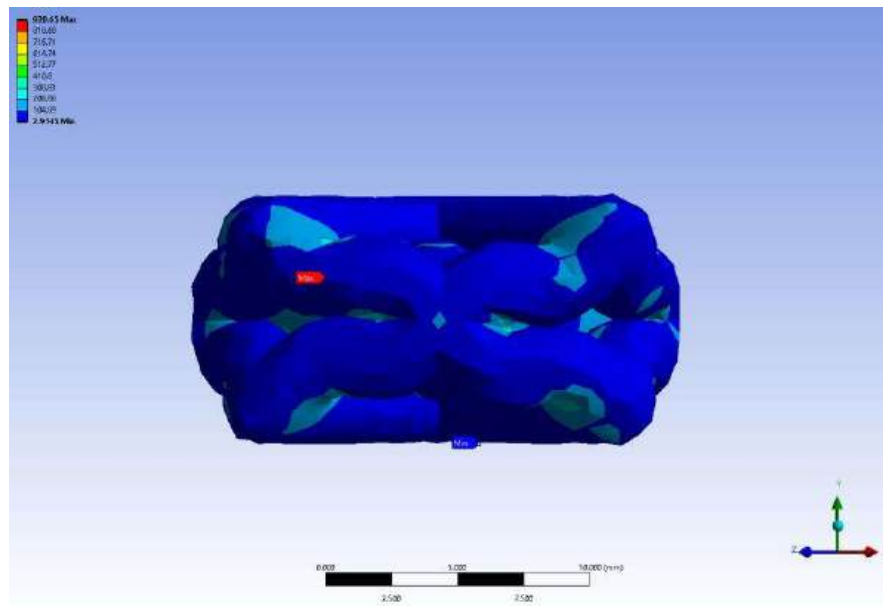


Figure 116: Equivalent Stress for R1.5mm L9.0mm with 1mm mesh.

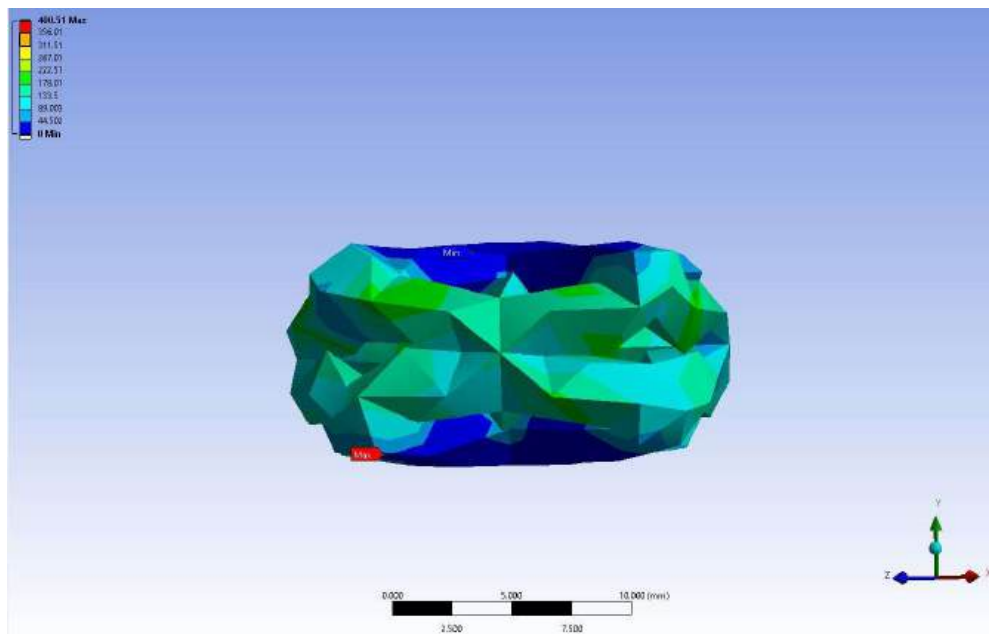


Figure 117: Equivalent Stress for R1.5mm L9.0mm with 3mm mesh.

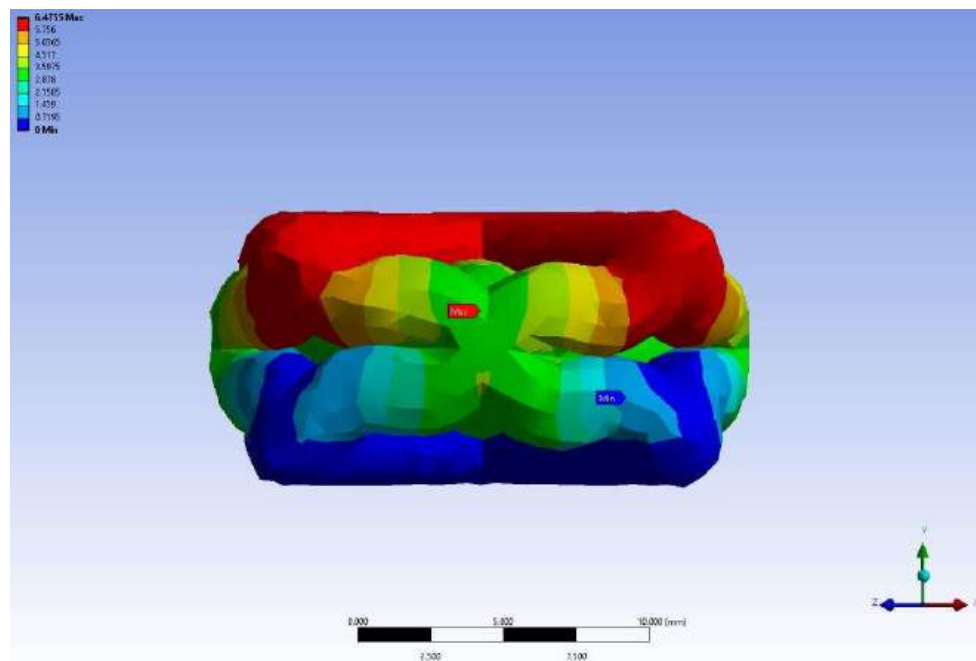


Figure 118: Total Deformation for R1.5mm L9.0mm with 1mm mesh.

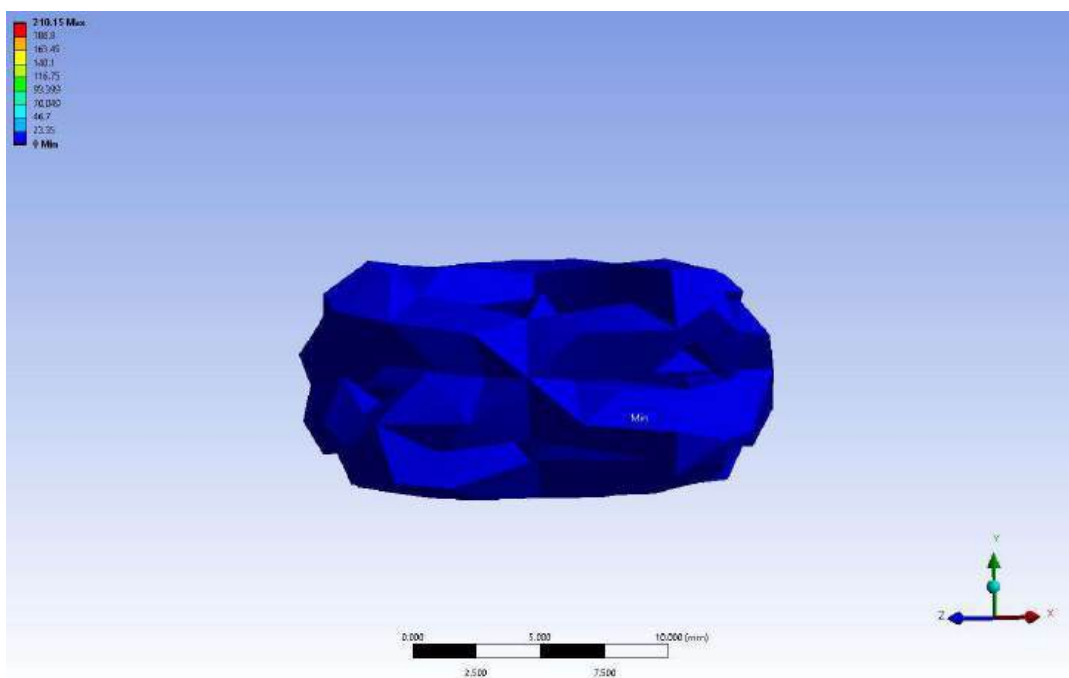


Figure 119: Total Deformation for R1.5mm L9.0mm with 3mm mesh.

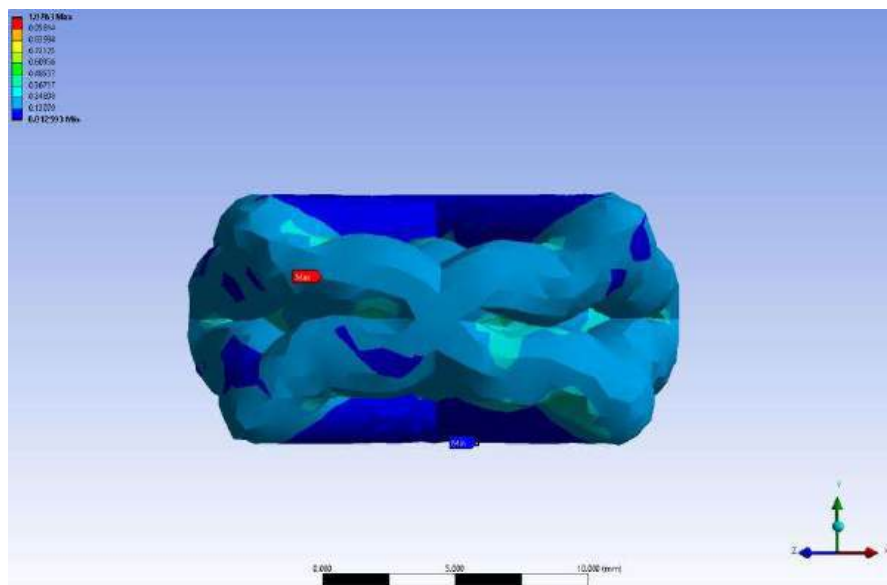


Figure 120: Elastic Strain for R1.5mm L9.0mm with 1mm mesh.

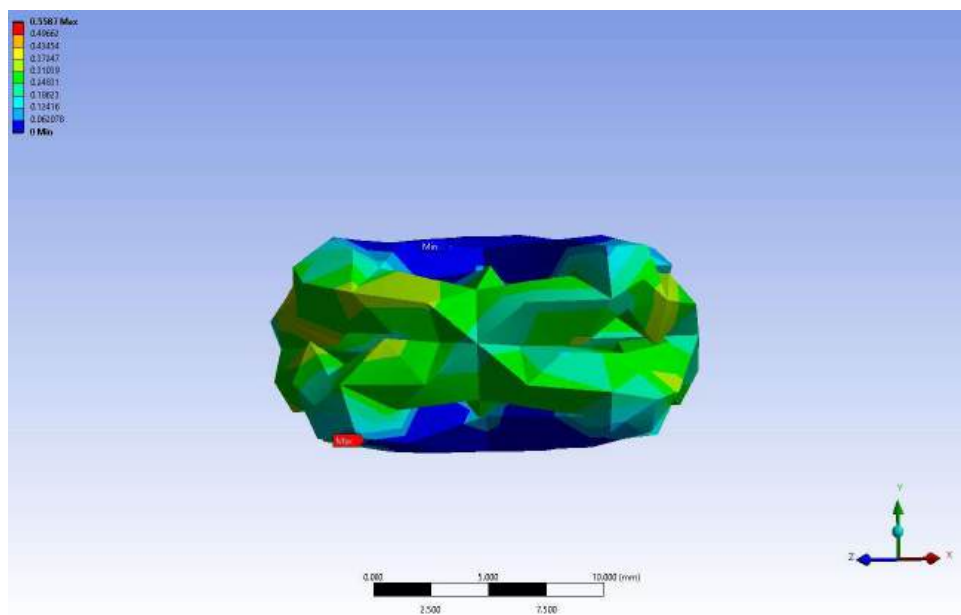


Figure 121: Elastic Strain for R1.5mm L9.0mm with 3mm mesh.

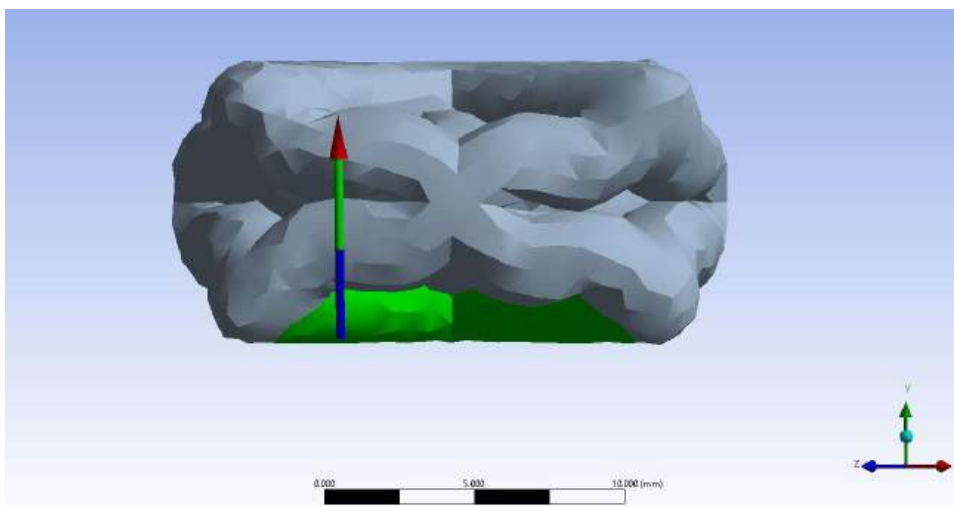


Figure 122: Force reaction for R1.5mm L9.0mm with 1mm mesh.

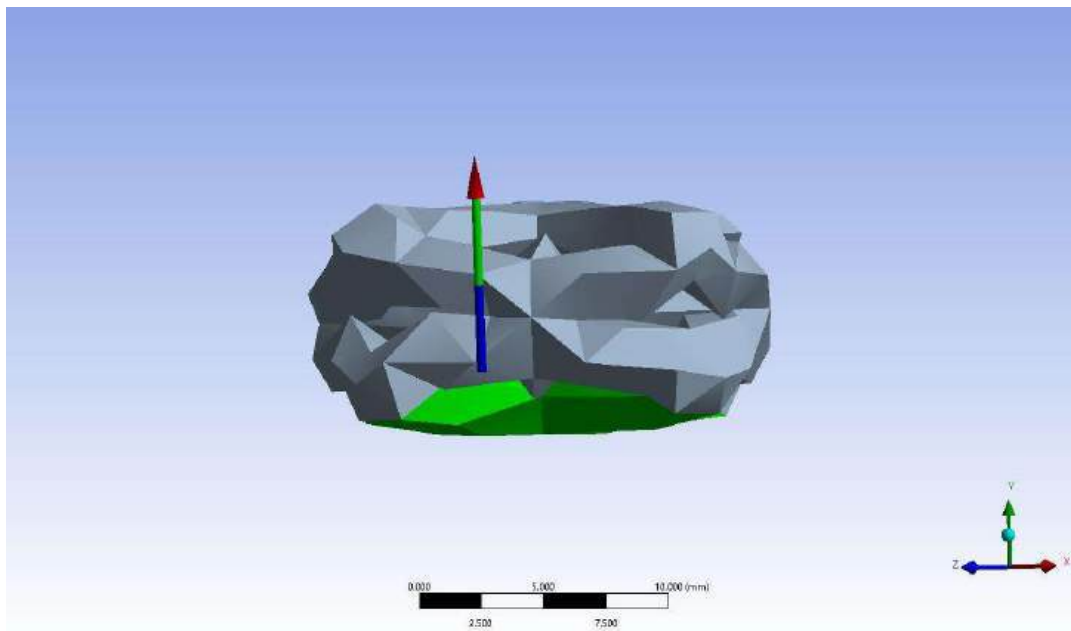


Figure 123: Force reaction for R1.5mm L9.0mm with 3mm mesh.

7.5.1.3.2 Unit Cell R 1.5 mm L 10.80mm

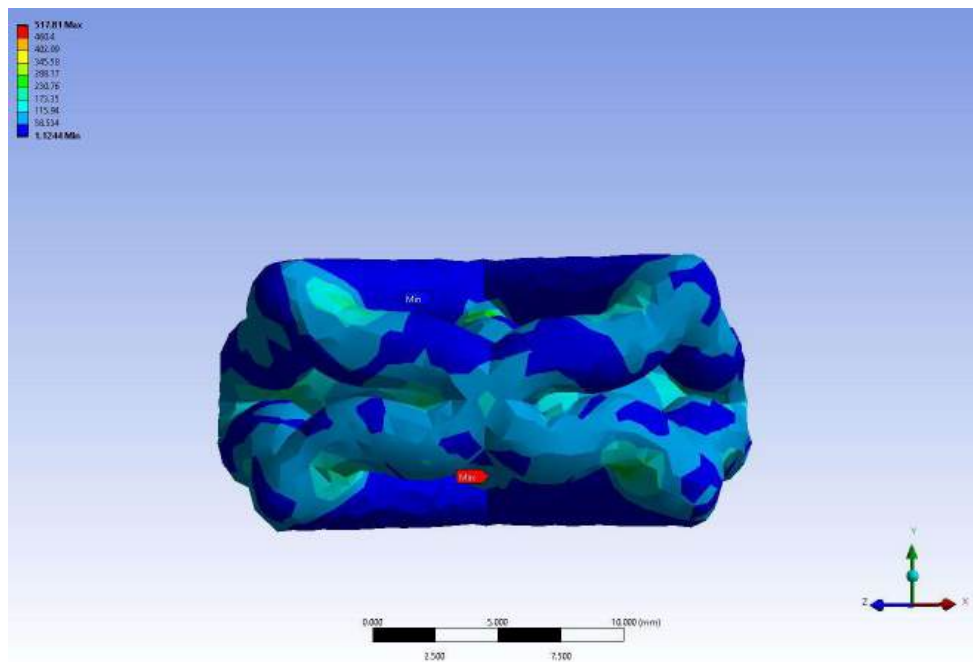


Figure 124: Equivalent Stress for R1.5mm L10.80mm with 1mm mesh.

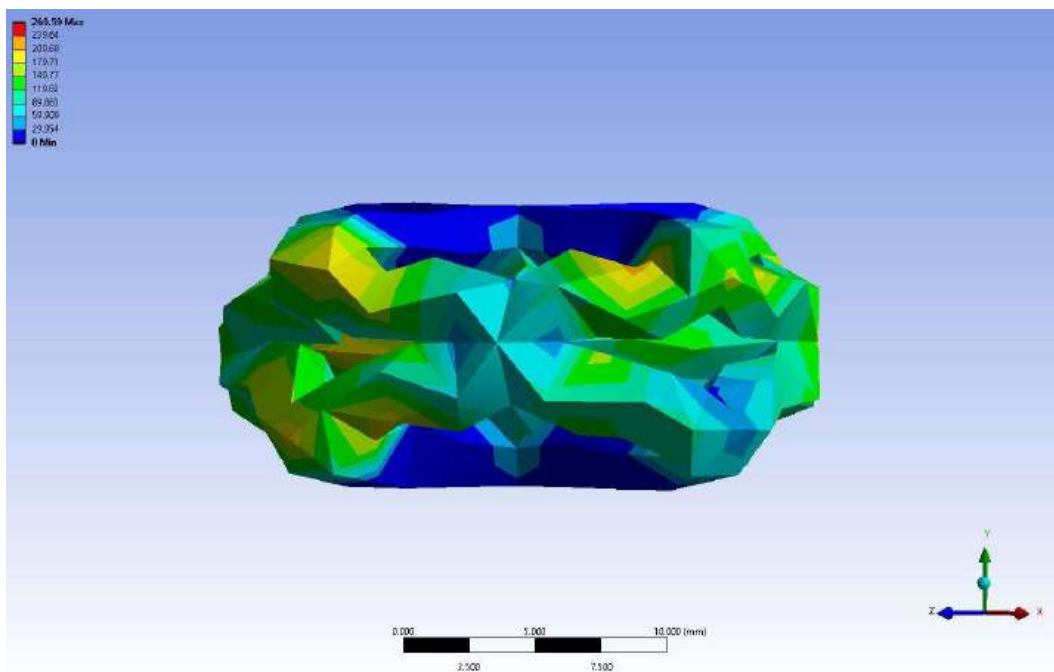


Figure 125: Equivalent Stress for R1.5mm L10.80mm with 3mm mesh.

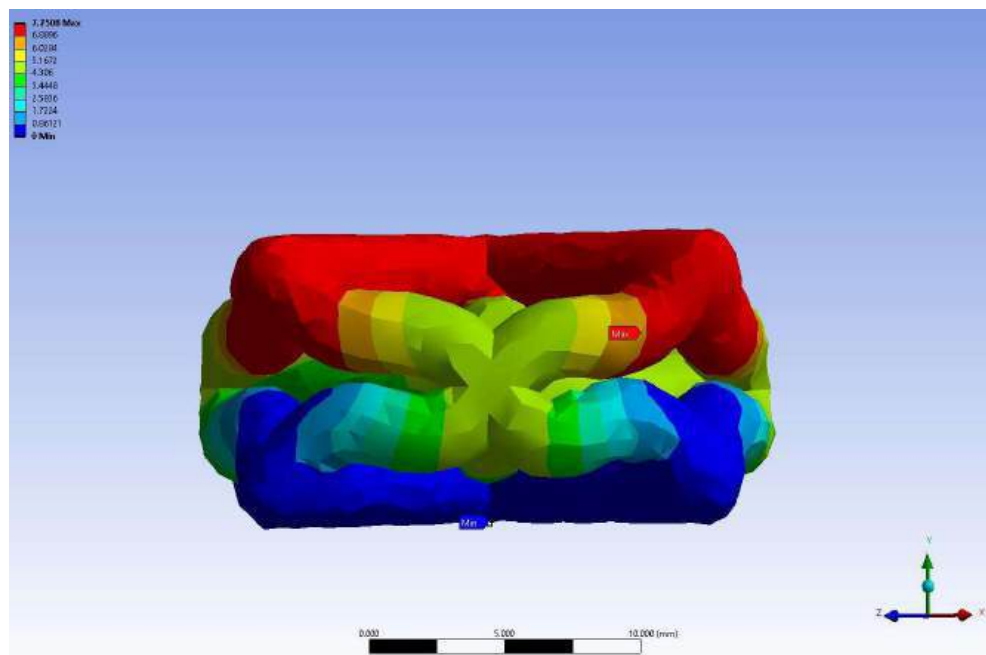


Figure 126: Total Deformation for R1.5mm L10.80mm with 1mm mesh.

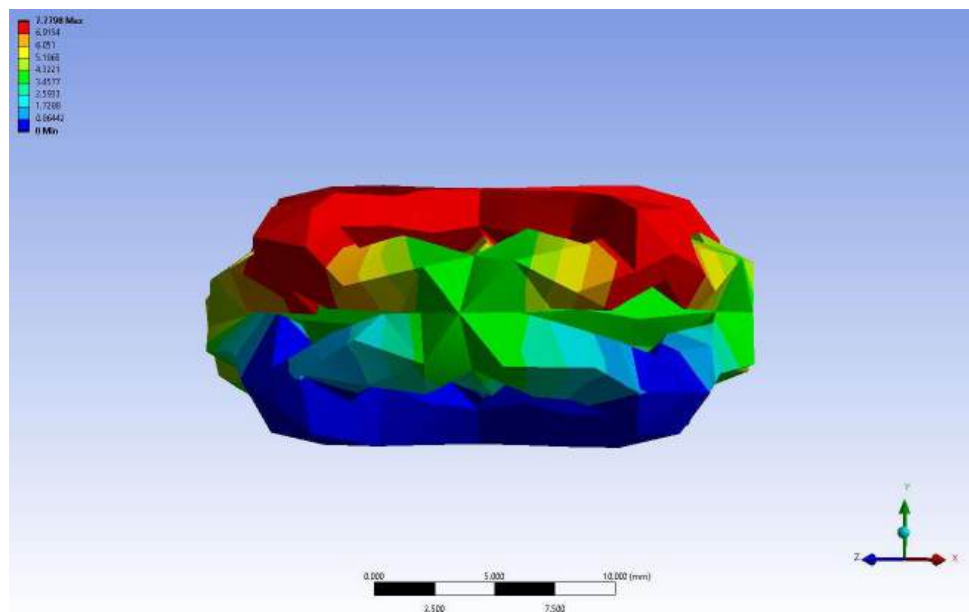


Figure 127: Total Deformation for R1.5mm L10.80mm with 3mm mesh.

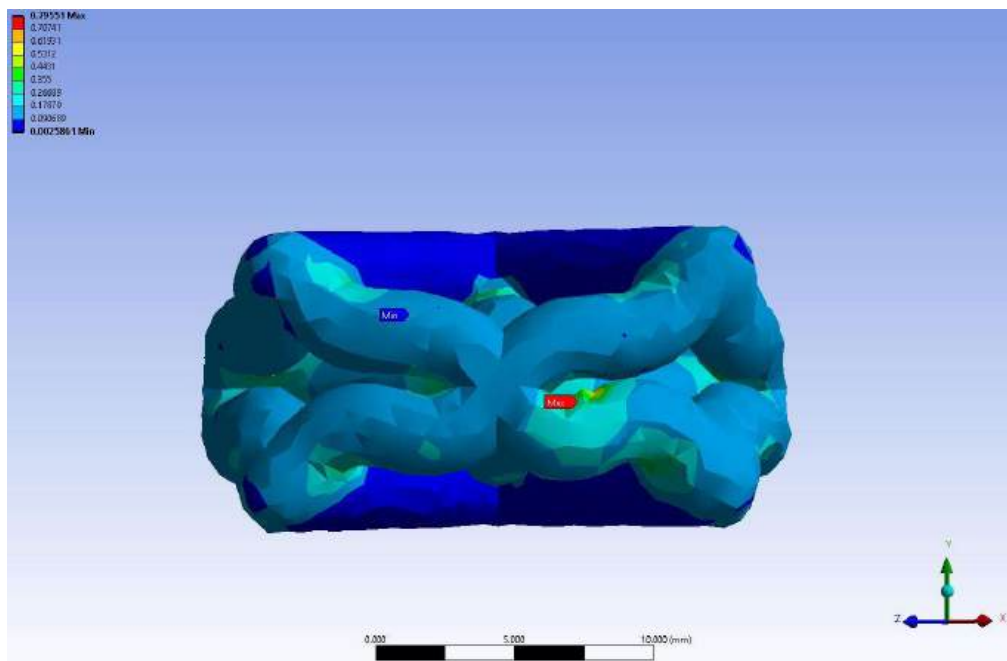


Figure 128: Elastic Strain for R1.5mm L10.80mm with 1mm mesh.

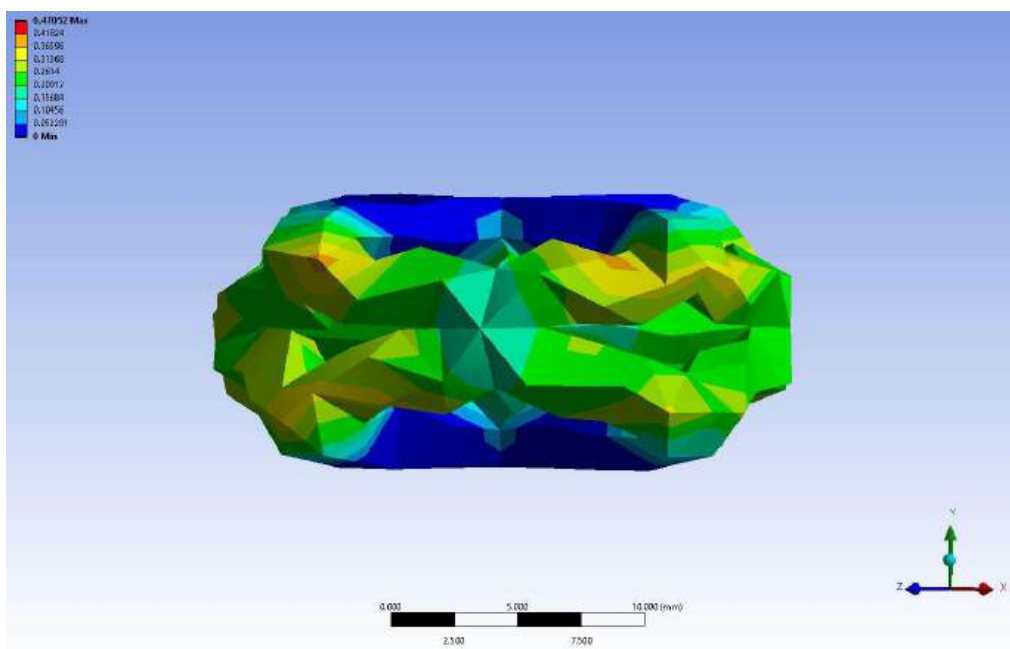


Figure 129: Elastic Strain for R1.5mm L10.80mm with 3mm mesh.

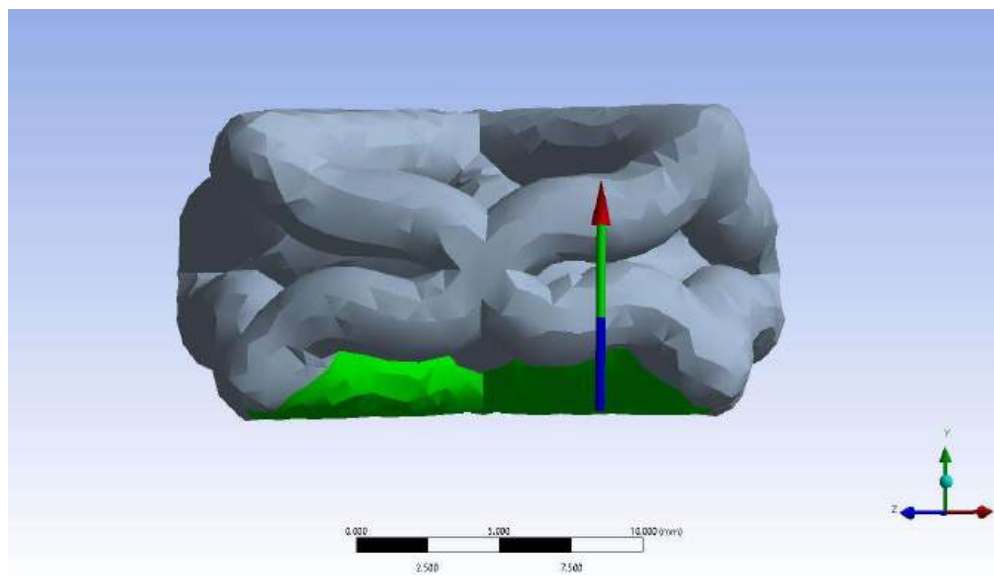


Figure 130: Force reaction for R1.5mm L10.80mm with 1mm mesh.

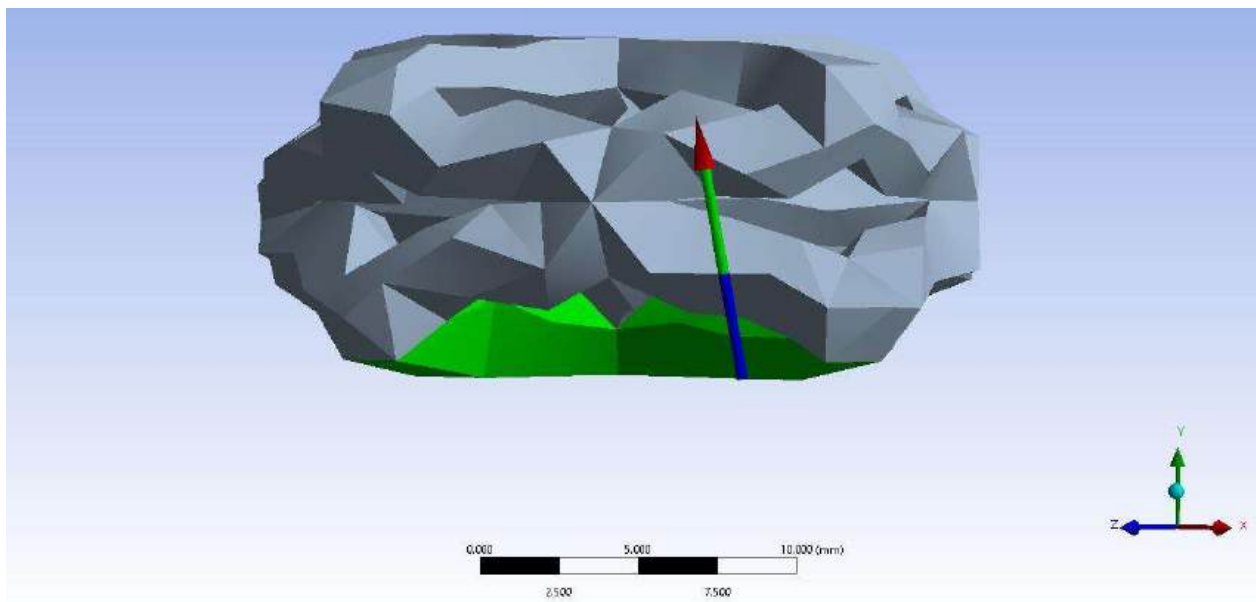


Figure 131: Force reaction for R1.5mm L10.80mm with 3mm mesh.

7.5.1.3.3 Unit Cell R 1.5mm L 13.50mm

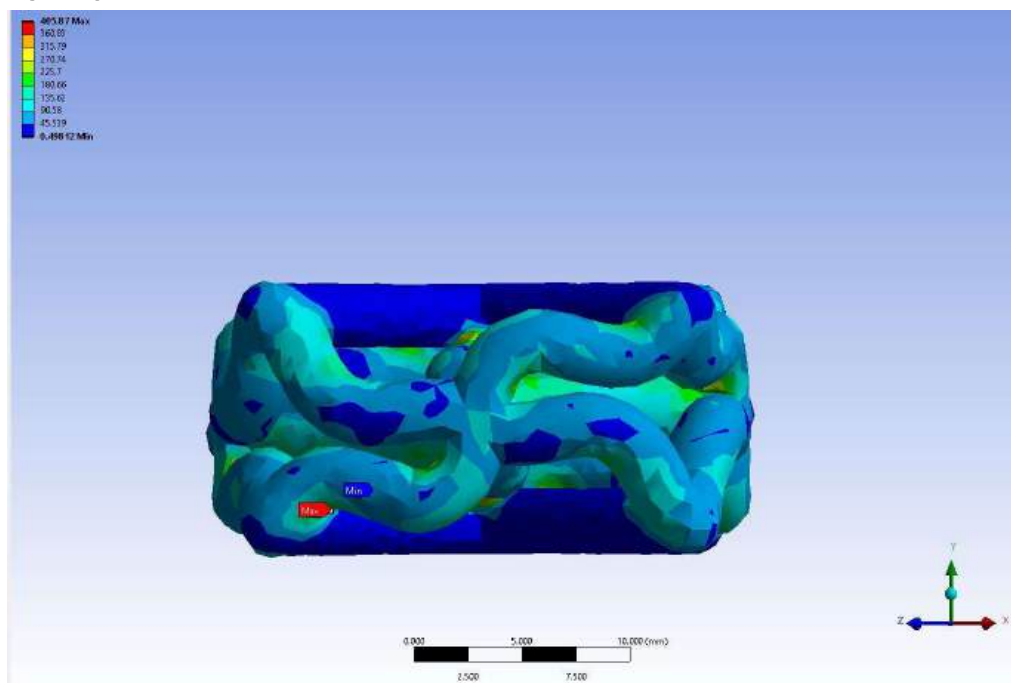


Figure 132: Equivalent Stress for R1.5mm L13.50mm with 1mm mesh.

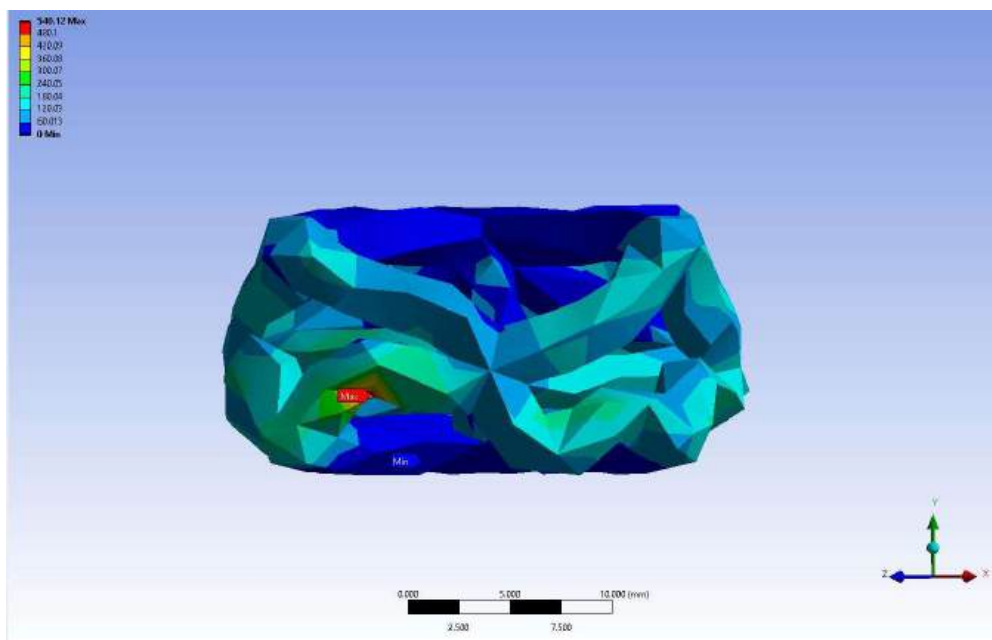


Figure 133: Equivalent Stress for R1.5mm L13.50mm with 3mm mesh.

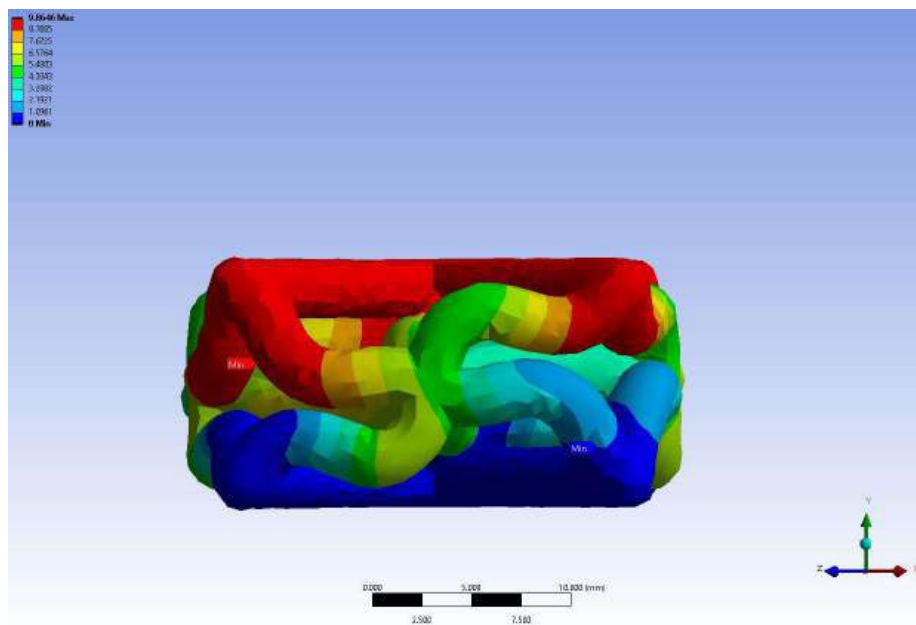


Figure 134: Total Deformation for R1.5mm L13.50mm with 1mm mesh.

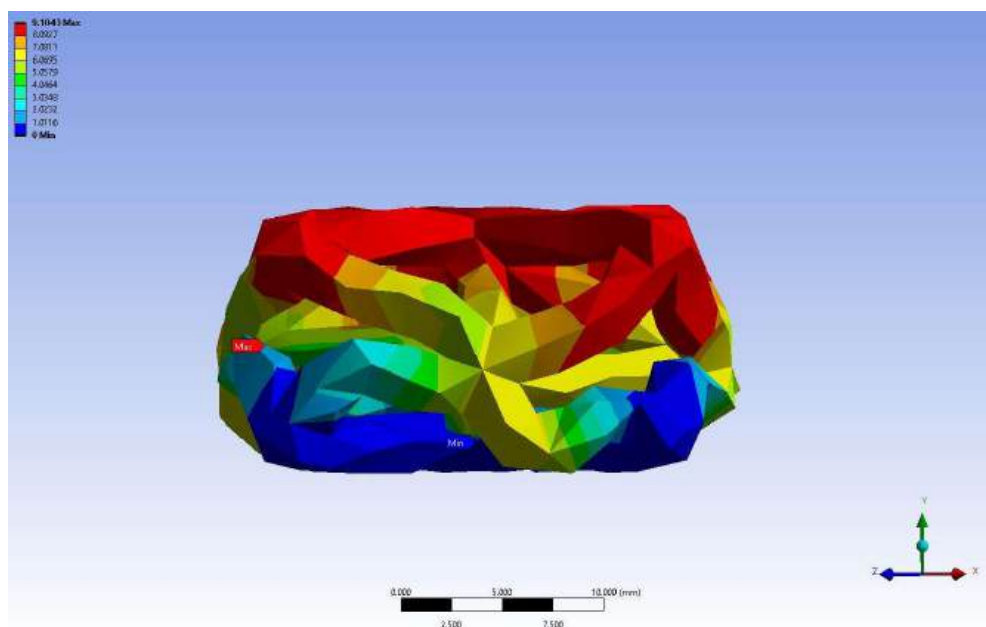


Figure 135: Total Deformation for R1.5mm L13.50mm with 3mm mesh.

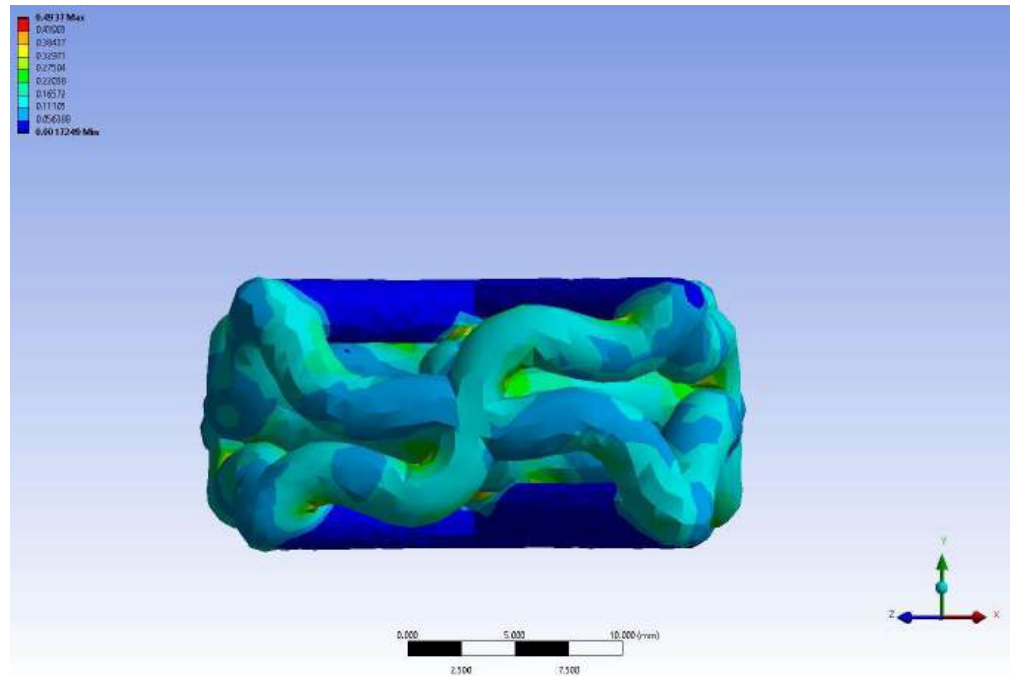


Figure 136: Elastic Strain for R1.5 mm L13.50 mm with 1 mm mesh.

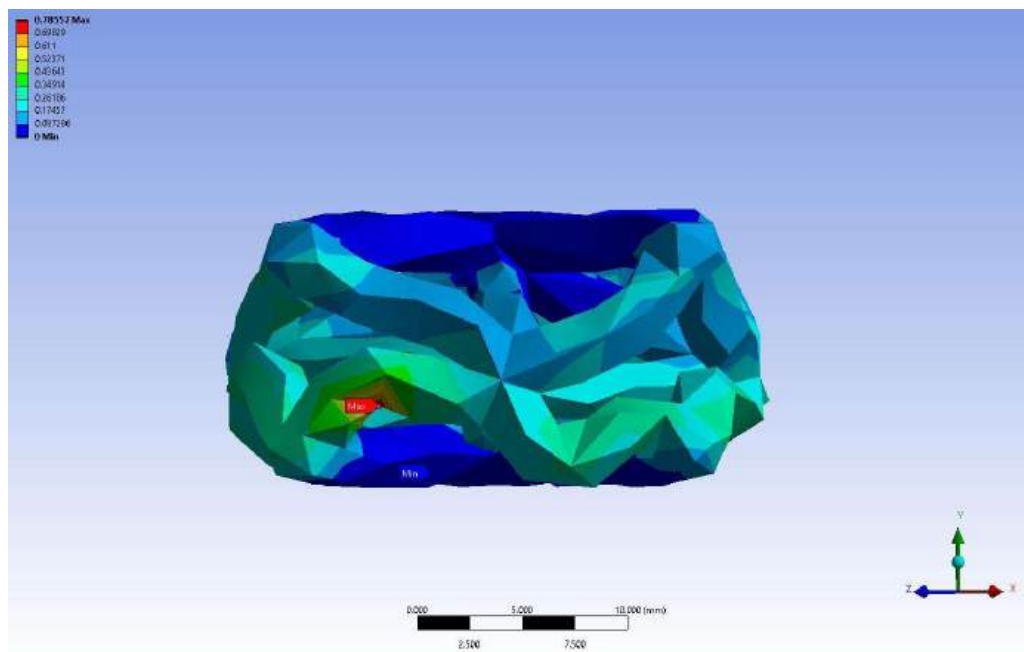


Figure 137: Elastic Strain for R1.5 mm L13.50 mm with 3 mm mesh.

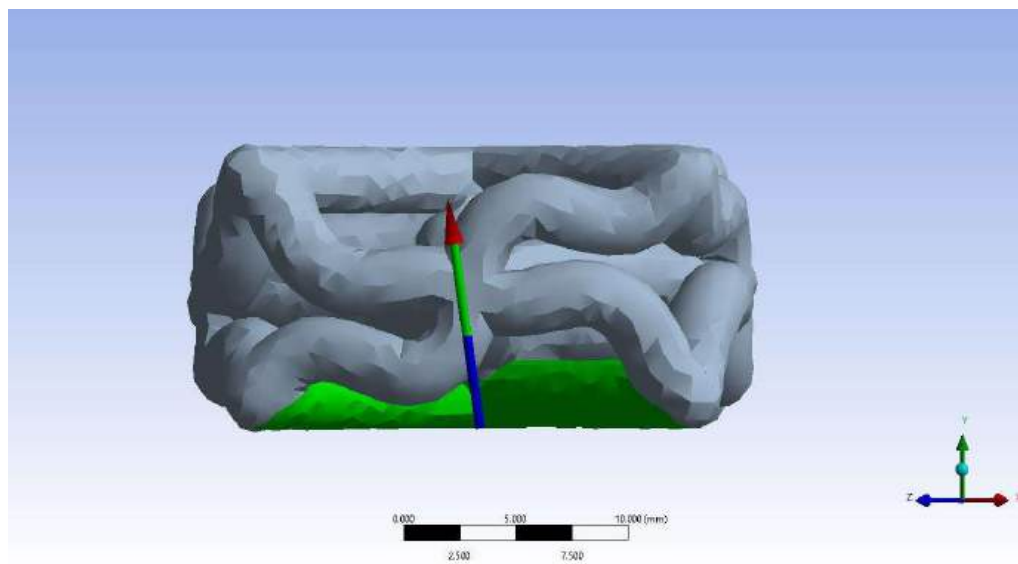


Figure 138: Force reaction for R1.5 mm L13.50 mm with 1 mm mesh.

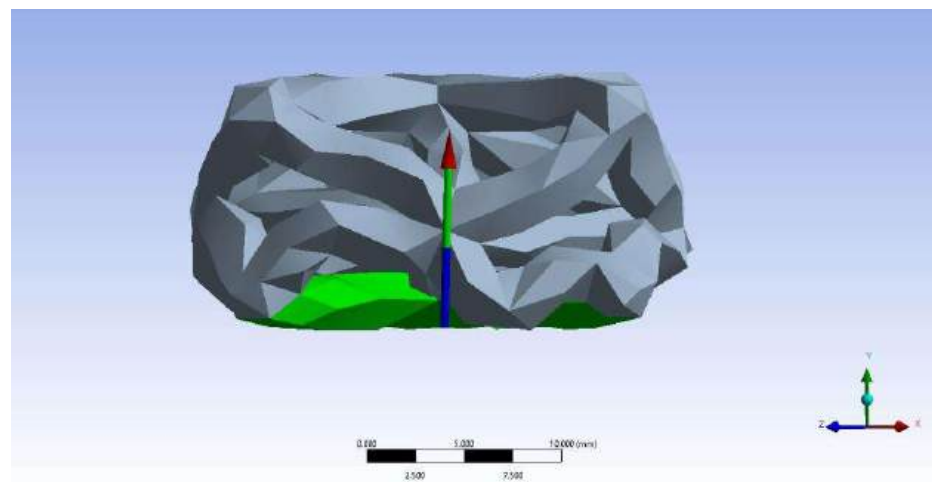


Figure 139: Force reaction for R1.5 mm L13.50 mm with 3 mm mesh.

7.5.1.3.4 Unit Cell R 1.5mm L 18.00mm

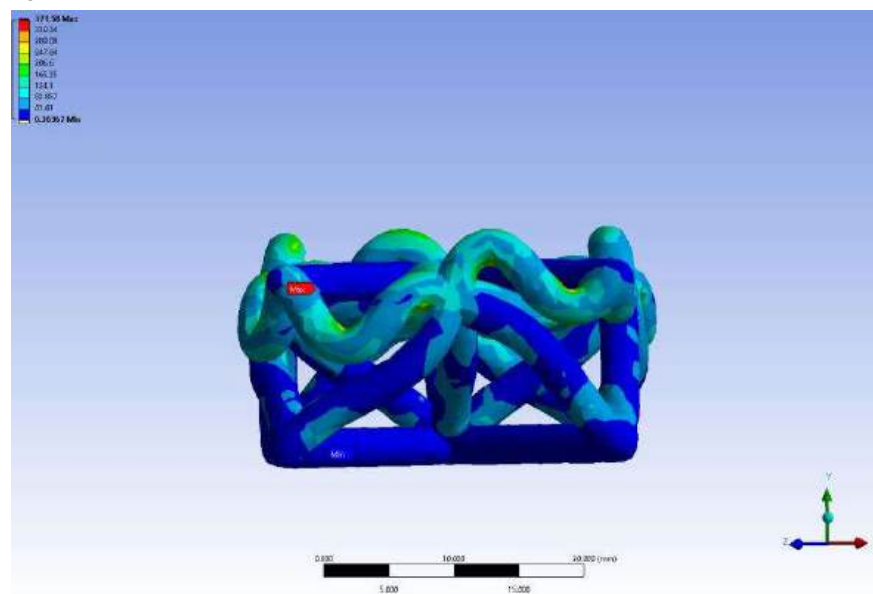


Figure 140: Equivalent Stress for R1.5 mm L18.0 mm with 1 mm mesh.

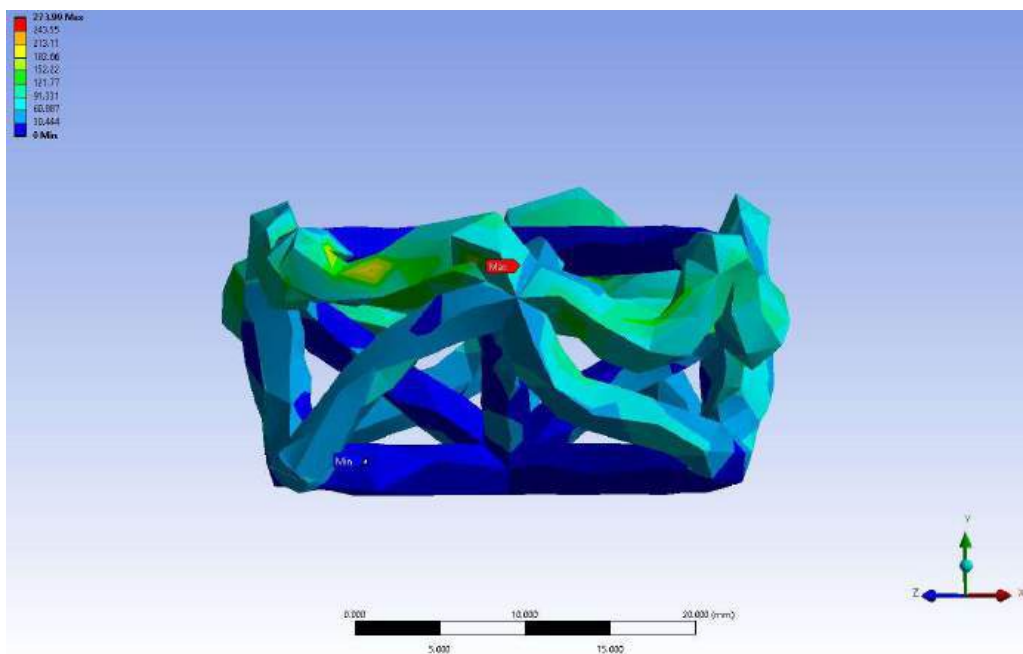


Figure 141: Equivalent Stress for R1.5 mm L18.0 mm with 3 mm mesh.

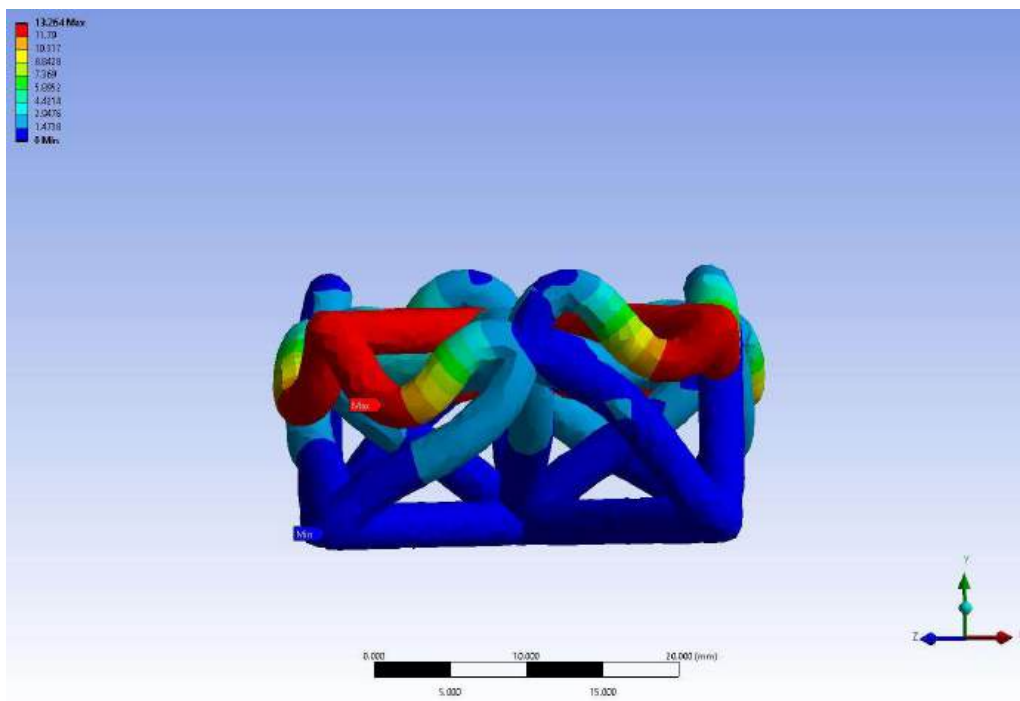


Figure 142: Total Deformation for R1.5 mm L18.0 mm with 1 mm mesh.

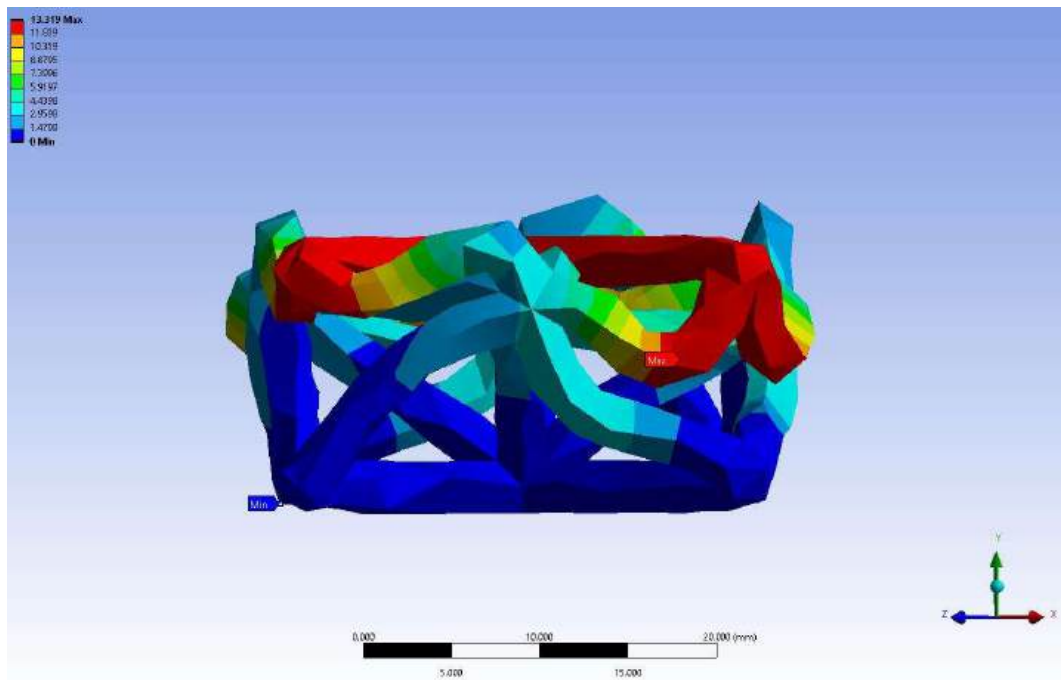


Figure 143: Total Deformation for R1.5 mm L18.0 mm with 3 mm mesh.

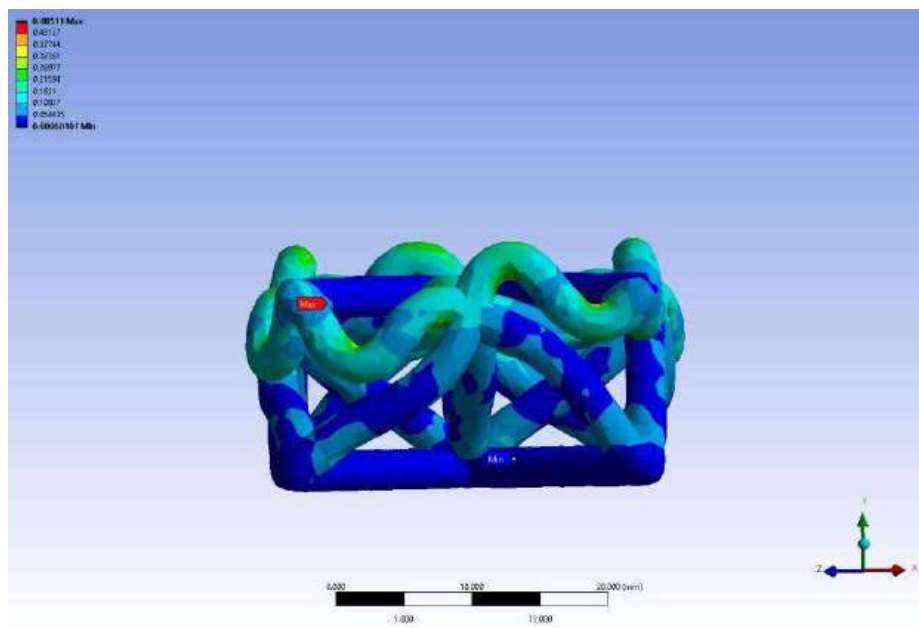


Figure 144: Elastic Strain for R1.5 mm L18.0 mm with 1 mm mesh.

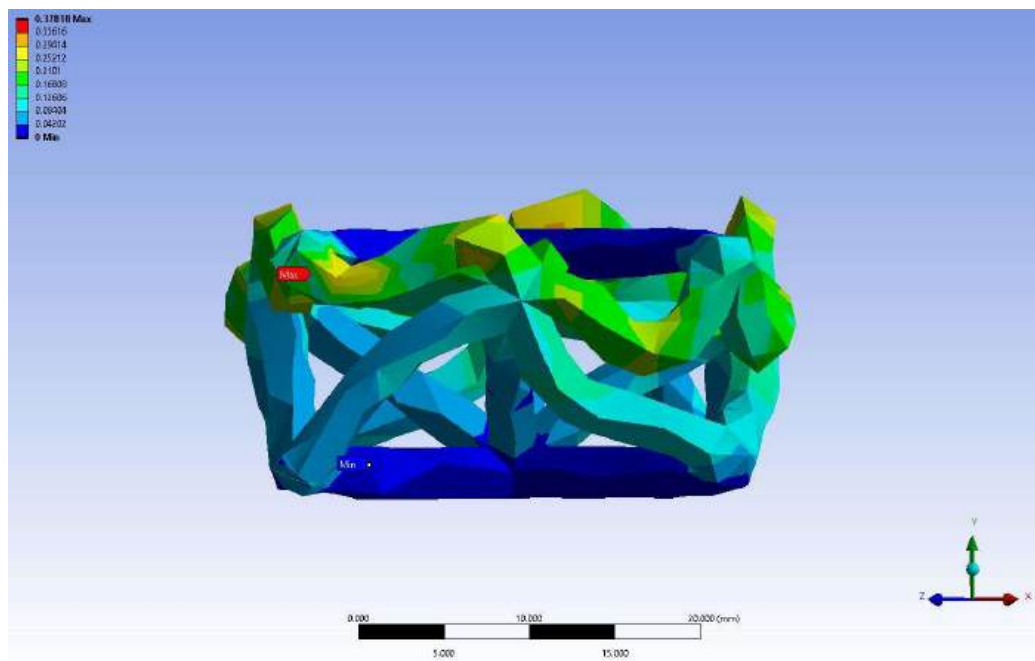


Figure 145: Elastic Strain for R1.5 mm L18.0 mm with 3 mm mesh.

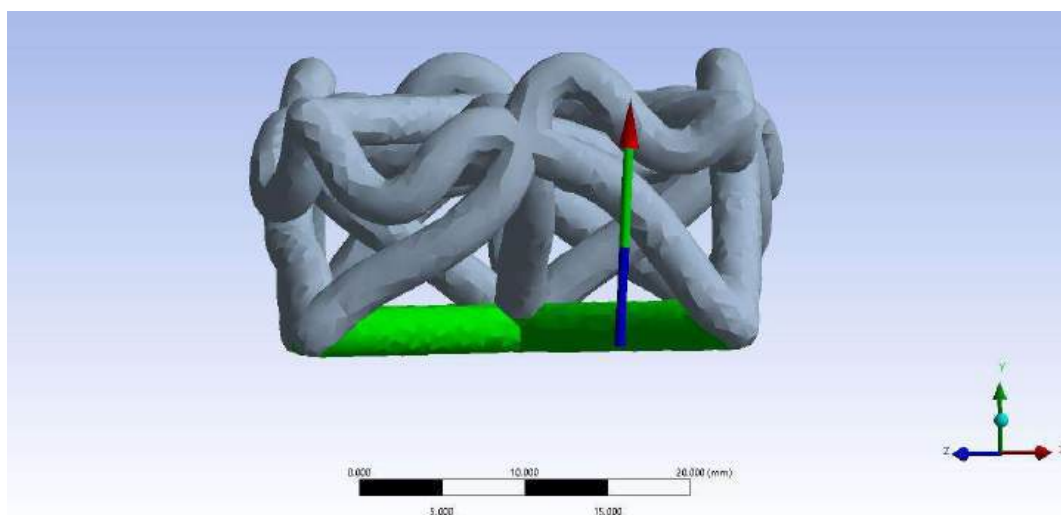


Figure 146: Force reaction for R1.5 mm L18.0 mm with 1 mm mesh.

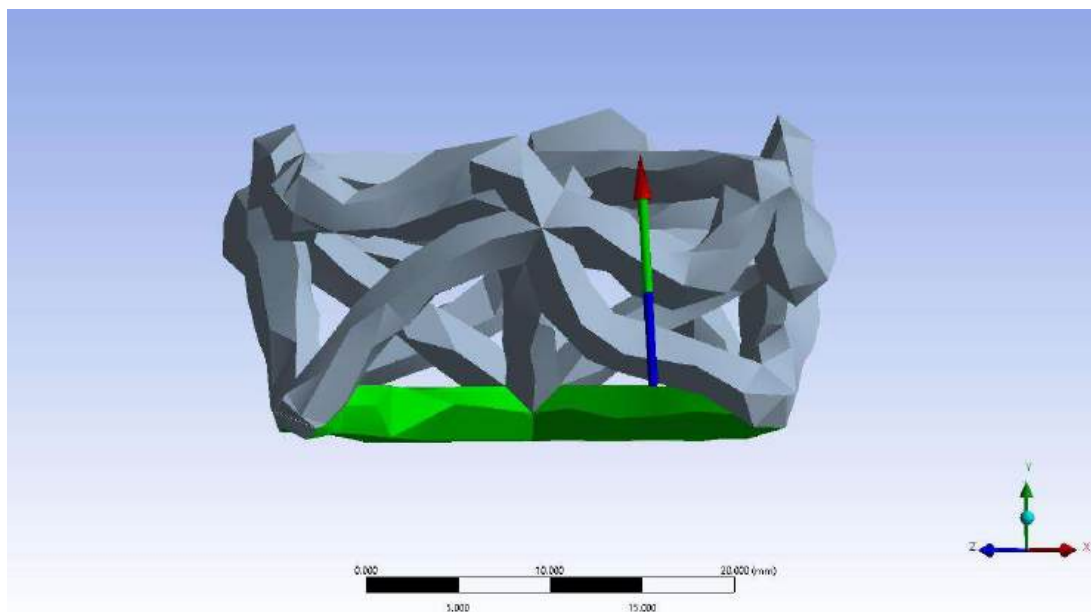


Figure 147: Force reaction for R1.5 mm L18.0 mm with 3 mm mesh.

7.5.2 Cell Structures

7.5.2.1 3x3x3 Structures

7.5.2.1.1 Cell Structure 3x3x3 R0.5 mm

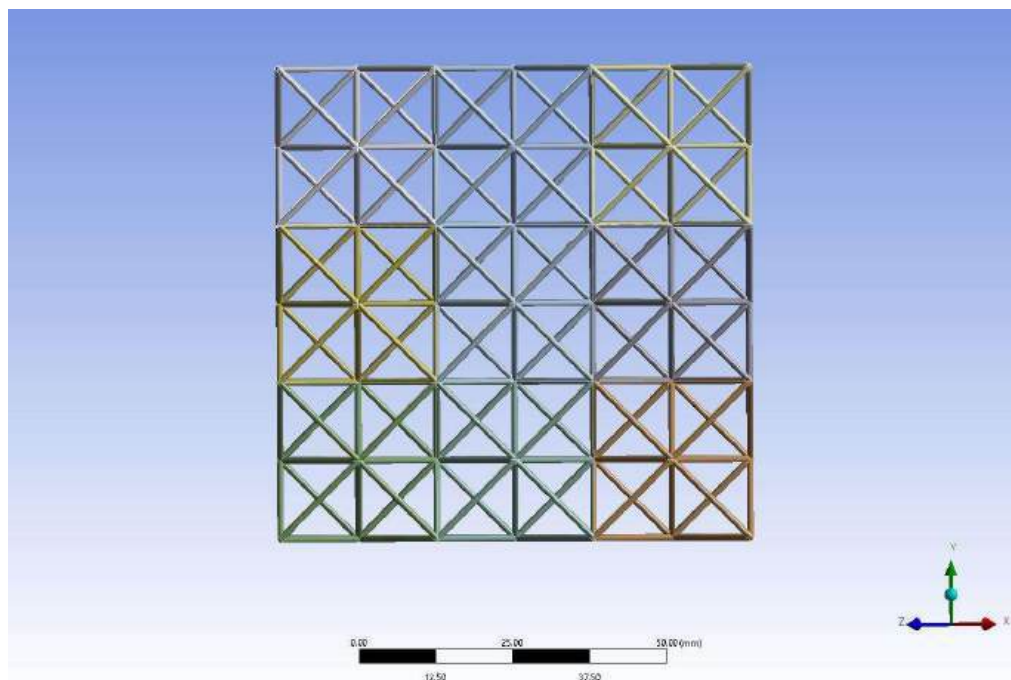


Figure 148: Equivalent Stress for 3x3x3 R0.5 mm Cell Structure with 3 mm (Coarse) mesh.

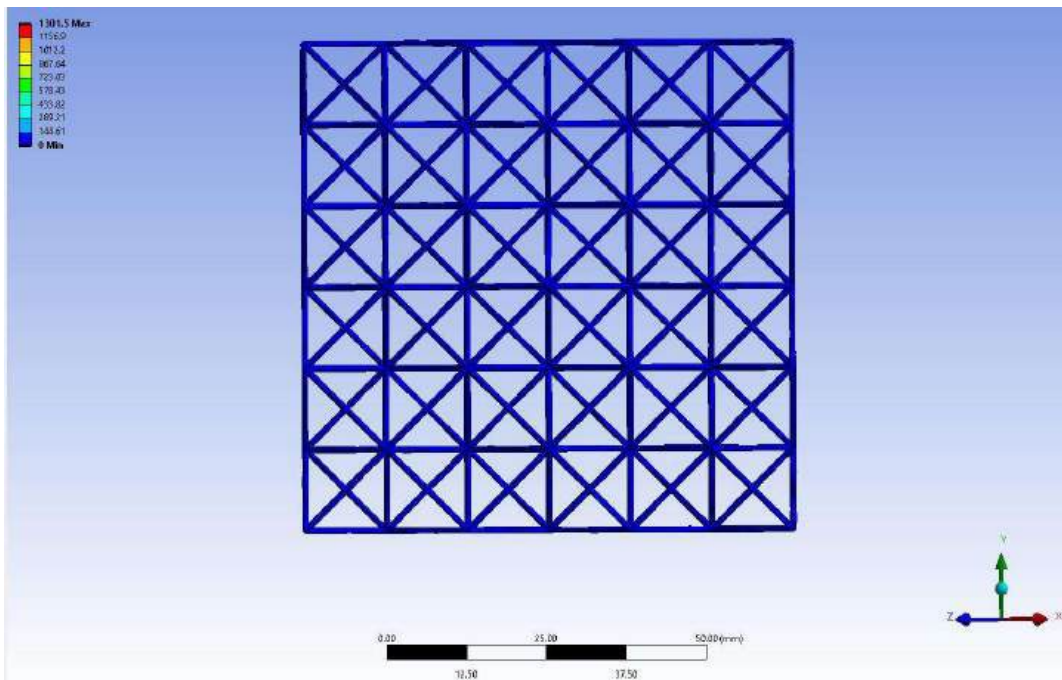


Figure 149: Total Deformation for 3x3x3 R0.5 mm Cell Structure with 3 mm mesh.

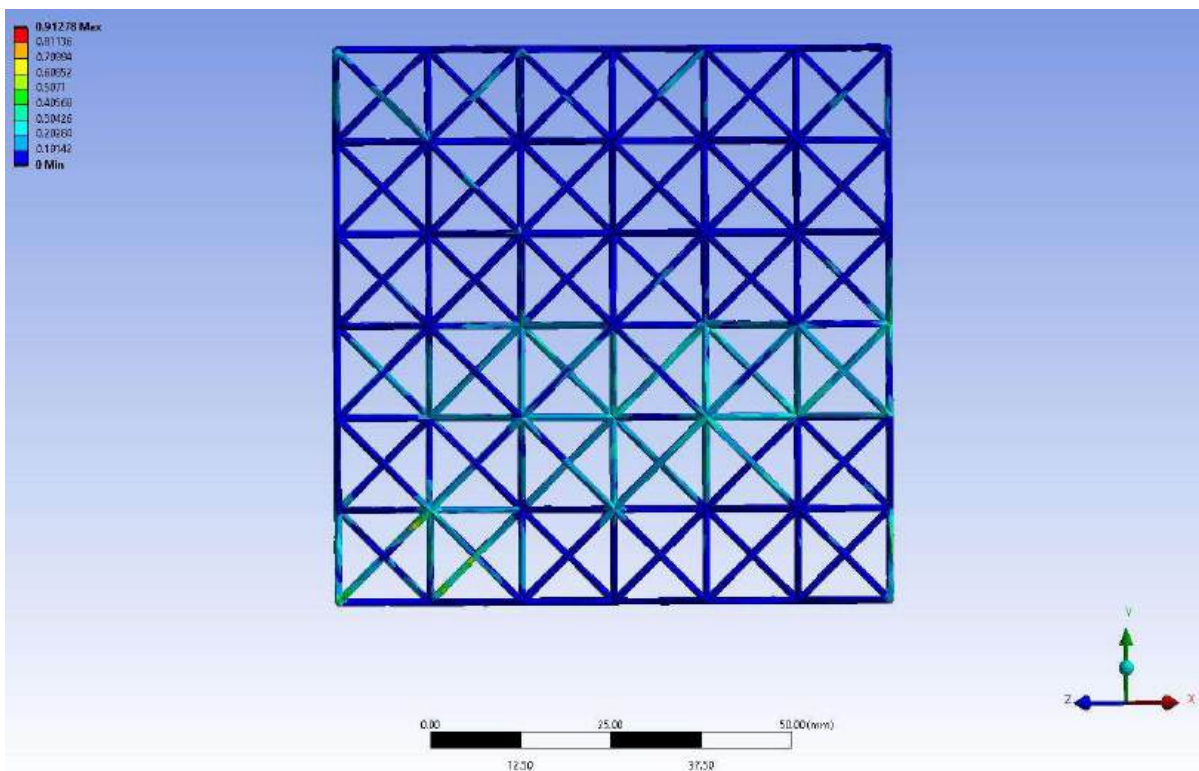


Figure 150: Elastic Strain for 3x3x3 R0.5 mm Cell Structure with 3 mm mesh

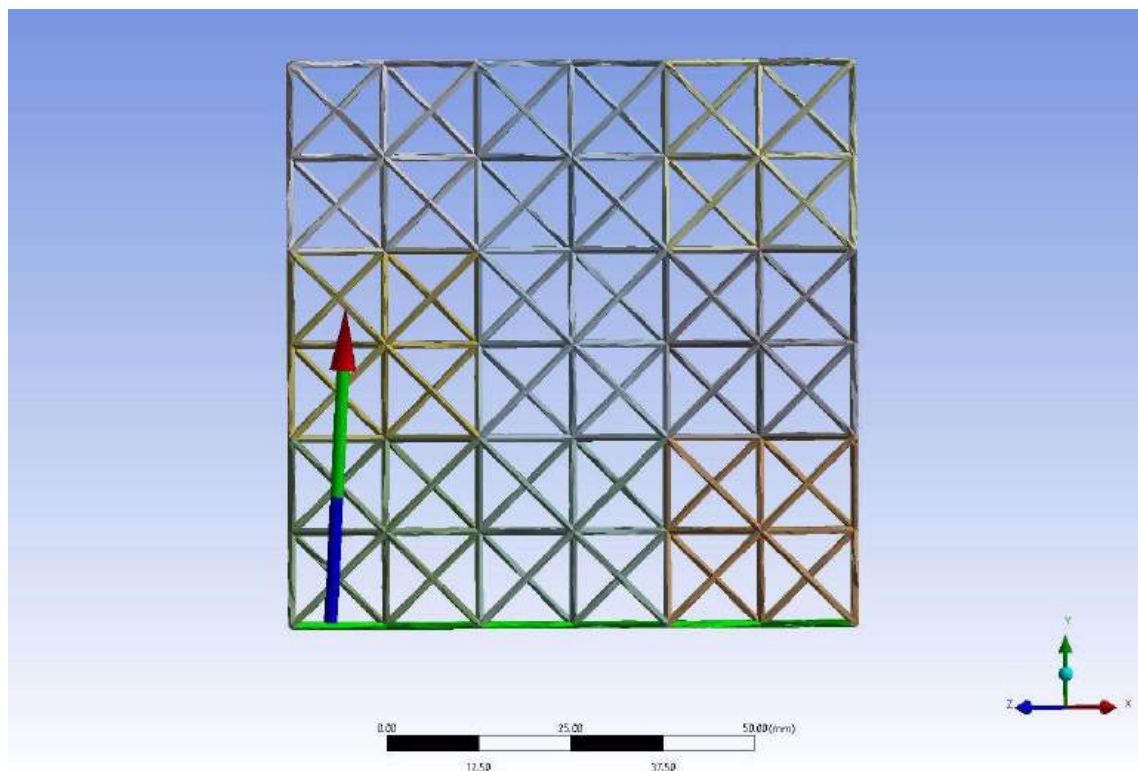


Figure 151: Force reaction for 3x3x3 R0.5 mm Cell Structure with 3 mm mesh

7.5.2.1.2 Cell Structure 3x3x3 R1.0 mm

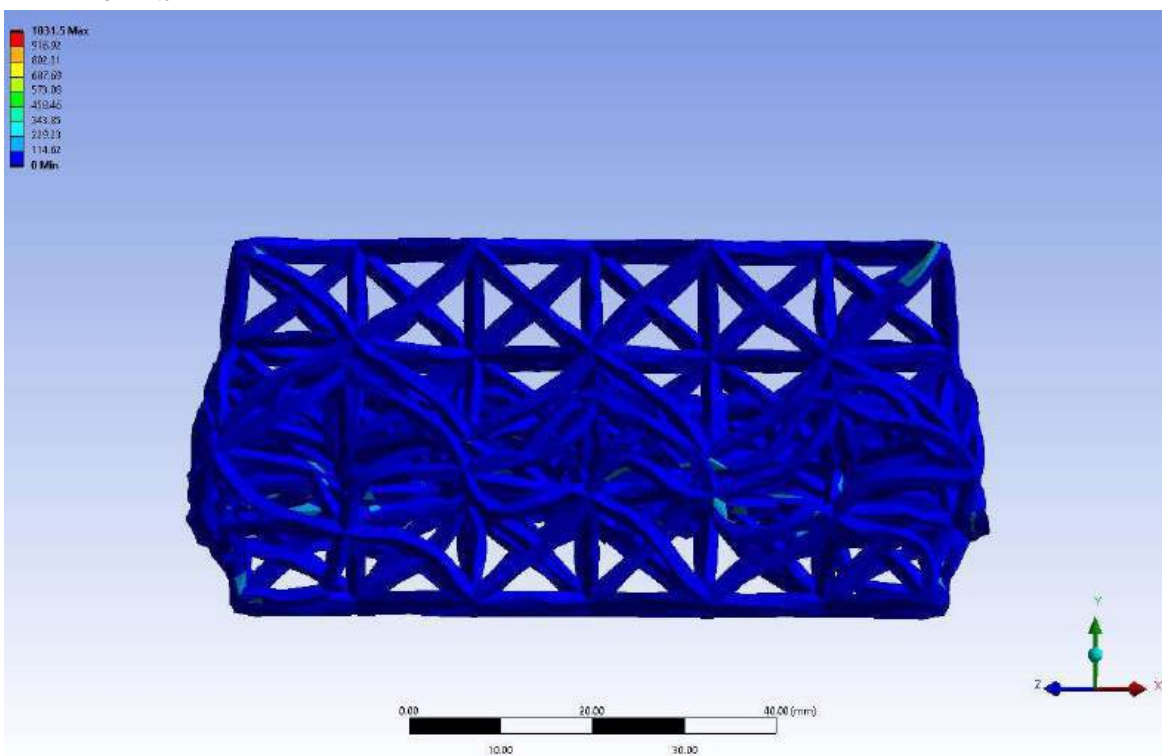


Figure 152: Equivalent Stress for 3x3x3 R1.0 mm Cell Structure with 3 mm (Coarse) mesh

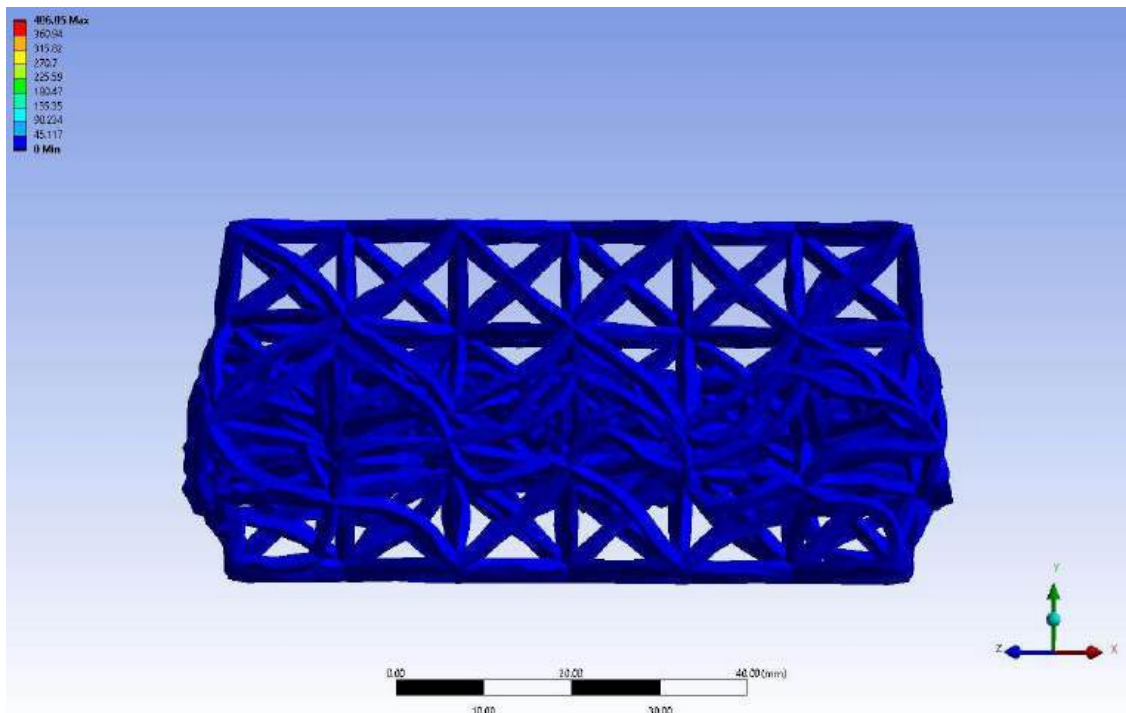


Figure 153: Total Deformation for 3x3x3 R1.0 mm Cell Structure with 3 mm mesh

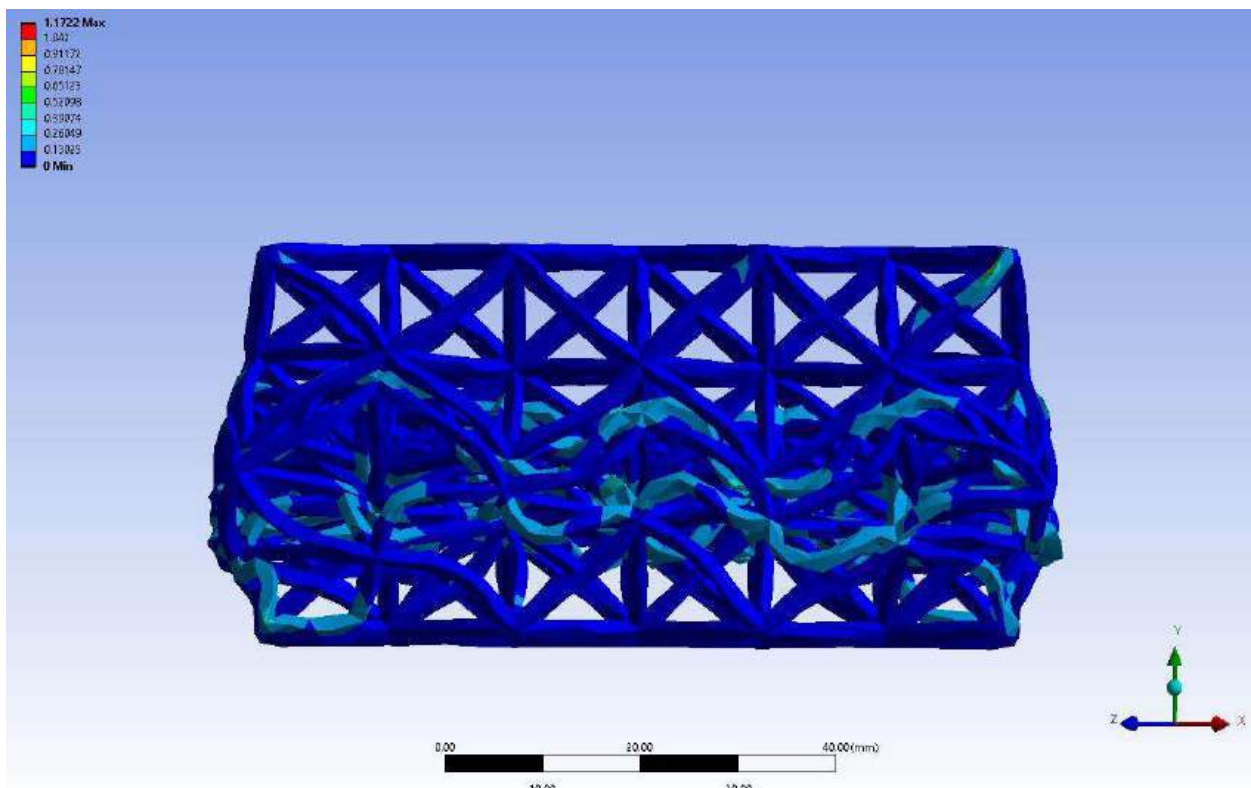


Figure 154: Elastic Strain for 3x3x3 R1.0 mm Cell Structure with 3 mm mesh

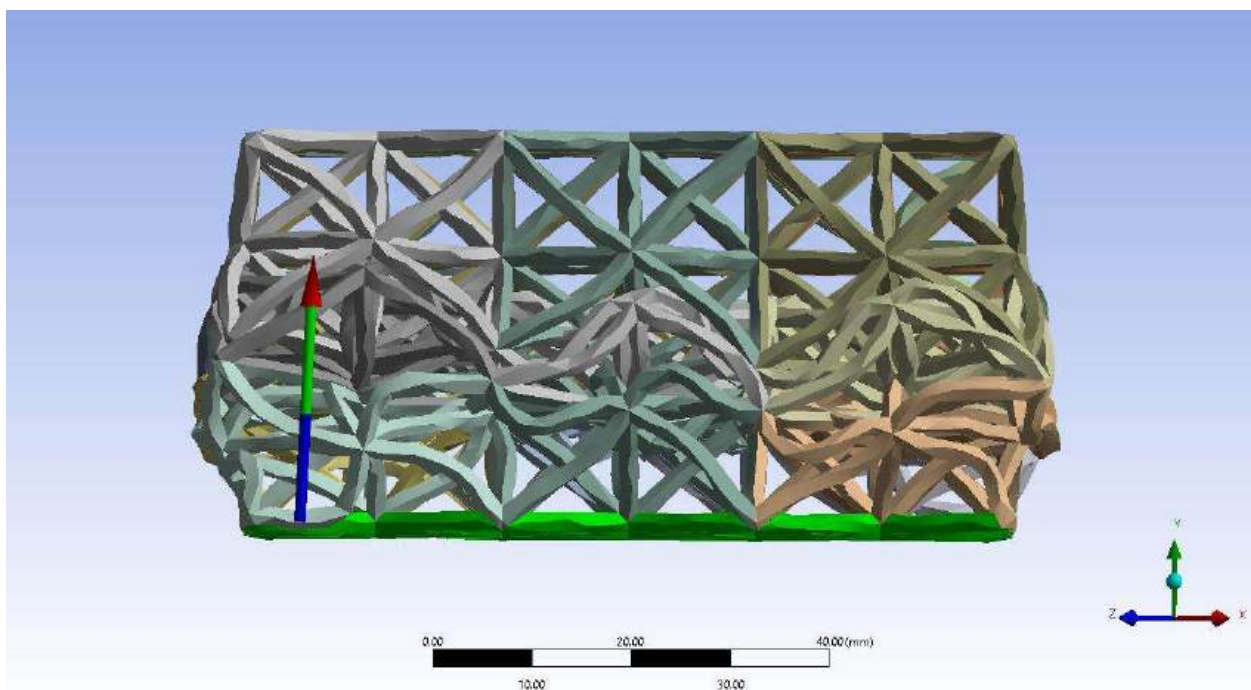


Figure 155: Force reaction for 3x3x3 R1.0 mm Cell Structure with 3 mm mesh

7.5.2.1.3 Cell Structure 3x3x3 R1.5 mm

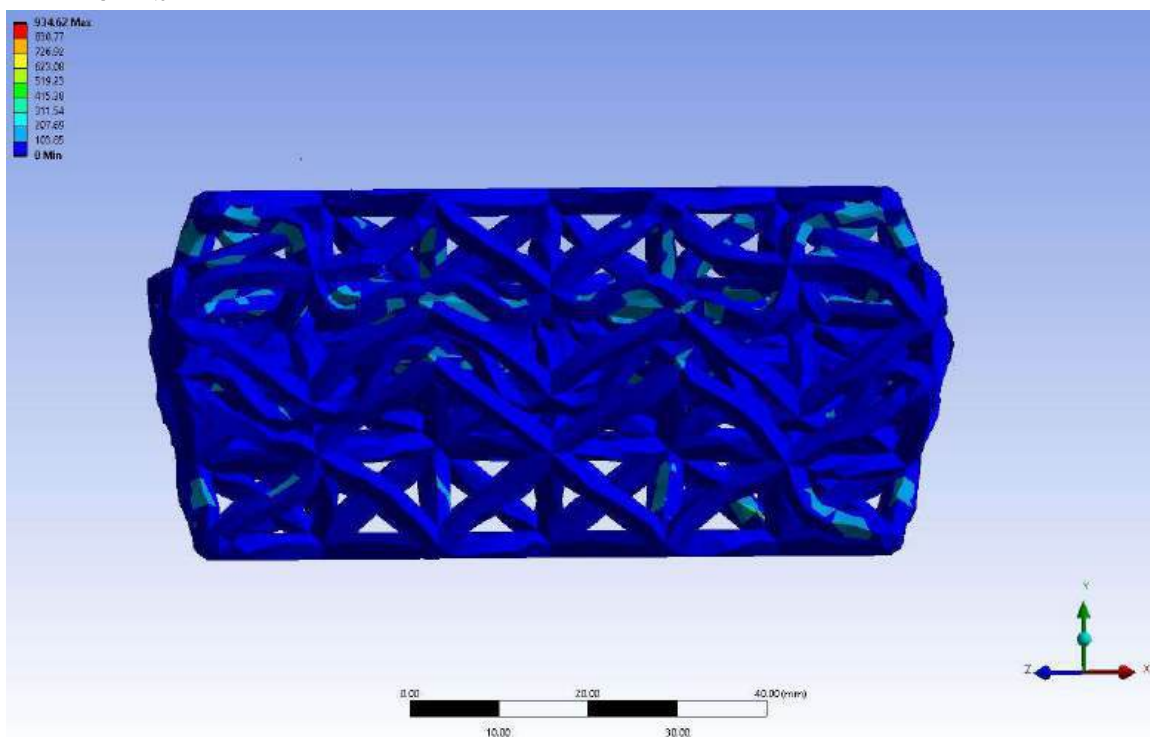


Figure 156: Equivalent Stress for 3x3x3 R1.5 mm Cell Structure with 3 mm mesh

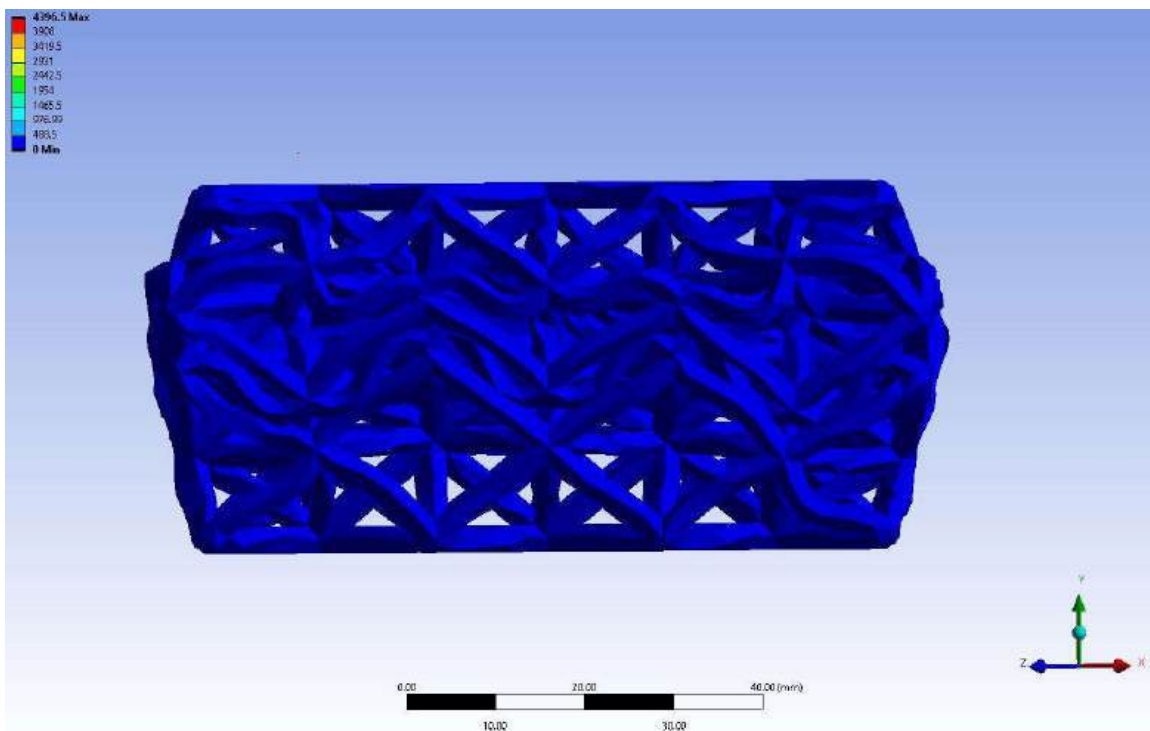


Figure 157: Total Deformation for 3x3x3 R1.5 mm Cell Structure with 3 mm mesh

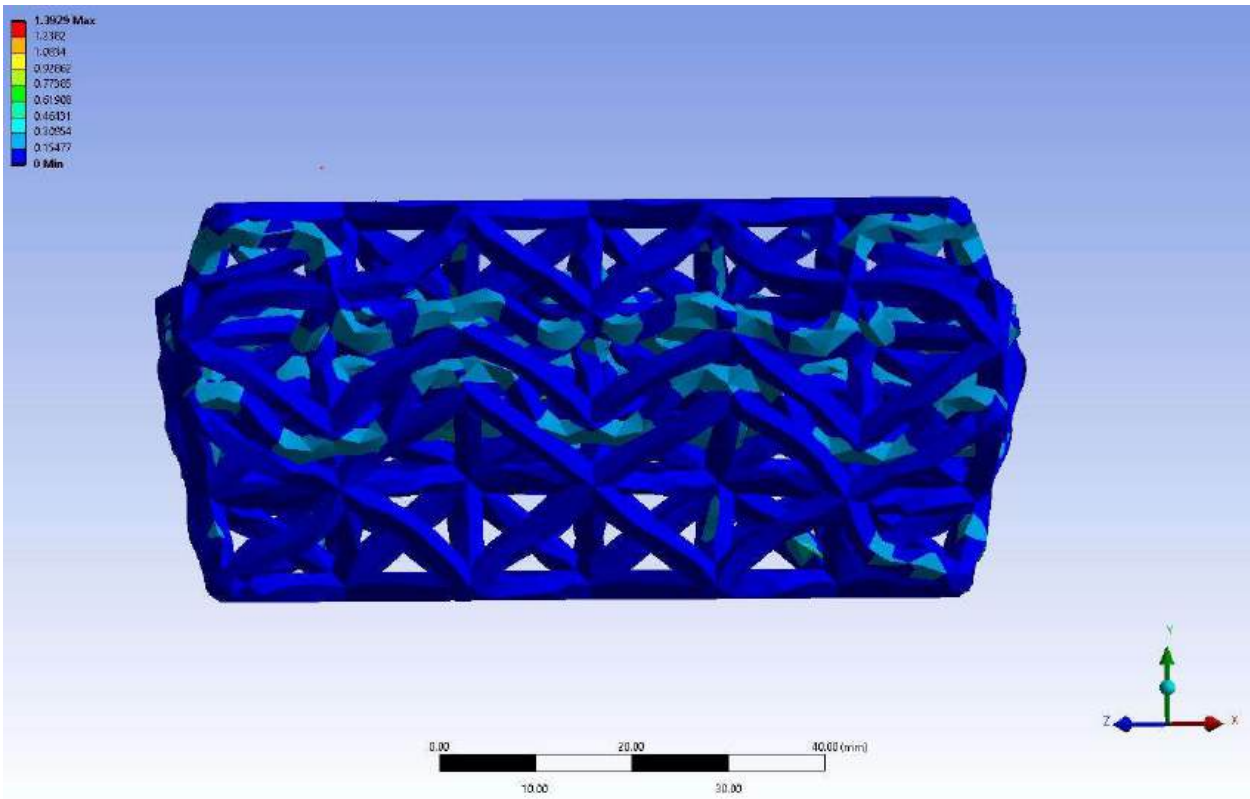


Figure 158: Elastic Strain for 3x3x3 R1.5 mm Cell Structure with 3 mm mesh

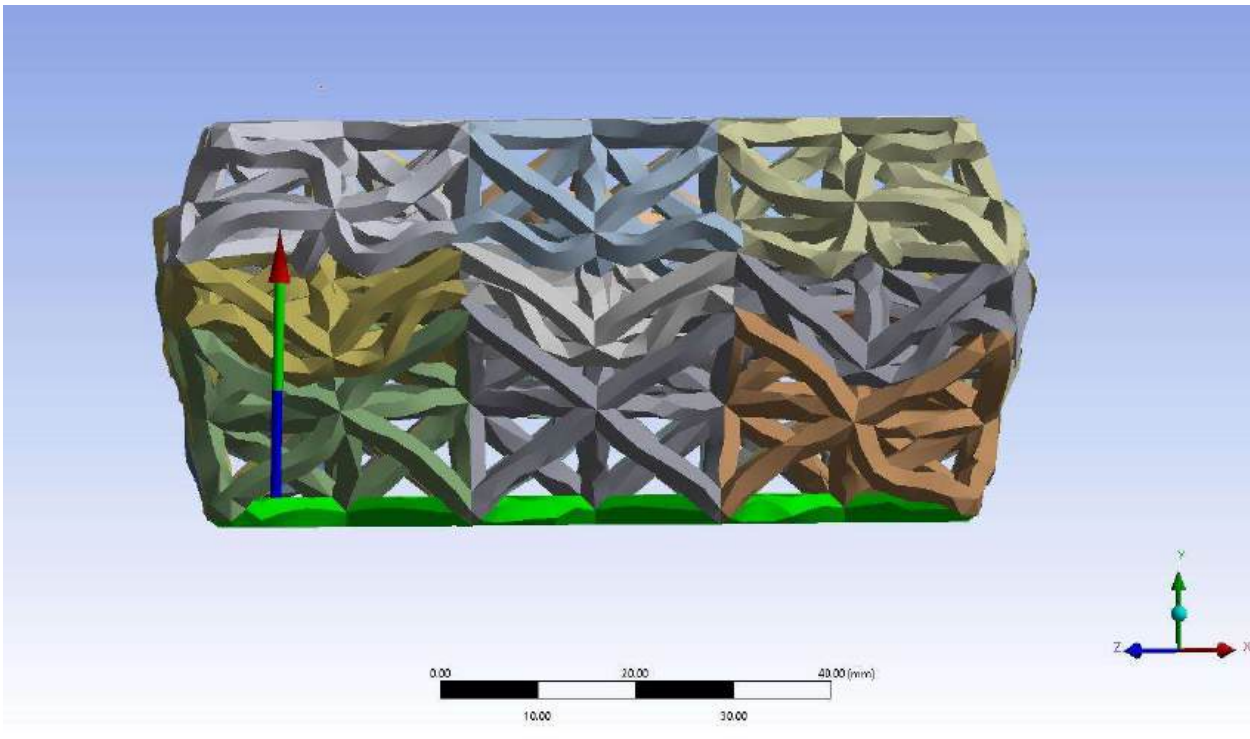


Figure 159: Force reaction for 3x3x3 R1.5 mm Cell Structure with 3 mm mesh

7.5.2.2 4x4x4 Structures

7.5.2.2.1 Cell Structure 4x4x4 0.5 mm

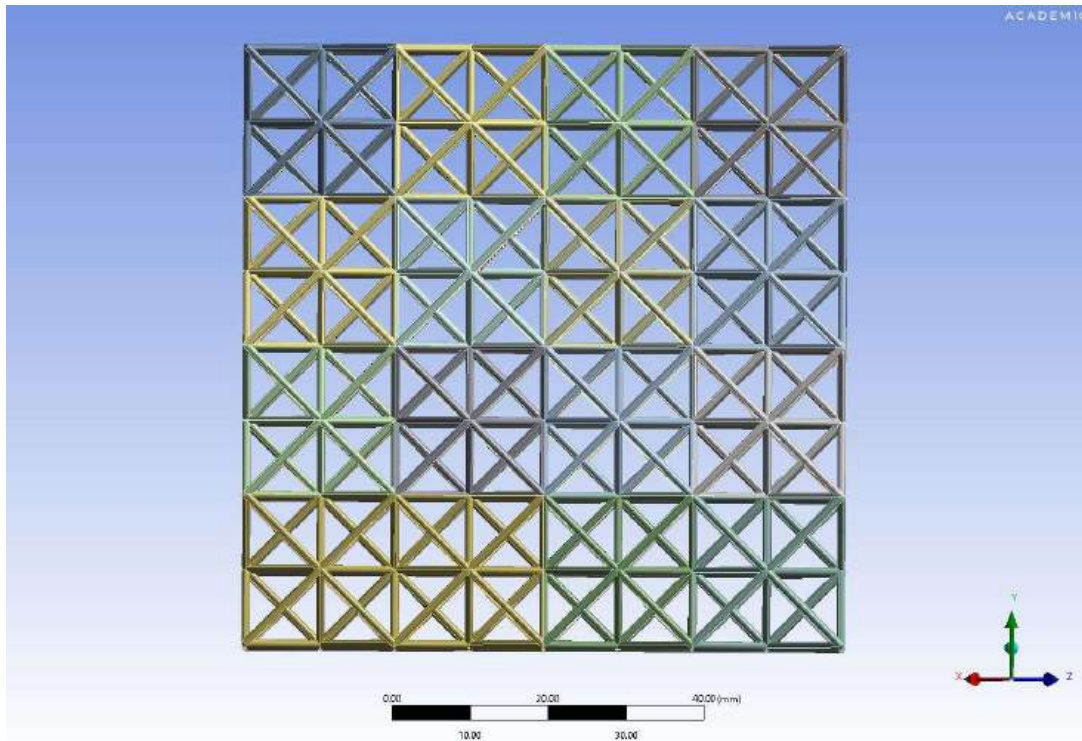


Figure 160: Equivalent Stress for 4x4x4 R0.5 mm with 3 mm (Coarse) mesh

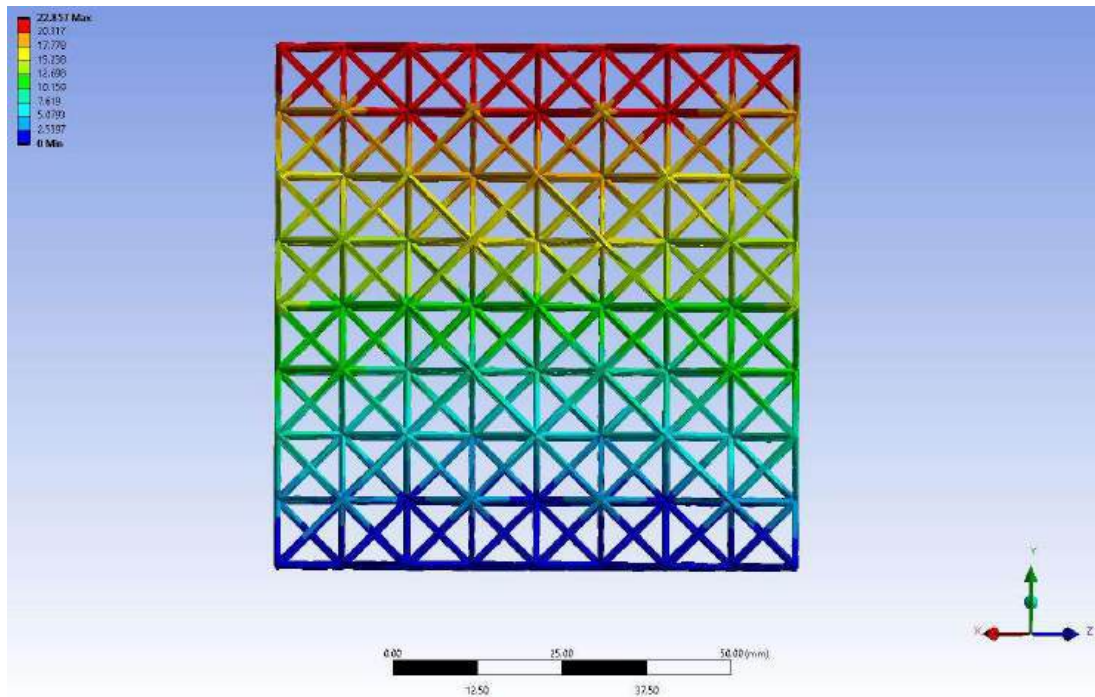


Figure 161: Total Deformation for 4x4x4 R0.5 mm Cell Structure with 3 mm mesh

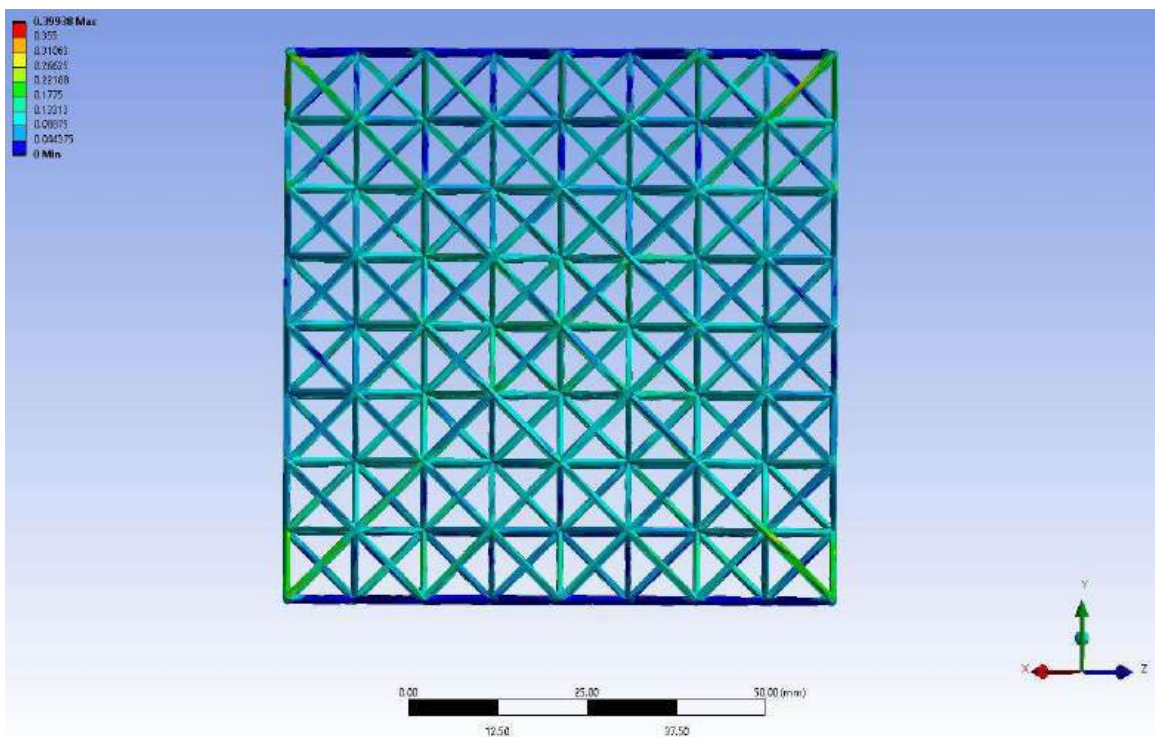


Figure 162: Elastic Strain for 4x4x4 R0.5 mm Cell Structure with 3 mm mesh

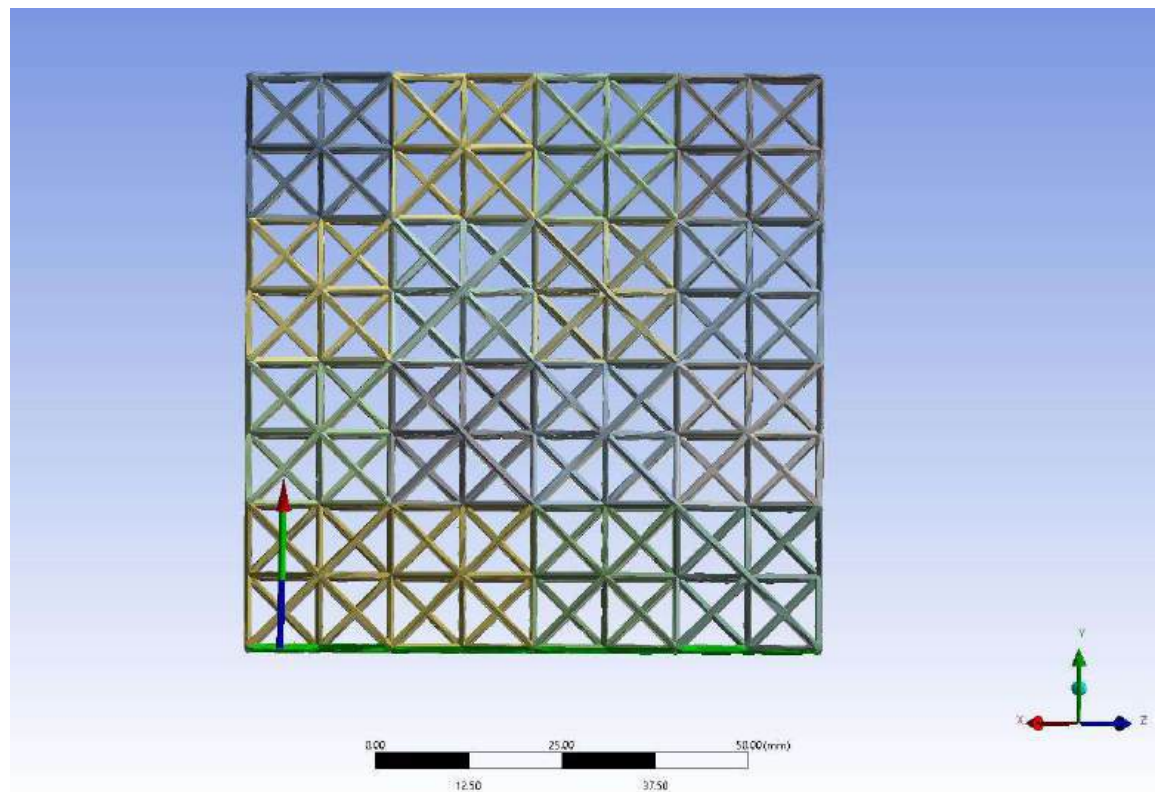


Figure 163: Force reaction for 4x4x4 R0.5 mm Cell Structure with 3 mm mesh

7.5.2.2.2 Cell Structure 4x4x4 1.5 mm

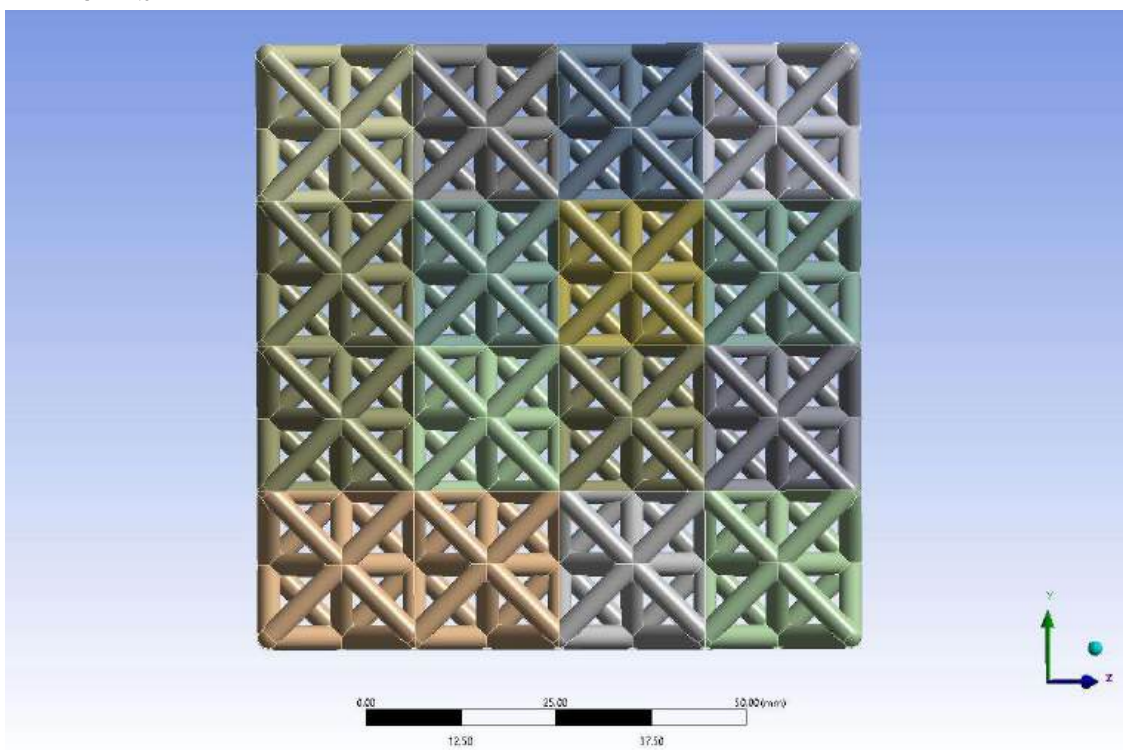


Figure 164: Equivalent Stress for 4x4x4 R1.5 mm Cell Structure with 3 mm mesh

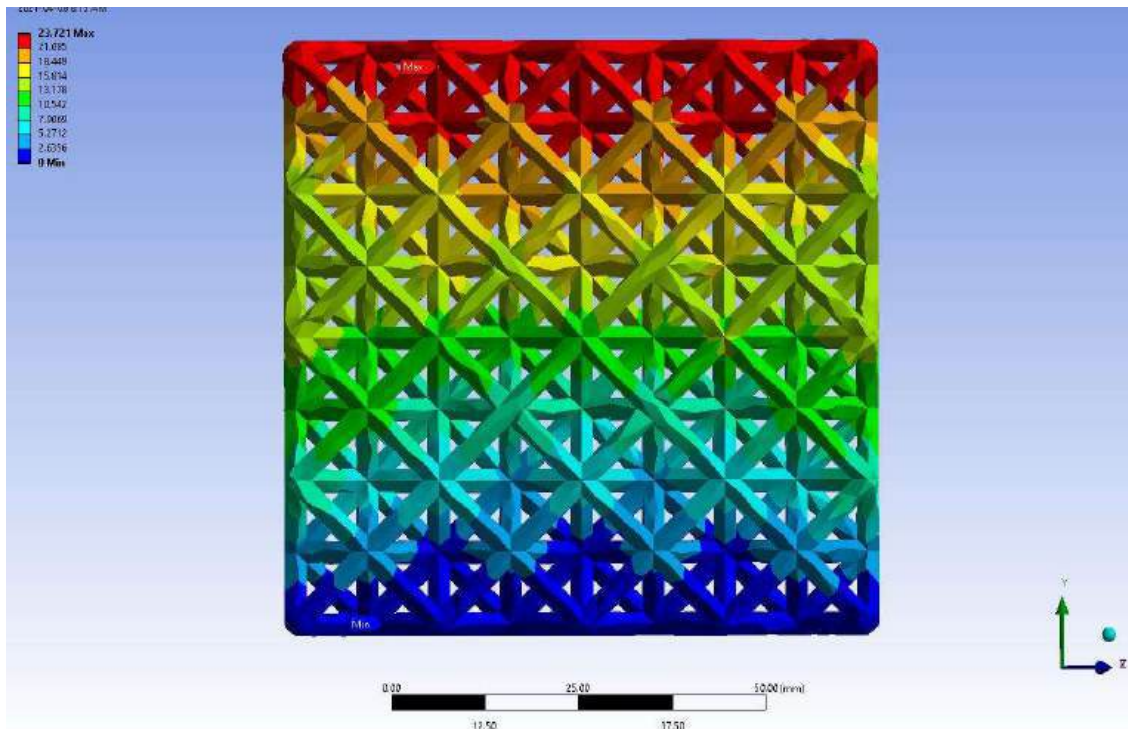


Figure 165: Total Deformation for 4x4x4 R1.5 mm Cell Structure with 3 mm mesh

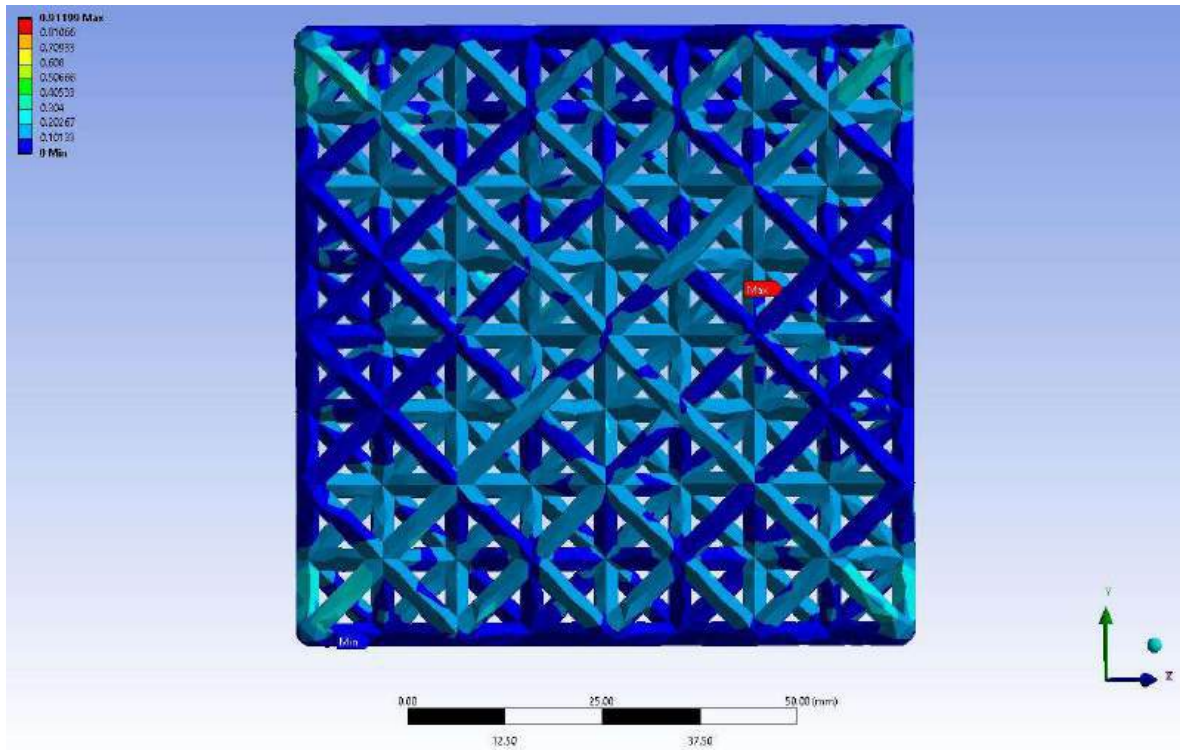


Figure 166: Elastic Strain for 4x4x4 R1.5 mm Cell Structure with 3 mm mesh

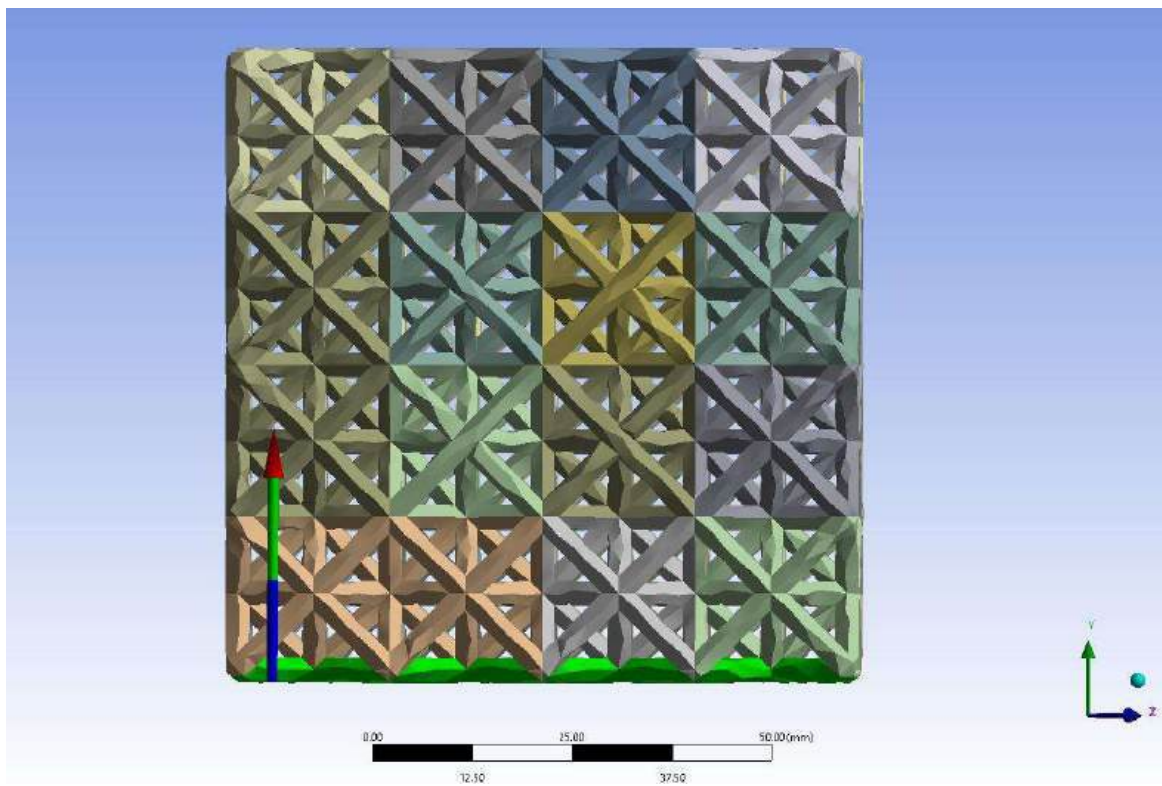


Figure 167: Force reaction for 4x4x4 R1.5 mm Cell Structure with 3 mm mesh

7.5.2.3 5x5x5 Structures

7.5.2.3.1 Cell Structure 5x5x5 0.5 mm

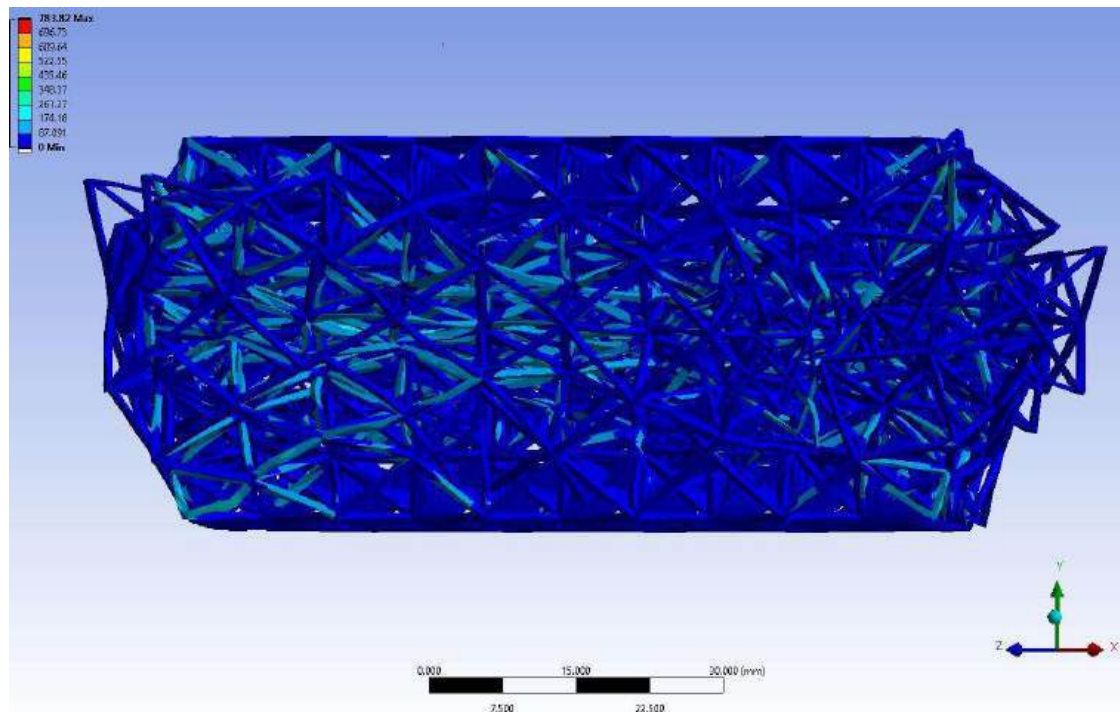


Figure 168: Equivalent Stress for 5x5x5 R0.5 mm Cell Structure with 3 mm (Coarse) mesh

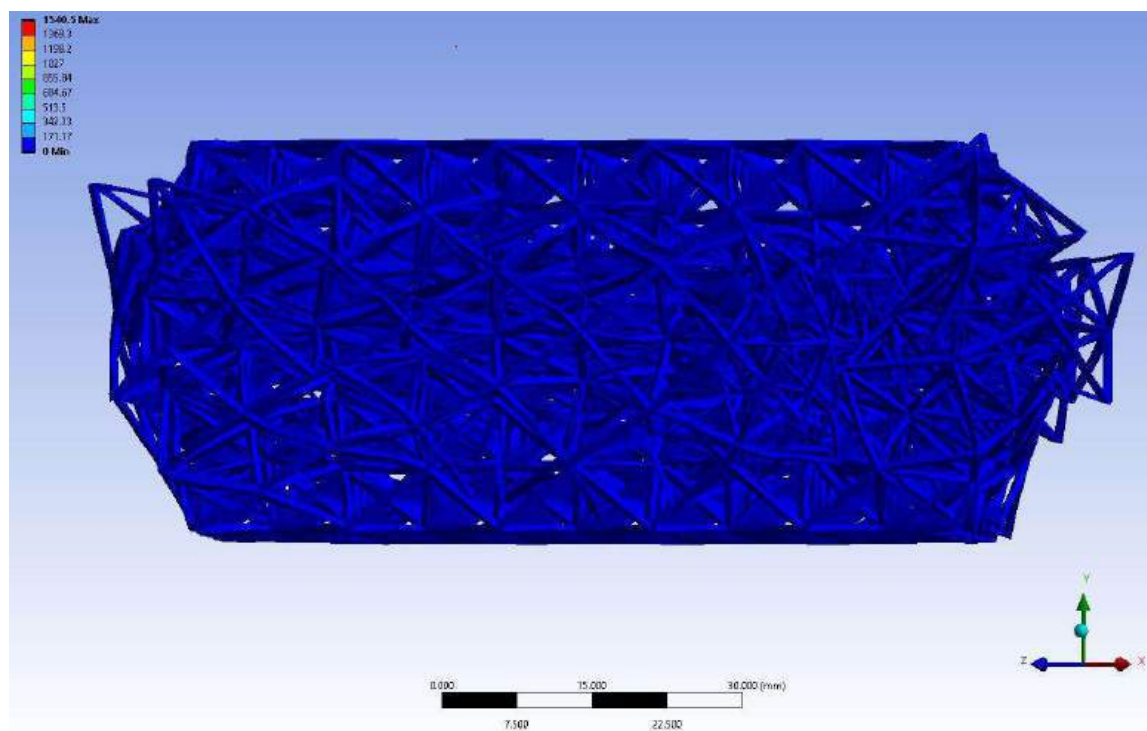


Figure 169: Total Deformation for 5x5x5 R0.5 mm Cell Structure with 3 mm mesh

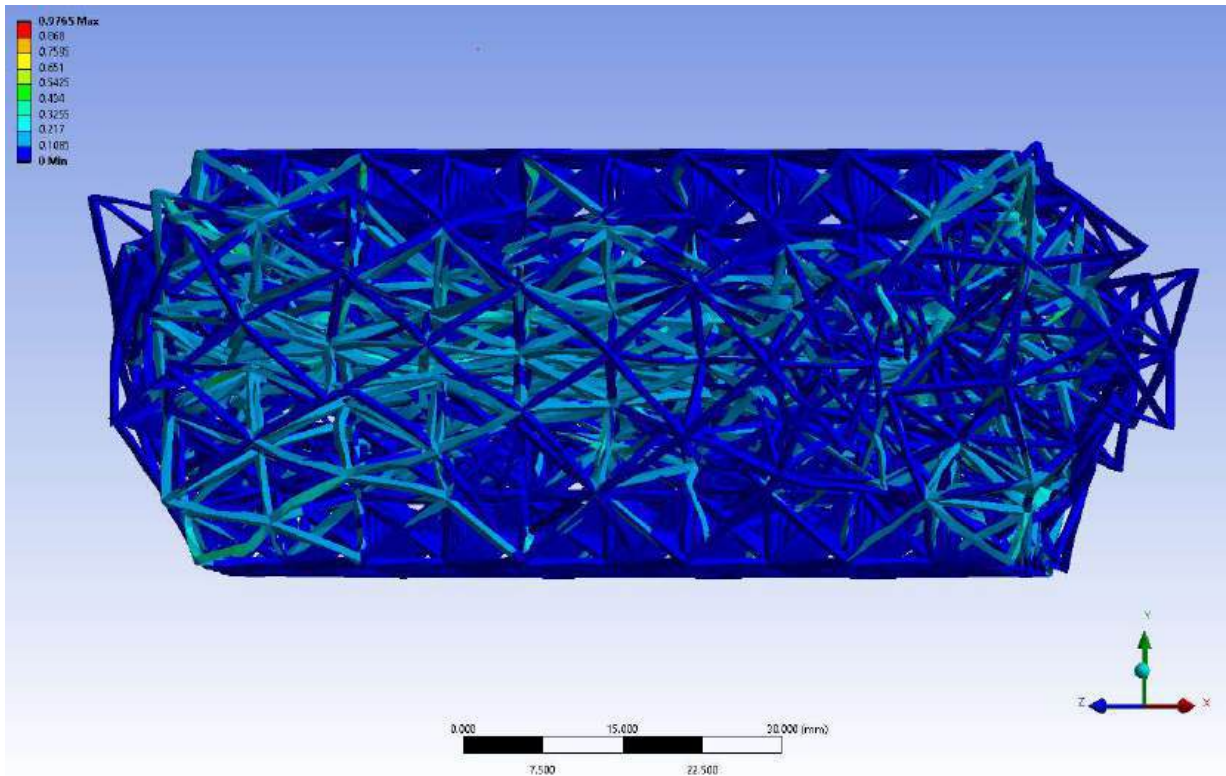


Figure 170: Elastic Strain for 5x5x5 R0.5 mm Cell Structure with 3 mm mesh

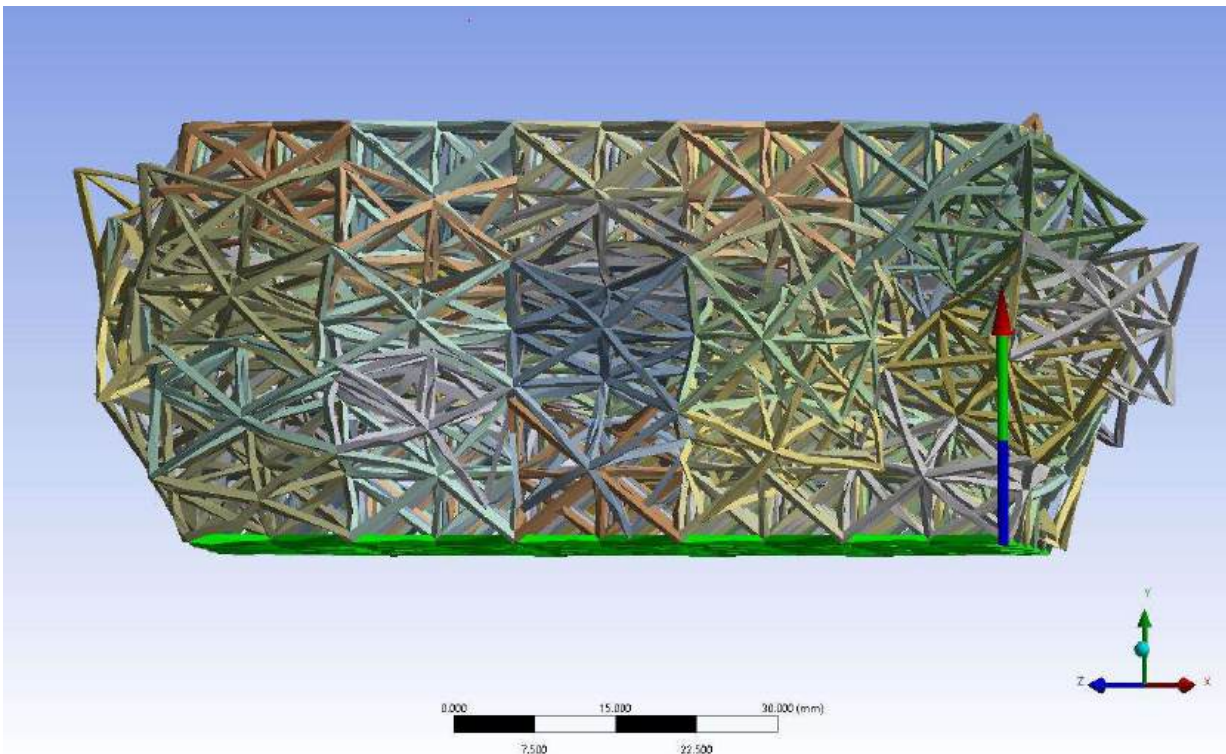


Figure 171: Force reaction for 5x5x5 R0.5 mm Cell Structure with 3 mm mesh

7.5.2.3.2 Cell Structure 5x5x5 1.0 mm

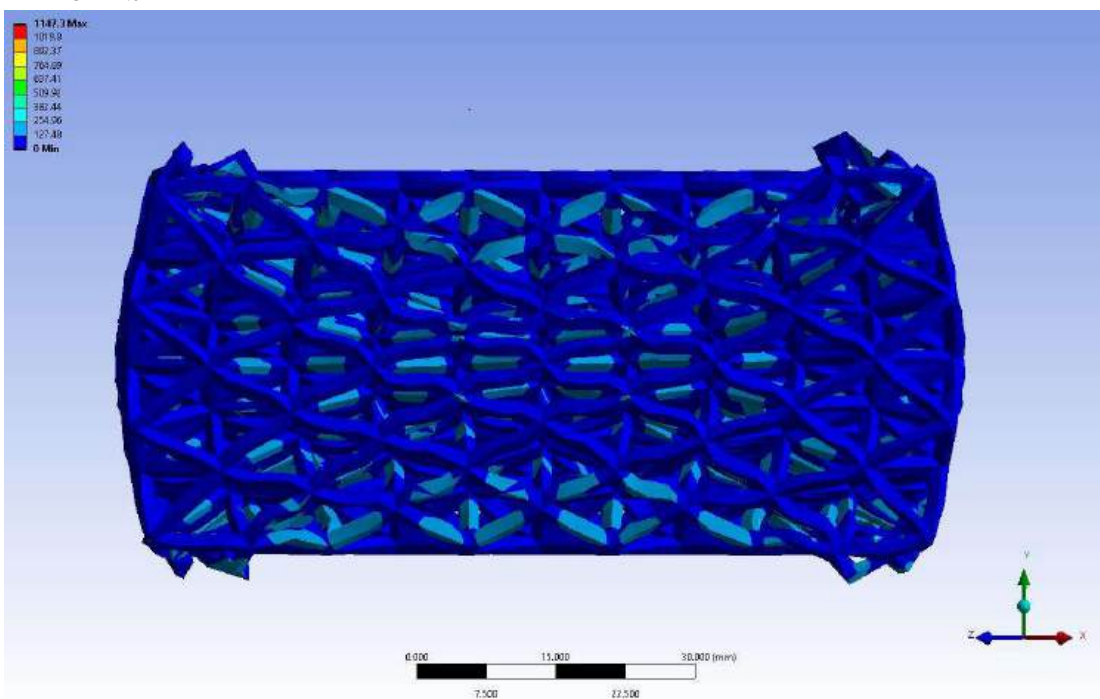


Figure 172: Equivalent Stress for 5x5x5 R1.0 mm Cell Structure with 3 mm (Coarse) mesh

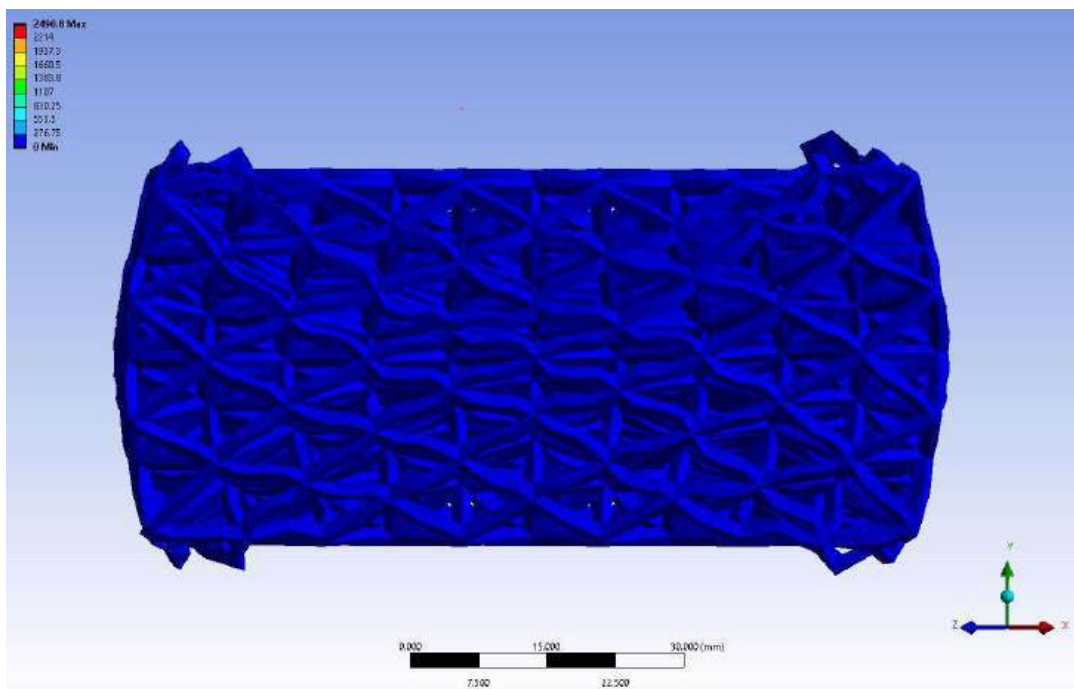


Figure 173: Total Deformation for 5x5x5 R1.0 mm Cell Structure with 3 mm mesh

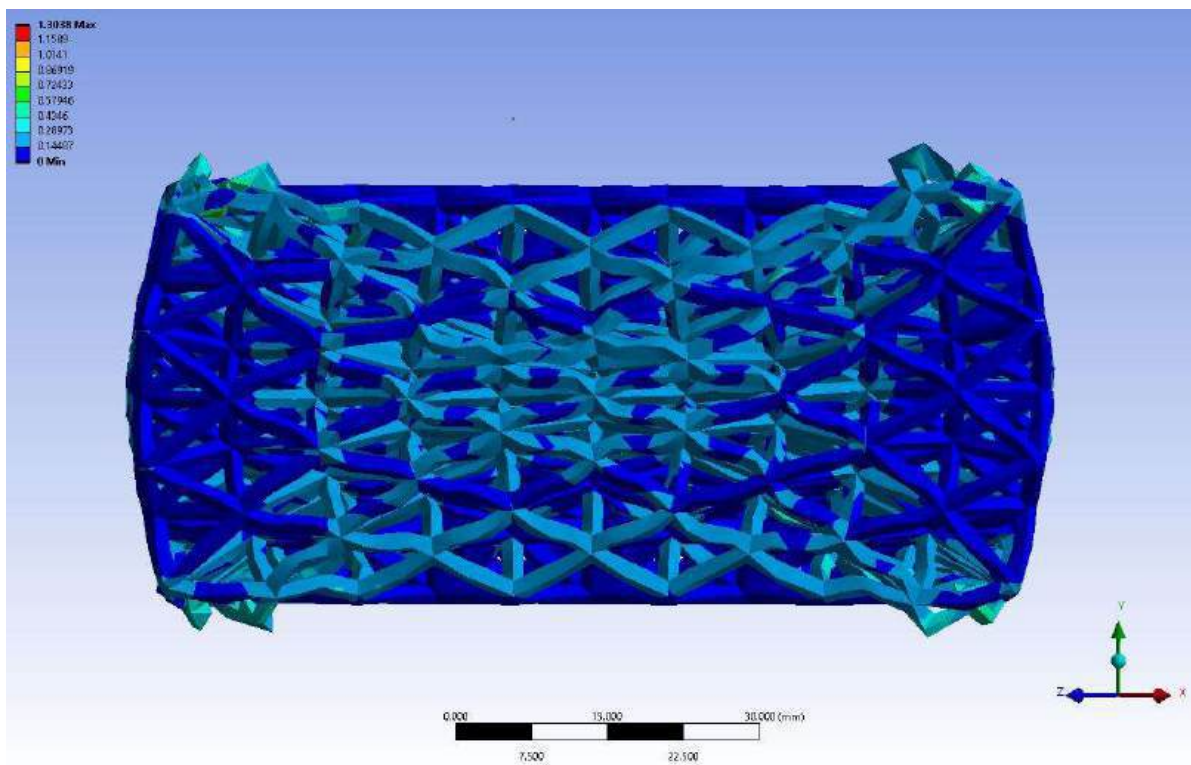


Figure 174: Elastic Strain for 5x5x5 R1.0 mm Cell Structure with 3 mm mesh

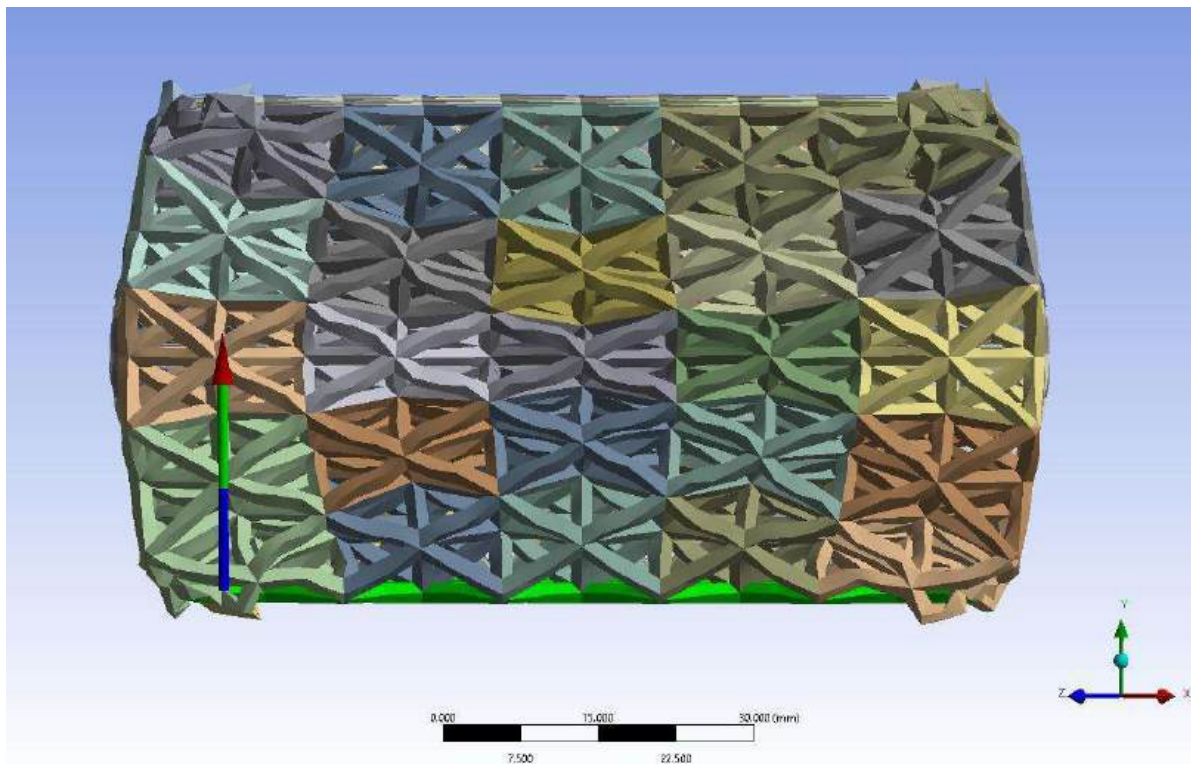


Figure 175: Force reaction for 5x5x5 R1.0 mm Cell Structure with 3 mm mesh

7.5.2.3.3 Cell Structure 5x5x5 1.5 mm

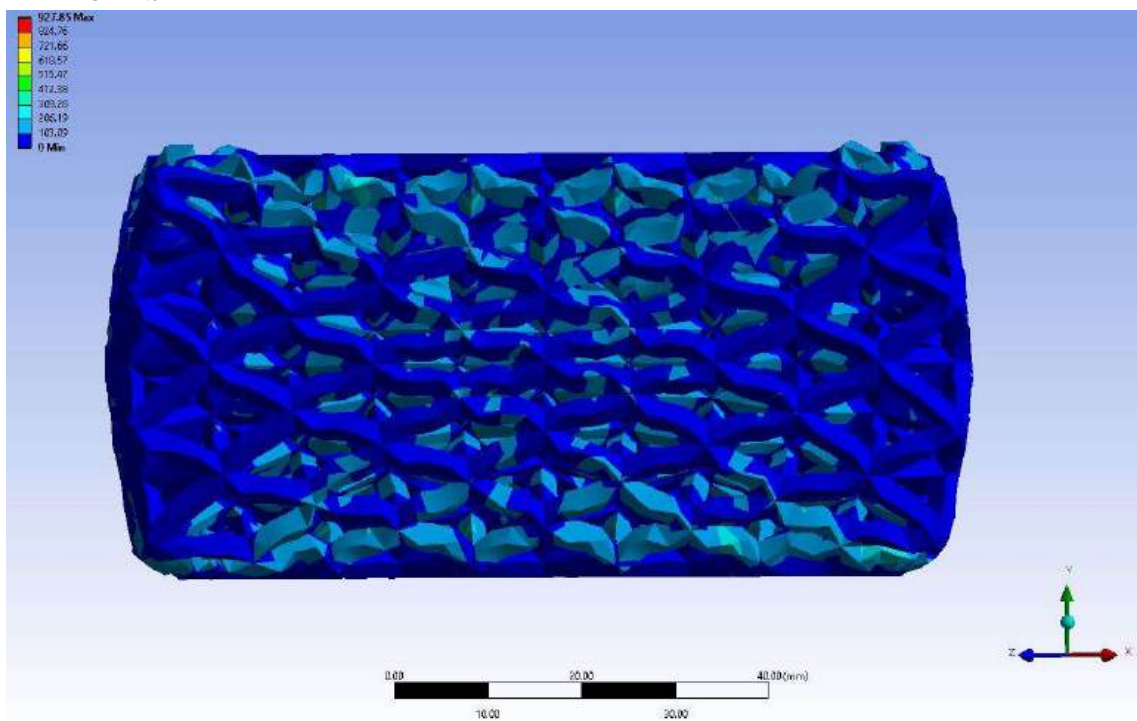


Figure 176: Equivalent Stress for 5x5x5 R1.5 mm Cell Structure with 3 mm (Coarse) mesh

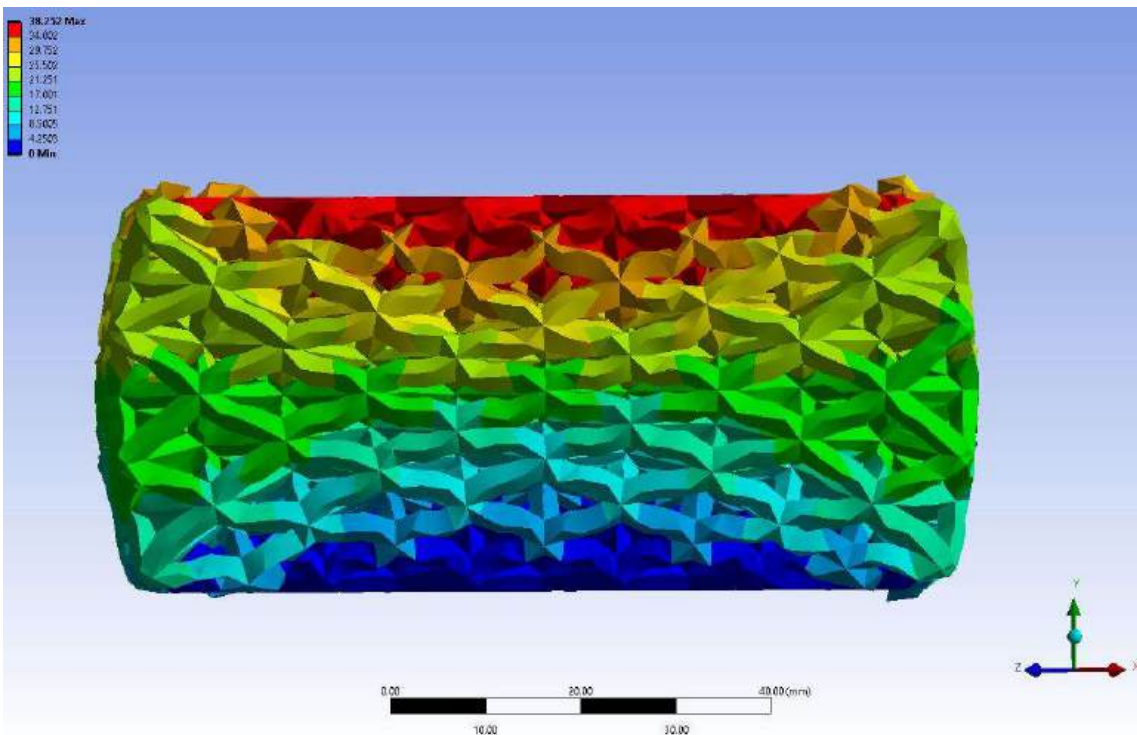


Figure 177: Total Deformation for 5x5x5 R1.5 mm Cell Structure with 3 mm mesh

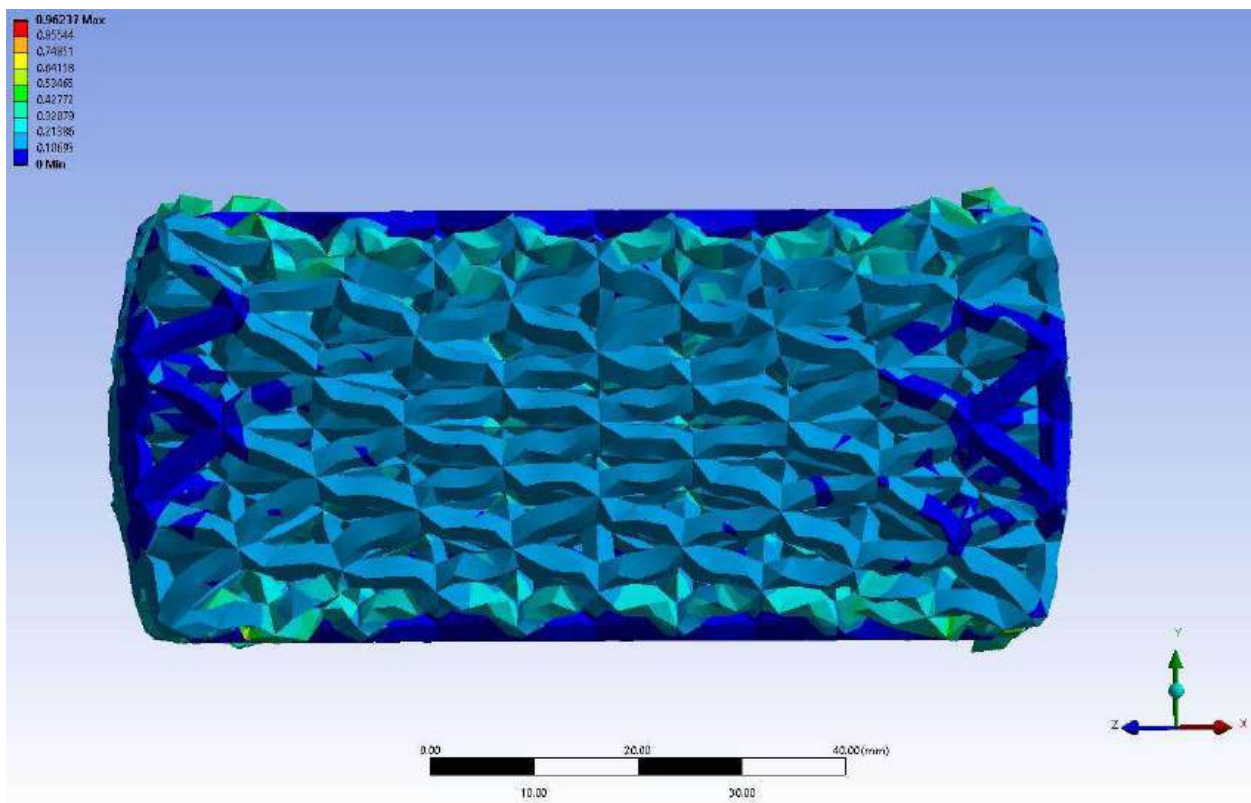


Figure 178: Elastic Strain for 5x5x5 R1.5 mm Cell Structure with 3 mm mesh

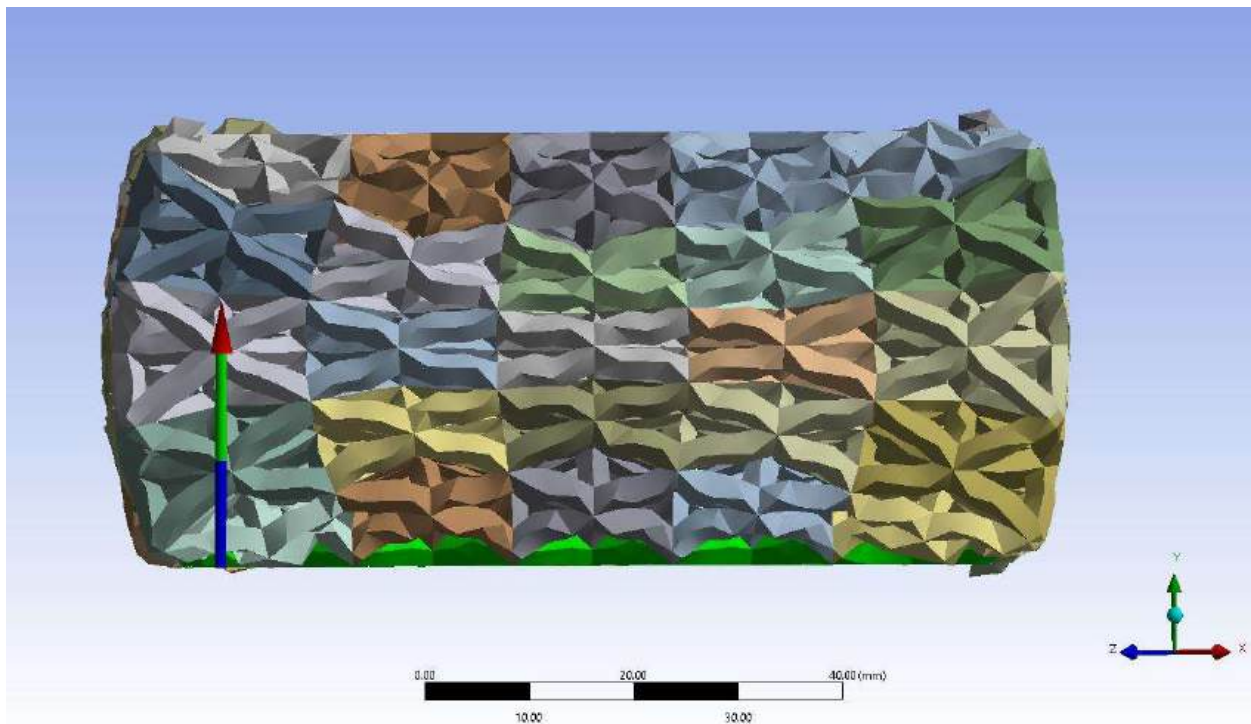


Figure 179: Force reaction for 5x5x5 R1.5 mm Cell Structure with 3 mm mesh

7.5.2.4 6x6x6 Structures

7.5.2.4.1 Cell Structure 6x6x6 0.5 mm

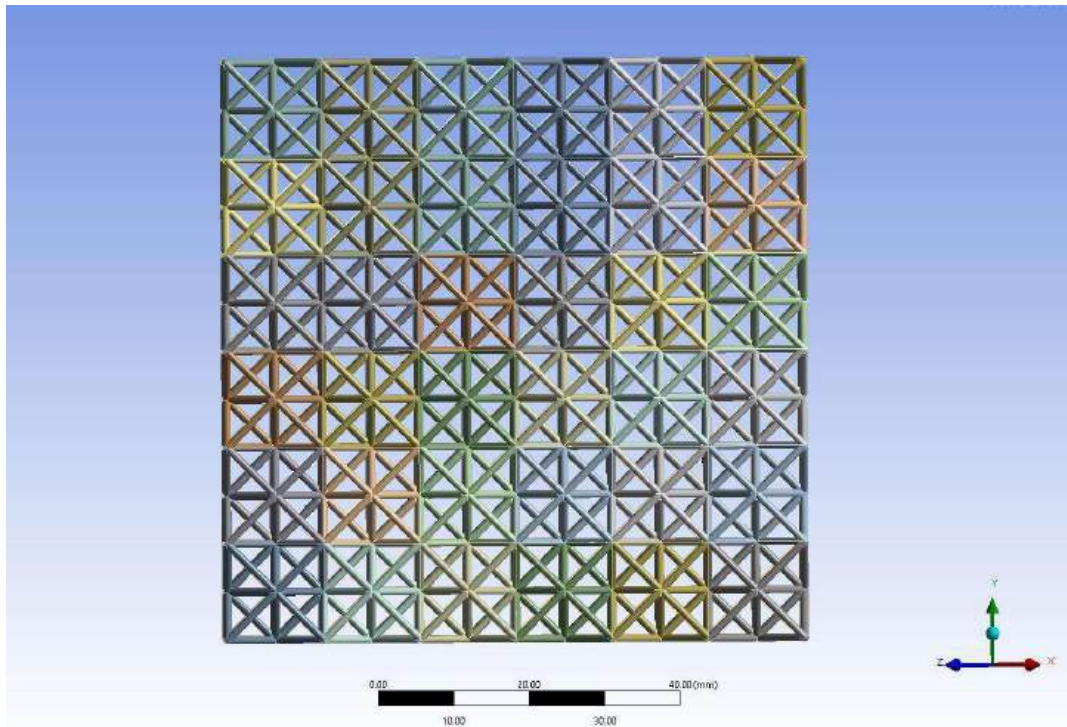


Figure 180: Equivalent Stress for 6x6x6 R0.5 mm Cell Structure with 3 mm (Coarse) mesh

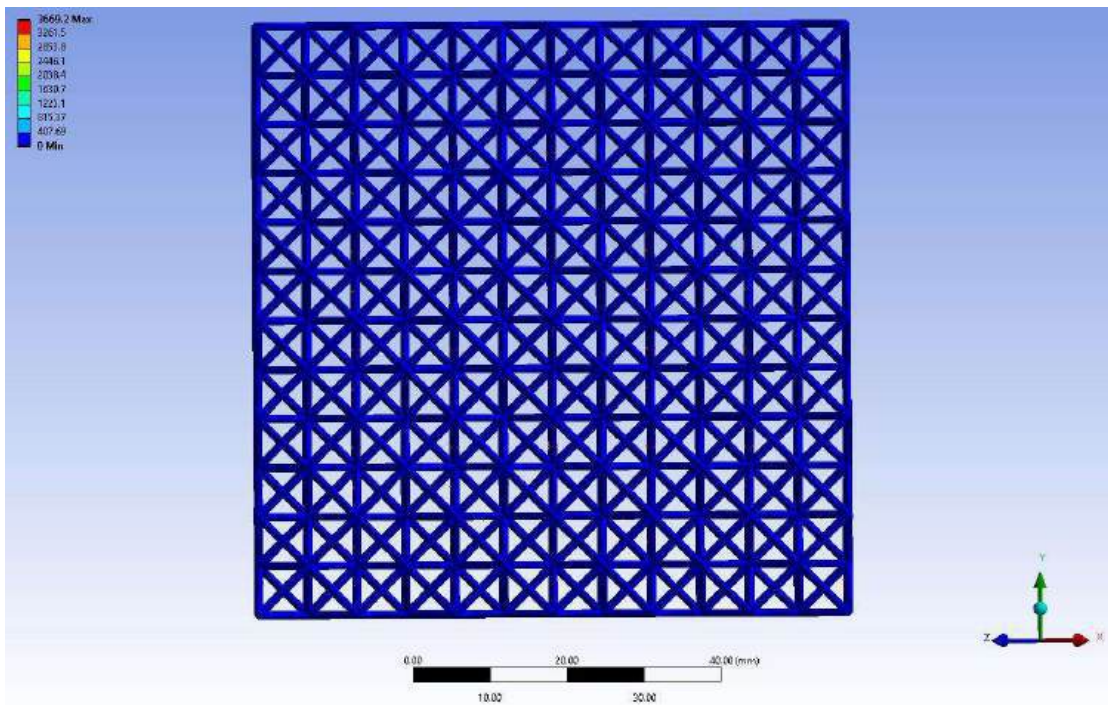


Figure 181: Total Deformation for 6x6x6 R0.5 mm Cell Structure with 3 mm mesh

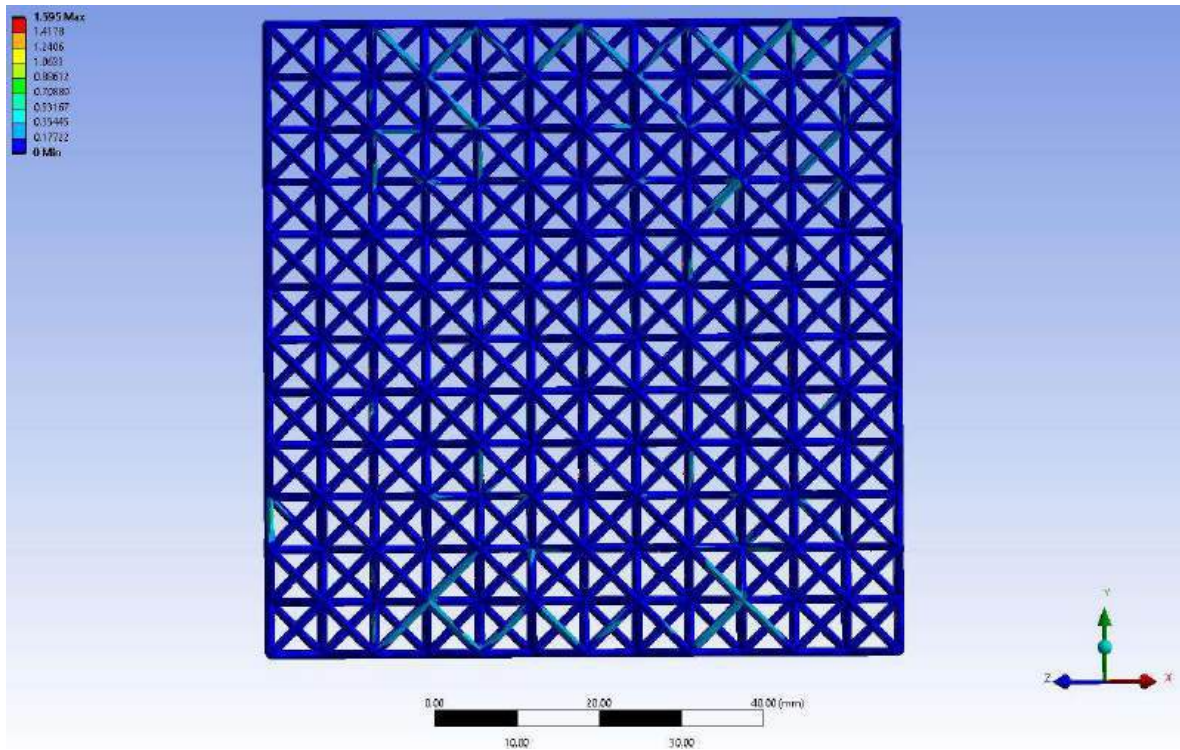


Figure 182: Elastic Strain for 6x6x6 R0.5 mm Cell Structure with 3 mm mesh

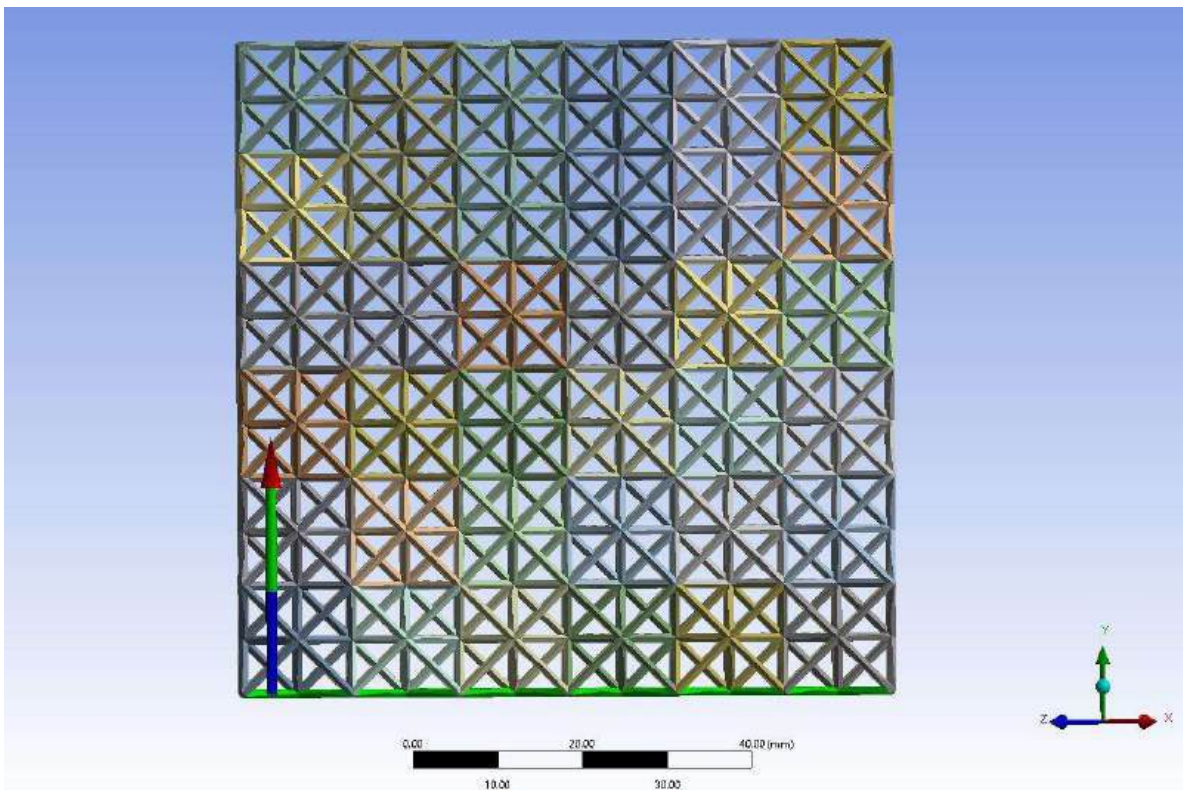


Figure 183: Force reaction for 6x6x6 R0.5 mm Cell Structure with 3 mm mesh

7.5.2.4.2 Cell Structure 6x6x6 1.0 mm

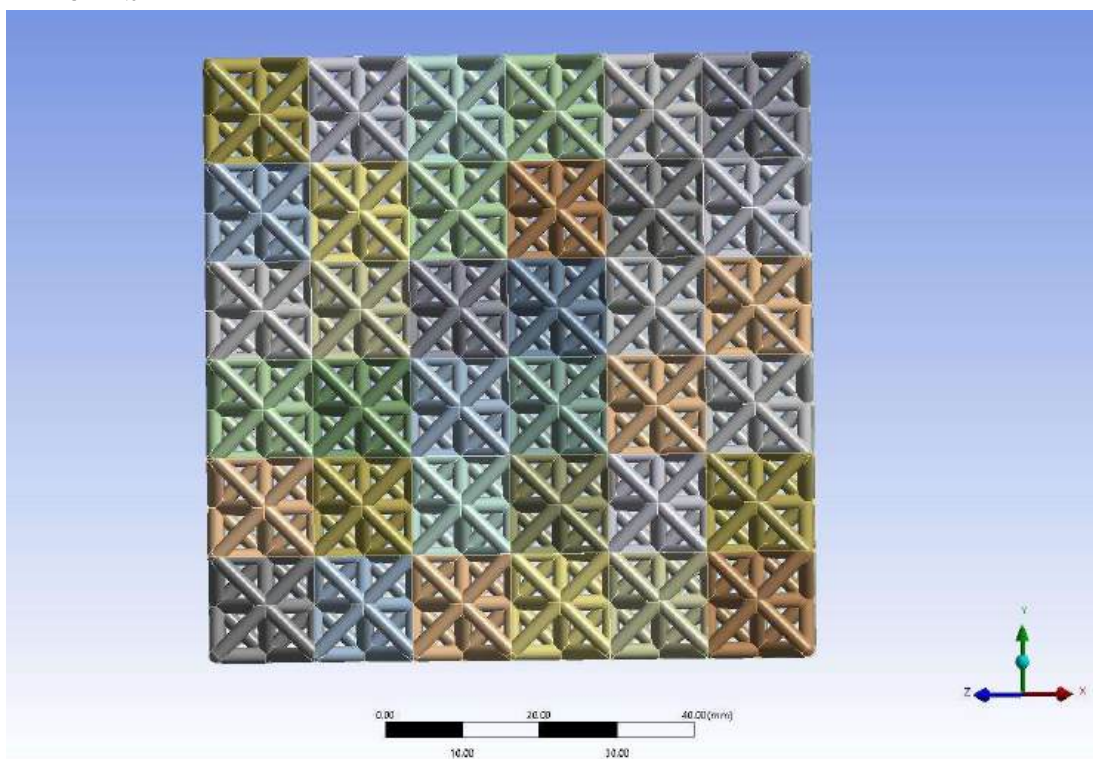


Figure 184: Equivalent Stress for 6x6x6 R1.0 mm Cell Structure with 3 mm (Coarse) mesh

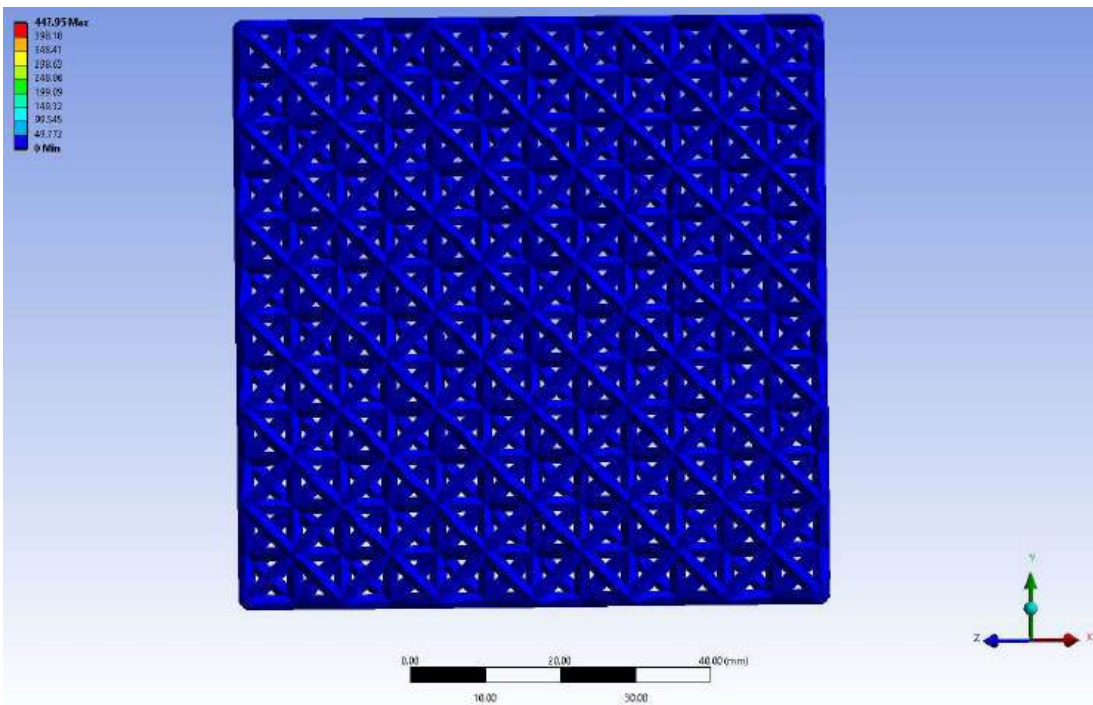


Figure 185: Total Deformation for 6x6x6 R1.0 mm Cell Structure with 3 mm mesh

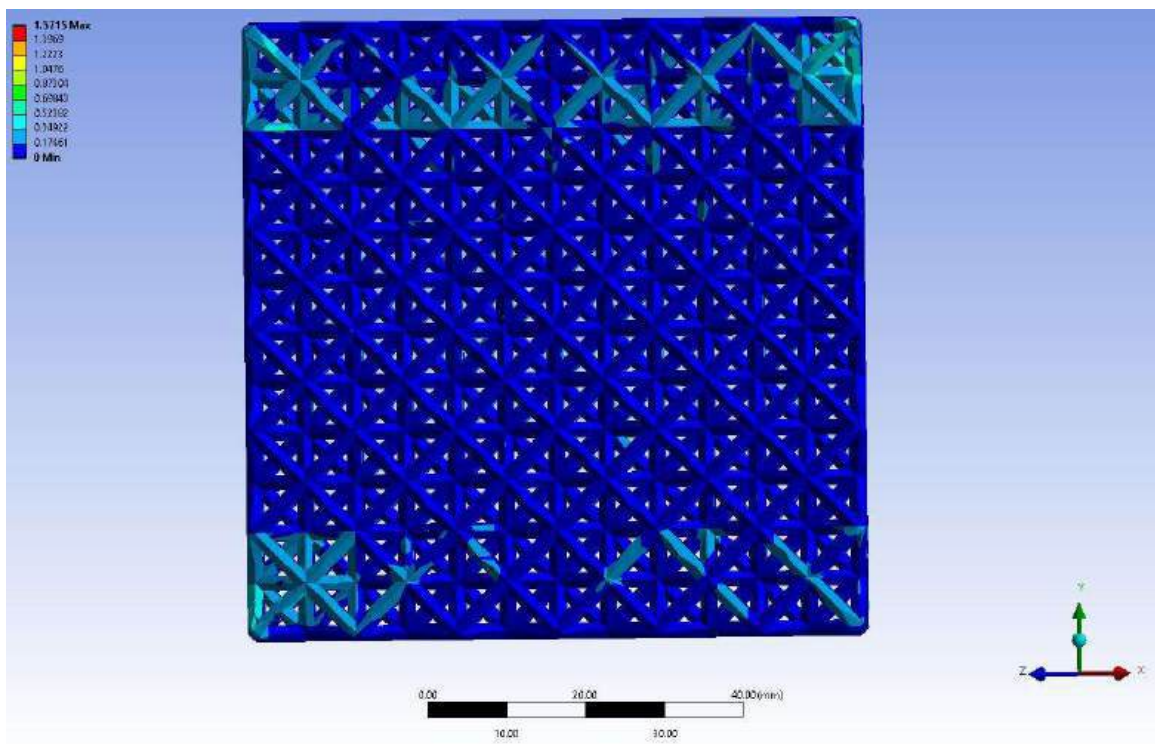


Figure 186: Elastic Strain for 6x6x6 R1.0 mm Cell Structure with 3 mm mesh

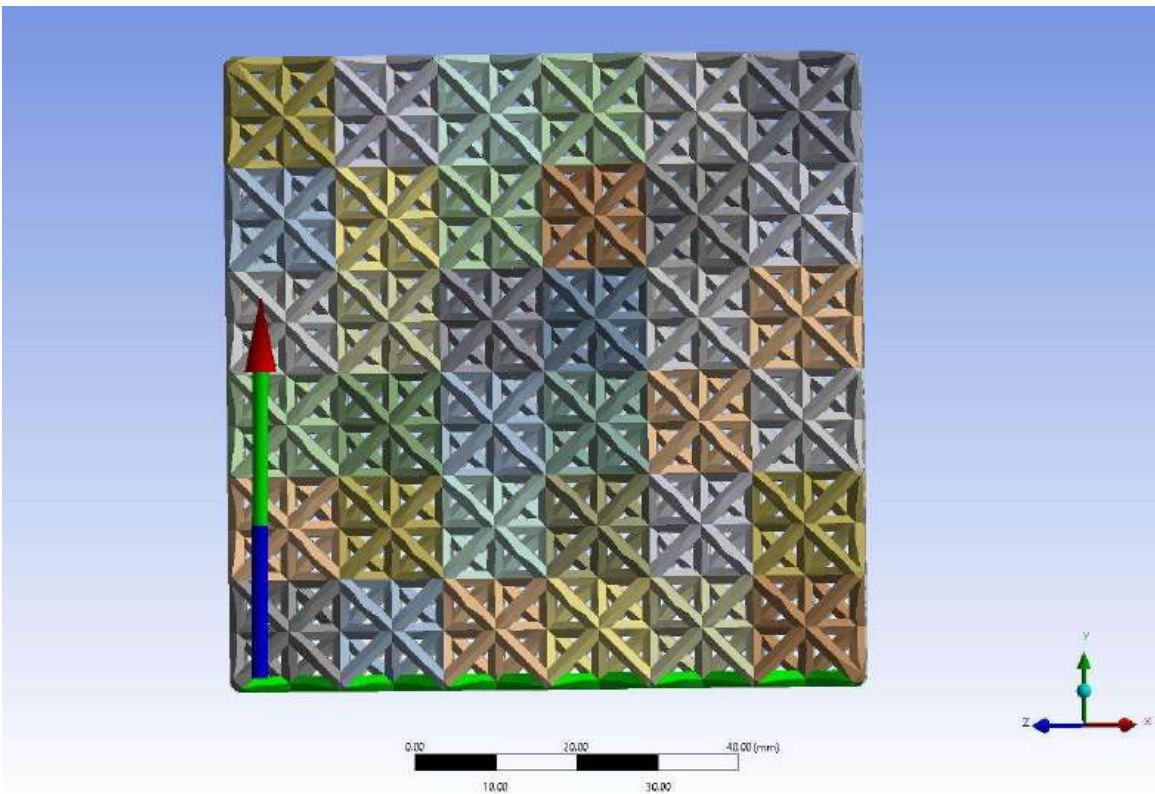


Figure 187: Force reaction for 6x6x6 R1.0 mm Cell Structure with 3 mm mesh

7.5.2.4.3 Cell Structure 6x6x6 1.5 mm

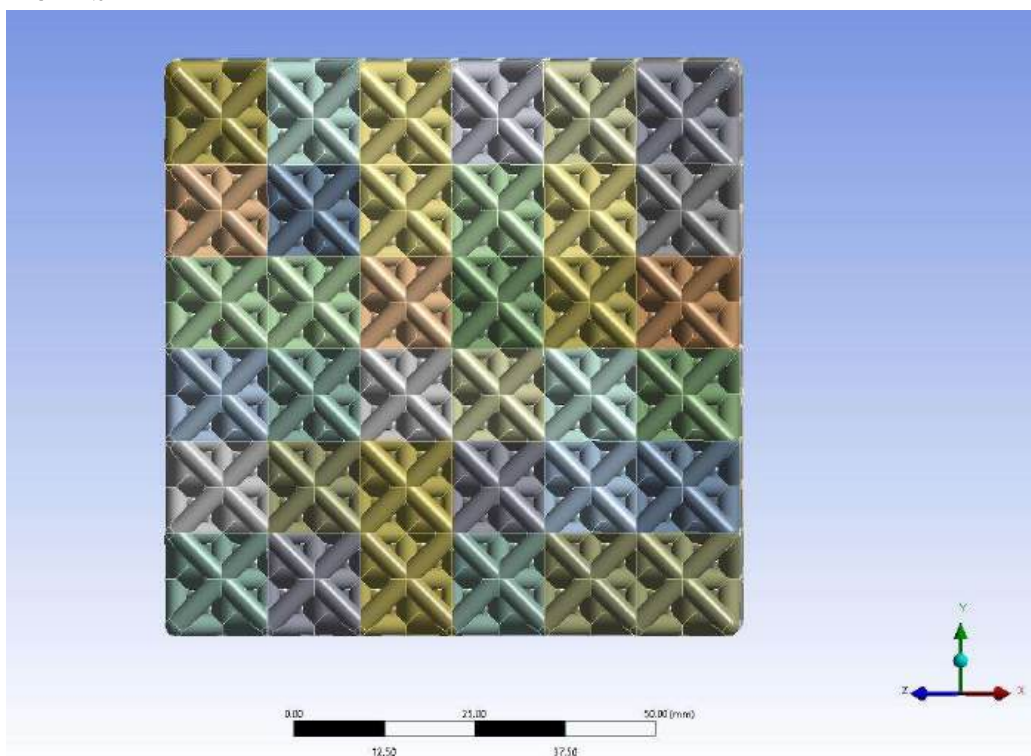


Figure 188: Equivalent Stress for 6x6x6 R1.5 mm Cell Structure with 3 mm (Coarse) mesh

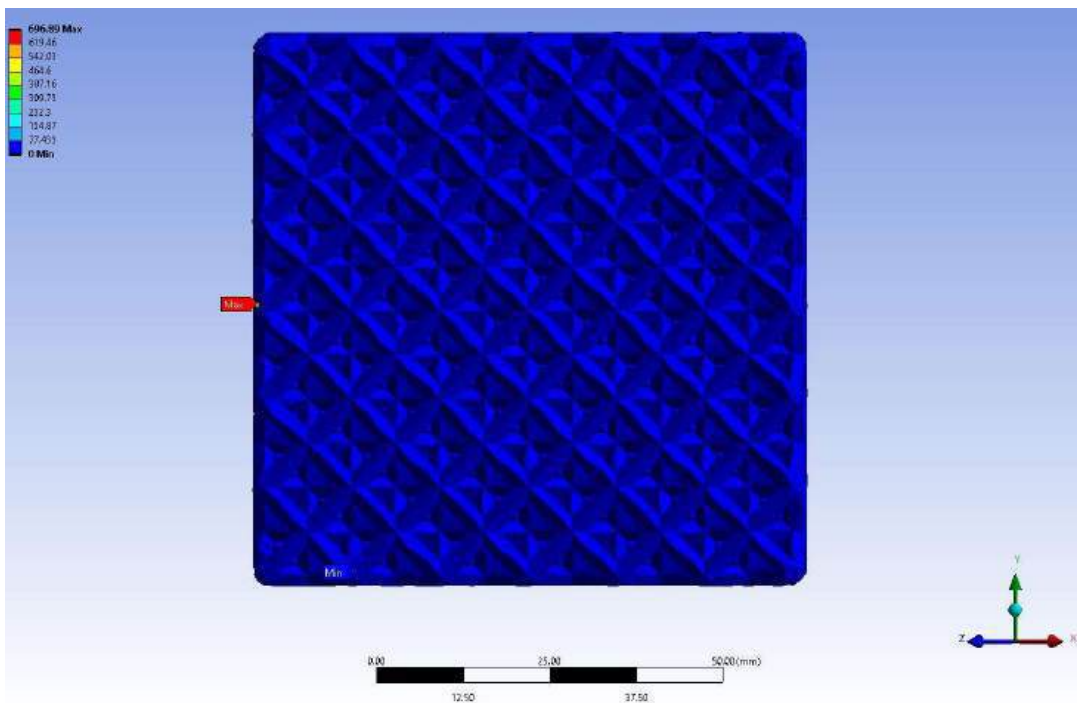


Figure 189: Total Deformation for 6x6x6 R1.5 mm Cell Structure with 3 mm mesh

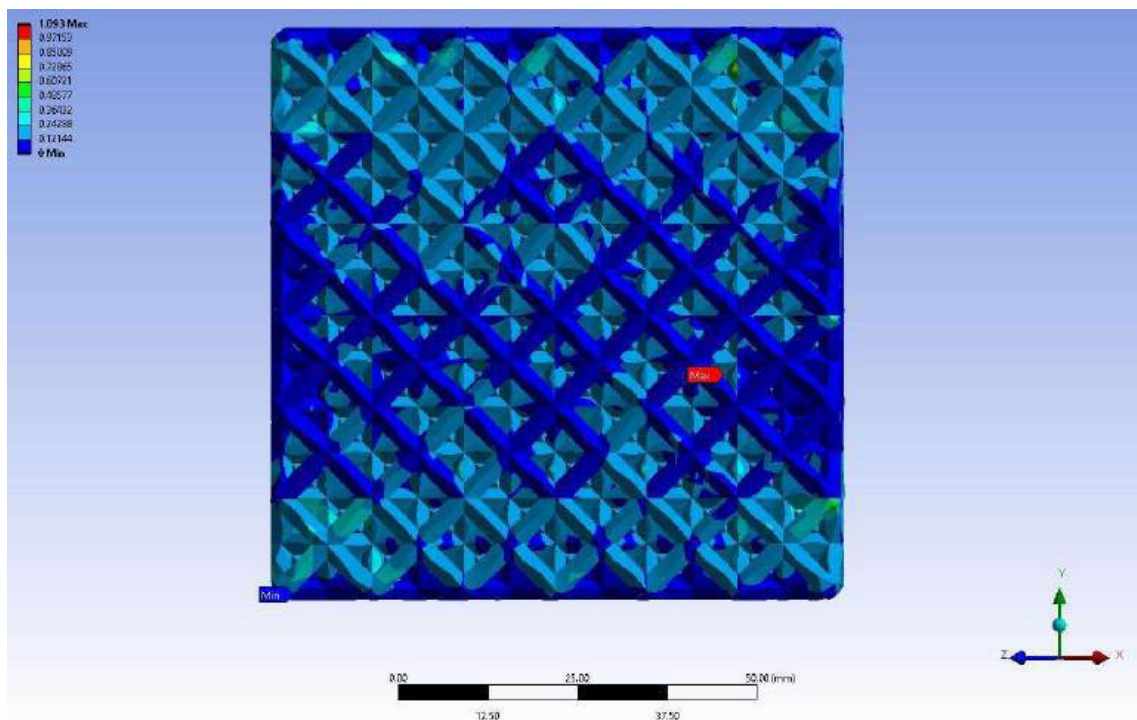


Figure 190: Elastic Strain for 6x6x6 R1.5 mm Cell Structure with 3 mm mesh

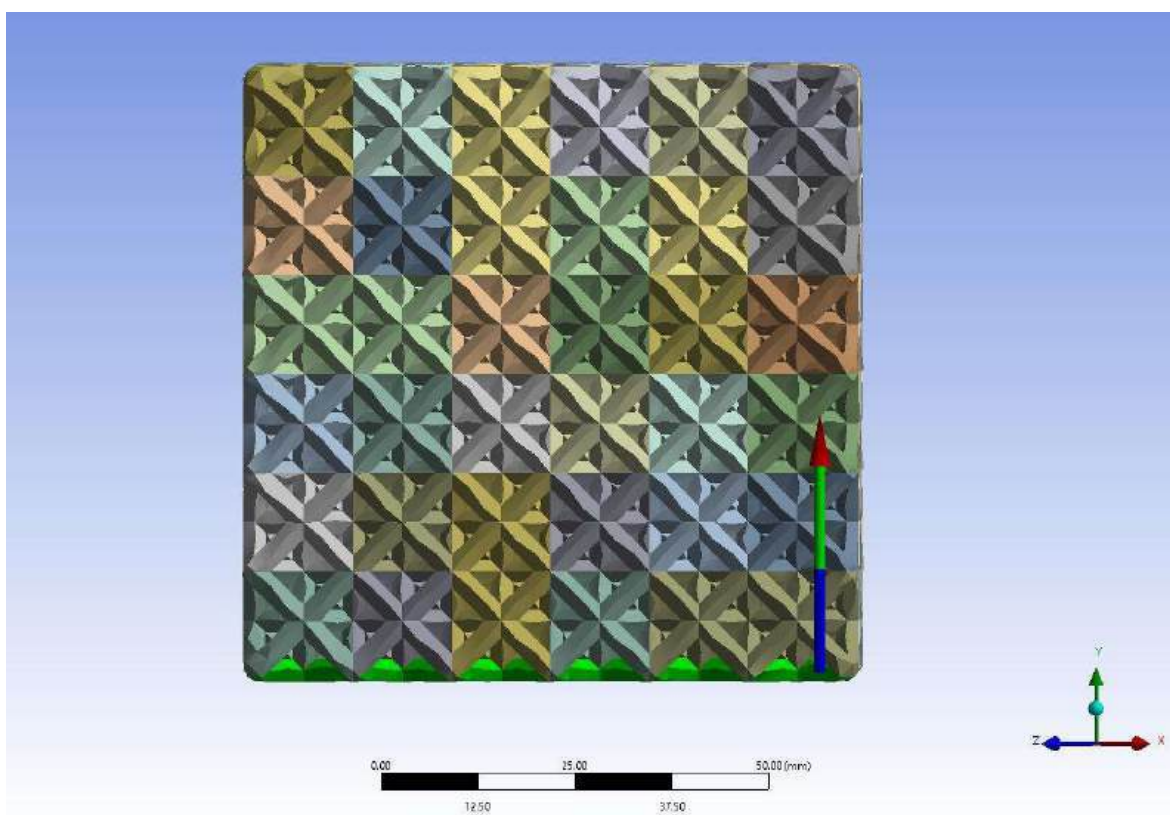


Figure 191: Force reaction for 6x6x6 R1.5 mm Cell Structure with 3 mm mesh

7.7 Ansys Detailed Forces and Energies

7.7.1 Unit Cell Fine Mesh (1 mm) Results

7.7.1.1 Unit Cells of R 0.5 mm

Table 22: Unit Cell of Radius 0.5 mm Length 9.0 mm Forces and Calculated Energy ($m = 2.75\text{e-}4 \text{ kg}$)

Displacement (mm)	Force (N)	Energy (Joules)	SEA (J/kg)
0	0.00E+00	0.00E+00	0.00E+00
0.636	9.33E+01	2.97E+04	1.08E+08
1.272	1.34E+02	1.02E+05	3.71E+08
1.908	1.43E+02	1.90E+05	6.91E+08
2.544	1.44E+02	2.81E+05	1.02E+09
3.18	1.38E+02	3.75E+05	1.36E+09
3.816	1.30E+02	4.65E+05	1.69E+09
4.452	1.24E+02	5.50E+05	2.00E+09
5.088	1.03E+02	6.36E+05	2.31E+09
5.724	6.40E+01	7.13E+05	2.59E+09
6.36	5.21E+01	7.58E+05	2.75E+09

Table 23: Unit Cell of Radius 0.5 mm Length 10.80 mm Forces and Calculated Energy ($m = 3.35\text{e-}4 \text{ kg}$)

Displacement (mm)	Force (N)	Energy (Joules)	SEA (J/kg)
0	0.00E+00	0.00E+00	0.00E+00
0.764	1.08E+02	4.13E+04	1.23E+08
1.528	1.23E+02	1.30E+05	3.87E+08
2.292	1.23E+02	2.24E+05	6.67E+08
3.056	1.19E+02	3.19E+05	9.51E+08
3.82	1.18E+02	4.10E+05	1.22E+09
4.584	1.12E+02	5.03E+05	1.50E+09
5.348	1.01E+02	5.93E+05	1.77E+09
6.112	1.08E+02	6.73E+05	2.01E+09

6.876	6.18E+01	7.73E+05	2.31E+09
7.64	5.02E+01	8.25E+05	2.46E+09

Table 24: Unit Cell of Radius 0.5 mm Length 13.50 mm Forces and Calculated Energy ($m = 4.25\text{e-}4 \text{ kg}$)

Displacement (mm)	Force (N)	Energy (Joules)	SEA (J/kg)
0	0.00E+00	0.00E+00	0.00E+00
0.955	5.89E+01	2.81E+04	6.62E+07
1.91	6.08E+01	8.53E+04	2.01E+08
2.865	6.02E+01	1.44E+05	3.38E+08
3.82	5.91E+01	2.02E+05	4.75E+08
4.775	5.74E+01	2.59E+05	6.09E+08
5.73	5.10E+01	3.17E+05	7.45E+08
6.685	5.56E+01	3.68E+05	8.65E+08
7.64	4.64E+01	4.25E+05	1.00E+09
8.595	3.80E+01	4.74E+05	1.11E+09
9.55	1.02E+01	5.23E+05	1.23E+09

Table 25: Unit Cell of Radius 0.5 mm Length 18.00 mm Forces and Calculated Energy ($m = 5.75\text{e-}4 \text{ kg}$)

Displacement (mm)	Force (N)	Energy (Joules)	SEA (J/kg)
0	0.00E+00	0.00E+00	0.00E+00
1.273	2.90E+01	1.85E+04	3.21E+07
2.546	3.19E+01	5.73E+04	9.97E+07
3.819	3.01E+01	9.90E+04	1.72E+08
5.092	3.16E+01	1.38E+05	2.41E+08
6.365	2.95E+01	1.80E+05	3.13E+08
7.638	3.06E+01	2.18E+05	3.80E+08
8.911	2.57E+01	2.60E+05	4.53E+08
10.184	2.52E+01	2.93E+05	5.10E+08
11.457	2.26E+01	3.27E+05	5.69E+08
12.73	5.08E+00	3.67E+05	6.39E+08

7.7.1.2 Unit Cells of R 1.0 mm

Table 26: Unit Cell of Radius 1.0 mm Length 9.0 mm Forces and Calculated Energy ($m = 1.0e-3 \text{ kg}$)

Displacement (mm)	Force (N)	Energy (Joules)	SEA (J/kg)
0	0.00E+00	0.00E+00	0.00E+00
0.636	6.34E+02	2.02E+05	2.01E+08
1.272	1.19E+03	7.83E+05	7.80E+08
1.908	1.69E+03	1.70E+06	1.70E+09
2.544	2.10E+03	2.91E+06	2.90E+09
3.18	2.39E+03	4.33E+06	4.32E+09
3.816	2.41E+03	5.86E+06	5.84E+09
4.452	2.31E+03	7.42E+06	7.39E+09
5.088	1.63E+03	9.11E+06	9.07E+09
5.724	1.39E+03	1.02E+07	1.02E+10
6.36	1.27E+03	1.11E+07	1.11E+10

Table 27: Unit Cell of Radius 1.0 mm Length 10.80 mm Forces and Calculated Energy ($m = 1.24e-3 \text{ kg}$)

Displacement (mm)	Force (N)	Energy (Joules)	SEA (J/kg)
0	0.00E+00	0.00E+00	0.00E+00
0.764	5.70E+02	2.18E+05	1.75E+08
1.528	1.08E+03	8.49E+05	6.83E+08
2.292	1.51E+03	1.84E+06	1.48E+09
3.056	1.62E+03	3.03E+06	2.44E+09
3.82	1.65E+03	4.28E+06	3.44E+09
4.584	1.64E+03	5.54E+06	4.46E+09
5.348	1.52E+03	6.84E+06	5.50E+09
6.112	1.23E+03	8.11E+06	6.52E+09
6.876	1.04E+03	9.12E+06	7.33E+09
7.64	8.17E+02	1.00E+07	8.04E+09

Table 28: Unit Cell of Radius 1.0 mm Length 13.50 mm Forces and Calculated Energy ($m = 1.60\text{e-}3 \text{ kg}$)

Displacement (mm)	Force (N)	Energy (Joules)	SEA (J/kg)
0	0.00E+00	0.00E+00	0.00E+00
0.955	5.38E+02	2.57E+05	1.60E+08
1.91	9.83E+02	9.83E+05	6.13E+08
2.865	1.07E+03	1.96E+06	1.22E+09
3.82	1.08E+03	2.99E+06	1.87E+09
4.775	1.06E+03	4.04E+06	2.52E+09
5.73	1.05E+03	5.06E+06	3.15E+09
6.685	1.01E+03	6.08E+06	3.79E+09
7.64	7.71E+02	7.16E+06	4.47E+09
8.595	3.94E+02	8.08E+06	5.04E+09
9.55	2.46E+02	8.53E+06	5.32E+09

Table 29: Unit Cell of Radius 1.0 mm Length 18.00 mm Forces and Calculated Energy ($m = 2.20\text{e-}3 \text{ kg}$)

Displacement (mm)	Force (N)	Energy (Joules)	SEA (J/kg)
0	0.00E+00	0.00E+00	0.00E+00
1.273	4.91E+02	3.12E+05	1.42E+08
2.546	5.66E+02	9.85E+05	4.47E+08
3.819	5.64E+02	1.71E+06	7.75E+08
5.092	5.73E+02	2.43E+06	1.10E+09
6.365	5.67E+02	3.16E+06	1.44E+09
7.638	5.46E+02	3.90E+06	1.77E+09
8.911	5.40E+02	4.60E+06	2.09E+09
10.184	3.38E+02	5.41E+06	2.46E+09
11.457	3.07E+02	5.87E+06	2.66E+09
12.73	1.74E+02	6.34E+06	2.88E+09

7.7.1.3 Unit Cells of R 1.5 mm

Table 30: Unit Cell of Radius 1.5 mm Length 9.0 mm Forces and Calculated Energy ($m = 2.04\text{e-}3 \text{ kg}$)

Displacement (mm)	Force (N)	Energy (Joules)	SEA (J/kg)
0	0.00E+00	0.00E+00	0.00E+00
0.636	1.92E+03	6.11E+05	3.00E+08
1.272	3.79E+03	2.43E+06	1.19E+09
1.908	5.56E+03	5.40E+06	2.65E+09
2.544	7.14E+03	9.43E+06	4.63E+09
3.18	8.35E+03	1.44E+07	7.05E+09
3.816	8.23E+03	1.97E+07	9.68E+09
4.452	7.67E+03	2.51E+07	1.23E+10
5.088	6.34E+03	3.04E+07	1.49E+10
5.724	6.09E+03	3.45E+07	1.70E+10
6.36	6.94E+03	3.87E+07	1.90E+10

Table 31: Unit Cell of Radius 1.5 mm Length 10.80 mm Forces and Calculated Energy ($m = 2.58\text{e-}3 \text{ kg}$)

Displacement (mm)	Force (N)	Energy (Joules)	SEA (J/kg)
0	0.00E+00	0.00E+00	0.00E+00
0.764	1.62E+03	6.17E+05	2.40E+08
1.528	3.19E+03	2.45E+06	9.52E+08
2.292	4.54E+03	5.41E+06	2.10E+09
3.056	5.74E+03	9.33E+06	3.62E+09
3.82	6.65E+03	1.41E+07	5.46E+09
4.584	6.91E+03	1.92E+07	7.47E+09
5.348	6.58E+03	2.46E+07	9.56E+09
6.112	5.03E+03	3.03E+07	1.17E+10
6.876	4.47E+03	3.43E+07	1.33E+10
7.64	4.50E+03	3.77E+07	1.46E+10

Table 32: Unit Cell of Radius 1.5 mm Length 13.50 mm Forces and Calculated Energy ($m = 3.39e-3$ kg)

Displacement (mm)	Force (N)	Energy (Joules)	SEA (J/kg)
0	0.00E+00	0.00E+00	0.00E+00
0.955	1.45E+03	6.94E+05	2.05E+08
1.91	2.68E+03	2.67E+06	7.87E+08
2.865	3.76E+03	5.74E+06	1.69E+09
3.82	4.63E+03	9.75E+06	2.88E+09
4.775	5.17E+03	1.44E+07	4.26E+09
5.73	5.29E+03	1.94E+07	5.73E+09
6.685	5.32E+03	2.45E+07	7.23E+09
7.64	3.72E+03	3.03E+07	8.95E+09
8.595	3.24E+03	3.41E+07	1.01E+10
9.55	2.99E+03	3.73E+07	1.10E+10

Table 33: Unit Cell of Radius 1.5 mm Length 18.00 mm Forces and Calculated Energy ($m = 4.74e-3$ kg)

Displacement (mm)	Force (N)	Energy (Joules)	SEA (J/kg)
0	0.00E+00	0.00E+00	0.00E+00
1.273	1.24E+03	7.91E+05	1.67E+08
2.546	2.33E+03	3.06E+06	6.46E+08
3.819	2.91E+03	6.40E+06	1.35E+09
5.092	2.94E+03	1.01E+07	2.14E+09
6.365	2.86E+03	1.39E+07	2.94E+09
7.638	2.88E+03	1.76E+07	3.71E+09
8.911	2.82E+03	2.13E+07	4.49E+09
10.184	2.41E+03	2.51E+07	5.30E+09
11.457	1.75E+03	2.86E+07	6.04E+09
12.73	1.29E+03	3.11E+07	6.57E+09

7.7.2 Unit Cell Coarse Mesh (3 mm) Results

7.7.2.1 Unit Cells of R 0.5 mm

Table 34: Unit Cell of Radius 0.5 mm Length 9.0 mm Forces and Calculated Energy ($m = 2.75\text{e-}4 \text{ kg}$)

Displacement (mm)	Force (N)	Energy (Joules)	SEA (J/kg)
0	0.00E+00	0.00E+00	0.00E+00
0.636	1.12E+02	3.56E+04	1.29E+08
1.272	2.17E+02	1.40E+05	5.09E+08
1.908	3.20E+02	3.11E+05	1.13E+09
2.544	4.14E+02	5.44E+05	1.98E+09
3.18	5.02E+02	8.36E+05	3.04E+09
3.816	5.81E+02	1.18E+06	4.29E+09
4.452	6.44E+02	1.57E+06	5.70E+09
5.088	7.05E+02	2.00E+06	7.26E+09
5.724	7.50E+02	2.46E+06	8.94E+09
6.36	7.67E+02	2.94E+06	1.07E+10

Table 35: Unit Cell of Radius 0.5 mm Length 10.80 mm Forces and Calculated Energy ($m = 3.35\text{e-}4 \text{ kg}$)

Displacement (mm)	Force (N)	Energy (Joules)	SEA (J/kg)
0	0.00E+00	0.00E+00	0.00E+00
0.764	1.08E+02	4.13E+04	1.23E+08
1.528	1.28E+02	1.31E+05	3.92E+08
2.292	1.29E+02	2.30E+05	6.85E+08
3.056	1.29E+02	3.29E+05	9.81E+08
3.82	1.26E+02	4.28E+05	1.28E+09
4.584	1.21E+02	5.26E+05	1.57E+09
5.348	1.18E+02	6.20E+05	1.85E+09
6.112	9.80E+01	7.17E+05	2.14E+09
6.876	5.78E+01	8.08E+05	2.41E+09
7.64	6.15E+01	8.53E+05	2.55E+09

Table 36: Unit Cell of Radius 0.5 mm Length 13.50 mm Forces and Calculated Energy ($m = 4.25\text{e-}4 \text{ kg}$)

Displacement (mm)	Force (N)	Energy (Joules)	SEA (J/kg)
0	0.00E+00	0.00E+00	0.00E+00
0.955	7.96E+01	3.80E+04	8.95E+07
1.91	8.69E+01	1.18E+05	2.77E+08
2.865	8.56E+01	2.01E+05	4.74E+08
3.82	7.35E+01	2.89E+05	6.79E+08
4.775	7.35E+01	3.59E+05	8.45E+08
5.73	6.94E+01	4.31E+05	1.01E+09
6.685	6.64E+01	4.99E+05	1.17E+09
7.64	6.22E+01	5.64E+05	1.33E+09
8.595	5.41E+01	6.27E+05	1.48E+09
9.55	4.60E+01	6.83E+05	1.61E+09

Table 37: Unit Cell of Radius 0.5 mm Length 18.00 mm Forces and Calculated Energy ($m = 5.75\text{e-}4 \text{ kg}$)

Displacement (mm)	Force (N)	Energy (Joules)	SEA (J/kg)
0	0.00E+00	0.00E+00	0.00E+00
1.273	8.05E+01	5.12E+04	8.92E+07
2.546	1.46E+02	1.95E+05	3.40E+08
3.819	1.67E+02	3.94E+05	6.86E+08
5.092	1.68E+02	6.07E+05	1.06E+09
6.365	1.75E+02	8.26E+05	1.44E+09
7.638	1.42E+02	1.07E+06	1.86E+09
8.911	1.79E+02	1.27E+06	2.22E+09
10.184	1.58E+02	1.52E+06	2.64E+09
11.457	1.17E+02	1.74E+06	3.03E+09
12.73	1.82E+02	1.93E+06	3.37E+09

7.7.2.2 Unit Cells of R 1.0 mm

Table 38: Unit Cell of Radius 1.0 mm Length 9.0 mm Forces and Calculated Energy ($m = 1.0e-3 \text{ kg}$)

Displacement (mm)	Force (N)	Energy (Joules)	SEA (J/kg)
0	0.00E+00	0.00E+00	0.00E+00
0.636	5.15E+02	1.64E+05	1.63E+08
1.272	9.94E+02	6.44E+05	6.41E+08
1.908	1.45E+03	1.42E+06	1.41E+09
2.544	1.84E+03	2.46E+06	2.46E+09
3.18	2.15E+03	3.73E+06	3.72E+09
3.816	2.43E+03	5.19E+06	5.17E+09
4.452	2.62E+03	6.80E+06	6.77E+09
5.088	2.62E+03	8.46E+06	8.43E+09
5.724	2.43E+03	1.02E+07	1.02E+10
6.36	2.53E+03	1.18E+07	1.17E+10

Table 39: Unit Cell of Radius 1.0 mm Length 10.80 mm Forces and Calculated Energy ($m = 1.24e-3 \text{ kg}$)

Displacement (mm)	Force (N)	Energy (Joules)	SEA (J/kg)
0	0.00E+00	0.00E+00	0.00E+00
0.764	4.04E+02	1.54E+05	1.24E+08
1.528	7.78E+02	6.06E+05	4.87E+08
2.292	1.11E+03	1.33E+06	1.07E+09
3.056	1.38E+03	2.28E+06	1.83E+09
3.82	1.47E+03	3.37E+06	2.71E+09
4.584	1.12E+03	4.63E+06	3.72E+09
5.348	1.44E+03	5.61E+06	4.51E+09
6.112	8.25E+02	6.94E+06	5.58E+09
6.876	1.02E+03	7.64E+06	6.15E+09
7.64	9.17E+02	8.46E+06	6.80E+09

Table 40: Unit Cell of Radius 1.0 mm Length 13.50 mm Forces and Calculated Energy ($m = 1.60\text{e-}3 \text{ kg}$)

Displacement (mm)	Force (N)	Energy (Joules)	SEA (J/kg)
0	0.00E+00	0.00E+00	0.00E+00
0.955	4.49E+02	2.15E+05	1.34E+08
1.91	8.72E+02	8.45E+05	5.27E+08
2.865	1.26E+03	1.86E+06	1.16E+09
3.82	1.59E+03	3.22E+06	2.01E+09
4.775	1.85E+03	4.86E+06	3.03E+09
5.73	2.06E+03	6.72E+06	4.19E+09
6.685	2.19E+03	8.75E+06	5.45E+09
7.64	2.27E+03	1.09E+07	6.78E+09
8.595	1.98E+03	1.32E+07	8.22E+09
9.55	2.07E+03	1.51E+07	9.42E+09

Table 41: Unit Cell of Radius 1.0 mm Length 18.00 mm Forces and Calculated Energy ($m = 2.20\text{e-}3 \text{ kg}$)

Displacement (mm)	Force (N)	Energy (Joules)	SEA (J/kg)
0	0.00E+00	0.00E+00	0.00E+00
1.273	3.46E+02	2.20E+05	1.00E+08
2.546	6.41E+02	8.49E+05	3.85E+08
3.819	7.13E+02	1.71E+06	7.77E+08
5.092	7.44E+02	2.64E+06	1.20E+09
6.365	7.60E+02	3.60E+06	1.63E+09
7.638	7.90E+02	4.58E+06	2.08E+09
8.911	7.73E+02	5.60E+06	2.54E+09
10.184	5.96E+02	6.70E+06	3.04E+09
11.457	5.80E+02	7.46E+06	3.39E+09
12.73	4.19E+02	8.30E+06	3.77E+09

7.7.2.3 Unit Cells of R1.5 mm

Table 42: Unit Cell of Radius 1.5 mm Length 9.0 mm Forces and Calculated Energy ($m = 2.04\text{e-}3 \text{ kg}$)

Displacement (mm)	Force (N)	Energy (Joules)	SEA (J/kg)
0	0.00E+00	0.00E+00	0.00E+00
0.636	1.50E+03	4.77E+05	2.34E+08
1.272	2.96E+03	1.89E+06	9.31E+08
1.908	4.36E+03	4.22E+06	2.07E+09
2.544	5.66E+03	7.41E+06	3.64E+09
3.18	6.84E+03	1.14E+07	5.59E+09
3.816	7.80E+03	1.60E+07	7.88E+09
4.452	8.66E+03	2.13E+07	1.04E+10
5.088	9.07E+03	2.69E+07	1.32E+10
5.724	8.46E+03	3.29E+07	1.61E+10
6.36	7.93E+03	3.84E+07	1.89E+10

Table 43: Unit Cell of Radius 1.5 mm Length 10.80 mm Forces and Calculated Energy ($m = 2.58\text{e-}3 \text{ kg}$)

Displacement (mm)	Force (N)	Energy (Joules)	SEA (J/kg)
0	0.00E+00	0.00E+00	0.00E+00
0.764	1.19E+03	4.54E+05	1.76E+08
1.528	2.32E+03	1.79E+06	6.96E+08
2.292	3.32E+03	3.95E+06	1.53E+09
3.056	4.21E+03	6.82E+06	2.65E+09
3.82	4.92E+03	1.03E+07	4.00E+09
4.584	5.47E+03	1.43E+07	5.54E+09
5.348	5.54E+03	1.85E+07	7.17E+09
6.112	5.76E+03	2.28E+07	8.85E+09
6.876	5.27E+03	2.74E+07	1.06E+10
7.64	4.69E+03	3.16E+07	1.23E+10

Table 44: Unit Cell of Radius 1.5 mm Length 13.50 mm Forces and Calculated Energy ($m = 3.39e-3$ kg)

Displacement (mm)	Force (N)	Energy (Joules)	SEA (J/kg)
0	0.00E+00	0.00E+00	0.00E+00
0.955	1.05E+03	5.03E+05	1.48E+08
1.91	2.01E+03	1.97E+06	5.81E+08
2.865	2.85E+03	4.29E+06	1.27E+09
3.82	3.53E+03	7.33E+06	2.16E+09
4.775	4.05E+03	1.09E+07	3.23E+09
5.73	4.38E+03	1.50E+07	4.42E+09
6.685	4.53E+03	1.92E+07	5.68E+09
7.64	4.48E+03	2.36E+07	6.96E+09
8.595	3.87E+03	2.81E+07	8.31E+09
9.55	4.04E+03	3.19E+07	9.43E+09

Table 45: Unit Cell of Radius 1.5 mm Length 18.00 mm Forces and Calculated Energy ($m = 4.74e-3$ kg)

Displacement (mm)	Force (N)	Energy (Joules)	SEA (J/kg)
0	0.00E+00	0.00E+00	0.00E+00
1.273	9.46E+02	6.02E+05	1.27E+08
2.546	1.76E+03	2.33E+06	4.91E+08
3.819	2.44E+03	5.00E+06	1.05E+09
5.092	2.83E+03	8.35E+06	1.76E+09
6.365	2.87E+03	1.20E+07	2.53E+09
7.638	2.86E+03	1.56E+07	3.30E+09
8.911	2.85E+03	1.93E+07	4.07E+09
10.184	2.58E+03	2.31E+07	4.87E+09
11.457	2.17E+03	2.66E+07	5.62E+09
12.73	1.34E+03	2.99E+07	6.31E+09

7.7.3 Cell Structure Mesh (3 mm) Results

7.7.3.1 Link Radius of R 0.5 mm

Table 46: 3x3x3 Cell Structure with a Link Radius of 0.5 mm Forces and Calculated Energy ($m = 1.20\text{e-}2 \text{ kg}$)

Displacement (mm)	Force (N)	Energy (Joules)	SEA (J/kg)
0	0.00E+00	0.00E+00	0.00E+00
3.8	4.33E+02	8.22E+05	6.87E+07
7.6	8.69E+02	3.30E+06	2.75E+08
11.4	1.21E+03	7.26E+06	6.06E+08
15.2	1.40E+03	1.22E+07	1.02E+09
19	1.46E+03	1.77E+07	1.48E+09
22.8	1.36E+03	2.34E+07	1.96E+09
26.6	1.22E+03	2.89E+07	2.41E+09
30.4	1.03E+03	3.39E+07	2.83E+09
34.2	0.00E+00	3.97E+07	3.32E+09
38	0.00E+00	3.97E+07	3.32E+09

Table 47: 4x4x4 Cell Structure with a Link Radius of 0.5 mm Forces and Calculated Energy ($m = 2.02\text{e-}2 \text{ kg}$)

Displacement (mm)	Force (N)	Energy (Joules)	SEA (J/kg)
0	0.00E+00	0.00E+00	0.00E+00
3.8	9.59E+02	1.82E+06	9.04E+07
7.6	2.04E+03	7.52E+06	3.73E+08
11.4	2.79E+03	1.67E+07	8.28E+08
15.2	3.33E+03	2.83E+07	1.40E+09
19	3.85E+03	4.19E+07	2.08E+09
22.8	4.13E+03	5.71E+07	2.83E+09
26.6	0.00E+00	8.07E+07	4.00E+09
30.4	0.00E+00	8.07E+07	4.00E+09
34.2	0.00E+00	8.07E+07	4.00E+09
38	0.00E+00	8.07E+07	4.00E+09

Table 48: 5x5x5 Cell Structure with a Link Radius of 0.5 mm Forces and Calculated Energy ($m = 3.02\text{e-}2 \text{ kg}$)

Displacement (mm)	Force (N)	Energy (Joules)	SEA (J/kg)
0	0.00E+00	0.00E+00	0.00E+00
3.8	9.65E+02	1.83E+06	6.08E+07
7.6	2.16E+03	7.77E+06	2.58E+08
11.4	3.14E+03	1.78E+07	5.91E+08
15.2	3.79E+03	3.10E+07	1.03E+09
19	4.12E+03	4.61E+07	1.53E+09
22.8	4.12E+03	6.17E+07	2.05E+09
26.6	3.93E+03	7.77E+07	2.58E+09
30.4	4.26E+03	9.33E+07	3.09E+09
34.2	4.19E+03	1.10E+08	3.63E+09
38	4.24E+03	1.26E+08	4.16E+09

Table 49: 6x6x6 Cell Structure with a Link Radius of 0.5 mm Forces and Calculated Energy ($m = 4.18\text{e-}2 \text{ kg}$)

Displacement (mm)	Force (N)	Energy (Joules)	SEA (J/kg)
0	0.00E+00	0.00E+00	0.00E+00
3.8	1.69E+03	3.20E+06	7.67E+07
7.6	3.98E+03	1.40E+07	3.34E+08
11.4	5.69E+03	3.23E+07	7.74E+08
15.2	6.58E+03	5.57E+07	1.33E+09
19	7.21E+03	8.19E+07	1.96E+09
22.8	6.07E+03	1.11E+08	2.67E+09
26.6	6.37E+03	1.35E+08	3.23E+09
30.4	6.60E+03	1.60E+08	3.82E+09
34.2	0.00E+00	1.97E+08	4.72E+09
38	0.00E+00	1.97E+08	4.72E+09

7.7.3.2 Link Radius of R 1.0 mm

Table 50: 3x3x3 Cell Structure with a Link Radius of 1.0 mm Forces and Calculated Energy ($m = 4.53\text{e-}2 \text{ kg}$)

Displacement (mm)	Force (N)	Energy (Joules)	SEA (J/kg)
0	0.00E+00	0.00E+00	0.00E+00
3.8	1.87E+03	3.55E+06	7.84E+07
7.6	3.88E+03	1.45E+07	3.20E+08
11.4	5.17E+03	3.17E+07	7.00E+08
15.2	5.72E+03	5.24E+07	1.16E+09
19	5.48E+03	7.45E+07	1.65E+09
22.8	2.75E+03	1.01E+08	2.22E+09
26.6	4.64E+03	1.15E+08	2.53E+09
30.4	5.66E+03	1.34E+08	2.96E+09
34.2	5.48E+03	1.56E+08	3.45E+09
38	3.41E+03	1.81E+08	3.99E+09

Displacement (mm)	Force (N)	Energy (Joules)	SEA (J/kg)
0	NO DATA	NO DATA	NO DATA
3.8	NO DATA	NO DATA	NO DATA
7.6	NO DATA	NO DATA	NO DATA
11.4	NO DATA	NO DATA	NO DATA
15.2	NO DATA	NO DATA	NO DATA
19	NO DATA	NO DATA	NO DATA
22.8	NO DATA	NO DATA	NO DATA
26.6	NO DATA	NO DATA	NO DATA
30.4	NO DATA	NO DATA	NO DATA
34.2	NO DATA	NO DATA	NO DATA
38	NO DATA	NO DATA	NO DATA

[NO DATA AVAILABLE FOR 4x4x4 R1.0 ($m = 7.44\text{e-}2 \text{ kg}$)]

Table 51: 5x5x5 Cell Structure with a Link Radius of 1.0 mm Forces and Calculated Energy ($m = 1.09e-1$ kg)

Displacement (mm)	Force (N)	Energy (Joules)	SEA (J/kg)
0	0.00E+00	0.00E+00	0.00E+00
3.8	7.53E+03	1.43E+07	1.32E+08
7.6	1.26E+04	5.26E+07	4.84E+08
11.4	1.83E+04	1.11E+08	1.03E+09
15.2	2.25E+04	1.89E+08	1.74E+09
19	2.52E+04	2.80E+08	2.57E+09
22.8	2.65E+04	3.78E+08	3.48E+09
26.6	2.61E+04	4.80E+08	4.41E+09
30.4	2.79E+04	5.82E+08	5.36E+09
34.2	2.80E+04	6.88E+08	6.33E+09
38	2.93E+04	7.97E+08	7.34E+09

Table 52: 6x6x6 Cell Structure with a Link Radius of 1.0 mm Forces and Calculated Energy ($m = 1.47e-1$ kg)

Displacement (mm)	Force (N)	Energy (Joules)	SEA (J/kg)
0	0.00E+00	0.00E+00	0.00E+00
3.8	8.45E+03	1.61E+07	1.09E+08
7.6	1.67E+04	6.39E+07	4.35E+08
11.4	2.40E+04	1.41E+08	9.62E+08
15.2	3.19E+04	2.47E+08	1.69E+09
19	3.66E+04	3.78E+08	2.57E+09
22.8	3.96E+04	5.22E+08	3.56E+09
26.6	4.08E+04	6.75E+08	4.60E+09
30.4	3.97E+04	8.32E+08	5.67E+09
34.2	0.00E+00	1.06E+09	7.21E+09
38	0.00E+00	1.06E+09	7.21E+09

7.7.3.3 Link Radius of R 1.5 mm

Table 53: 3x3x3 Cell Structure with a Link Radius of 1.5 mm Forces and Calculated Energy ($m = 9.60\text{e-}2 \text{ kg}$)

Displacement (mm)	Force (N)	Energy (Joules)	SEA (J/kg)
0	0.00E+00	0.00E+00	0.00E+00
3.8	5.96E+03	1.13E+07	1.18E+08
7.6	1.15E+04	4.46E+07	4.64E+08
11.4	1.51E+04	9.51E+07	9.91E+08
15.2	1.76E+04	1.57E+08	1.64E+09
19	1.79E+04	2.25E+08	2.34E+09
22.8	1.63E+04	2.96E+08	3.08E+09
26.6	1.56E+04	3.59E+08	3.74E+09
30.4	1.86E+04	4.24E+08	4.42E+09
34.2	1.80E+04	4.96E+08	5.17E+09
38	1.51E+04	5.70E+08	5.94E+09

Table 54: 4x4x4 Cell Structure with a Link Radius of 1.5 mm Forces and Calculated Energy ($m = 1.54\text{e-}1 \text{ kg}$)

Displacement (mm)	Force (N)	Energy (Joules)	SEA (J/kg)
0.00	0.00E+00	0.00E+00	0.00E+00
3.8	1.26E+04	2.39E+07	1.56E+08
7.6	2.07E+04	8.73E+07	5.68E+08
11.40	3.10E+04	1.86E+08	1.21E+09
15.2	3.61E+04	3.13E+08	2.04E+09
19	4.16E+04	4.61E+08	3.00E+09
22.80	4.33E+04	6.22E+08	4.05E+09
26.6	4.28E+04	7.88E+08	5.13E+09
30.4	0.00E+00	1.03E+09	6.71E+09
34.20	0.00E+00	1.03E+09	6.71E+09
38	0.00E+00	1.03E+09	6.71E+09

Table 55: 5x5x5 Cell Structure with a Link Radius of 1.5 mm Forces and Calculated Energy ($m = 2.18e-1$ kg)

Displacement (mm)	Force (N)	Energy (Joules)	SEA (J/kg)
0	0.00E+00	0.00E+00	0.00E+00
3.8	1.84E+04	3.49E+07	1.60E+08
7.6	3.59E+04	1.38E+08	6.34E+08
11.4	5.11E+04	3.03E+08	1.39E+09
15.2	5.97E+04	5.14E+08	2.36E+09
19	7.18E+04	7.64E+08	3.51E+09
22.8	7.57E+04	1.04E+09	4.79E+09
26.6	7.82E+04	1.34E+09	6.14E+09
30.4	7.65E+04	1.64E+09	7.52E+09
34.2	7.81E+04	1.93E+09	8.87E+09
38	7.78E+04	2.23E+09	1.02E+10

Table 56: 6x6x6 Cell Structure with a Link Radius of 1.5 mm Forces and Calculated Energy ($m = 2.84e-1$ kg)

Displacement (mm)	Force (N)	Energy (Joules)	SEA (J/kg)
0	0.00E+00	0.00E+00	0.00E+00
3.8	2.74E+04	5.20E+07	1.83E+08
7.6	5.51E+04	2.09E+08	7.33E+08
11.4	8.22E+04	4.69E+08	1.65E+09
15.2	1.06E+05	8.27E+08	2.91E+09
19	1.26E+05	1.27E+09	4.46E+09
22.8	1.43E+05	1.78E+09	6.25E+09
26.6	1.45E+05	2.33E+09	8.18E+09
30.4	0.00E+00	3.15E+09	1.11E+10
34.2	0.00E+00	3.15E+09	1.11E+10
38	0.00E+00	3.15E+09	1.11E+10

7.8 Force and Energy Absorption Graphs

7.8.1 Unit Cell Fine (1 mm) vs. Coarse (3 mm) Mesh Results Comparison

7.8.1.1 Constant Link length Comparison

7.8.1.1.1 Force vs. Displacement

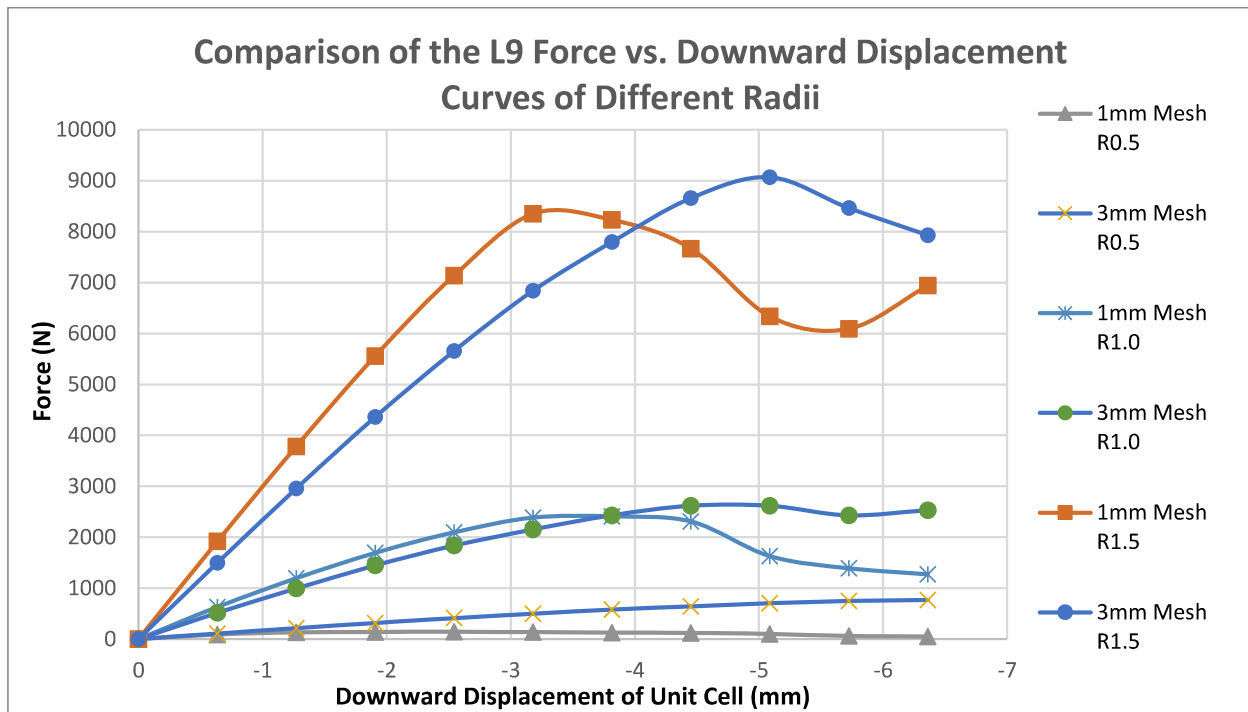


Figure 192: Comparison of Fine vs. Coarse Mesh Results using Force vs. Displacement data of Different Radii for Link length 9 mm Unit Cell.

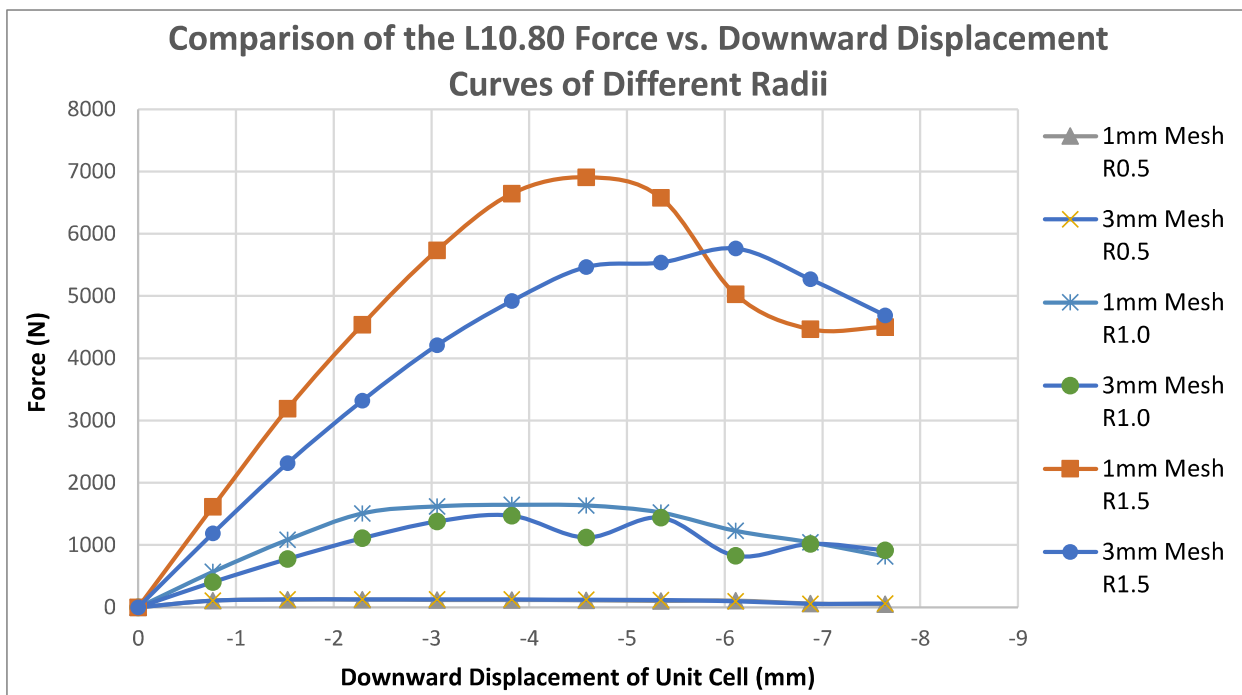


Figure 193: Comparison of Fine vs. Coarse Mesh Results using Force vs. Displacement data of Different Radii for Link length 10.80 mm Unit Cell.

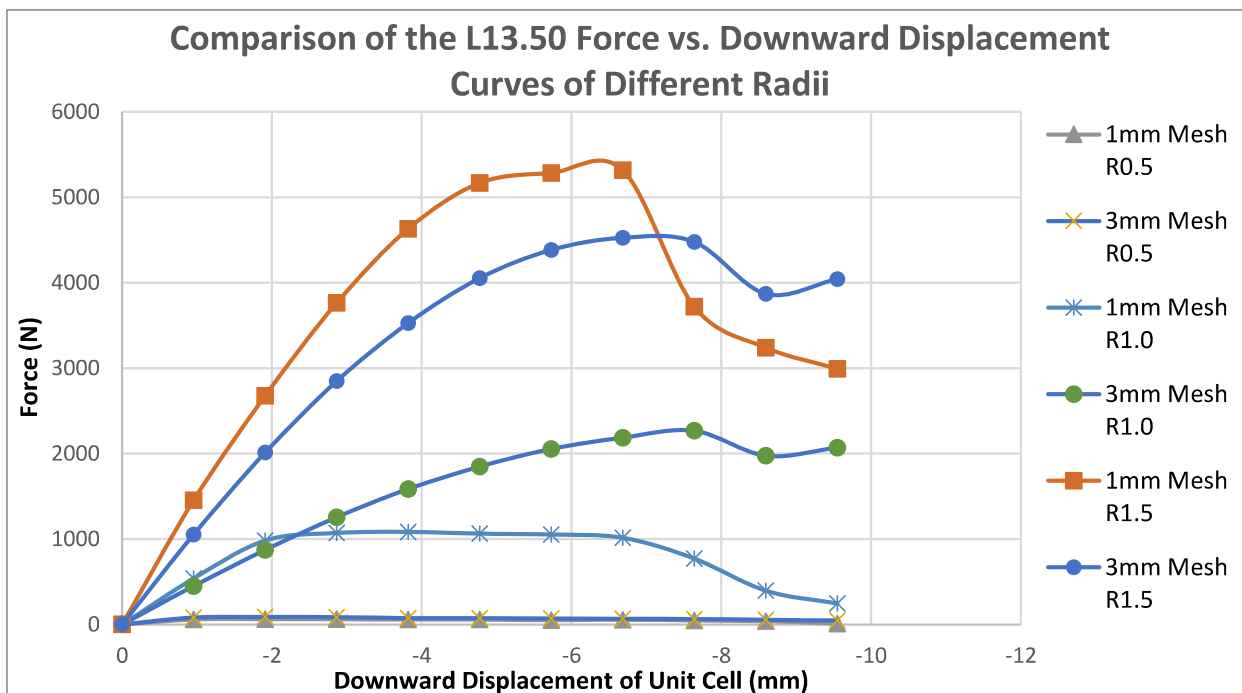


Figure 194: Comparison of Fine vs. Coarse Mesh Results using Force vs. Displacement data of Different Radii for Link length 13.50 mm Unit Cell.

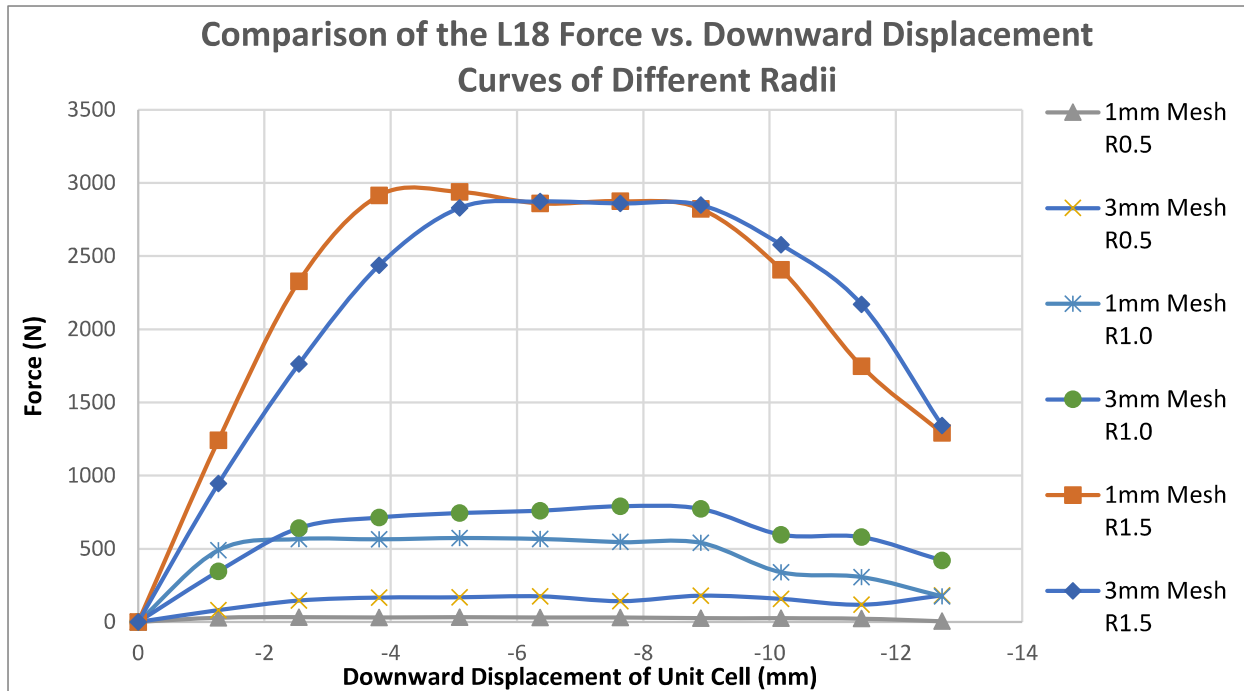


Figure 195: Comparison of Fine vs. Coarse Mesh Results using Force vs. Displacement data of Different Radii for Link length 18 mm Unit Cell.

7.8.1.1.2 Energy vs. Displacement

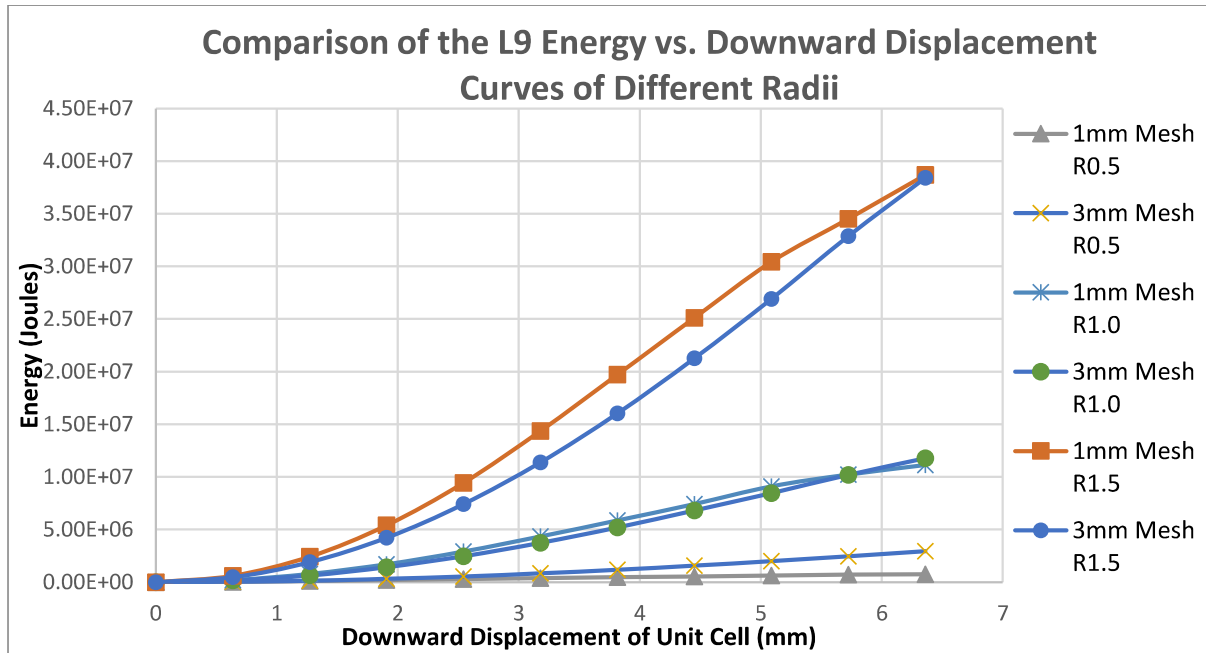


Figure 196: Comparison of Fine vs. Coarse Mesh Results using Energy vs. Displacement data of Different Radii for Link length 9 mm Unit Cell.

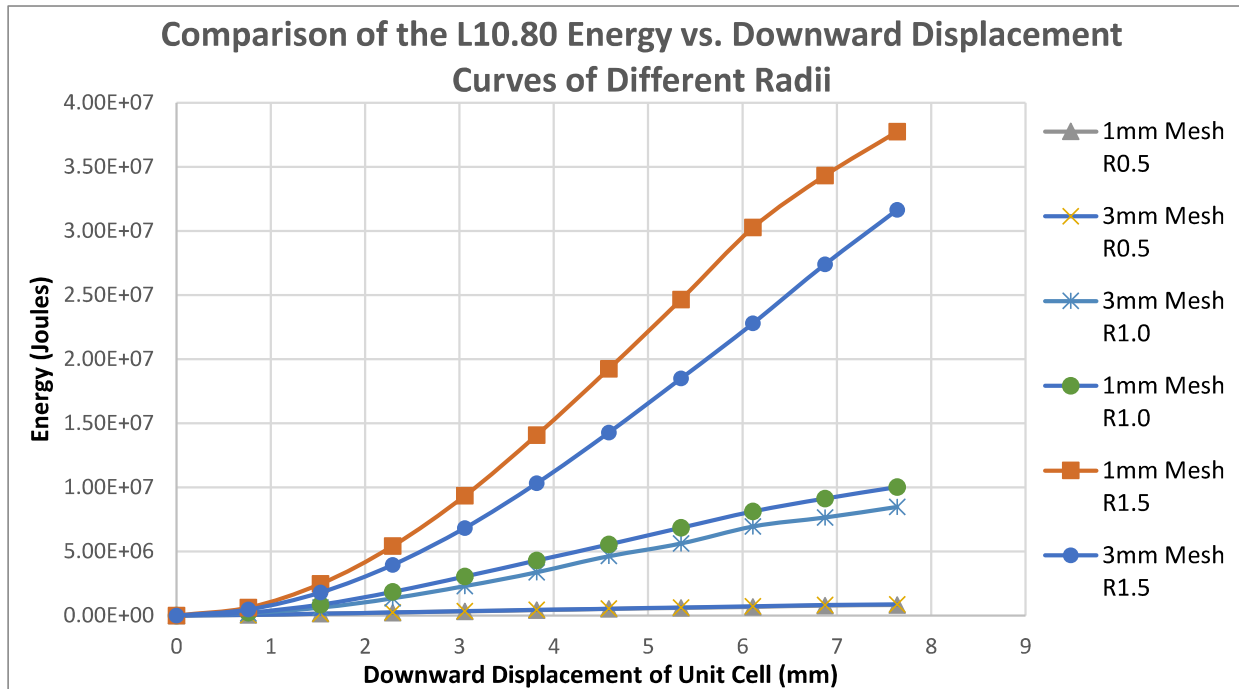


Figure 197: Comparison of Fine vs. Coarse Mesh Results using Energy vs. Displacement data of Different Radii for Link length 10.80 mm Unit Cell.

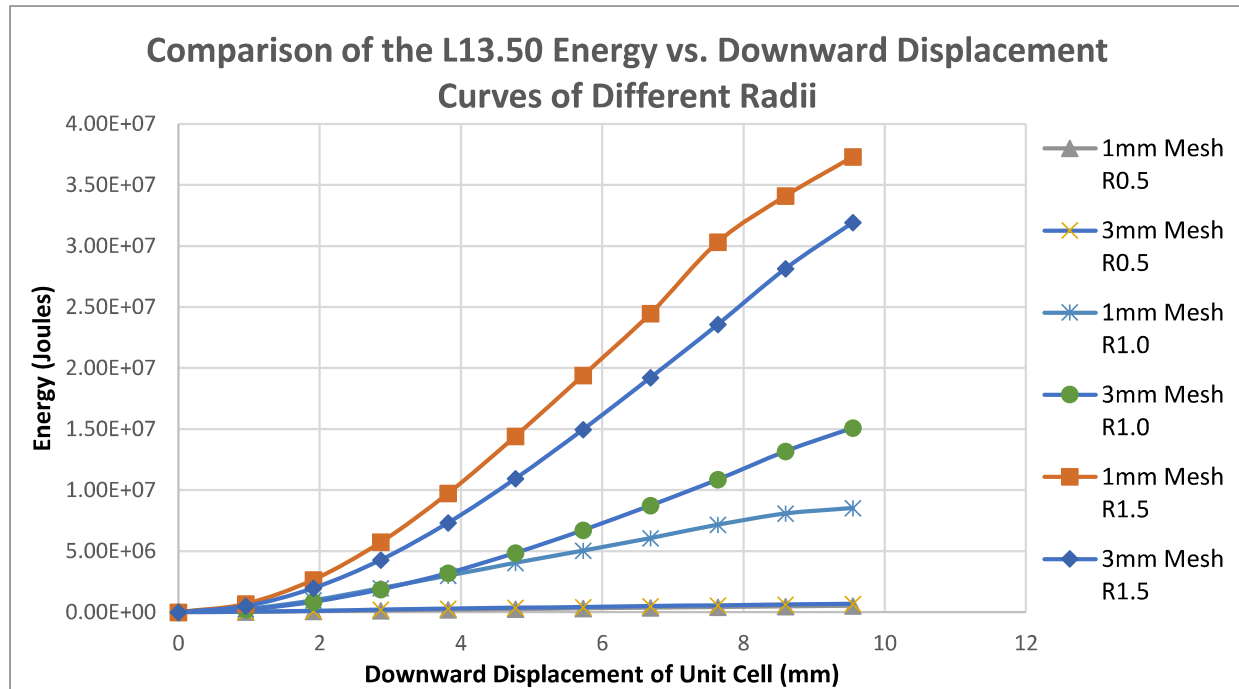


Figure 198: Comparison of Fine vs. Coarse Mesh Results using Energy vs. Displacement data of Different Radii for Link length 13.50 mm Unit Cell.

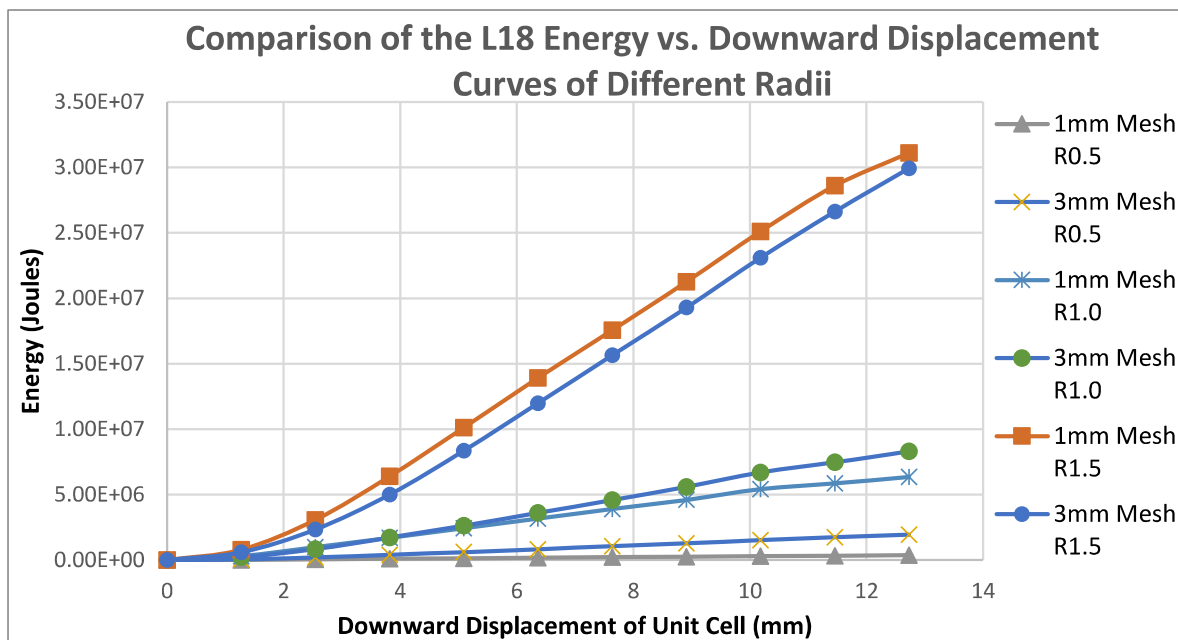


Figure 199: Comparison of Fine vs. Coarse Mesh Results using Energy vs. Displacement data of Different Radii for Link length 18 mm Unit Cell.

7.8.2 Cell Structure Mesh (3 mm) Results

7.8.2.1 Constant Cell Structure Comparison

7.8.2.1.1 Force vs. Displacement

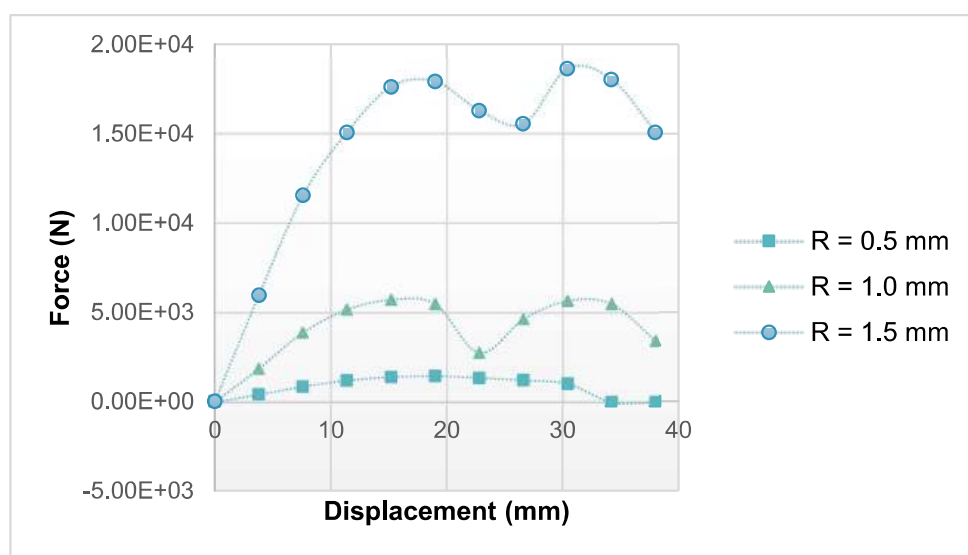


Figure 200: 3x3x3 Force vs. Displacement Curve

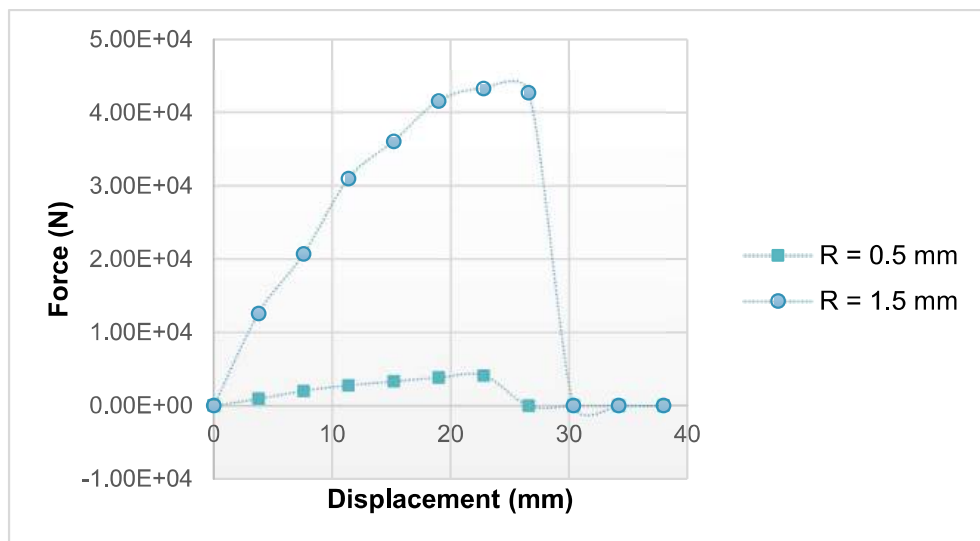


Figure 201: 4x4x4 Force vs. Displacement Curve [4x4x4 R1.0 data not included]

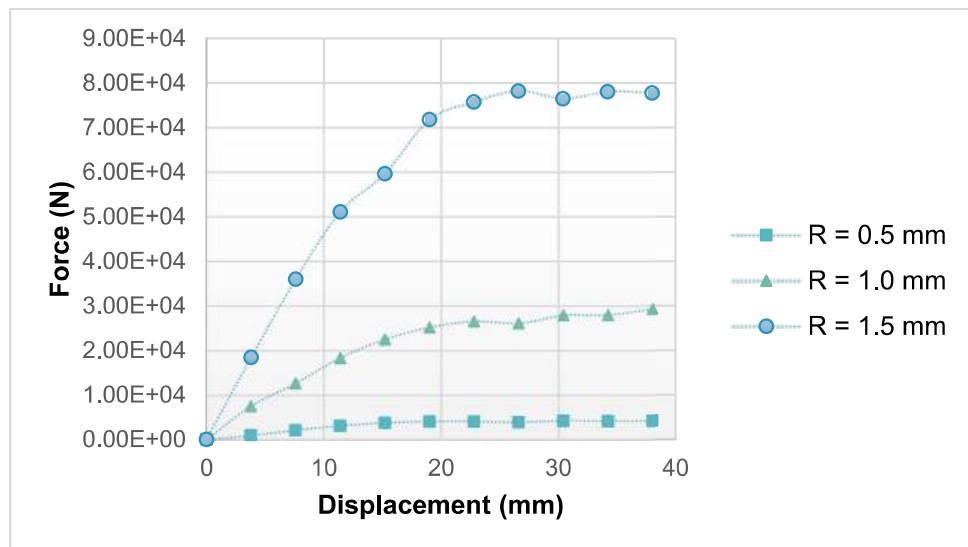


Figure 202: 5x5x5 Force vs. Displacement Curve

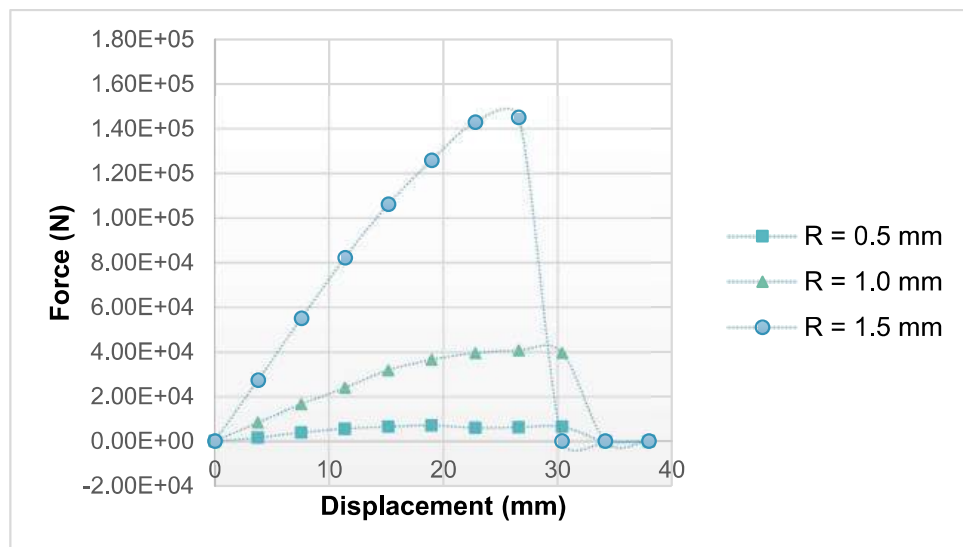


Figure 203: 6x6x6 Force vs. Displacement Curve

7.8.2.1.2 Energy vs. Displacement

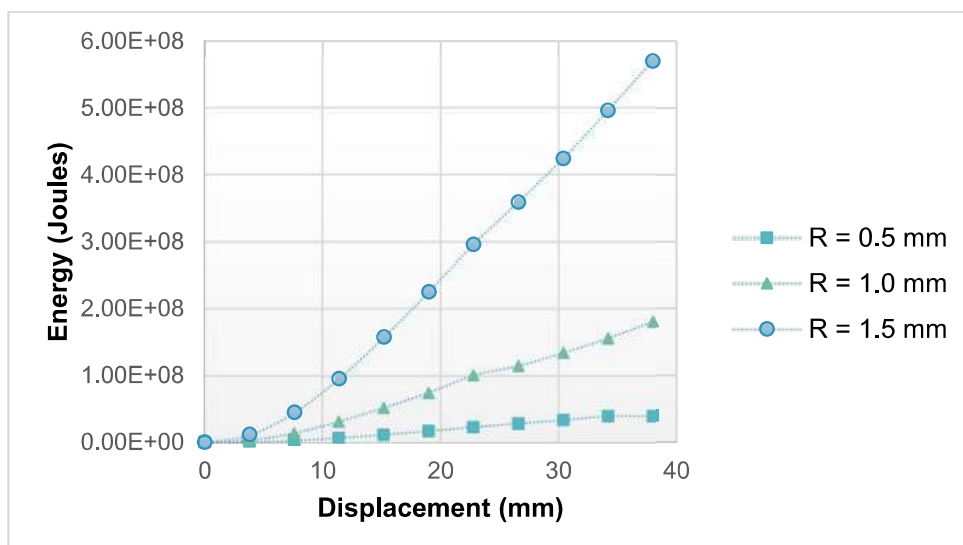


Figure 204: 3x3x3 Energy vs. Displacement Curve

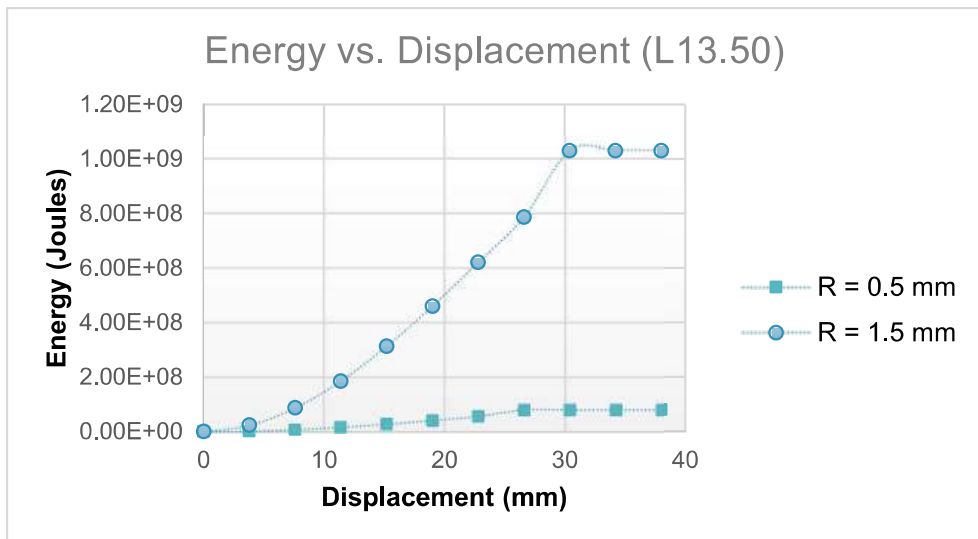


Figure 205: 4x4x4 Force vs. Displacement Curve [4x4x4 R1.0 data not included]

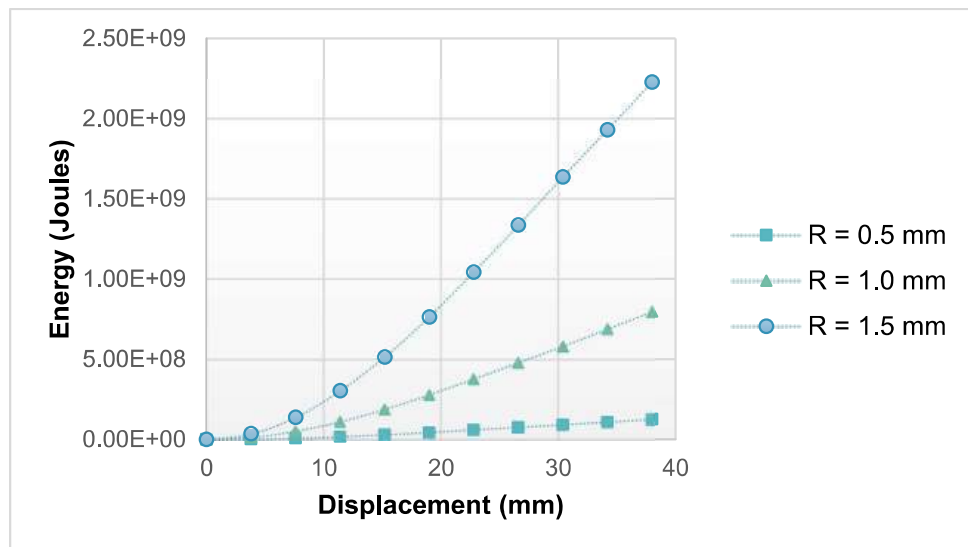


Figure 206: 5x5x5 Energy vs. Displacement Curve

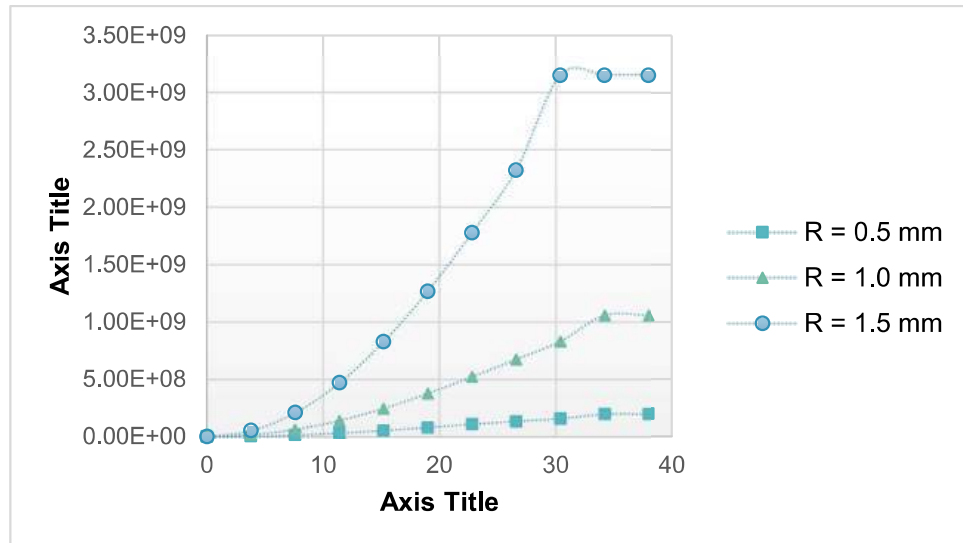


Figure 207: 6x6x6 Energy vs. Displacement Curve

7.8.2.2 Constant Radius Comparison

7.8.2.2.1 Force vs. Displacement

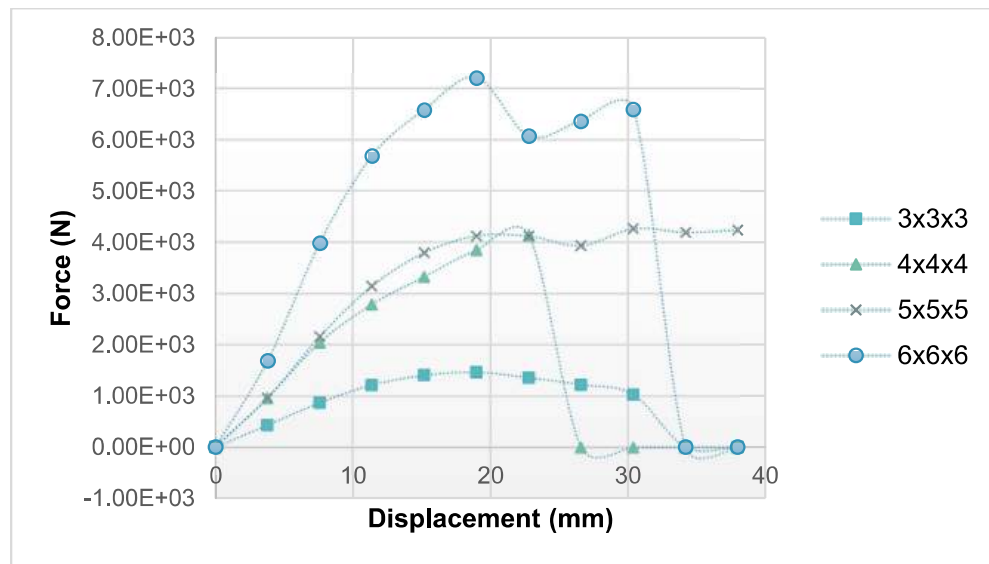


Figure 208: Force vs. Displacement Curve for Each Cell Structure of Link Radius 0.5 mm

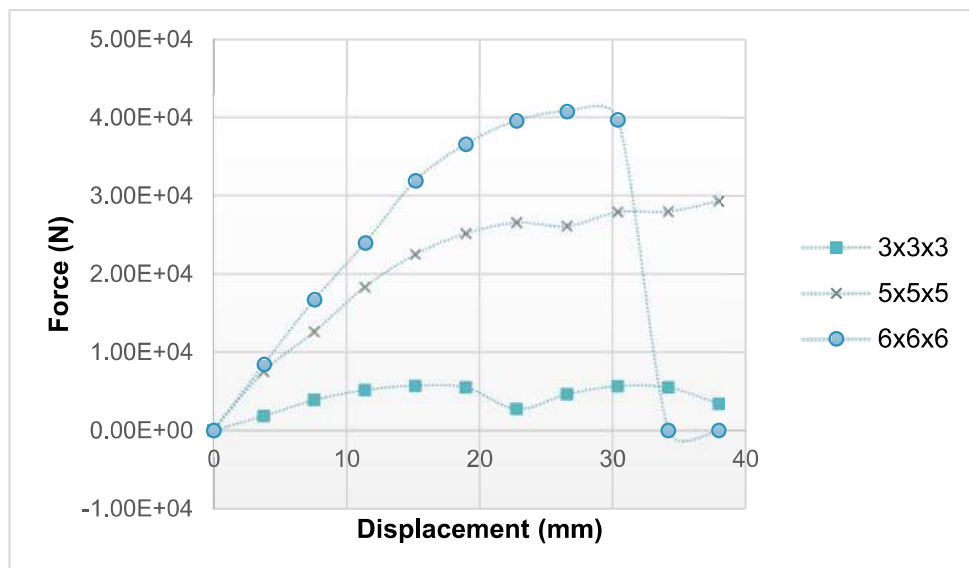


Figure 209: Force vs. Displacement Curve for Each Cell Structure of Link Radius 1.0 mm [4x4x4 data not included]

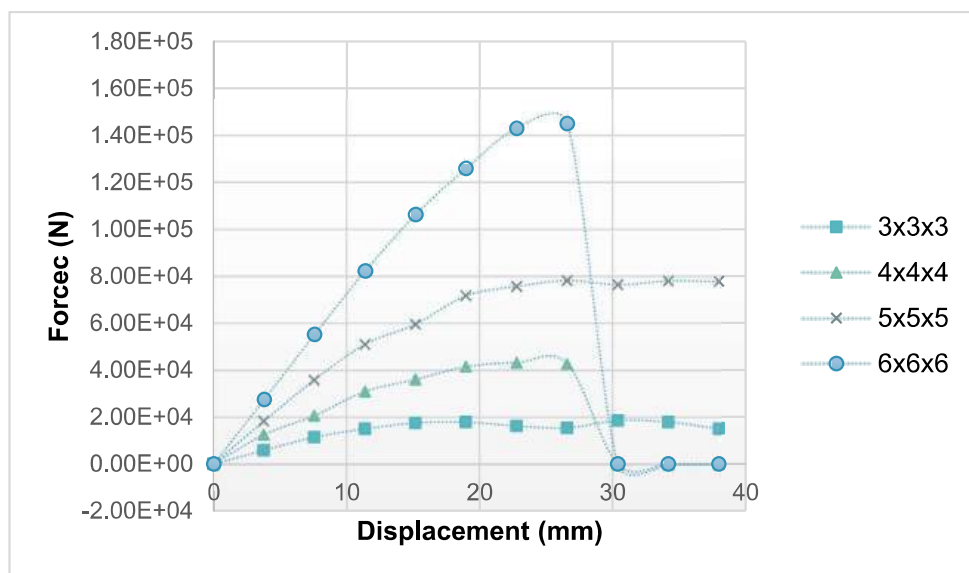


Figure 210: Force vs. Displacement Curve for Each Cell Structure of Link Radius 1.5 mm

7.8.2.2.2 Energy vs. Displacement

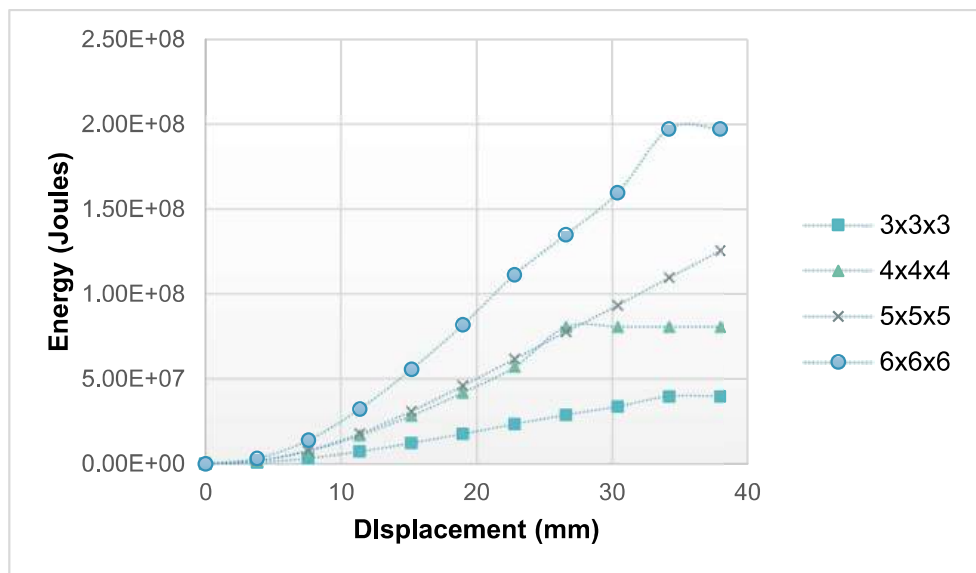


Figure 211: Energy vs. Displacement Curve for Each Cell Structure of Link Radius 0.5 mm

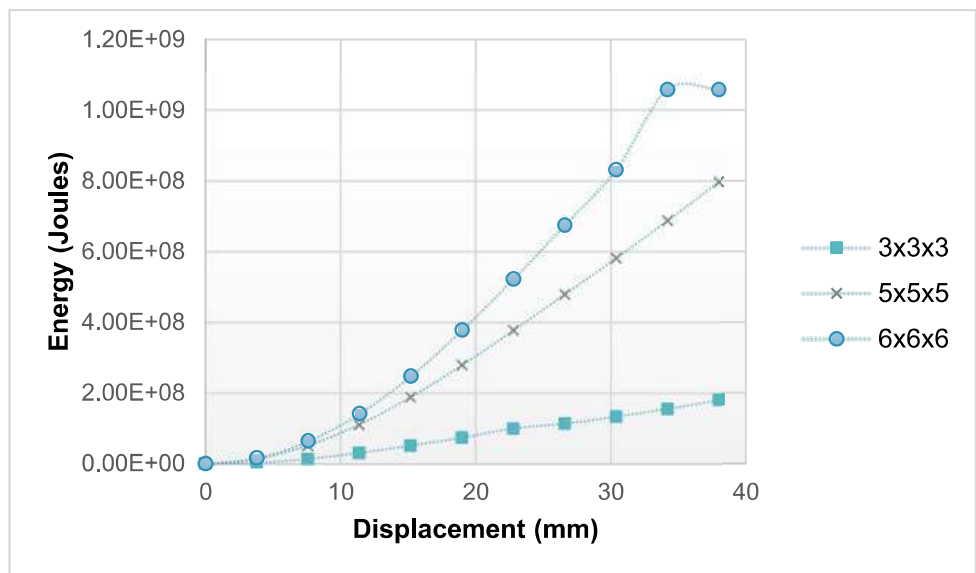


Figure 212: Energy vs. Displacement Curve for Each Cell Structure of Link Radius 1.0 mm [4x4x4 not included]

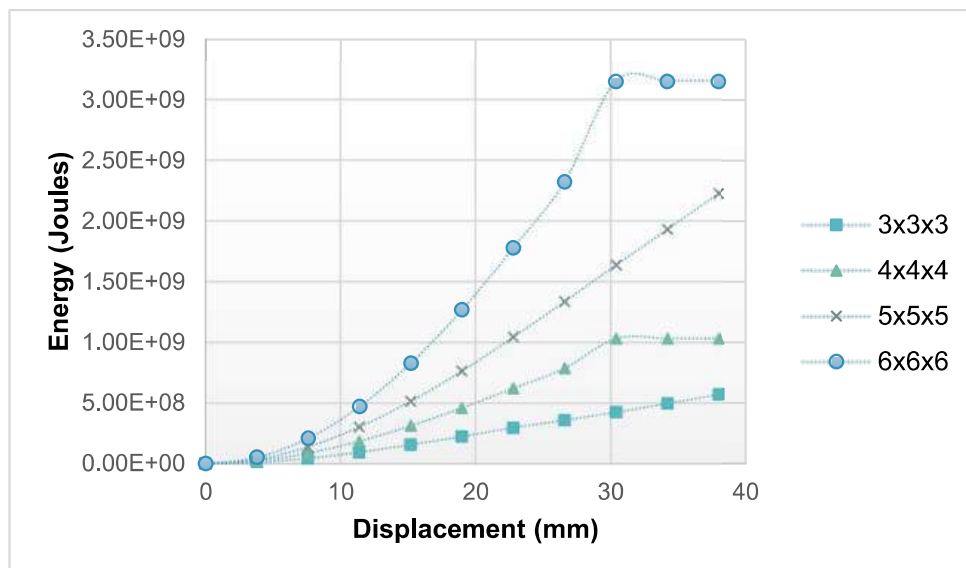


Figure 213: Energy vs. Displacement Curve for Each Cell Structure of Link Radius 1.5 mm

7.9 Specific Energy Absorption (SEA) Graphs

7.9.1 SEA of Fine Mesh (1mm Mesh) Unit Cells

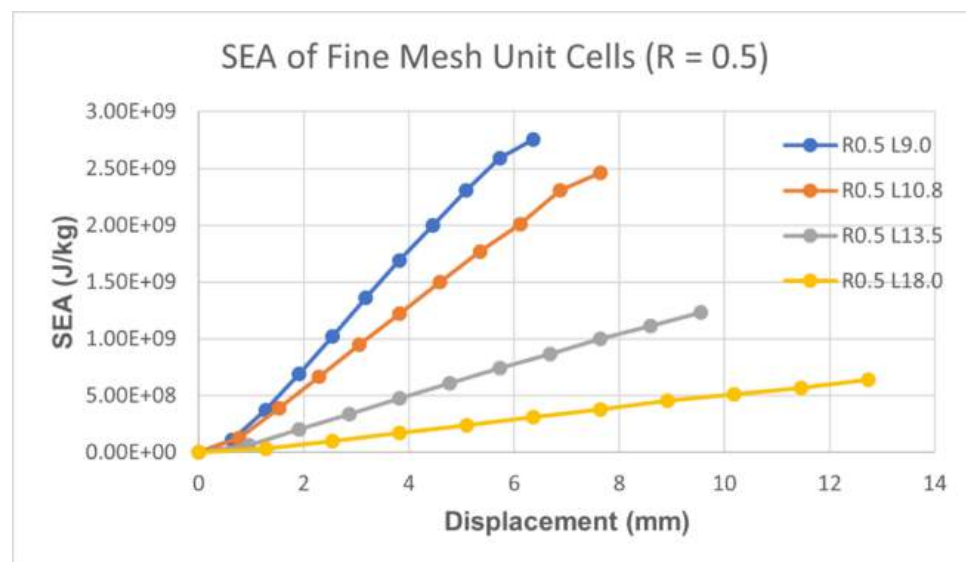


Figure 214: SEA vs. Displacement Curve for Fine Mesh Unit Cell of Link Radius 0.5 mm

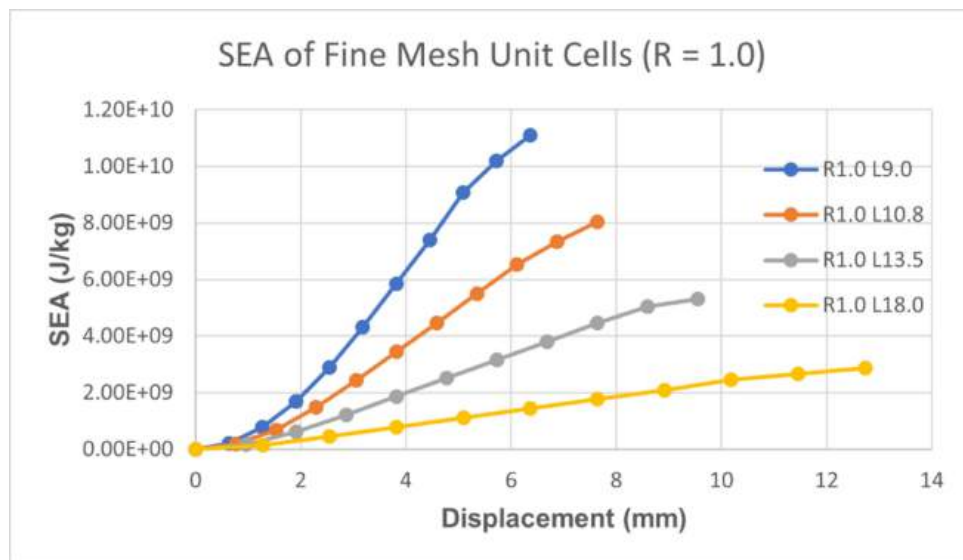


Figure 215: SEA vs. Displacement Curve for Fine Mesh Unit Cell of Link Radius 1.0 mm

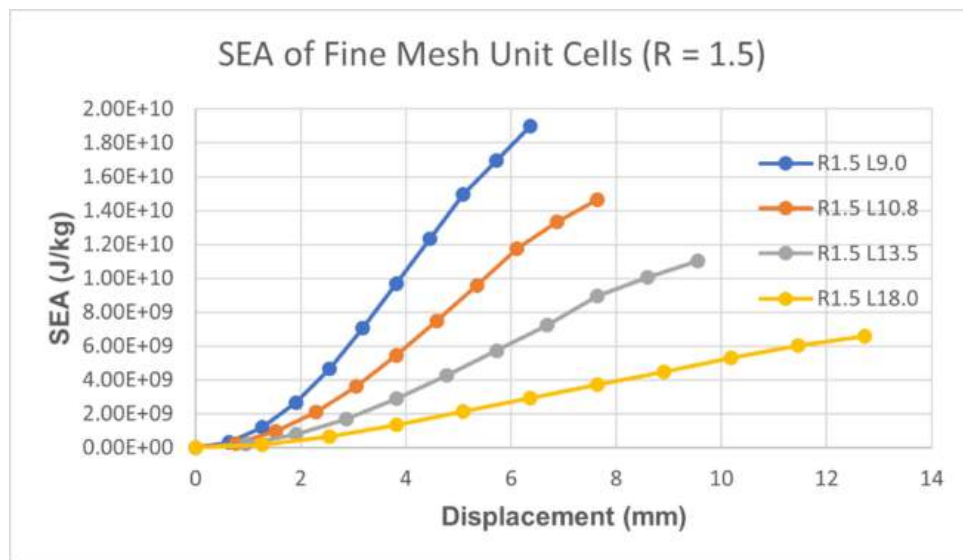


Figure 216: SEA vs. Displacement Curve for Fine Mesh Unit Cell of Link Radius 1.5 mm

7.9.2 SEA of Coarse Mesh (3mm Mesh) Unit Cells

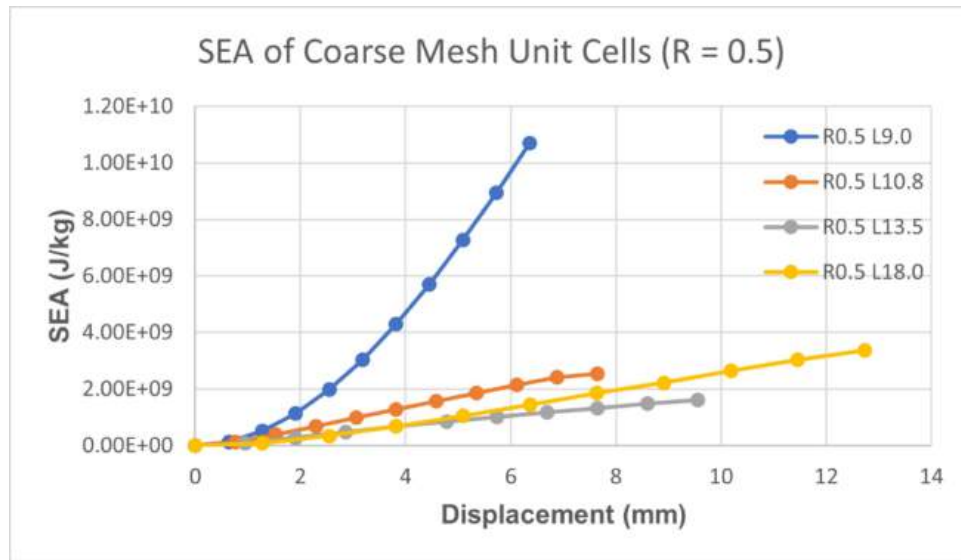


Figure 217: SEA vs. Displacement Curve for Coarse Mesh Unit Cell of Link Radius 0.5 mm

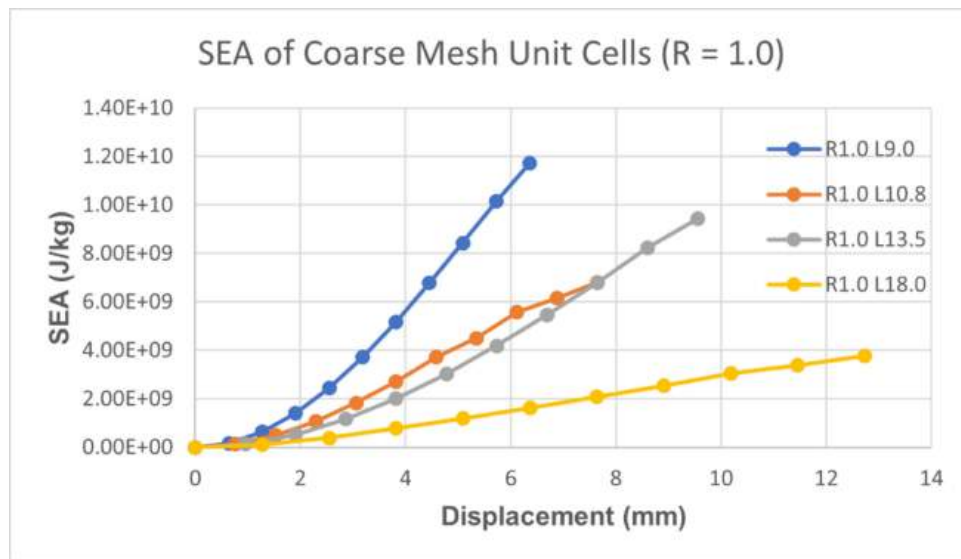


Figure 218: SEA vs. Displacement Curve for Coarse Mesh Unit Cell of Link Radius 1.0 mm

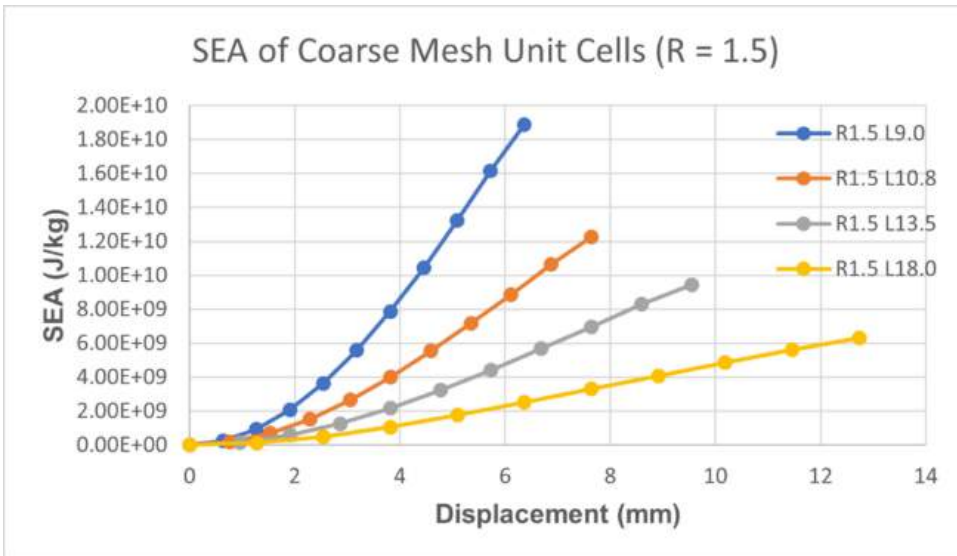


Figure 219: SEA vs. Displacement Curve for Coarse Mesh Unit Cell of Link Radius 1.5 mm

7.9.3 SEA of Cell Structures (3mm Mesh)

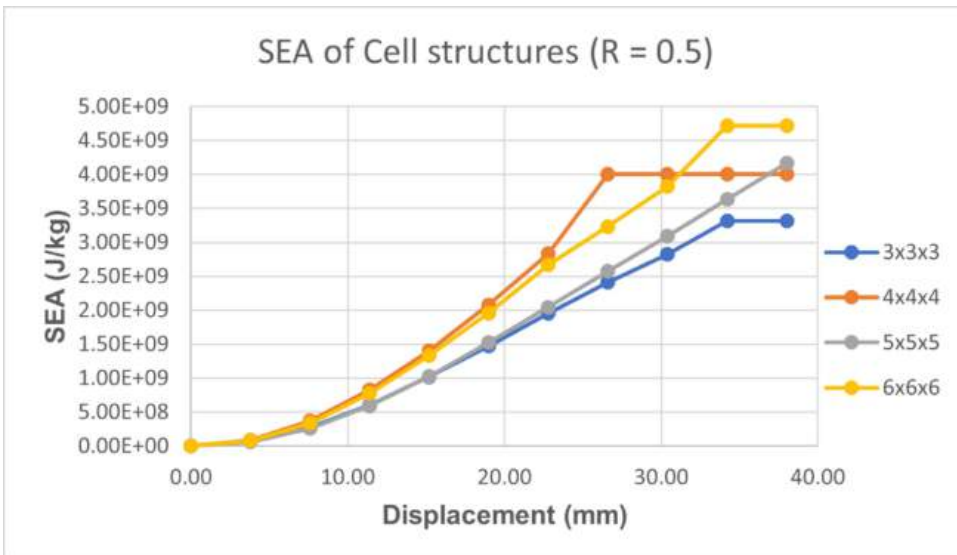


Figure 220: SEA vs. Displacement Curve for Cell Structures of Link Radius 0.5 mm

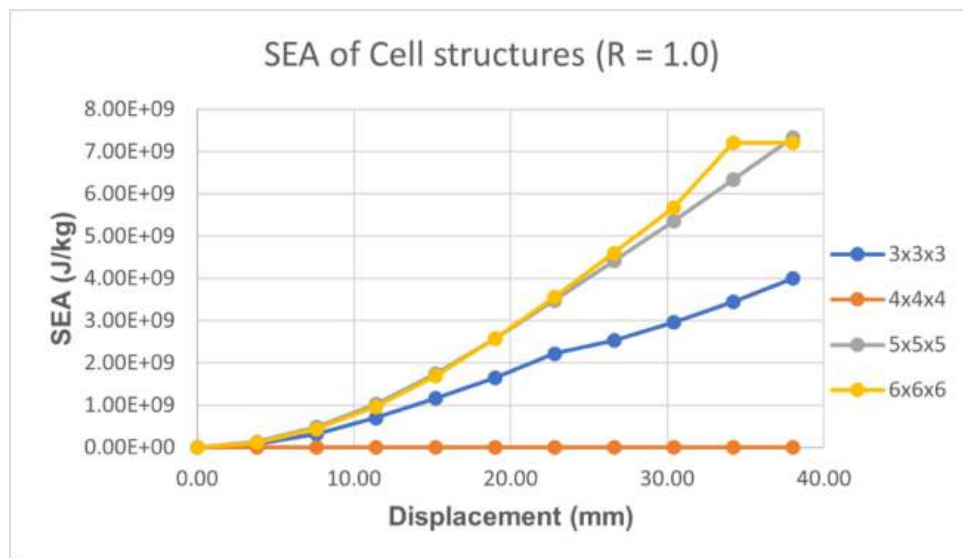


Figure 221: SEA vs. Displacement Curve for Cell Structures of Link Radius 1.0 mm

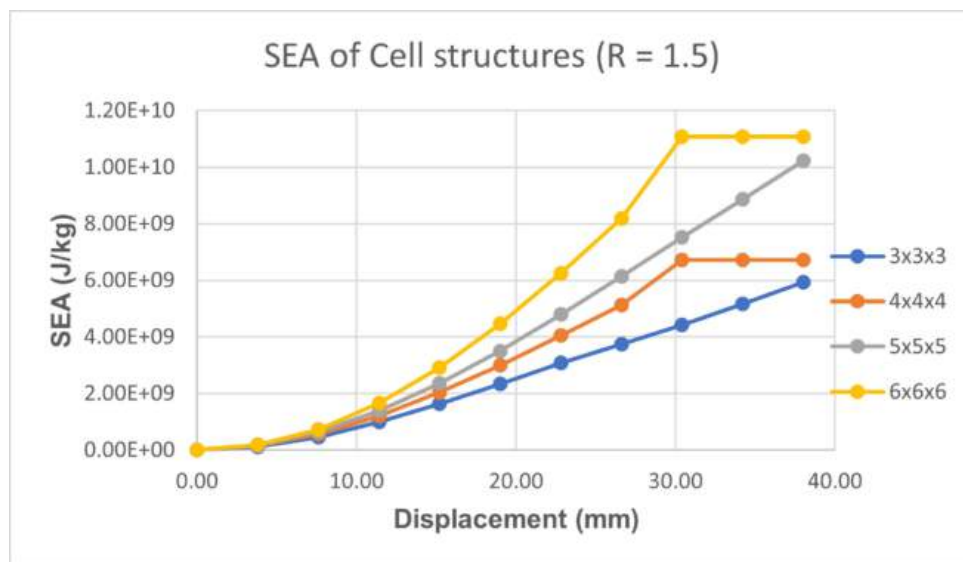


Figure 222: SEA vs. Displacement Curve for Cell Structures of Link Radius 1.5 mm

7.10 Stress Versus Strain Graphs

7.10.1 Unit Cells with Fine and Coarse Mesh vs. their accompanying Assembled Cell Structures

7.10.1.1 Link Length 9.0 mm

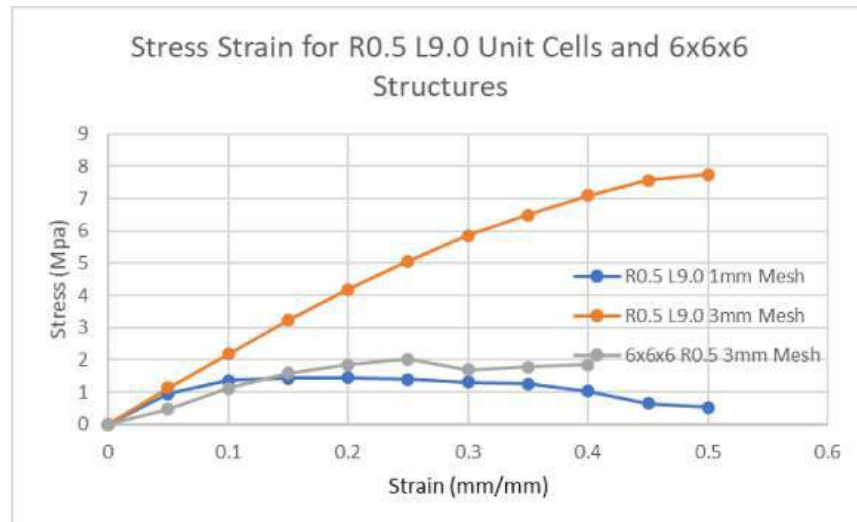


Figure 223: Stress Strain Curves of L9.0 mm R0.5 mm Unit Cells and its 6x6x6 Cell Structure vs. Displacement data for Fine and Coarse Mesh.

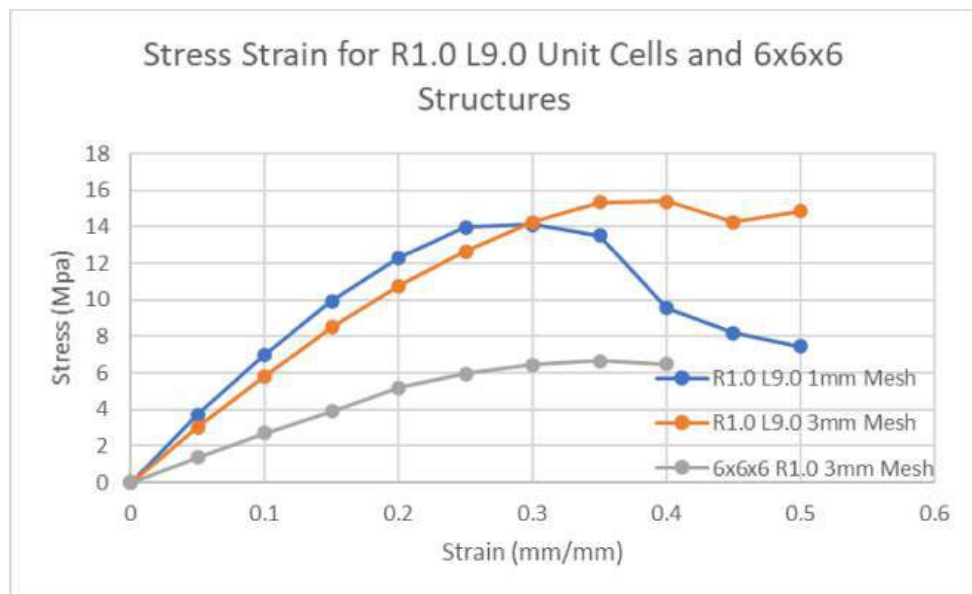


Figure 224: Stress Strain Curves of L9.0 mm R1.0 mm Unit Cells and its 6x6x6 Cell Structure vs. Displacement data for Fine and Coarse Mesh.

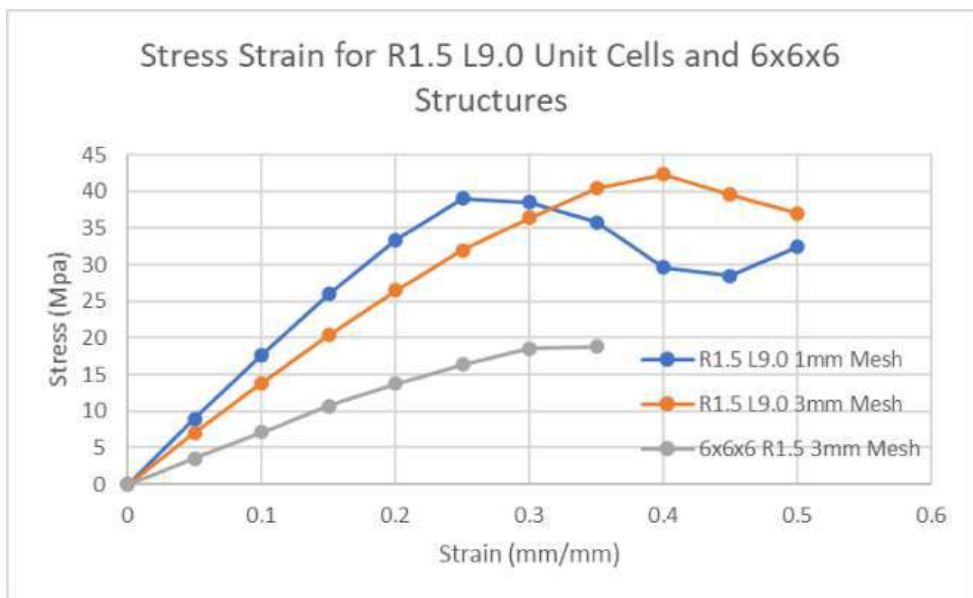


Figure 225: Stress Strain Curves of L9.0 mm R1.5 mm Unit Cells and its 6x6x6 Cell Structure vs. Displacement data for Fine and Coarse Mesh.

7.10.1.2 Link Length 10.80 mm

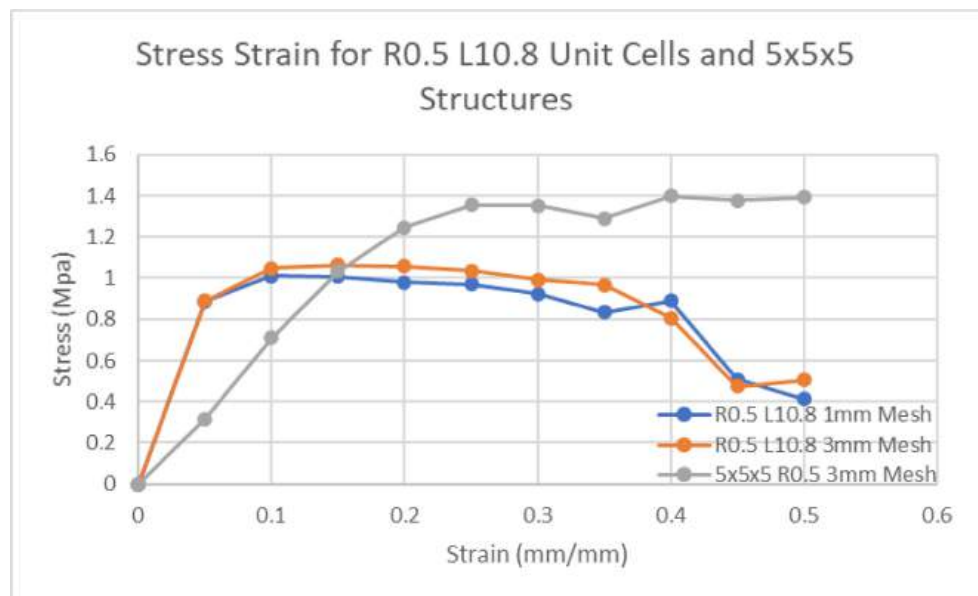


Figure 226: Stress Strain Curves of L10.80 mm R0.5 mm Unit Cells and its 5x5x5 Cell Structure vs. Displacement data for Fine and Coarse Mesh.

Stress Strain for R1.0 L10.8 Unit Cells and 5x5x5 Structures

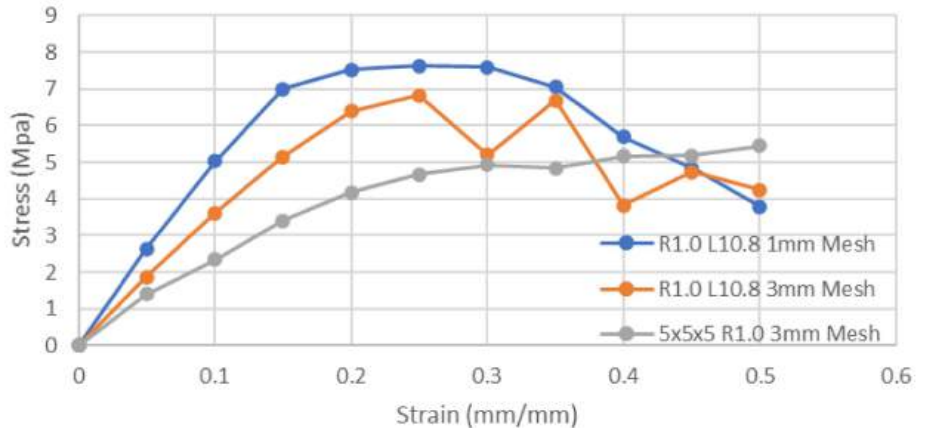


Figure 227: Stress Strain Curves of L10.80 mm R1.0 mm Unit Cells and its 5x5x5 Cell Structure vs. Displacement data for Fine and Coarse Mesh.

Stress Strain for R1.5 L10.8 Unit Cells and 5x5x5 Structures

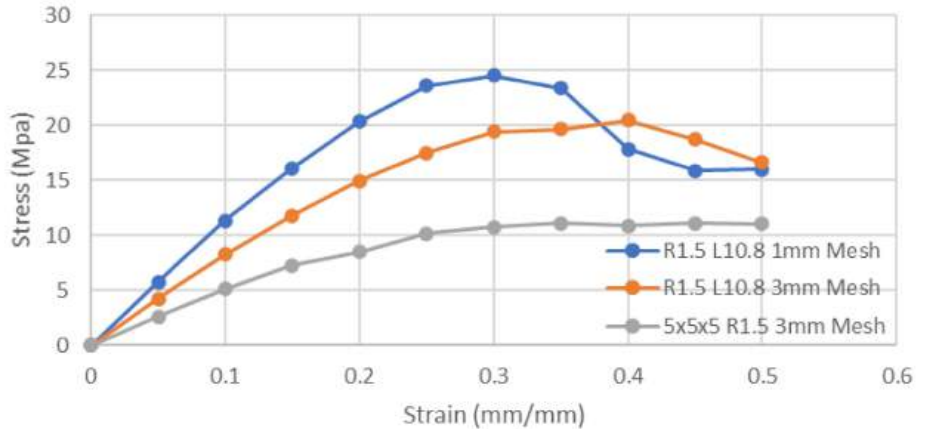


Figure 228: Stress Strain Curves of L10.80 mm R1.5 mm Unit Cells and its 5x5x5 Cell Structure vs. Displacement data for Fine and Coarse Mesh.

7.10.1.3 Link Length 13.50 mm

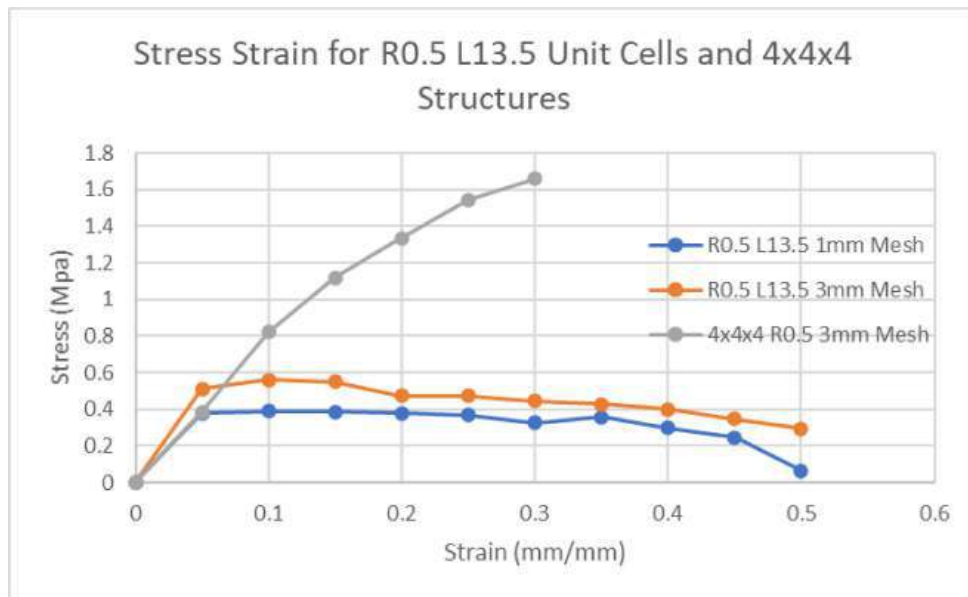


Figure 229: Stress Strain Curves of L13.50 mm R0.5 mm Unit Cells and its 4x4x4 Cell Structure vs. Displacement data for Fine and Coarse Mesh.

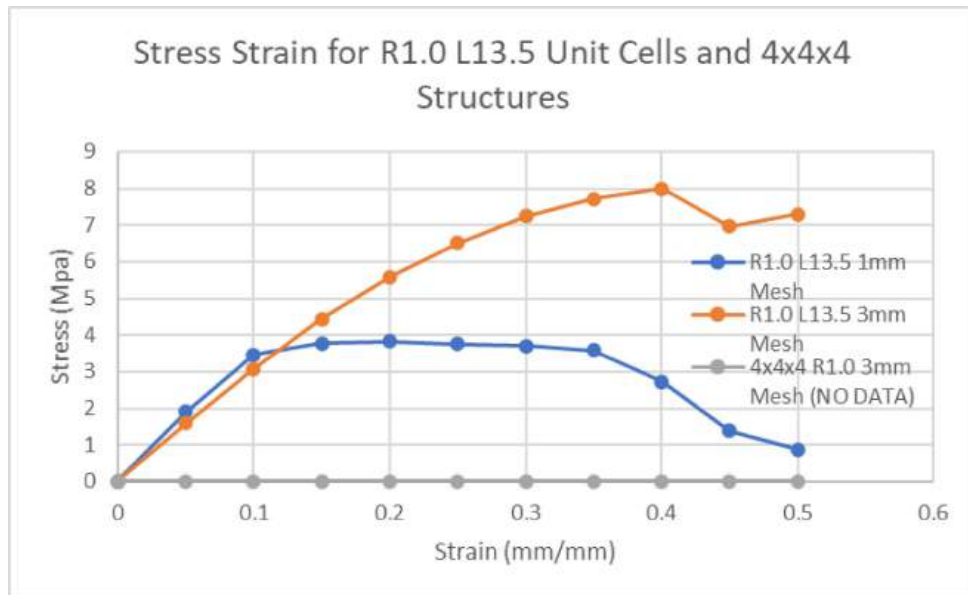


Figure 230: Stress Strain Curves of L13.50 mm R1.0 mm Unit Cells and its 4x4x4 Cell Structure vs. Displacement data for Fine and Coarse Mesh.

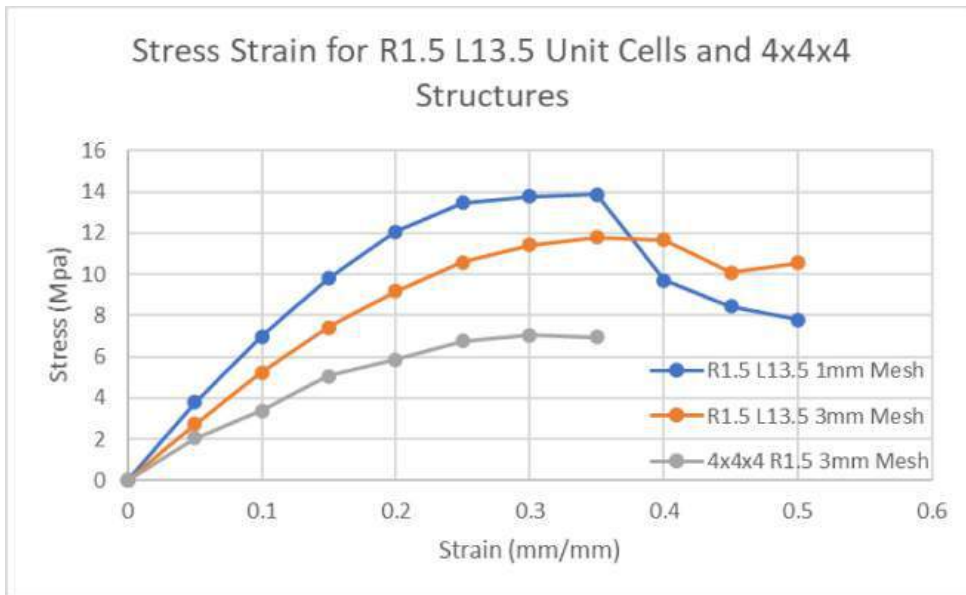


Figure 231: Stress Strain Curves of L13.50 mm R1.5 mm Unit Cells and its 4x4x4 Cell Structure vs. Displacement data for Fine and Coarse Mesh.

7.10.1.4 Link Length 18.0 mm

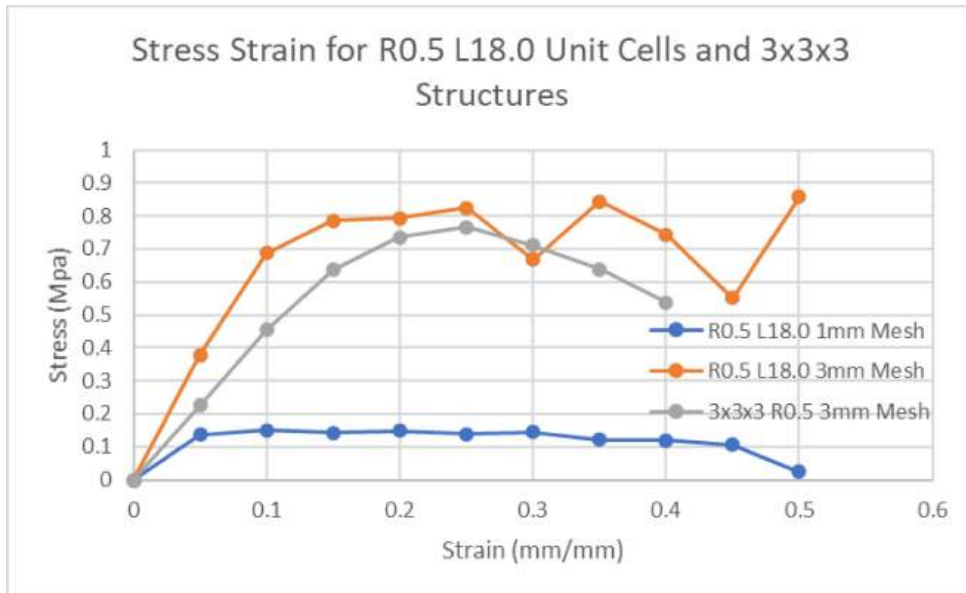


Figure 232: Stress Strain Curves of L18.0 mm R0.5 mm Unit Cells and its 3x3x3 Cell Structure vs. Displacement data for Fine and Coarse Mesh.

Stress Strain for R1.0 L18.0 Unit Cells and 3x3x3 Structures

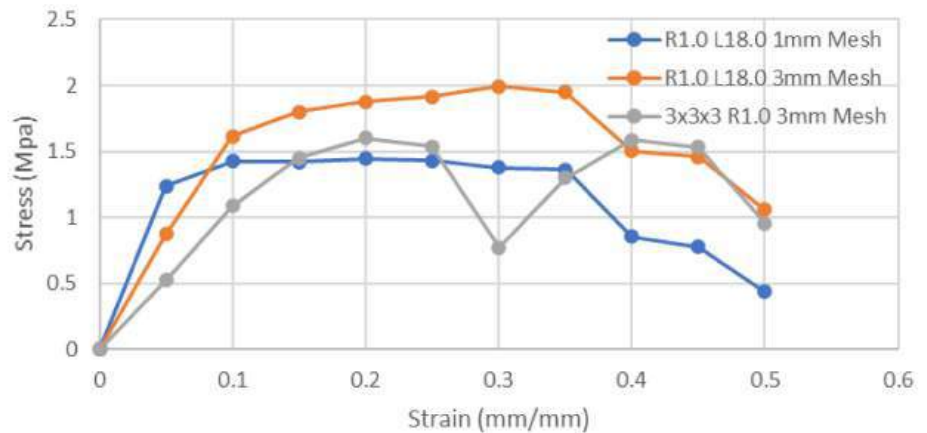


Figure 233: Stress Strain Curves of L18.0 mm R1.0 mm Unit Cells and its 3x3x3 Cell Structure vs. Displacement data for Fine and Coarse Mesh.

Stress Strain for R1.5 L18.0 Unit Cells and 3x3x3 Structures

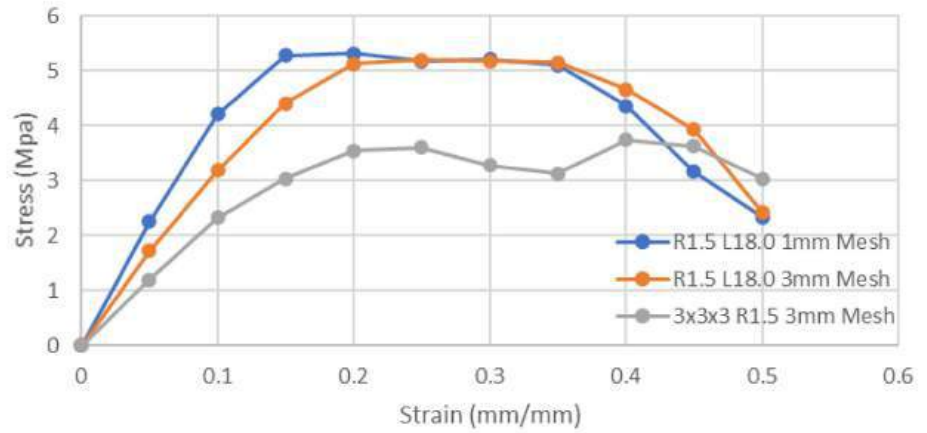


Figure 234: Stress Strain Curves of L18.0 mm R1.5 mm Unit Cells and its 3x3x3 Cell Structure vs. Displacement data for Fine and Coarse Mesh.

7.10.2 Varying Radiiuses with Constant Length

7.10.2.1 Unit Cells with 1.0 mm Fine Mesh

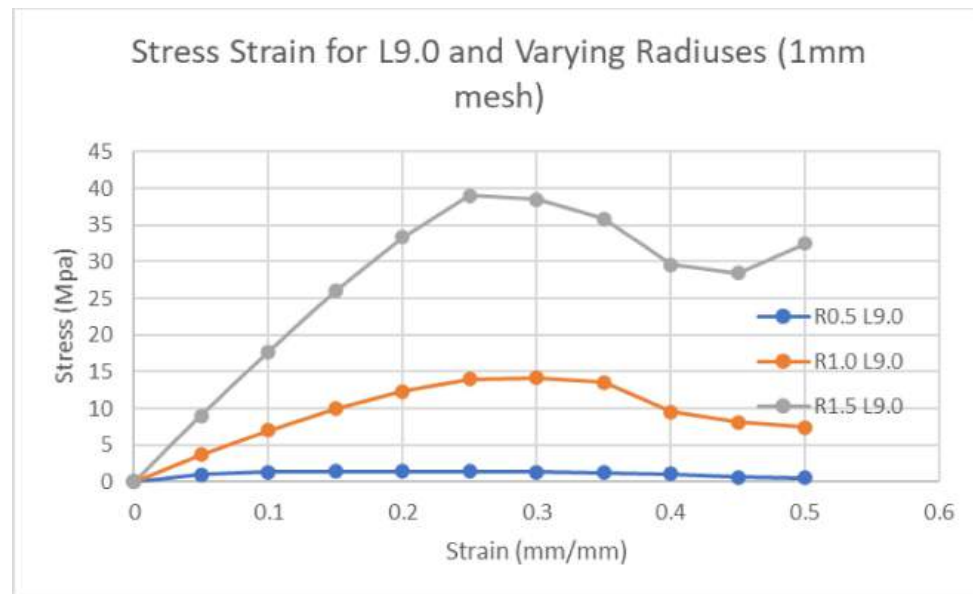


Figure 235: Stress Strain Curves of L9.0 mm Unit Cell w/ 1 mm Fine Mesh vs. Displacement data for Different Radii.

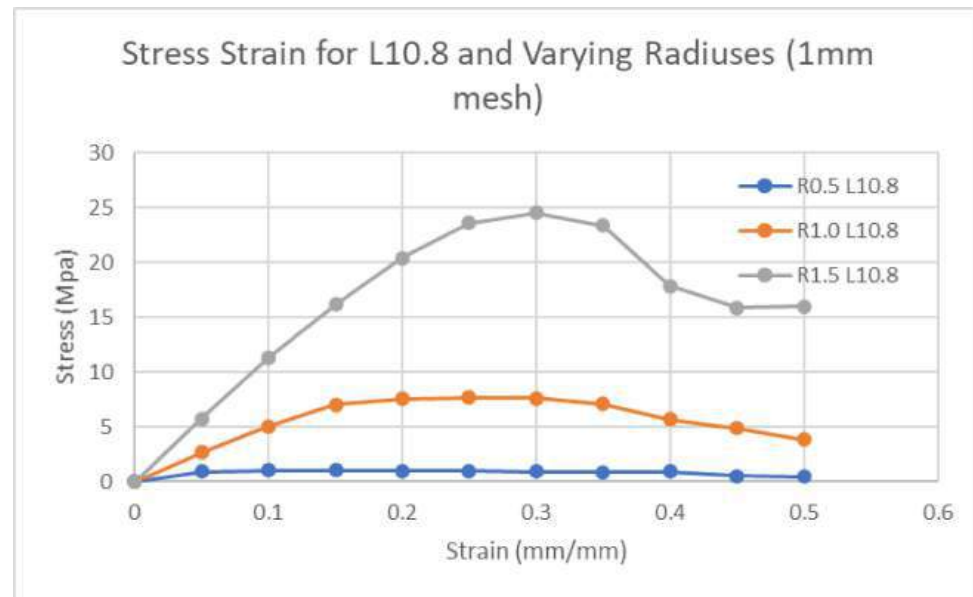


Figure 236: Stress Strain Curves of L10.80 mm Unit Cell w/ 1 mm Fine Mesh vs. Displacement data for Different Radii.

Stress Strain for L13.5 and Varying Radiiuses (1mm mesh)

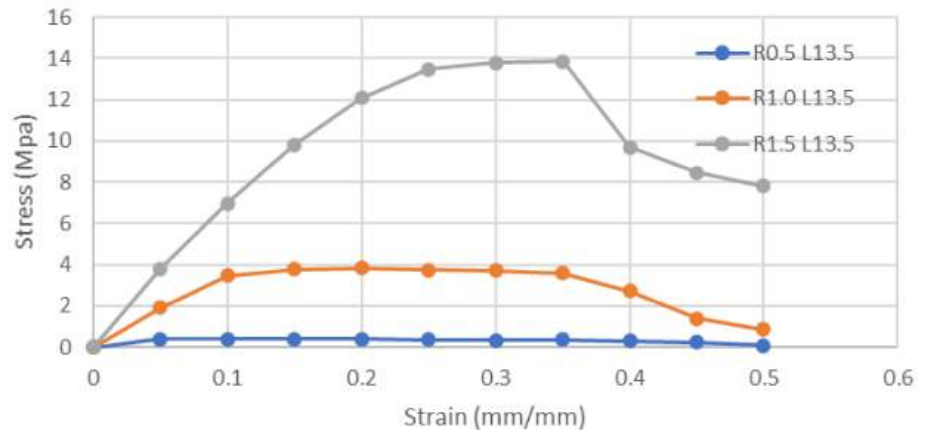


Figure 237: Stress Strain Curves of L13.50 mm Unit Cell w/ 1 mm Fine Mesh vs. Displacement data for Different Radii.

Stress Strain for L18.0 and Varying Radiiuses (1mm mesh)

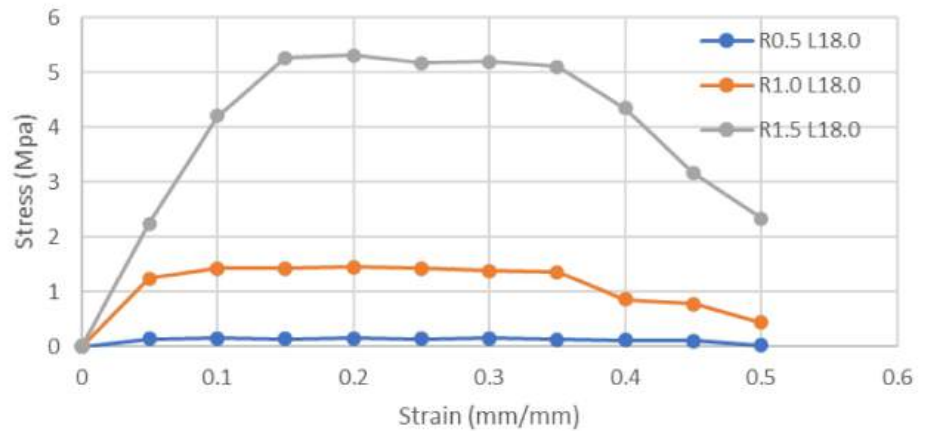


Figure 238: Stress Strain Curves of L9.0 mm Unit Cell w/ 1 mm Fine Mesh vs. Displacement data for Different Radii.

7.10.2.2 Unit Cells with 3.0 mm Coarse Mesh

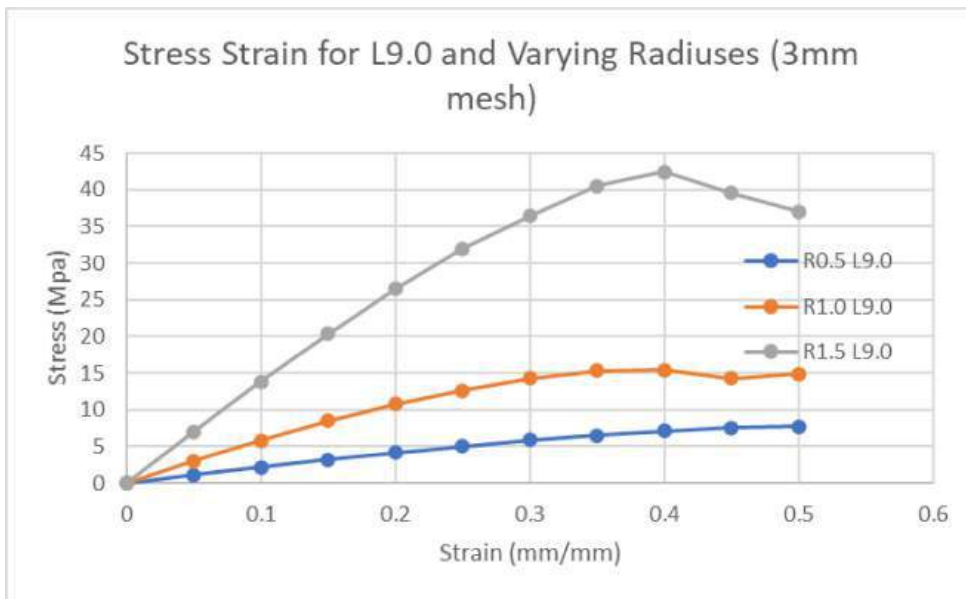


Figure 239: Stress Strain Curves of L9.0 mm Unit Cell w/ 3 mm Coarse Mesh vs. Displacement data for Different Radii.

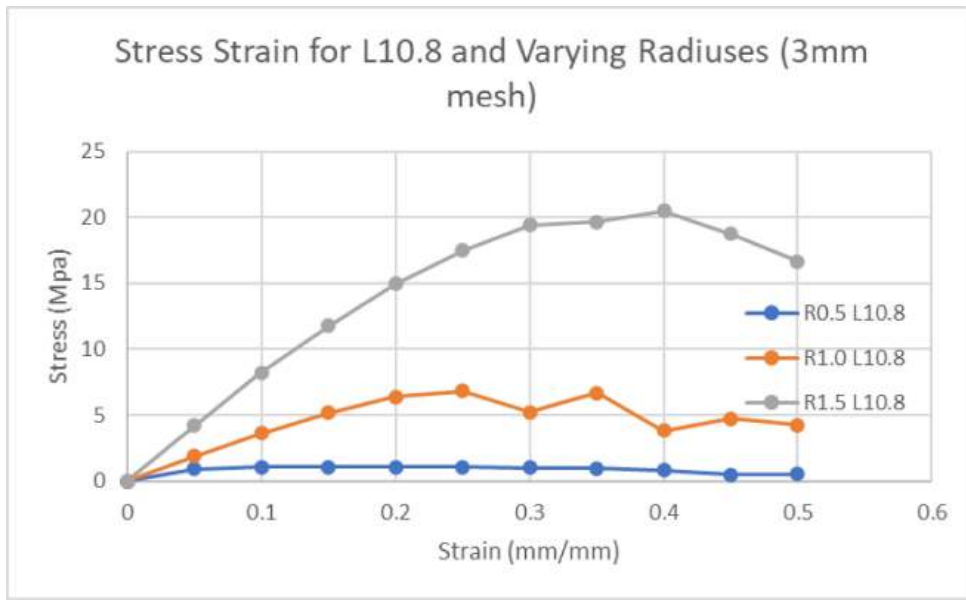


Figure 240: Stress Strain Curves of L10.80 mm Unit Cell w/ 3 mm Coarse Mesh vs. Displacement data for Different Radii.

Stress Strain for L13.5 and Varying Radiiuses (3mm mesh)

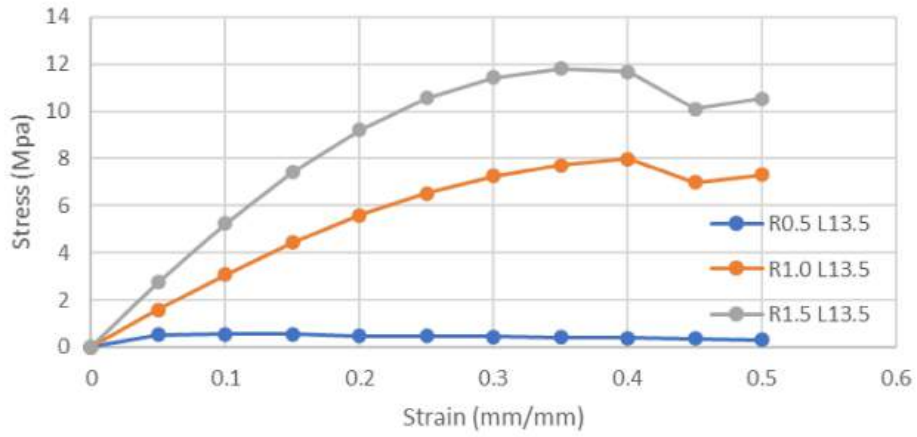


Figure 241: Stress Strain Curves of L13.50 mm Unit Cell w/ 3 mm Coarse Mesh vs. Displacement data for Different Radii.

Stress Strain for L18.0 and Varying Radiiuses (3mm mesh)

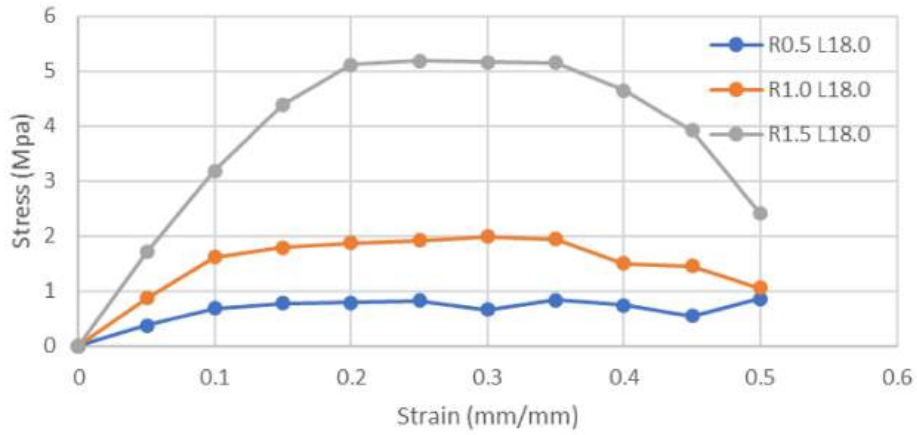


Figure 242: Stress Strain Curves of L18.0 mm Unit Cell w/ 3 mm Coarse Mesh vs. Displacement data for Different Radii.

7.10.2.3 Cell Structures with 3.0 mm Coarse Mesh

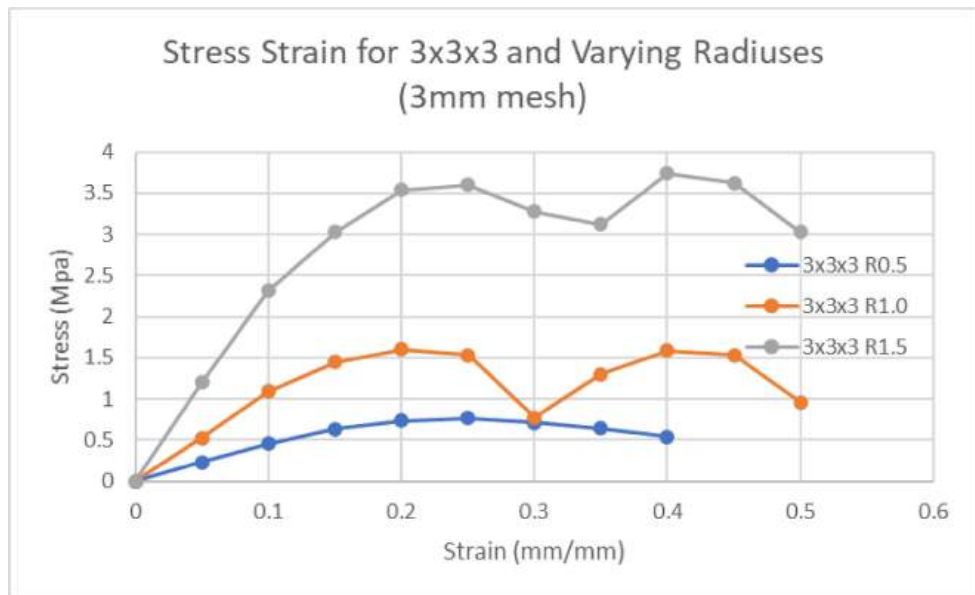


Figure 243: Stress Strain Curves of 3x3x3 Cell Structure w/ 3 mm Coarse Mesh vs. Displacement data for Different Radii.

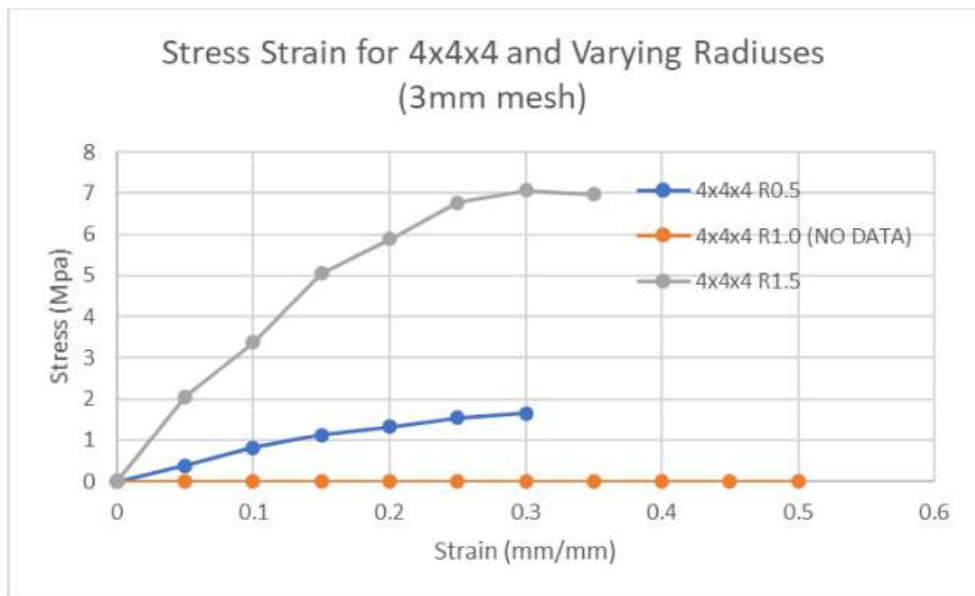


Figure 244: Stress Strain Curves of 4x4x4 Cell Structure w/ 3 mm Coarse Mesh vs. Displacement data for Different Radii.

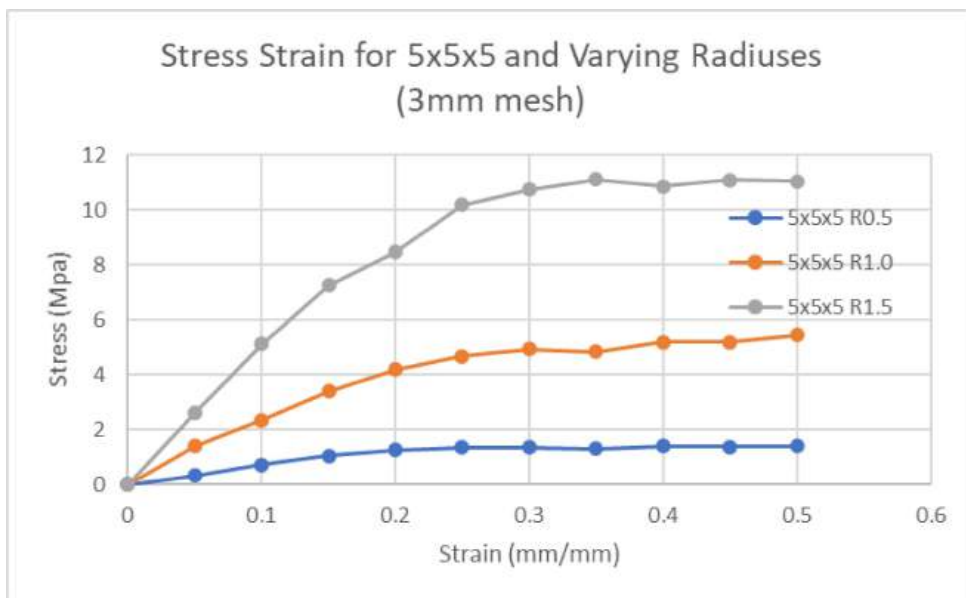


Figure 245: Stress Strain Curves of 5x5x5 Cell Structure w/ 3 mm Coarse Mesh vs. Displacement data for Different Radii.

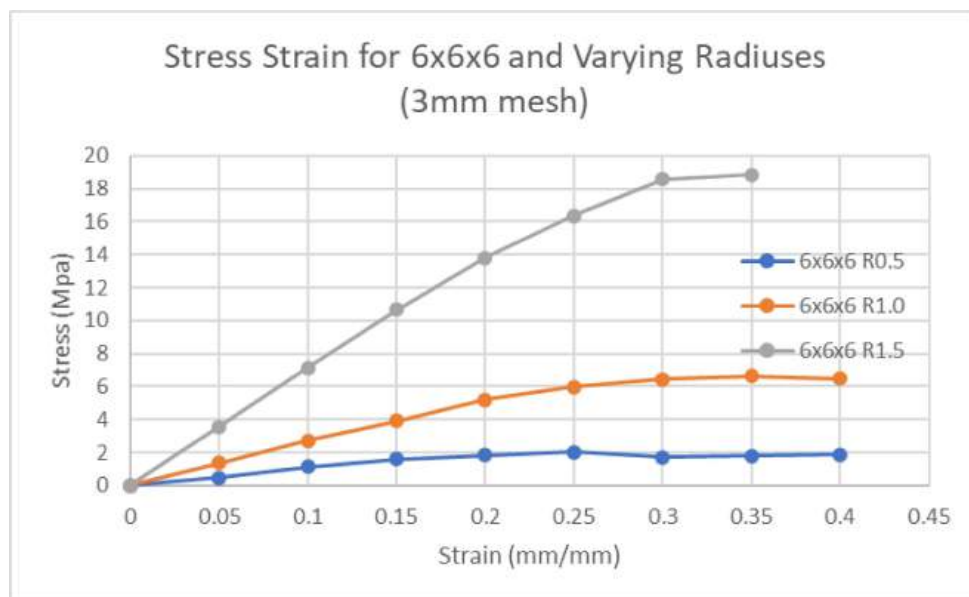


Figure 246: Stress Strain Curves of 6x6x6 Cell Structure w/ 3 mm Coarse Mesh vs. Displacement data for Different Radii.

7.10.3 Varying Lengths with Constant Radiiuses

7.10.3.1 Unit Cells with 1.0 mm Fine Mesh

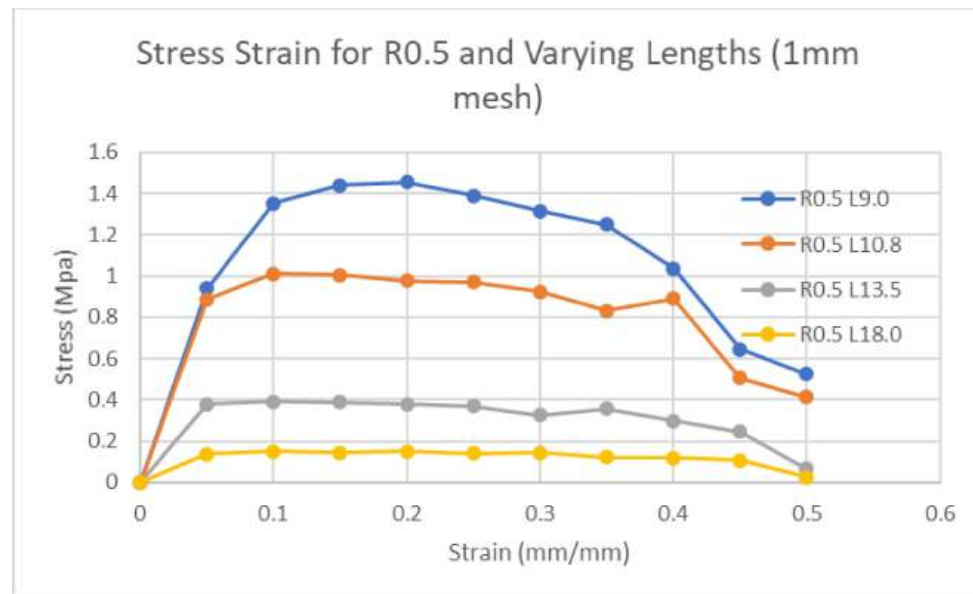


Figure 247: Stress Strain Curves of R0.5 mm Unit Cell w/ 1 mm Fine Mesh vs. Displacement data for Different Link Lengths.

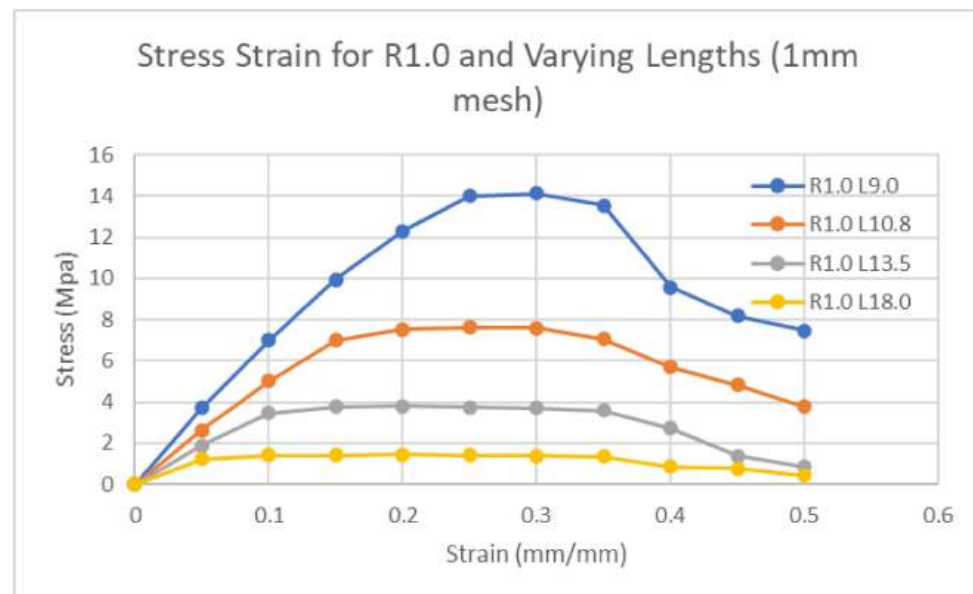


Figure 248: Stress Strain Curves of R1.0 mm Unit Cell w/ 1 mm Fine Mesh vs. Displacement data for Different Link Lengths.

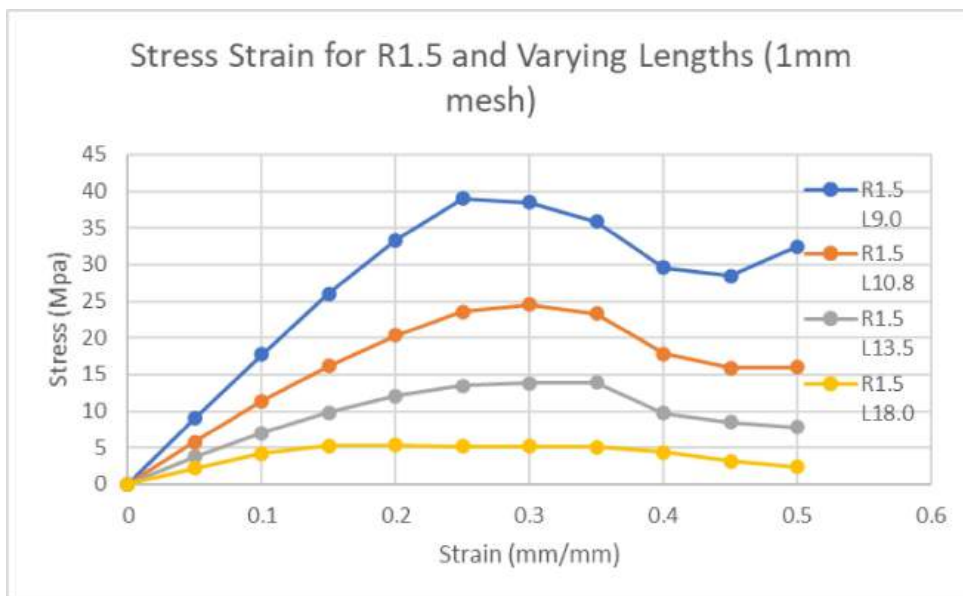


Figure 249: Stress Strain Curves of R1.5 mm Unit Cell w/ 1 mm Fine Mesh vs. Displacement data for Different Link Lengths.

7.10.3.2 Unit Cells with 3.0 mm Coarse Mesh

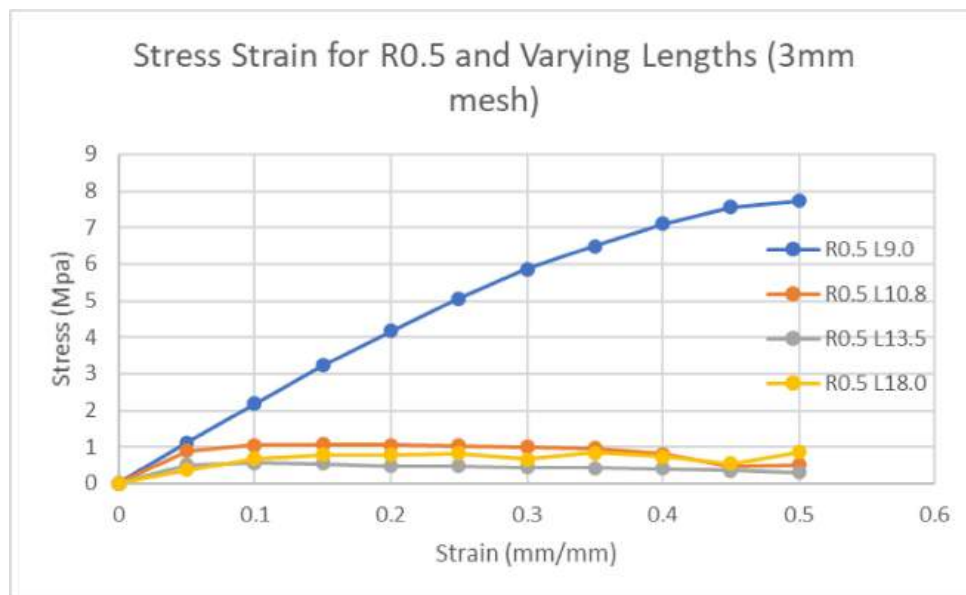


Figure 250: Stress Strain Curves of R0.5 mm Unit Cell w/ 3 mm Coarse Mesh vs. Displacement data for Different Link Lengths.

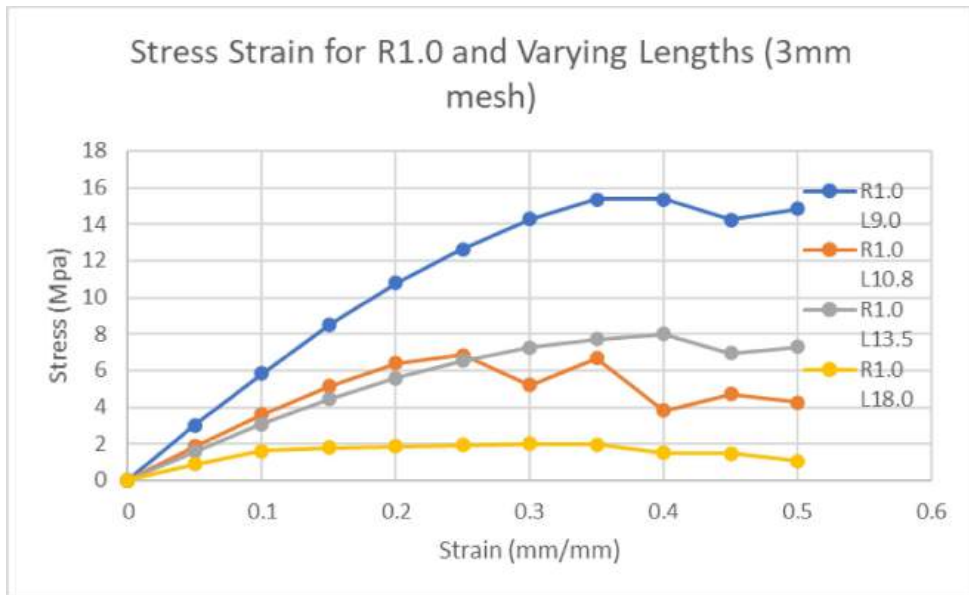


Figure 251: Stress Strain Curves of R1.0 mm Unit Cell w/ 3 mm Coarse Mesh vs. Displacement data for Different Link Lengths.

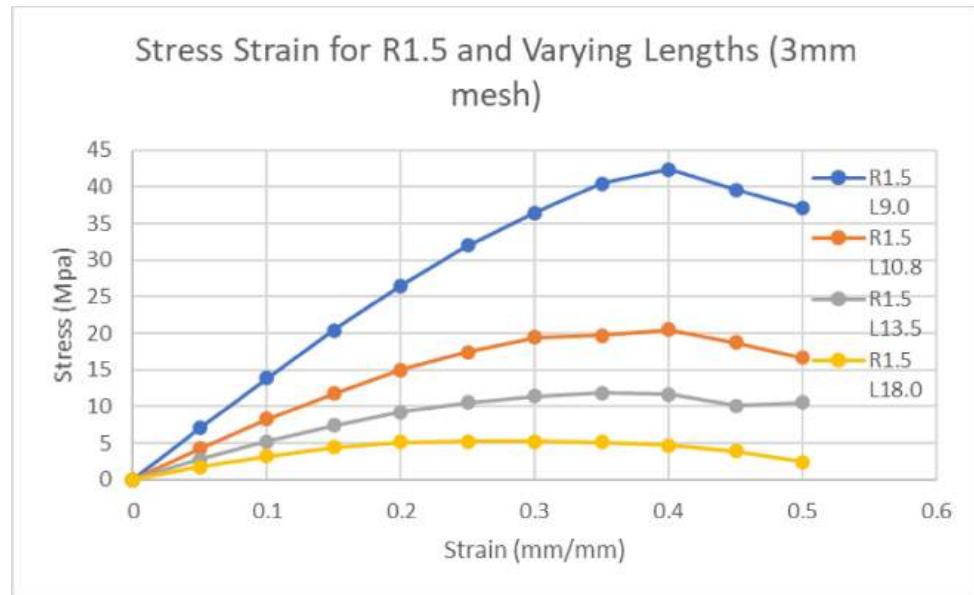


Figure 252: Stress Strain Curves of R1.5 mm Unit Cell w/ 3 mm Coarse Mesh vs. Displacement data for Different Link Lengths.

7.10.3.3 Cell Structures with 3.0 Coarse Mesh

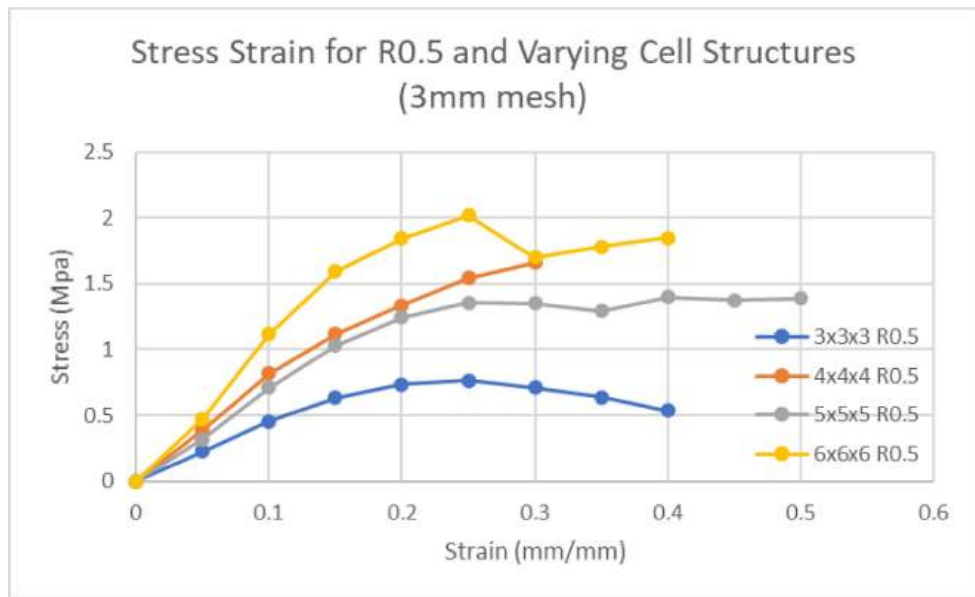


Figure 253: Stress Strain Curves of R0.5 mm Cell Structures w/ 3 mm Coarse Mesh vs. Displacement data for Different Link Lengths.

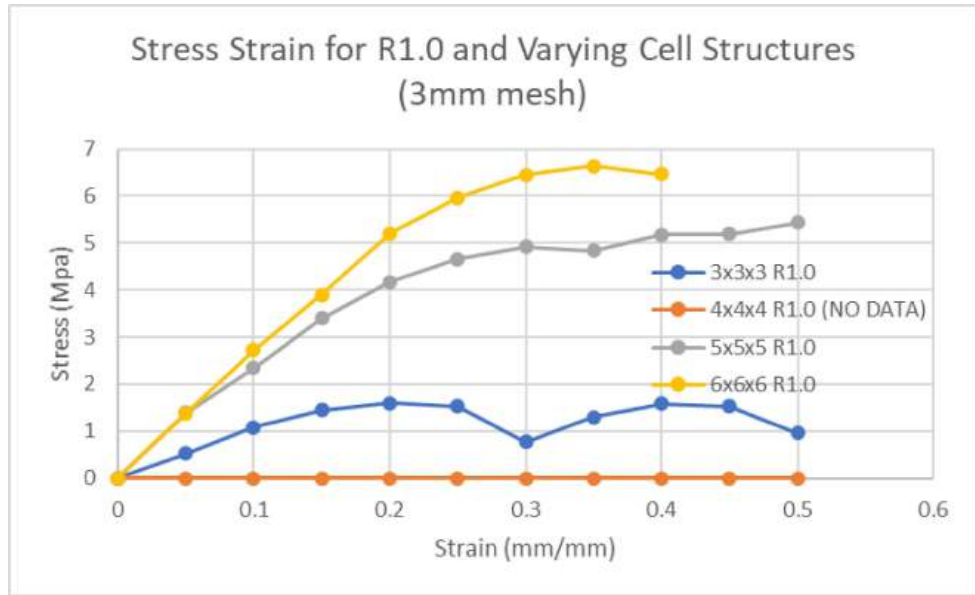


Figure 254: Stress Strain Curves of R1.0 mm Cell Structures w/ 3 mm Coarse Mesh vs. Displacement data for Different Link Lengths.

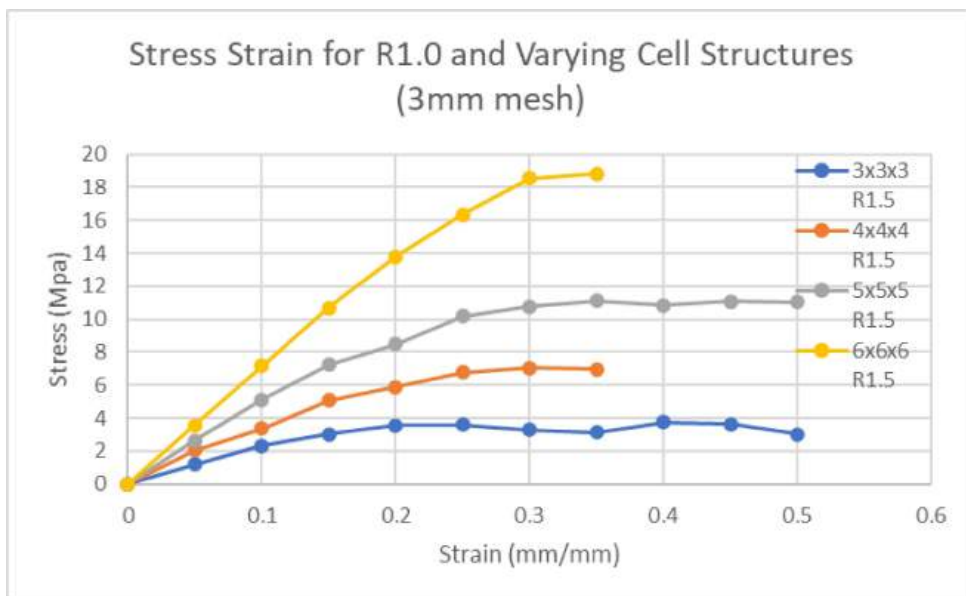


Figure 255: Stress Strain Curves of R1.5 mm Cell Structures w/ 3 mm Coarse Mesh vs. Displacement data for Different Link Lengths.

7.11 Impact Test on Single and Multiple 3x3x3 Cell Structures

7.11.1 Impact Test on Single 3x3x3 Cell Structure

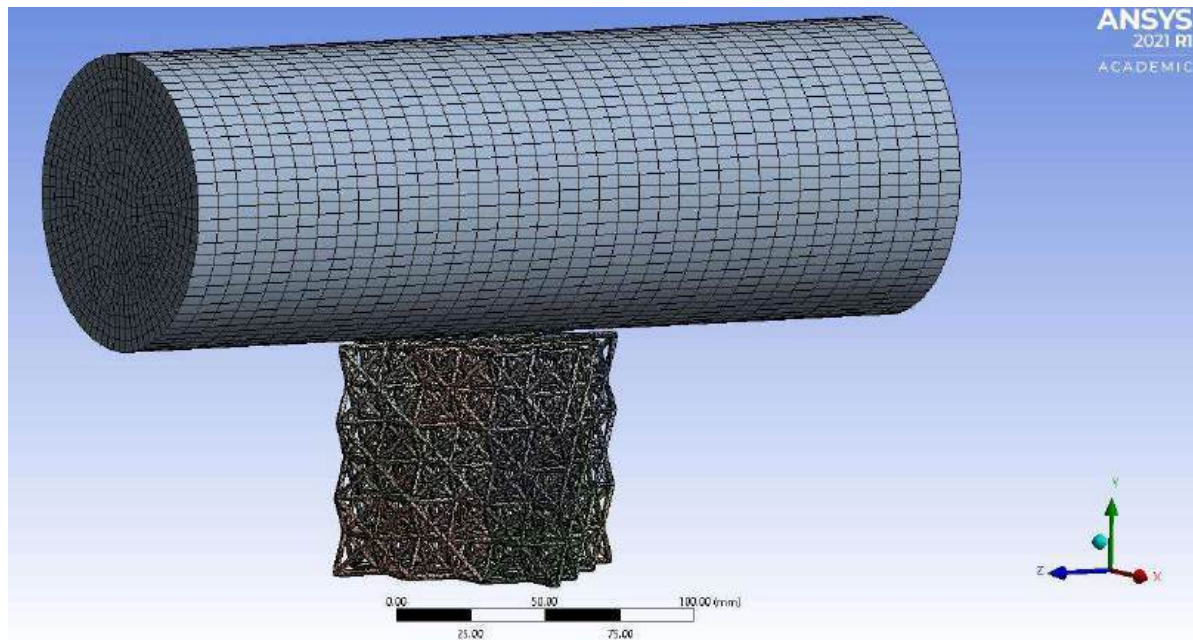


Figure 256: Impact Test of Cylinder (arm) on a single 3x3x3 Cell Structure w/ 3mm Mesh. Mesh Size varies on Cylinder.

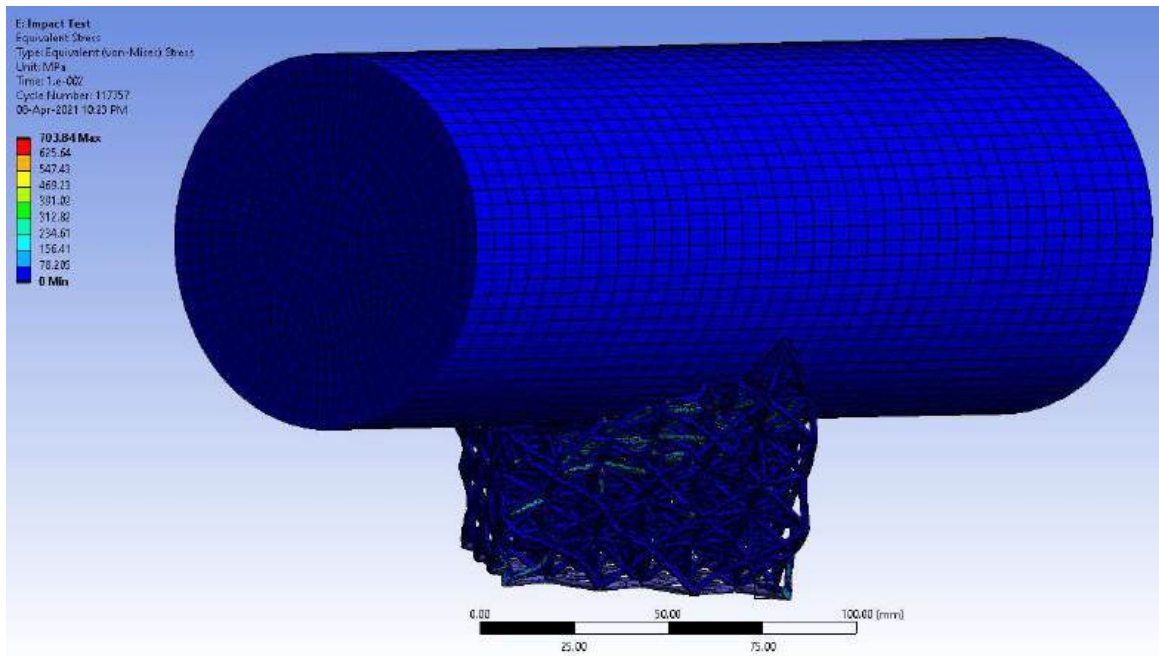


Figure 257: Equivalent Stress of Impact Test on Cylinder (arm) on a single 3x3x3 Cell Structure w/ 3mm Mesh. Mesh Size varies on Cylinder. Fixed Support in purple.

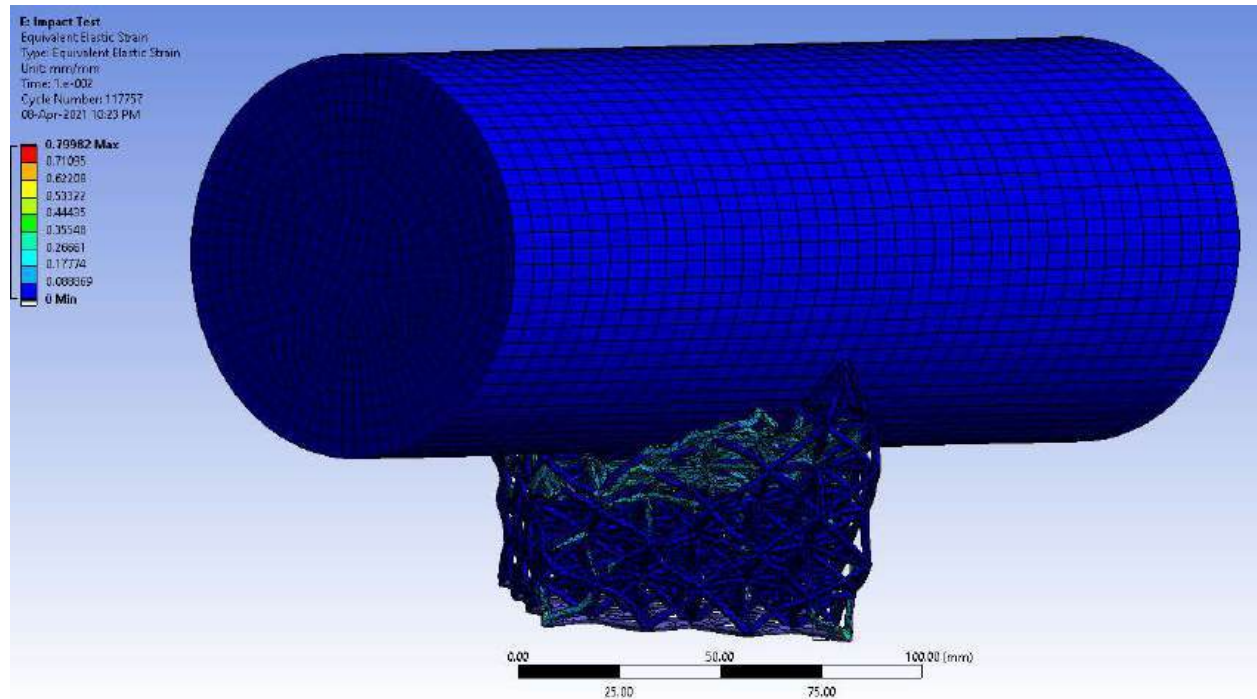


Figure 258: Elastic Strain of Impact Test on Cylinder (arm) on a single 3x3x3 Cell Structure w/ 3mm Mesh. Mesh Size varies on Cylinder.

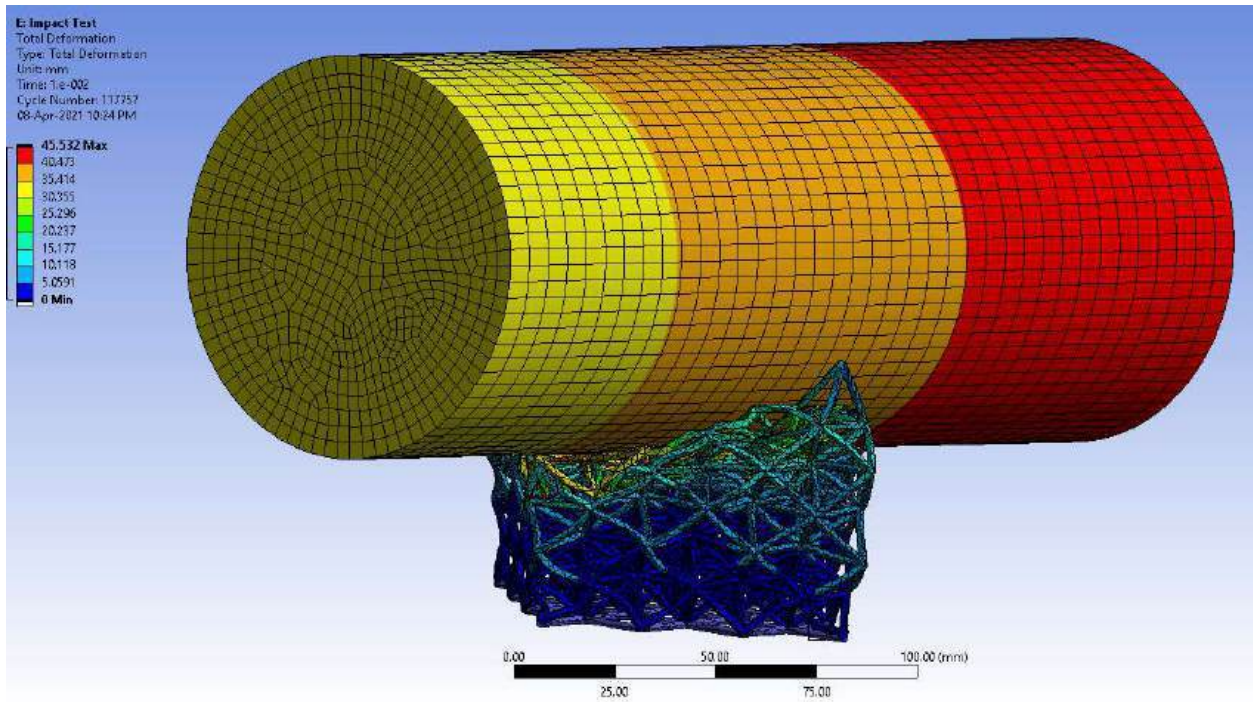


Figure 259: Total Deformation of Impact Test on Cylinder (arm) on a single 3x3x3 Cell Structure w/ 3mm Mesh. Mesh Size varies on Cylinder.

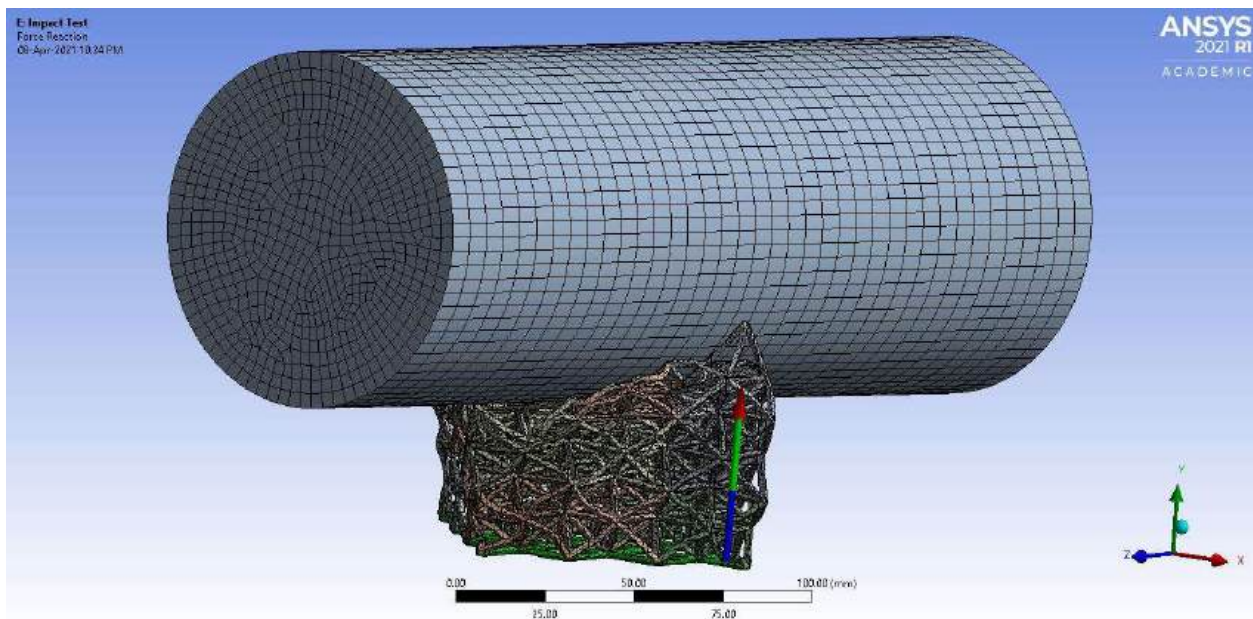


Figure 260: Force Reaction of Impact Test on Cylinder (arm) on a single 3x3x3 Cell Structure w/ 3mm Mesh. Mesh Size varies on Cylinder.

7.11.2 Impact Test on 2x2 Sheet of Cell Structures

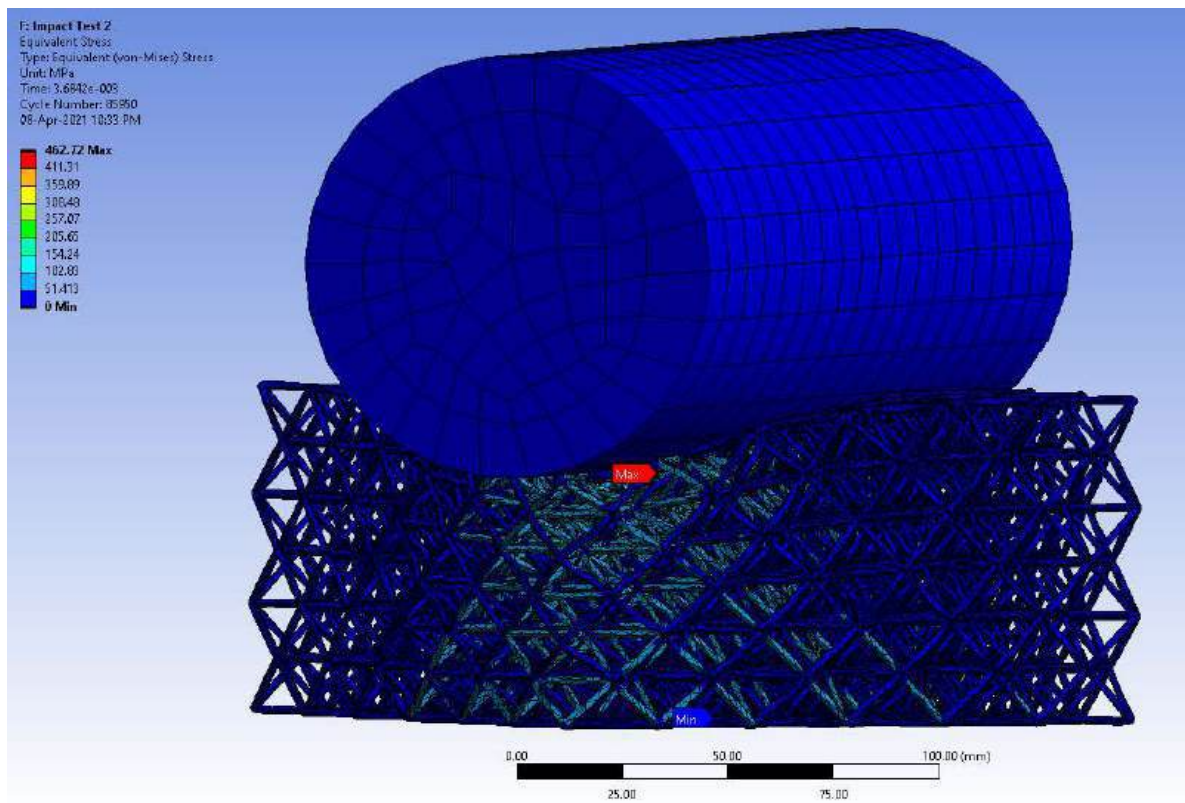


Figure 261: Equivalent Stress of Impact Test on Cylinder (arm) on multiple 3x3x3 Cell Structures (2x2 Sheet) w/ 3mm Mesh. Mesh Size varies on Cylinder.

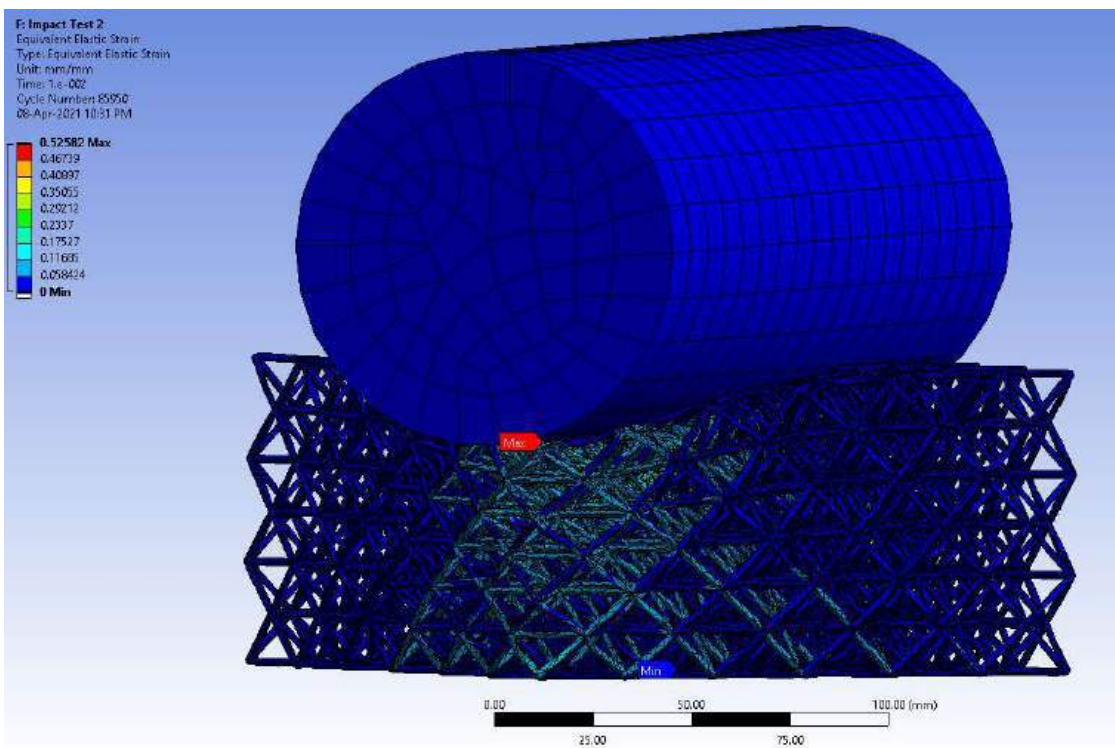


Figure 262: Elastic Strain of Impact Test on Cylinder (arm) on multiple 3x3x3 Cell Structures (2x2 Sheet) w/ 3mm Mesh. Mesh Size varies on Cylinder.

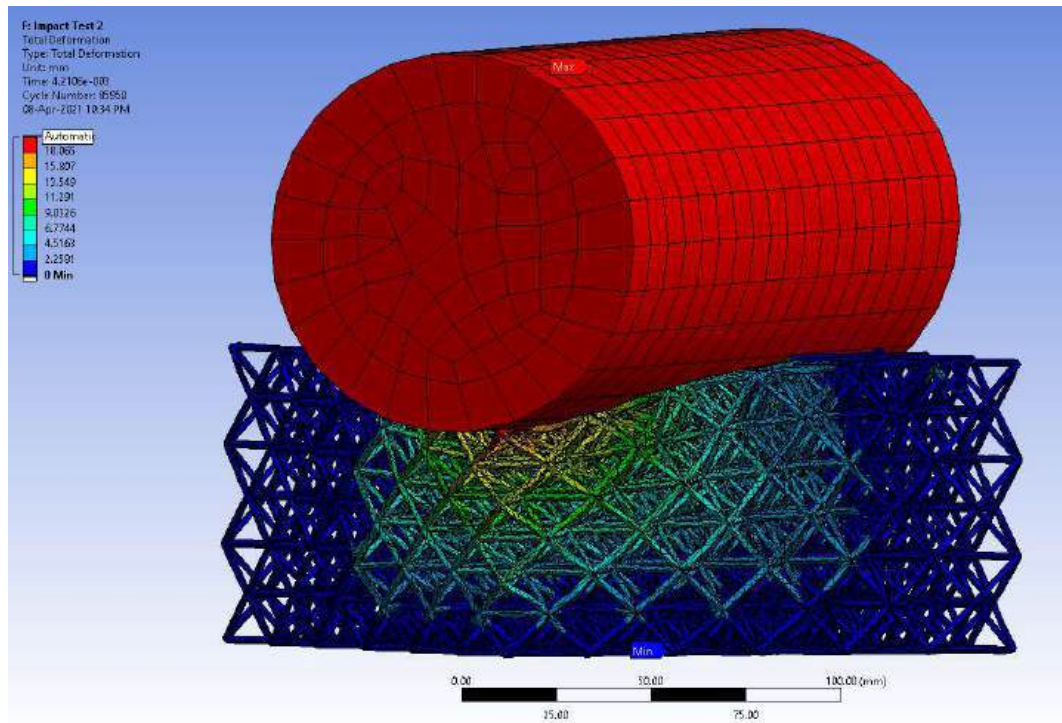


Figure 263: Total Deformation of Impact Test on Cylinder (arm) on multiple 3x3x3 Cell Structures (2x2 Sheet) w/ 3mm Mesh. Mesh Size varies on Cylinder.

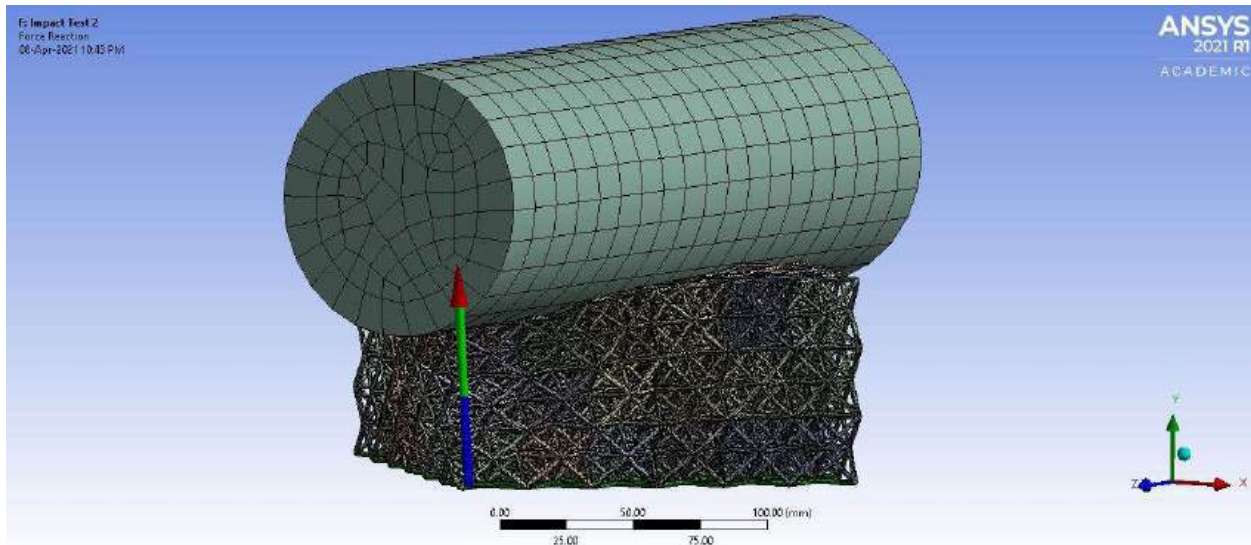


Figure 264: Force Reaction of Impact Test on Cylinder (arm) on multiple 3x3x3 Cell Structures (2x2 Sheet) w/ 3mm Mesh. Mesh Size varies on Cylinder.

7.12 Decision Matrix Tools

7.12.1 Ranking Metrics

Table 57: Fine Mesh Ranking Metrics

Rank	Lower Range	Upper Range
10	1.72E+10	1.90E+10
9	1.53E+10	1.72E+10
8	1.35E+10	1.53E+10
7	1.17E+10	1.35E+10
6	9.82E+09	1.17E+10
5	7.98E+09	9.82E+09
4	6.14E+09	7.98E+09
3	4.31E+09	6.14E+09
2	2.47E+09	4.31E+09
1	6.39E+08	2.47E+09

Table 58: Coarse Mesh Ranking Metrics

Rank	Lower Range	Upper Range
10	1.71E+10	1.89E+10
9	1.54E+10	1.71E+10
8	1.37E+10	1.54E+10
7	1.20E+10	1.37E+10
6	1.02E+10	1.20E+10
5	8.51E+09	1.02E+10
4	6.78E+09	8.51E+09
3	5.06E+09	6.78E+09
2	3.33E+09	5.06E+09
1	1.61E+09	3.33E+09

Table 59: Cell Structure Ranking Metrics

Rank	Lower Range	Upper Range
10	1.03E+10	1.11E+10
9	9.53E+09	1.03E+10
8	8.75E+09	9.53E+09
7	7.98E+09	8.75E+09
6	7.20E+09	7.98E+09
5	6.42E+09	7.20E+09
4	5.65E+09	6.42E+09
3	4.87E+09	5.65E+09
2	4.09E+09	4.87E+09
1	3.32E+09	4.09E+09

Table 60: Theoretical Density Ranking Metrics

Rank	Lower Range	Upper Range
1	6.68E-01	7.40E-01
2	5.96E-01	6.68E-01
3	5.25E-01	5.96E-01

4	4.53E-01	5.25E-01
5	3.81E-01	4.53E-01
6	3.09E-01	3.81E-01
7	2.37E-01	3.09E-01
8	1.65E-01	2.37E-01
9	9.26E-02	1.65E-01
10	2.06E-02	9.26E-02

Table 61: Unit Cell Volume Ranking Metrics

Rank	Lower Range	Upper Range
1	3.64E+03	4.02E+03
2	3.26E+03	3.64E+03
3	2.88E+03	3.26E+03
4	2.50E+03	2.88E+03
5	2.12E+03	2.50E+03
6	1.75E+03	2.12E+03
7	1.37E+03	1.75E+03
8	9.90E+02	1.37E+03
9	6.11E+02	9.90E+02
10	2.33E+02	6.11E+02

Table 62: Cell Structure Volume Ranking Metrics

Rank	Lower Range	Upper Range
1	2.18E+05	2.41E+05
2	1.95E+05	2.18E+05
3	1.72E+05	1.95E+05
4	1.49E+05	1.72E+05
5	1.26E+05	1.49E+05
6	1.03E+05	1.26E+05
7	7.94E+04	1.03E+05
8	5.63E+04	7.94E+04
9	3.32E+04	5.63E+04

10	1.02E+04	3.32E+04
----	----------	----------

Table 63: Simplicity of Application Ranking Metrics

Rank	Lower Range	Upper Range
1	24.75	27.00
2	22.50	24.75
3	20.25	22.50
4	18.00	20.25
5	15.75	18.00
6	13.50	15.75
7	11.25	13.50
8	9.00	11.25
9	6.75	9.00
10	4.50	6.75

7.12.2 Ranking

Table 64: Fine Mesh SEA Ranking

ID	SEA	Ranking
R0.5 L9	2.75E+09	2
R0.5 L10.80	2.46E+09	1
R0.5 L13.50	1.23E+09	1
R0.5 L18.00	6.39E+08	1
R1.0 L9	1.11E+10	6
R1.0 L10.80	8.04E+09	5
R1.0 L13.50	5.32E+09	3
R1.0 L18.00	2.88E+09	2
R1.5 L9	1.90E+10	10
R1.5 L10.80	1.46E+10	8
R1.5 L13.50	1.10E+10	6
R1.5 L18.00	6.57E+09	4

Table 65: Coarse Mesh SEA Ranking

ID	SEA	Ranking
R0.5 L9	1.07E+10	6
R0.5 L10.80	2.55E+09	1
R0.5 L13.50	1.61E+09	1
R0.5 L18.00	3.37E+09	2
R1.0 L9	1.17E+10	6
R1.0 L10.80	6.80E+09	4
R1.0 L13.50	9.42E+09	5
R1.0 L18.00	3.77E+09	2
R1.5 L9	1.89E+10	10
R1.5 L10.80	1.23E+10	7
R1.5 L13.50	9.43E+09	5
R1.5 L18.00	6.31E+09	3

Table 66: Cell Structure SEA Ranking

ID	SEA	Ranking
R0.5 6x6x6	4.72E+09	2
R0.5 5x5x5	4.16E+09	2
R0.5 4x4x4	4.00E+09	1
R0.5 3x3x3	3.32E+09	1
R1.0 6x6x6	7.21E+09	6
R1.0 5x5x5	7.34E+09	6
R1.0 4x4x4	0.00E+00	INVALID DATA
R1.0 3x3x3	3.99E+09	1
R1.5 6x6x6	1.11E+10	10
R1.5 5x5x5	1.02E+10	9
R1.5 4x4x4	6.71E+09	5
R1.5 3x3x3	5.94E+09	4

Table 67: Theoretical Density Ranking

ID	Theoretical Densities	Ranking
R0.5 L9	0.08228	10
R0.5 L10.8	0.05714	10
R0.5 L13.5	0.03657	10
R0.5 L18	0.02057	10
R1 L9	0.32910	6
R1 L10.8	0.22854	8
R1 L13.5	0.14627	9
R1 L18	0.08228	10
R1.5 L9	0.74048	1
R1.5 L10.8	0.51422	4
R1.5 L13.5	0.32910	6
R1.5 L18	0.18512	8

Table 68: Unit Cell Volume Ranking

ID	Volumes	Ranking
R0.5 L9	2.33E+02	10
R0.5 L10.80	2.84E+02	10
R0.5 L13.50	3.60E+02	10
R0.5 L18.00	4.87E+02	10
R1.0 L9	8.51E+02	9
R1.0 L10.80	1.05E+03	8
R1.0 L13.50	1.36E+03	8
R1.0 L18.00	1.87E+03	6
R1.5 L9	1.73E+03	7
R1.5 L10.80	2.18E+03	5
R1.5 L13.50	2.87E+03	4
R1.5 L18.00	4.02E+03	1

Table 69: Cell Structure Volume Ranking

ID	Volumes	Ranking
R0.5 L9	3.54E+04	9
R0.5 L10.80	2.56E+04	10
R0.5 L13.50	1.71E+04	10
R0.5 L18.00	1.02E+04	10
R1.0 L9	1.24E+05	6
R1.0 L10.80	9.21E+04	7
R1.0 L13.50	6.31E+04	8
R1.0 L18.00	3.84E+04	9
R1.5 L9	2.41E+05	1
R1.5 L10.80	1.85E+05	3
R1.5 L13.50	1.30E+05	5
R1.5 L18.00	8.14E+04	7

Table 70: Simplicity of Application Ranking

ID	Measurement Factor	Ranking
R0.5 L9	4.5	10
R0.5 L10.80	5.4	10
R0.5 L13.50	6.75	9
R0.5 L18.00	9	8
R1.0 L9	9	8
R1.0 L10.80	10.8	8
R1.0 L13.50	13.5	6
R1.0 L18.00	18	4
R1.5 L9	13.5	6
R1.5 L10.80	16.2	5
R1.5 L13.50	20.25	3
R1.5 L18.00	27	1